

DISSERTATIONES CHIMICAE UNIVERSITATIS TARTUENSIS

100

DARJA LAVÕGINA

Development of protein kinase
inhibitors based on adenosine
analogue-oligoarginine conjugates



TARTU UNIVERSITY
PRESS

Institute of Chemistry, Faculty of Science and Technology, University of Tartu,
Estonia

Dissertation is accepted for the commencement of the degree of Doctor of
Philosophy in Chemistry on September 7, 2010 by the Doctoral Committee of
the Institute of Chemistry, University of Tartu

Supervisor: Asko Uri (PhD), Leading Scientist, Institute of Chemistry,
University of Tartu, Estonia

Opponent: Stefan Knapp (PhD), Professor and Principal Investigator,
Phosphorylation Dependent Signaling Group,
University of Oxford, UK

Commencement: at 2 PM on November 10, 2010; in room 1021, Chemikum,
14A Ravila St., Tartu



Euroopa Liit
Euroopa Sotsiaalfond



Eesti tuleviku heaks

ISSN 1406–0299

ISBN 978–9949–19–471–1 (trükis)

ISBN 978–9949–19–472–8 (PDF)

Autoriõigus: Darja Lavõgina, 2010

Tartu Ülikooli Kirjastus

www.tyk.ee

Tellimus nr. 510

CONTENTS

LIST OF ORIGINAL PUBLICATIONS	7
ABBREVIATIONS	8
ABSTRACT	11
LITERATURE OVERVIEW	12
1. Protein kinases	12
1.1. General features	12
1.2. AGC-group PKs	13
1.2.1. PKA	15
1.2.2. PKG	19
1.2.3. ROCK	23
1.2.4. PKB	25
1.3. PKs in disease	27
2. Protein kinase inhibitors	30
2.1. General features	30
2.2. Characteristics and general principles of design of PK inhibitors	31
2.2.1. Affinity and inhibitory potency	31
2.2.2. Rational design of PK inhibitors	36
2.2.3. Selectivity issues	38
2.3. Main classes of PK inhibitors	42
2.3.1. Irreversible mono-ligand inhibitors	43
2.3.2. Reversible mono-ligand inhibitors. Special case: ATP-competitive inhibitors	46
2.3.3. Reversible mono-ligand inhibitors. Special case: Protein/peptide substrate-competitive inhibitors	53
2.3.4. Reversible mono-ligand inhibitors. Special case: Allosteric inhibitors and inhibitors of activation	62
2.3.5. Reversible biligand inhibitors. Special case: Bisubstrate inhibitors	65
METHODS	72
1. Solid phase peptide synthesis	72
2. Biochemical <i>in vitro</i> assays for the assessment of PK inhibitors	76
2.1. Inhibition assays versus binding assays	76
2.2. Radiometric methods	77
2.3. Fluorescence techniques	78
2.3.1. Fluorescence phenomenon	78
2.3.2. Measurement of fluorescence intensity (FI)	81
2.3.3. Measurement of fluorescence intensity (FI). Special case: Förster-type resonance energy transfer (FRET)	82
2.3.4. Measurement of fluorescence anisotropy (FA)	84
3. Protein crystallography	86
3.1. General features	86

3.2. Models of diffraction.....	90
3.3. Crystal structures of PKAc.....	93
3.3.1. General features.....	93
3.3.2. Ternary complex of PKAc with AMP-PNP and PKI(5...24).....	96
3.3.3. Conformational versatility of PKs.....	100
3.3.4. PKAr subunits and holoenzyme	105
AIMS OF THE STUDY	112
RESULTS AND DISCUSSION	113
1. Development of ARC-II conjugates [Paper 1: Enkvist <i>et al.</i> , 2006, Paper 3: Lavogina <i>et al.</i> , 2010a]	113
2. Confirmation of the bisubstrate character of ARC-IIs [Paper 1: Enkvist <i>et al.</i> , 2006, Paper 3: Lavogina <i>et al.</i> , 2010a]	117
3. Crystallographic studies of ARC-II conjugates [Paper 2: Lavogina <i>et al.</i> , 2009, Paper 3: Lavogina <i>et al.</i> , 2010a, Paper 5: Pflug <i>et al.</i> , 2010]	120
3.1. PKAc – ARC-1034 complex (PDB 3BWJ) [Paper 2: Lavogina <i>et al.</i> , 2009, Paper 3: Lavogina <i>et al.</i> , 2010a]	120
3.2. PKAc – ARC-670 complex (PDB 3AGM) [Paper 3: Lavogina <i>et al.</i> , 2010a, Paper 5: Pflug <i>et al.</i> , 2010].....	123
4. Development of ARC-III conjugates [Paper 2: Lavogina <i>et al.</i> , 2009, Paper 3: Lavogina <i>et al.</i> , 2010a]	128
5. Crystallographic studies of ARC-III conjugates [Paper 5: Pflug <i>et</i> <i>al.</i> , 2010]	133
5.1. PKAc – ARC-1012 complex (PDB 3AG9).....	133
5.2. PKAc – ARC-1039 complex (PDB 3AGL)	136
6. Application of ARC-II and ARC-III conjugates as inhibitors and fluorescent probes of PKGI α [Paper 4: Lavogina <i>et al.</i> , 2010b]	139
6.1. Development of assays.....	139
6.2. Studies of binding and inhibition mechanism.....	142
7. Measurement of physiological effects of ARC-903 in isolated rat arteries [Paper 4: Lavogina <i>et al.</i> , 2010b]	143
CONCLUSIONS.....	145
SUMMARY IN ESTONIAN	147
REFERENCES	149
APPENDICES	164
Appendix 1. Selectivity profiling of ARC-902, ARC-903, ARC-1028 and ARC-664	164
PUBLICATIONS	167
CURRICULUM VITAE	239
ELULOOKIRJELDUS.....	241

LIST OF ORIGINAL PUBLICATIONS

- I. Enkvist E., **Lavogina D.**, Raidaru G., Vaasa A., Viil I., Lust M., Viht K., Uri A., Conjugation of adenosine and hexa-(D-arginine) leads to a nanomolar bisubstrate-analog inhibitor of basophilic protein kinases. *Journal of Medicinal Chemistry* (2006), 49, 7150–7159
- II. **Lavogina D.**, Lust M., Viil I., König N., Raidaru G., Rogozina J., Enkvist E., Uri A., Bossemeyer D., Structural Analysis of ARC-Type Inhibitor (ARC-1034) Binding to Protein Kinase A Catalytic Subunit and Rational Design of Bisubstrate Analogue Inhibitors of Basophilic Protein Kinases. *Journal of Medicinal Chemistry* (2009), 52, 308–321
- III. **Lavogina D.**, Enkvist E., Uri A., Bisubstrate Inhibitors of Protein Kinases: from Principle to Practical Applications. *ChemMedChem* (2010), 5, 23–34
- IV. **Lavogina D.**, Nickl C. K., Enkvist E., Raidaru G., Lust M., Vaasa A., Uri A., Dostmann W. R., Adenosine analogue-oligo-arginine conjugates (ARCs) serve as high-affinity inhibitors and fluorescence probes of type I cGMP-dependent protein kinase (PKGI α). *Biochimica et Biophysica Acta-Proteins and Proteomics* (2010), 1804, 1857–1868
- V. Pflug A., Rogozina J., **Lavogina D.**, Enkvist E., Uri A., Engh R. A., Bossemeyer D., Diversity of bisubstrate binding modes of adenosine analogue-oligoarginine conjugates in protein kinase A and implications for protein substrate interactions. *Journal of Molecular Biology* (2010), doi: 10.1016/j.jmb.2010.08.028

Author's contribution:

- Paper I:** The author performed synthesis of compounds **2–5**, **7**, **8**, **11**, **25**, **26**, and participated in writing of the manuscript.
- Paper II:** The author carried out synthesis of all ARC-type inhibitors, performed co-crystallization of **ARC-1034** with PKAc, participated in the design of novel ARCs, and was responsible for data analysis and writing of the manuscript.
- Paper III:** The author participated in the collection of data from the relevant publications, and was responsible for data analysis and writing of the manuscript.
- Paper IV:** The author carried out synthesis of compounds **ARC-341**, **ARC-349**, **ARC-902**, **ARC-903**, **ARC-905**, **ARC-1028**, **ARC-1044**, **ARC-1042** and **ARC-1059**, performed FA-, FI-, FRET- and radio-metric assays, participated in the ARC internalization studies, and was responsible for data analysis and writing of the manuscript.
- Paper V:** The author carried out synthesis of compounds **ARC-1012** and **ARC-1039**, performed co-crystallization of **ARC-1012** with PKAc, and participated in data analysis and writing of the manuscript.

ABBREVIATIONS

AC	adenylate cyclase
ACI	ATP-competitive inhibitors
ABPP	activity-based protein profiling
Adc	adenosine 4'-dehydroxymethyl-4'-carboxylic acid moiety
ADP	adenosine 5'-diphosphate
Ahx	6-aminohexanoic acid moiety
AKAP	A-kinase anchoring protein
ALI	allosteric inhibitor
AMP	adenosine 5'-monophosphate
ARC	adenosine analogue-oligoarginine conjugate
ATP	adenosine 5'-triphosphate
BCR-Abl	fusion protein consisting of the BCR (breakpoint cluster region) protein and the Abl (Abelson) tyrosine kinase
Boc	tert-Butoxycarbonyl
BODIPY FL	4,4-difluoro-5,7-dimethyl-4-bora-3a,4a-diaza-S-indacene-3-propionic acid
BSI	bisubstrate inhibitor
CAMK	calcium/calmodulin-dependent protein kinase
cAMP	cyclic adenosine 3',5'-monophosphate
CDK	cyclin-dependent protein kinase
cGMP	cyclic guanosine 3',5'-monophosphate
CK	casein kinase
c-Kit	cytokine receptor tyrosine kinase
CML	chronic myeloid leukemia
CPP	cell-penetrating peptide
CREB	cAMP response element-binding protein
Csk	c-Src tyrosine kinase
EGFR	epidermal growth factor receptor 1 tyrosine kinase
EPAC	exchange factor directly activated by cAMP
FA	fluorescence anisotropy
FI	fluorescence intensity
Fmoc	9-fluorenyl-methoxycarbonyl
FP	fluorescence polarization
FRET	Förster resonance energy transfer
GFP	green fluorescent protein
GSK	glycogen synthase kinase
HER2	human epidermal growth factor receptor 2 tyrosine kinase
HTS	high-throughput screening
I κ B	inhibitor of NF κ B
IP ₃	inositol(1,4,5)triphosphate
IRAG	IP ₃ receptor-associated substrate
IRK	insulin receptor tyrosine kinase

K _D	equilibrium dissociation constant obtained from binding assays
K _d	dissociation constant obtained from displacement assays
K _i	inhibition constant
Lck	leukocyte-specific protein tyrosine kinase
MAPK	mitogen-activated protein kinase
MEK	MAPK kinase
MEKK	MEK kinase
MLC ₂₀	20 kDa regulatory light chain of myosin II
MLCK	Ca ²⁺ /calmodulin-dependent myosin light-chain kinase
MSK1	mitogen- and stress-activated protein kinase
mTOR	mammalian target of rapamycin
mTORC1	mTOR complex 1 composed of mTOR, regulatory associated protein of mTOR (Raptor), mammalian LST8/G-protein β-subunit like protein (mLST8/GβL) and other binding partners
mTORC2	mTOR complex 1 composed of mTOR, rapamycin-insensitive companion of mTOR (Rictor), mammalian LST8/G-protein β-subunit like protein (mLST8/GβL) and other binding partners
MYPT	MLC phosphatase
NFAT3	nuclear factor of activated T cells-3
NFκB	nuclear factor κ-light-chain-enhancer of activated B cells
NMR	nuclear magnetic resonance
NPR	natriuretic peptide receptor
PBC	phosphate-binding cassette
PCI	protein substrate-competitive inhibitor
PDE	phosphodiesterase
PDGFR	platelet-derived growth factor receptor kinase
PDK	phosphoinositide-dependent kinase
PEG	polyethylene glycol
PI3K	phosphoinositide-3-kinase
PH	pleckstrin homology (domain)
PK	protein kinase
PKA	cAMP-dependent protein kinase
PKAc	PKA catalytic subunit
PKAr	PKA regulatory subunit
PKB	protein kinase B (Akt)
PKC	protein kinase C
PKG	cGMP-dependent protein kinase
PKI	heat-stable protein kinase inhibitor
PP	protein phosphatase
PtdInsP ₃	phosphatidylinositol(3,4,5)triphosphate
Rho	homologue of small GTPase Ras
ROCK	Rho-dependent protein kinase
ROF	rule-of-five

Rp-8-pCPT-cGMPS	8-(para-chlorophenylthio)guanosine-3',5'-cyclic monophosphorothioate, Rp- isomer
Rp-8-Br-PET-cGMPS	8-Bromo- β -phenyl-1,N ² - ethenoguanosine-3', 5'-cyclic monophosphorothioate, Rp- isomer
RSK	ribosomal protein S6 kinase
SH	Src homology (domain)
SPPS	solid phase peptide synthesis
SPR	surface plasmon resonance
Src	family of proto-oncogenic (sarcoma) tyrosine kinases
Syk	spleen tyrosine kinase
TAMRA	carboxytetramethylrhodamine
TK	tyrosine kinase
TLC	thin layer chromatography
TSC	tuberous sclerosis protein
VEGFR	vascular endothelial growth factor receptor tyrosine kinase

ABSTRACT

Since the pioneering works by E. P. Kennedy, E. H. Fischer, E. G. Krebs, E. W. Sutherland and W. D. Wosilait in 1950s [Cohen P., 2002], protein phosphorylation has stayed one of the most thoroughly studied and discussed topics of the natural sciences. Protein kinases, the enzymes catalyzing phosphorylation have been termed “the machines of life” for being involved in most processes of cell regulation; the aberrant signalling of protein kinases has been connected to a variety of diseases, including cancer, diabetes, and asthma. Consequently, an increasing amount of effort has been focussed on the investigation and implication of mechanisms responsible for the regulation of protein kinase activity, giving stimulus for the intense development of protein kinase inhibitors.

This thesis describes the focussed design and synthesis of a family of protein kinase inhibitors represented by conjugates of adenosine analogues and arginine-rich peptides (ARCs) targeted to the basophilic protein kinases. Structure-affinity relationship studies as well as crystallographic evidence have been used to guide the development process to yield new generations of ARC-inhibitors, with most efficient compounds expressing subnanomolar affinity and tunable selectivity towards protein kinases of the AGC-group, including cyclic nucleotide-dependent protein kinases, pharmacologically important protein kinase B and Rho-dependent protein kinase. The remarkable inhibitory properties of ARCs in combination with their proteolytic stability and ability to penetrate the cell plasma membrane have enabled the successful application of **ARC-1059** in vasoconstriction experiments *via* targeting cAMP/PKA and cGMP/PKG pathways in isolated rat arteries, which confirmed the potential of bisubstrate inhibitor strategy as a whole.

LITERATURE OVERVIEW

I. Protein kinases

I.1. General features

Protein kinases (PKs) are enzymes that catalyze the phosphorylation reaction, *i.e.*, the transfer of a γ -phosphoryl group from a donor (nucleotide, usually ATP [Bostrom *et al.*, 2009; Shugar, 1996]) to an acceptor molecule (protein/peptide substrate) (Figure 1). As a result of phosphoryl transfer, a negative charge is incorporated into the hydroxyl-bearing side-chain of a Ser, Thr or Tyr residue of the substrate [Pinna and Ruzzene, 1996], and this relatively small change in the chemical composition of the phosphorylated amino acid triggers massive rearrangement of its neighboring microenvironment [Steichen *et al.*, 2010]. The phosphorylation reaction thus serves as a molecular switch, causing a change of the protein substrate conformation and rendering its ability to participate in a variety of cellular processes, ranging from differentiation, transcription and apoptosis to cytoskeletal rearrangement, cell movement and responsiveness to extracellular stimuli [Manning B. D. and Cantley, 2007; Shabb, 2001].

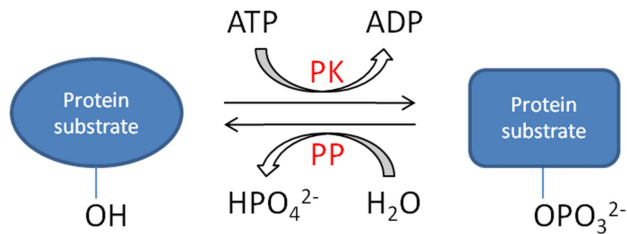


Figure 1. Scheme of protein phosphorylation. PK, protein kinase; PP, protein phosphatase.

The spatiotemporal control of activity of PKs themselves is performed by several mechanisms, including expression within a certain stage of cell cycle [Murray A. W., 2004], localization in subcellular compartments [Tasken and Aandahl, 2004], positive or negative feedback-loops, *etc.* PKs participate in large intracellular information currents, all of them leading to a certain outcome event involving the examples provided below:

- repetitive autophosphorylation and phosphorylation steps (*i.e.*, PK cascades [Chang and Karin, 2001]);
- intertwined signaling of PKs and protein phosphatases (PP, enzymes catalyzing the hydrolytic removal of phosphoryl groups from protein substrates) [Pidoux and Tasken, 2010];
- conjunction of PK functioning with gradients of activating secondary messengers or ligands [Wilson L. S. *et al.*, 2008].

Not surprisingly, taking advantage of the phosphorylation reaction as such and PKs as its catalyzing 'machinery' for the sustainment of life is utilized throughout the nature, both by prokaryotic [Leonard *et al.*, 1998] and eukaryotic organisms [Lee J. and Rudd, 2002; Miranda-Saavedra *et al.*, 2007]. In humans, 518 PKs are encoded in genome, of which 40 are atypical and 50 predicted to be catalytically inactive due to the lack of at least one of the conserved catalytic residues [Hanks, 2003; Manning G. *et al.*, 2002]. The efforts to systematize the set of human PKs (termed human kinome) on the basis of sequence comparison of PK catalytic and other domains, biological functions, and a similar classification of kinomes of other organisms, have resulted in generation of phylogenetic maps, where PKs are divided into groups, families, and subfamilies [InvitrogenTM Human Kinome Map; Kinnings and Jackson, 2009; Manning G. *et al.*, 2002]. The main phylogenetic groups of PKs are as follows [Manning G. *et al.*, 2002; Parsons *et al.*, 2005]:

- AGC (containing members of PKA, PKG, and PKC families, which are often activated by second messengers and mostly phosphorylate substrates rich in basic amino acid residues);
- CAMK (calcium/calmodulin-dependent PKs, which also frequently phosphorylate substrates rich in basic amino acid residues);
- CMGC (containing members of CDK, MAPK, GSK3, and CLK families, which often phosphorylate substrates rich in Pro residues);
- CK1 (casein kinase 1 family, which preferably phosphorylate motifs rich in acidic residues);
- STE (homologs of yeast Sterile 7, Sterile 11, and Sterile 20 kinases, including PKs involved in MAPK activation and related kinases);
- TK (tyrosine kinases, including receptor TKs and non-receptor TKs);
- TKL (tyrosine kinase-like PKs, which share high domain similarity with TKs, but are Ser/Thr kinases).

1.2. AGC-group PKs

The term AGC-group was introduced by Steven Hanks and Tony Hunter in 1995 to delimit PKs that share a high similarity of primary amino acid sequence in their catalytic kinase domains with cAMP-dependent PK (PKA), cGMP-dependent PK (PKG), and protein kinase C (PKC) [Hanks and Hunter, 1995]. In humans, AGC-group contains 60 PKs, whereas the majority of members possess several isoforms and splice variants, further enhancing the diversity of this group.

Representatives of the AGC-group are activated downstream of a wide range of extracellular stimuli, and several levels of activity (*i.e.*, basal, partial, or full) may exist, tuned through a variety of mechanisms. The full activation is usually acquired *via* the two following mechanisms:

- (auto)phosphorylation of the two highly conserved regulatory motifs (the activation loop located inside the catalytic core and the hydrophobic motif positioned in a non-catalytic region following the kinase domain) [Smith J. A. *et al.*, 1996; Steichen *et al.*, 2010];
- binding of one or more low-molecular weight messenger molecules (*i.e.*, cyclic nucleotides, phospholipids, phosphoinositides, or members of Rho GTPase family) to the regulatory domain of PK [Liu P. *et al.*, 2009; Poppe *et al.*, 2008; Somlyo and Somlyo, 2000].

In several cases, divalent cations (Mg^{2+} , Ca^{2+}) are also required for the catalytic functioning [Herberg *et al.*, 1999; Lin X. *et al.*, 2005].

The majority of PKs of the AGC-group are the basophilic Ser/Thr PKs, meaning that they phosphorylate substrates on side-chains of Ser or Thr residues preferably flanked by basic amino acids (Lys or Arg; (Table 1) [Pearce *et al.*, 2010]. Due to the similar consensus sequences of substrates, several AGC-group PKs can phosphorylate the same protein *in vivo* (*i.e.*, PKB, RSK, PKA, PKC and S6K isoforms phosphorylate the same Ser residue at the N-terminus of glycogen synthase kinase 3 [Frame and Cohen, 2001]), such cross-reactivity demonstrating the importance and the scope of confluence in PK pathways.

Table 1. Examples of substrate consensus sequences of AGC-group members (adapted from Pearce *et al.*, 2010).

<i>Protein kinase</i>	<i>Substrate consensus sequence^a</i>
PKAc	Arg-Arg-Xaa- Ser/Thr -Hyd
PKB	Arg-Xaa-Arg-Xaa-Xaa- Ser/Thr -Hyd
PKC (for isoform α)	Arg-Lys-Xaa- Ser/Thr -Xaa-Arg/Lys
PKG	Arg/Lys _{2...3} -Xaa- Ser/Thr
ROCK	Arg/Lys-Arg/Lys-Xaa- Ser/Thr
S6K	Arg/Lys-Xaa-Arg-Xaa-Xaa- Ser/Thr

^a The phosphorylatable residue (*i.e.*, position P0) is indicated in bold; Hyd, amino acid with bulky hydrophobic side-chain; Xaa, any amino acid

A brief review about the members of AGC-group within the scope of studies of the given thesis is given below.

1.2.1. PKA

Since the beginning of the human kinome research era, PKA has been one of the most extensively studied PKs, both due to the importance of its signaling throughout the body systems and its attractive features as a model kinase (high expression and purification yield, good crystallization properties, activation by a comparatively uncomplicated mechanism, *etc.*).

PKA is one of the major downstream effectors of the secondary messenger cAMP, and the “classical” PKA activation cascade involves several steps linking an extracellular event with an intracellular outcome (Figure 2; [Skallhegg *et al.*, 2005]). Binding of a ligand to the extracellular part of a G_s-protein coupled receptor triggers conformational change, which is translated to the intracellular G_s-protein, causing substitution of GTP for GDP in the latter and subsequent dissociation of the activated G_s-protein into an α -subunit and a $\beta\gamma$ -heterodimer [Nelson *et al.*, 2000]. The α -subunit of G_s subsequently binds to and activates a member of adenylate cyclase (AC) family of transmembrane proteins, comprising nine closely related isoforms in mammals; alternatively, ACs can be directly activated by small-molecular weight compounds (*i.e.*, forskolin) [Hanoune and Defer, 2001]. ACs then catalyze the conversion of ATP to cAMP, which in turn triggers several downstream events including the activation of the cyclic nucleotide-binding proteins PKA and EPAC [Cheng X. *et al.*, 2008].

The PKA holoenzyme consists of two regulatory and two catalytic subunits; when cAMP binds cooperatively to the regulatory subunits of the PKA holoenzyme (two cAMP molecules per regulatory subunit), the latter dissociates into a dimer of regulatory subunits (PKAr) and two catalytic subunits (PKAc) that represent the active form of PKA. It should be noted, however, that in order to become catalytically active, PKAc also requires phosphorylation at Thr197 (performed by PDK1 *in vivo*) and autophosphorylation at Ser338.

In normal tissues, the ratio of the PKAr:PKAc molar concentrations is relatively constant, being kept close to unity [Hofmann *et al.*, 1977]. Both regulatory and catalytic subunits of PKA are expressed as a variety of isoforms: PKArI α , PKArI β (with a molecular weight of 43–47 kDa), PKArII α and PKArII β (molecular weight of 49–55 kDa), or PKAc α , PKAc β , PKAc γ , and PRKX (with a molecular weight of 40 kDa), respectively [Diskar *et al.*, 2007; Skallhegg *et al.*, 1998]. The two classes of PKA holoenzymes are designated type I and type II according to the type of regulatory subunits; the apparent activation constant of PKA holoenzymes type I by cAMP is 110 nM, while for PKA holoenzymes type II it is 180 nM [Diskar *et al.*, 2007].

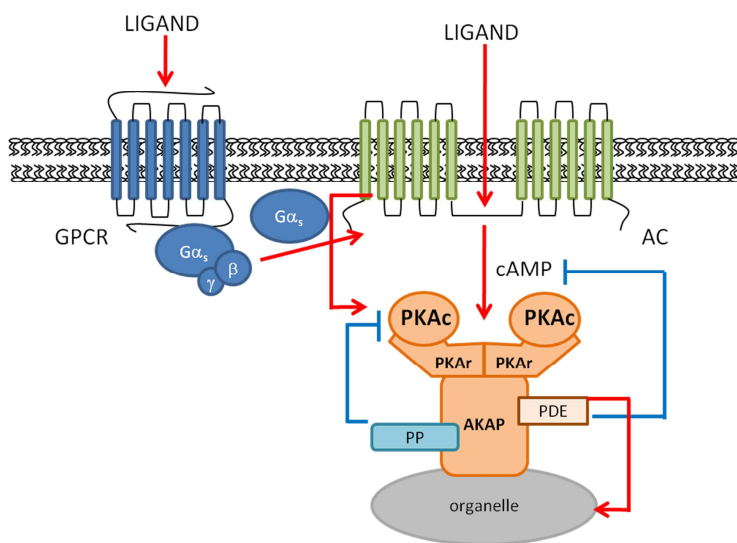


Figure 2. General scheme of PKAc activation and intracellular targeting. AC, adenylyl cyclase; GPCR, G-protein coupled receptor; PDE, phosphodiesterase; PP, protein phosphatase.

The region of PKAc where the regulatory subunits bind, partially coincides with the substrate-binding site of PKAc, and the regulatory subunits also contain the PKAc substrate consensus sequence [Taylor *et al.*, 2008]. Indeed, PKArII subunits are autophosphorylated by PKAc, while PKArI subunits contain Ala moiety instead of the phosphorylatable Ser or Thr residue and are therefore not autophosphorylated [Smith C. M. *et al.*, 1999]. Interestingly, the apparent activation constant of PKA holoenzymes containing phosphorylated PKArII is higher (340 nM) than for the non-phosphorylated form [Diskar *et al.*, 2007]. Another difference between type I and type II subunits lies in the fact that PKArI subunits require the presence of MgATP for the tight binding to PKAc whereas PKArII do not; this phenomenon has also been attributed to the presence or absence of the phosphorylatable residue in the composition of the regulatory subunit [Skalhegg *et al.*, 2005]. Overall, it has been demonstrated that the PKA holoenzyme type I is more sensitive to perturbations in the active site cleft and fixes PKAc in fully closed conformation that requires MgATP [Skalhegg *et al.*, 2005]. Moreover, the alanine residue in the P0¹ position of

¹ P0 position indicates the phosphorylatable residue of the substrate protein/peptide, or a residue corresponding to the phosphorylatable residue in the peptide substrate-mimicking inhibitor. Positions of amino acids residing to the N-terminus of the substrate from the phosphorylatable residue are designated as P-1, P-2, *etc.*, and the positions of amino acids residing to the C-terminus of the substrate as P+1, P+2, *etc.*

PKA α I prevents complete dissociation of the PKA holoenzyme type I in the presence of cAMP *in vivo* (however, the affinity of PKA α I towards PKA β is reduced almost 100-fold in the presence of cAMP)[Anand *et al.*, 2010]. The PKA holoenzyme type II, on the other hand, is less sensitive towards changes in the catalytic core, and the autophosphorylated form of RII enables PKA β to adopt a half-closed conformation; upon activation with cAMP, the PKA holoenzyme type II becomes fully dissociated [Skalhegg *et al.*, 2005].

The intracellular compartmentalization of the PKA holoenzyme is controlled by association of the regulatory subunits with A-kinase anchoring proteins (AKAPs) [Dibenedetto *et al.*, 2008; Pidoux and Tasken, 2010]. Primarily, only RII-targeting AKAPs have been identified, hence the PKA holoenzyme type I was regarded mainly cytoplasmic; however, AKAPs for RI have also been subsequently discovered [Huang L. J. *et al.*, 1997; Tasken and Aandahl, 2004]. Overall, AKAP family is represented in mammals by over 50 members; all of them contain a domain for binding PKA α subunits and a domain for directing the PKA holoenzyme-AKAP complex to subcellular structures, membranes, or organelles [Beene and Scott, 2007]. Moreover, AKAPs uphold the constitution of localized pools of cAMP-signalling, as in addition to PKA holoenzyme, AKAPs may bear binding domains also for phosphodiesterases (PDEs), which degrade cAMP, and even for PPs, which perform dephosphorylation [Pidoux and Tasken, 2010]. In some cases, the complexity of such pools of cAMP-signalling is further enhanced by negative feedback loops triggered by cross-activation of PDEs (*i.e.*, PDE3B, PDE4D3), deactivation of G $_s$ protein-coupled receptors (*i.e.*, D1-dopamine receptor) or even conversion of G $_s$ to G $_i$ (*i.e.*, in case of β 2- adrenergic receptor) *via* PKA β -catalyzed phosphorylation [Shabb, 2001].

PKA β dissociated from the holoenzyme may be located in the cytosol, or may enter the nucleus by passive diffusion through the pores in the nuclear envelope [Harootunian *et al.*, 1993]. The re-location of PKA β back to the cytosol is mediated by the family of heat-stable protein kinase inhibitors (PKIs) [Wen *et al.*, 1995]. PKIs are proteins comprising 70...75 amino acids and consisting of two domains: an N-terminal protein kinase inhibition domain mimicking the substrate consensus sequence of PKA β , and a C-terminal nuclear export signal [Dalton and Dewey, 2006]. The nuclear export signal that is located within residues 37–46 of PKI contains several hydrophobic leucine residues; in PKA β -unbound state of PKI, these residues are 'masked' and PKI moves freely between the cytosol and the nucleus [Dalton and Dewey, 2006]. Upon binding of PKI kinase inhibitory domain to PKA β , the nuclear export signal of PKI becomes exposed, and the PKA β -PKI complex is transported back to the cytosol, where PKI further acts as a potent endogenous PKA β inhibitor. The latter function of PKI becomes especially important if reduction of PKA β activity in the presence of cAMP is required, as PKI does not contain a cAMP-binding domain and retains its inhibitory functions in the conditions where PKA α subunits are “switched off”.

In the recent years, an increasing number of studies have provided evidence for another endogenous way of inhibition of PKA β that is retained in the

presence of cAMP and is performed by the complex of nuclear factor- κ B (NF κ B) with the unphosphorylated form of its natural inhibitor (I κ B). The exact mechanism of this PKAc inhibition is unknown, although it has been suggested that I κ B masks the ATP-binding site of PKAc [Zhong *et al.*, 1997]. The phosphorylation of I κ B catalyzed by I κ B kinase (stimulated by lipopolysaccharides or by vasoactive peptides), by ROCK or by MEKK1 triggers proteosomal degradation of pI κ B and thus causes the release of active PKAc [Dulin *et al.*, 2001; Ma Y. *et al.*, 2005; Profirovic *et al.*, 2005; Sriwai *et al.*, 2008].

PKA is an ubiquitous PK, being expressed in high concentration in several tissues (*i.e.*, skeletal, cardiac, smooth muscle, adipose, brain, endocrine tissue, *etc.*); consequently, PKAc phosphorylates a large variety of substrates localized either in the cytosol, in the nucleus, or even in the extracellular environment *in vivo* [Shabb, 2001]. Historically, PKAc was discovered as an enzyme stimulating glycogenolysis in muscle by phosphorylating cytosolic phosphorylase kinase, which in turn activates glycogen phosphorylase and thus triggers conversion of glycogen to glucose-1-phosphate [Walsh *et al.*, 1968]; PKAc further contributes to glycogenolysis by deactivating phosphorylation of glycogen synthase at Ser5 [Shabb, 2001]. PKAc also regulates metabolic processes in the liver by inhibition of glycolysis *via* deactivation of fructose-2,6-bisphosphatase and pyruvate kinase by PKAc-catalyzed phosphorylation at Ser32 and at Ser12, respectively [Shabb, 2001].

One of the most widely known PKA pathways in the nucleus involves phosphorylation of the cAMP response element-binding protein (CREB) at Ser133; in certain conditions, however, the phosphorylation of the same site can be performed by PKB [Du and Montminy, 1998], and phosphorylation of other sites (required for full activation of CREB) by Raf, MEK, or PKC [Johannessen and Moens, 2007]. Analogically, PKAc phosphorylates at Ser117 the homologous CRE modulator (CREM) [Rosenberg *et al.*, 2002]. Phosphorylated CREB (pCREB) binds subsequently the CREB-binding protein (CBP) that is a general transcriptional co-activator, and this interaction results in stimulation of the transcription [Rosenberg *et al.*, 2002]. Similarly, transcription is activated as a result of PKAc-catalyzed phosphorylation of NF- κ B; however, PKAc may also inhibit transcriptional activity, as exemplified by PKAc-catalyzed deactivating phosphorylation of the NFAT3 isoform [Shabb, 2001].

The ubiquitous functions of PKAc also involve destabilization of actin cytoskeleton, and suppression of apoptosis; additionally, there are several tissue-specific physiological tasks, such as stimulation of lipolysis in adipose tissue, regulation of ion conductance and cardiovascular relaxation in smooth muscle, inhibition of platelet aggregation, inhibition of antigen-induced B- and T-cell activation, *etc.* [Shabb, 2001, Skalhogg *et al.*, 2005, Hofmann *et al.*, 2009].

I.2.2. PKG

Along with PKA, another closely related member of the cyclic nucleotide-dependent PK family is PKG (Figure 3), which represents one of the major effectors in the cGMP signaling. Mammals possess two PKG genes termed PKGI and PKGII [Hofmann *et al.*, 2000; Smolenski *et al.*, 1998], whereas PKGI is mainly located in the cytoplasm and PKGII is usually myristylated and anchored to the plasma membrane [Vaandrager *et al.*, 2005]. The holoenzyme of PKGI is formed by N-terminal dimerization of monomeric chains; a monomeric chain has a molecular weight of 76 kDa and consists of several domains, including the N-terminal dimerization domain, autoinhibitory domain, regulatory domain carrying cGMP-binding sites, and catalytic domain bearing ATP- and protein/peptide substrate-binding sites [Hofmann *et al.*, 2009].

In the absence of cGMP, the PKGI holoenzyme is maintained in the basal state by association of the autoinhibitory domain of each monomer with the substrate-binding site located in the catalytic domain of the same chain; the basal activity of PKGI is surprisingly high, constituting 10% of the maximal activity, and it may be even more enhanced by autophosphorylation [Scholten *et al.*, 2008]. According to the mass-spectrometric studies, PKGI has at least two major autophosphorylation sites, Thr516 in the activation loop and Thr84 in the N-terminal part of the protein, whereas more Ser/Thr sites within the amino acid region 26–84 have also been identified [Alverdi *et al.*, 2008].

PKA α [Bos taurus], PubMed NP_777009

```

1  mgnaaaakkg  seqesvkefl  akakedflkk  wenpaqntah  ldqferikt1  gtgsfgrvml
61  vkhmetgnhy  amkildkqkv  vklkqieht1  nekri1qavn  fpflvk1efs  fkdnsnlymv
121 meyvpggemf  shlr1rigrfs  epharfyaag  ivltfeyl1hs  ldliyr1l1kp  enllidqggy
181 iqvt1dfgfak  rvkg1rtwt1c  gtpeylapei  ilskgynkav  dwwalgvli1y  emaagyp1ff
241 adqpiqiyek  ivsgkvr1fps  hfssdlkdl1  rnllqvdl1tk  rfgnlkngvn  diknhkw1fat
301 tdw1ai1yqrk  veapf1pkfk  gpgdtsnfdd  yeeee1rvsi  nekcgke1fse  f

```

PKG α [Bos taurus], PubMed CAA70155

```

1  mseleedfak  ilmlkeerik  eleklrseke  eeigelkrkl  hkcqsvlpvp  sthigpr1trr
61  aggisae1pqt  yrsfhd1lrqa  frkftk1sers  kdlikea1ild  ndfmkn1els  qi1geivdcm1y
121 pveygk1dsci  ikegdvg1slv  yvmedg1kvev  tkegvkl1ctm  gpgkvf1gela  il1y1nctrtat
181 vktl1vnvklw  aidrqcf1qti  mmrtg1likht  eyme1flk1svp  tfqslp1eeil  skladv1leet
241 hyenge1yiir  qgargd1tffi  isk1gk1v1ntr  eds1p1nedp1vf  lrt1lg1kgdw1f  gekalq1gedv
301 rtanvia1aaea  vtcl1vidrds  fkh1lig1gldd  vsnkay1edae  akaky1eaaea  f1fan1kl1sdf
361 niid1tl1gvvg  fgr1velv1qlk  seeskt1fank  ilkk1rh1vdt  rqqeh1r1sek  qimq1gah1sdf
421 ivrl1yrtfkd  sky1lyml1mea  clggel1wt1il  rdr1gs1fedst  trfyt1ac1vve  afay1l1hskgi
481 iyr1l1kpen1l  ildhrg1yakl  vdfgf1akk1ig  fgkkt1wt1fcg  tpeyv1apei1  l1nkgh1disad
541 ywsl1gilmye  lltgsp1pfsg  pdpmk1ty1nii  lrgid1mie1fp  kkiak1naa1nl  ikk1lcr1dnps
601 erlgn1lkngv  kdiq1khkw1fe  gfnw1egl1rkg  tltpp1i1psv  aspt1dts1nfd  sfped1ndepp
661 pddn1sgwdid  f

```

Figure 3. Comparison of sequences of PKA α and PKG α . The catalytically important regions of PKs are coloured, the catalytic domain of PKG α is gray.

PKGI is expressed in two splice variants, PKGI α and PKGI β that differ only in the 80–100 N-terminal amino acids; however, these structural variations cause substantial alterations of the cGMP binding pattern. While PKGI α comprises a high- and a low-affinity cGMP-binding site (K_D values towards cGMP of 10 nM and 150 nM, respectively) interconnected by the positive cooperativity, PKGI β has two low-affinity binding sites [Landgraf and Hofmann, 1989; Smith J. A. *et al.*, 2000]. Both PKGI splice variants bind cGMP with *ca* 100-fold selectivity over cAMP, as compared to only 50-fold selectivity of PKAr subunits towards cAMP over cGMP [Shabb and Corbin, 1992].

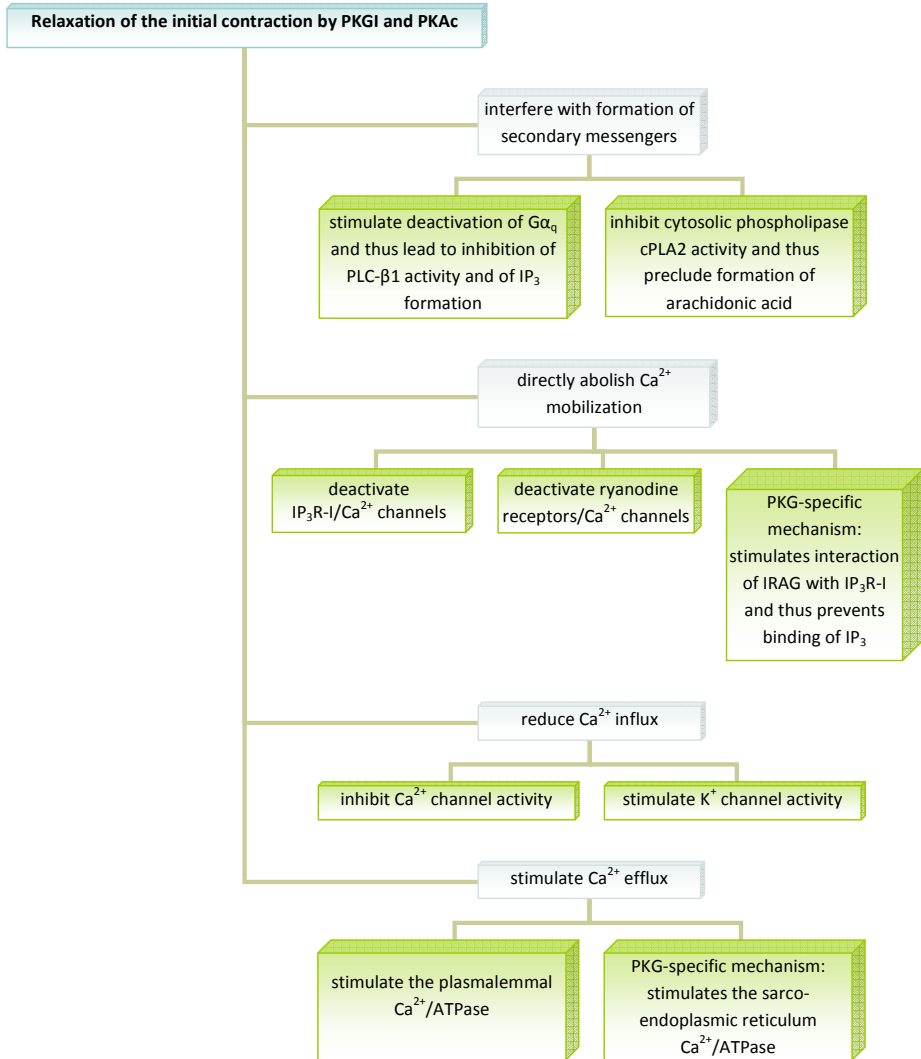
Analogically to cAMP/PKA pathway, the cGMP-PKGI signaling involves several positive and negative feedback loops connected to the production of cGMP from GTP, which might be connected either to the extracellular or to the intracellular event. In the first case, binding of natriuretic peptides to the transmembrane receptors NPRA and NPRB triggers receptor dimerization and induction of the intrinsic guanylyl cyclase (GC) activity, causing rapid increase in the intracellular cGMP concentration [Schultz *et al.*, 1989; Wilson E. M. and Chinkers, 1995]. Importantly, activation of GC activity also requires phosphorylation of NPRA and NPRB prior to the ligand binding, and recent studies have shown that this phosphorylation is catalyzed by PKGI [Airhart *et al.*, 2003]. The second mechanism of cGMP production involves NO-induced activation of the soluble guanylyl cyclase (sGC); dependent on the level of NO production, sGC may function *via* tonic or *via* acute signaling mode, correspondingly resulting in long-lasting low-level cGMP production or in sharp burst of cGMP concentration [Cary *et al.*, 2005].

The main responsibility for the amplitude and duration of the cGMP effect is controlled by the cyclic nucleotide phosphodiesterase PDE5, which selectively transforms cGMP into GMP. Interestingly, cGMP serves not only as a substrate but also as an activator of PDE5 [Rybalkin *et al.*, 2003], whereas the longer-lasting activation of PDE5 is achieved *via* PKGI-catalyzed phosphorylation at Ser92 [Rybalkin *et al.*, 2002]; most likely, the former mechanism is utilized for cleavage of sharp burst of cGMP, whereas the latter is more important for the tonic dissimulation. The quick cleavage of local high gradients of cGMP necessitates co-localization of GCs, PKGI, and PDE5; while in case of cAMP/PKA pathway the co-localization is achieved with the aid of AKAPs, the corresponding putative G-kinase anchoring proteins (GKAPs) have also been recently reported [Wilson L. S. *et al.*, 2008]. Another way for the compartmentalization of PKG signaling is the association of the latter with cGMP-producing NPRA or NPRB [Airhart *et al.*, 2003], or the interaction of PKGI *via* its N-terminal leucine zipper domain with various substrates, including inositol(1,4,5)triphosphate (IP₃) receptor-associated substrate (IRAG) [Desch *et al.*, 2010; Schlossmann *et al.*, 2000]. Interestingly, the latter is also responsible for the prevention of PKGI β (but not PKGI α) translocation to the nucleus in some cell types and suppression of PKGI β transcriptional activity [Casteel *et al.*, 2008].

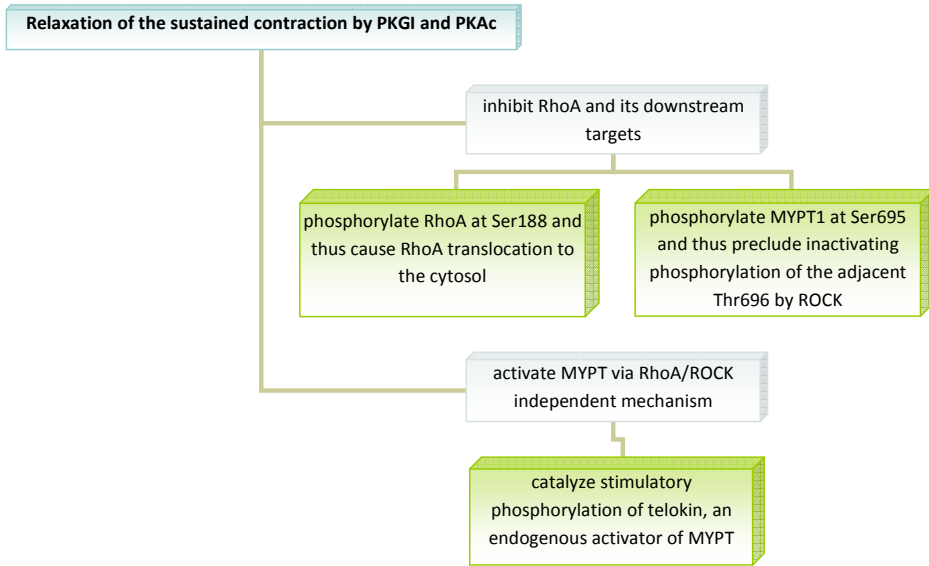
In the organism, PKGI is not as abundant as PKA, and is primarily found in the smooth muscles, platelets, lung, and cerebellum; PKGII, on the other hand prevails in the secretory epithelium of small intestine, juxta-glomerular cells, adrenal cortex, and several brain nuclei [Hofmann *et al.*, 2009]. Despite notable variations in the amino acid composition of the C-terminal fragments ATP-binding cleft and the surrounding loops, both cyclic nucleotide-dependent PKs have preference towards the similar substrate consensus sequences, and in some cases may phosphorylate the same substrates *in vivo* [Kumar and Walsh, 2002; Murthy *et al.*, 2003; Wood J. S. *et al.*, 1996]. One of the most important physiological examples of tight confluence between cGMP/PKGI and cAMP/PKA pathways is represented by the relaxation of vascular smooth muscle tone [Kuroki *et al.*, 2007; Murthy, 2006; Muzaffar *et al.*, 2008; Sanchez *et al.*, 2008].

Smooth muscle contraction requires phosphorylation of Ser19 on the 20 kDa regulatory light chain of myosin II (MLC₂₀); the initial contraction is performed by Ca²⁺/calmodulin-dependent myosin light-chain kinase (MLCK) as a response to increase in concentration of cytosolic Ca²⁺ [Murthy, 2006; Wooldridge *et al.*, 2004]. The mobilization of Ca²⁺ is performed by several pathways, *i.e.*, by IP₃-induced Ca²⁺ release *via* IP₃ receptors (IP₃R-I)/Ca²⁺ channels, or by arachidonic acid- and cyclic ADP ribose-induced Ca²⁺ release *via* ryanodine receptors/Ca²⁺ channels [Murthy, 2006]. As the initial rise of Ca²⁺ concentration is rapidly dissipated and MLCK becomes inactivated, a Ca²⁺-independent protein kinase is required to sustain the phosphorylation state of MLC₂₀. Whereas this protein kinase has not yet been unambiguously identified (although ZIP kinase has been suggested as a candidate), it has been demonstrated that the sustained contraction is upheld by RhoA/Rho kinase (ROCK) pathway that prevents the dephosphorylation of MLC₂₀ by MLC phosphatase (MYPT) [Murthy, 2006; Puetz *et al.*, 2009]. All of the aforementioned pathways may be blocked by the cyclic nucleotide-dependent PKs, which impede the initial contraction (Scheme 1) as well as sustained contraction of smooth muscle (Scheme 2) [Frei *et al.*, 2009; Wooldridge *et al.*, 2004].

Other related functions of PKGI involve cardiac and vascular remodeling; additionally, PKGI mediates anti-aggregatory effect in platelets, regulates several processes in central nervous system, and transcriptional activity in some cellular systems [Hofmann *et al.*, 2009]. PKGII, on the other hand, regulates gastrointestinal secretion, reduces renin secretion in juxta-glomerular cells, and is essential for the bone development [Hofmann *et al.*, 2009].



Scheme 1. Relaxation of the initial (*i.e.*, Ca^{2+} -dependent) contraction by PKGI and PKAc.



Scheme 2. Relaxation of the sustained (*i.e.*, Ca^{2+} -independent) contraction by PKGI and PKAc.

1.2.3. ROCK

A member of the AGC-group triggering physiological responses that often oppose those of cyclic nucleotides is ROCK, the principal mediator of the signaling pathways initiated by members of the Ras homolog gene family of small GTPases (RhoA or RhoE). ROCK has two isoforms, ROCK-I (ROCK β) and ROCK-II (ROCK α) that share 64% net sequence homology and possess a molecular weight of 160 kDa (Figure 4); both isoforms are activated by RhoA, but only ROCK-I may be activated by RhoE [Hahmann and Schroeter, 2010; LoGrasso and Feng, 2009]. In organism, ROCK is ubiquitously expressed, whereas ROCK-I is more prominent in lung, liver, spleen, kidneys, and testes, and ROCK-II expression is elevated in brain and heart [Hahmann and Schroeter, 2010].

ROCK comprises several domains, starting from the N-terminal kinase domain (where isoforms exhibit 89% homology) followed by the coiled-coil domain, Rho-binding (RB) domain, and finally the C-terminal pleckstrin homology (PH) domain split into two halves by an internal cysteine-rich (C1) domain [Jacobs *et al.*, 2006]. The crystallographic studies suggest that ROCK forms a head-to-head homodimer through N-terminal extension [Yamaguchi *et al.*, 2006a; Yamaguchi *et al.*, 2006b], whereas in the inactive state, the RB and the PH-C1 domains of ROCK sequester its N-terminal kinase domain and thus suppress its catalytic activity [Amano *et al.*, 1999].

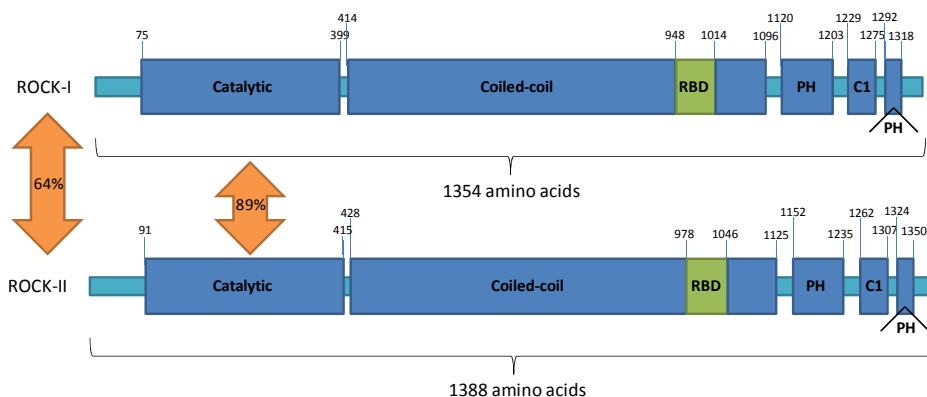


Figure 4. Domains of human ROCK-I and ROCK-II isoforms (adapted from Olson, 2008). Percentage reflects the sequence homology; RBD, Rho-binding domain.

The activation of ROCK does not require (auto)phosphorylation at any site of the kinase, but necessitates recruitment of both RhoA and ROCK to the plasma membrane, which is comprised as a result of a sequence of intracellular events. RhoA is a monomeric G-protein active when bound to GTP and inactive when bound to GDP [Somlyo and Somlyo, 2000]. In a resting state, the inactive form (RhoA-GDP) is stabilized by complexation with guanine nucleotide dissociation inhibitor (GDI); upon activation by guanine nucleotide exchange factors that stimulate GDP to GTP exchange on RhoA, RhoA-GTP dissociates from the complex with GDI and translocates to the plasma membrane [Somlyo and Somlyo, 2000].

The localization of ROCK, on the other hand, is regulated by its PH-C1 domains. Interestingly, the ROCK PH domain lacks the signature phosphoinositide-binding motif found in typical lipid-binding PH domains, and the ROCK C1 domain does not contain the diacylglycerol/phorbol ester binding pocket found in the canonical C1 domains [Wen *et al.*, 2008]. Instead, the folding pattern of ROCK PH-C1 domains exposes the unconventional positively charged surface that is responsible for the attachment of ROCK to the negatively charged membrane bilayers (possibly *via* the recognition of phosphatidylinositol-3,4,5-triphosphates, PtdInsP₃) [Wen *et al.*, 2008].

Binding of RhoA-GTP to ROCK interferes with the interaction of the ROCK N-terminal kinase domain with the C-terminal RB and the PH-C1 domains, resulting in a gain of catalytic activity [Jacobs *et al.*, 2006]. The RhoA/ROCK pathway has been especially thoroughly investigated in the context of regulation of smooth muscle contraction, where it opposes the effect of cAMP/PKA and cGMP/PKG pathways. As pointed out before, ROCK mediates phosphorylation of the regulatory subunit of MYPT1 at Thr696; as a result of this phosphorylation, MYPT1 dissociates from the catalytic subunit of the MLC phosphatase, and the phosphatase activity is reduced [Fukata *et al.*, 2001]. Furthermore, ROCK contributes to the sustained contraction of smooth muscle by catalyzing

phosphorylation of ZIPK, a kinase that enables preservation of the phosphorylated state of MLC₂₀ in the absence of Ca²⁺ [Murthy, 2006].

The down-regulation of MYPT1 and closely related MYPT2 activity by ROCK is also important for the remodeling of actin cytoskeleton inside the cells, as the sustainment of phosphorylated state of MLC₂₀ enables the latter to interact with filamentous actin (F-actin) [Fukata *et al.*, 2001]. An additional mechanism contributing to the ROCK-mediated actin-myosin contractile force generation is ROCK-catalyzed phosphorylation of LIM kinase (LIMK); LIMK in turn phosphorylates the ADF/cofilin family of proteins, and thus blocks their actin-depolymerizing activity [Maekawa *et al.*, 1999]. Other non-muscle cell functions regulated by RhoA/ROCK pathways involve contraction of endothelial cells, aggregation of platelets, neurite retraction, formation of microvilli, membrane ruffling and cell migration, *etc* [LoGrasso and Feng, 2009; Mulder *et al.*, 2004; Nakayama *et al.*, 2005; Olson, 2008; Paul *et al.*, 1999].

1.2.4. PKB

Another PK sharing high percent of sequence homology with PKA and PKG within the catalytic domain is PKB (Akt). PKB is expressed as three isoforms, PKB α (Akt1), PKB β (Akt2), and PKB γ (Akt3), which all possess similar structure, consisting of an N-terminal PH domain, a central catalytic domain, and a small C-terminal regulatory domain [Liu P. *et al.*, 2009; Manning B. D. and Cantley, 2007].

PKB activation relies on a variety of mechanisms Figure 5):

- firstly, activation of PKB (similarly to PKA) is connected with the extracellular event, through the receptor (*i.e.*, insulin receptor, growth factor receptors, GPCRs) \rightarrow phosphoinositide-3-kinase (PI3K) \rightarrow phosphatidylinositol(3,4,5)triphosphate (PtdInsP₃) pathway [Dilly and Rajala, 2008; Shah B. H. *et al.*, 2006];
- secondly, the subcellular localization of PKB is of crucial importance, as its activation is performed at the membrane *via* utilization of PtdInsP₃ (similarly to ROCK, S6K1, p90RSK, and PKC isoforms) [Currie *et al.*, 1999; Liu P. *et al.*, 2009];
- thirdly, PKB serves as an example of phosphorylation cascade, as PKB is a substrate protein for another kinase, 3-phosphoinositide-dependent protein kinase 1 (PDK1) [Calleja *et al.*, 2007];
- finally, full activation of PKB involves phosphorylation by mammalian target of rapamycin (mTOR), which is in turn one of the downstream targets of PKB itself [Facchinetti *et al.*, 2008; Sarbassov *et al.*, 2005; Toker, 2008].

The intracellular analyses proved the existence of a cytosolic pre-activation complex with PKB bound to PDK1, whereas the intramolecular interactions between the PH domain and the catalytic domain of PKB cause the absence of catalytic activity of the latter [Calleja *et al.*, 2007]. Binding of PtdInsP₃ to PDK1 and to the PH domain of PKB leads to the recruitment of PDK1-PKB

complex to the cell membrane, and induces a conformational change that relieves the autoinhibition within PKB molecule [Calleja *et al.*, 2007]. The activation loop of the PKB catalytic domain released from the intramolecular interaction becomes accessible for phosphorylation at Thr308 (PKB α numbering) catalyzed by PDK1, whereas it has been demonstrated that the interaction of PDK1 with PtdInsP3 enhances the rate at which PDK1 activates PKB [Currie *et al.*, 1999].

Importantly, the phosphorylated PKB may dissociate from the membrane and retain its active conformation when functioning in cytosol; still, the full activation requires another phosphorylation at Ser473 (PKB α numbering) in the hydrophobic motif of the C-terminal tail [Sarbasov *et al.*, 2005]. The exact role of this phosphorylation has not been resolved yet, and it has been even proposed that phosphorylation at Ser473 precedes the phosphorylation at Thr308 and contributes to the recognition of PKB by PDK1 [Sarbasov *et al.*, 2005]. The PK catalyzing phosphorylation at Ser473 has not been unequivocally identified, and a number of candidates have been proposed including PKC isoform $\beta 2$, DNA-dependent protein kinase, and PKB itself; however, most studies have pointed out the importance of mTOR complex 2 (mTORC2) in this process [Liu P. *et al.*, 2009]. mTORC2 consists of mTOR bound to the rapamycin-insensitive companion of mTOR (riCTOR) and several other mTOR-interacting proteins; according to the *in vitro* studies, mTORC2 directly phosphorylates PKB on Ser473 and also facilitates Thr308 phosphorylation by PDK1 [Sarbasov *et al.*, 2005; Toker, 2008]. It has also been suggested that mTORC2 is responsible for the phosphorylation of PKB at its turn motif (Thr450 in PKB α). This phosphorylation occurs probably during or shortly after the synthesis of PKB, and is required for the facilitation of carboxyl-terminal folding and for the stabilization of the newly synthesized PKB by interactions of phosphorylated Thr450 with the conserved basic residues in the kinase domain [Facchinetti *et al.*, 2008].

PKB itself has a colossal amount of protein substrates, whereas the first PKB target identified in cells was glycogen synthase kinase 3 (GSK3) [Cross *et al.*, 1995]. PKB phosphorylates GSK3 at a highly conserved N-terminal Ser residue (Ser21 in GSK3 α , Ser9 in GSK3 β), and this phosphorylation triggers inactivation of GSK3 resulting in stimulation of glycogen synthesis, promotion of lipid production, and in loss of GSK3 proapoptotic function [Frame and Cohen, 2001; Manning B. D. and Cantley, 2007; Yang J. *et al.*, 2002]. Recent data, however, suggests that in the absence of PKB, GSK3 may also be phosphorylated at the same Ser by other representatives of the AGC-group, *i.e.* ribosomal protein S6 kinase $\beta 1$ (S6K1), PKAc, or the most downstream kinase of the classical mitogen-activated protein kinase (MAPK) cascade called MAPK-activated protein kinase-1 (MAPKAP-K1 or RSK) [Frame and Cohen, 2001; Zhang H. H. *et al.*, 2006].

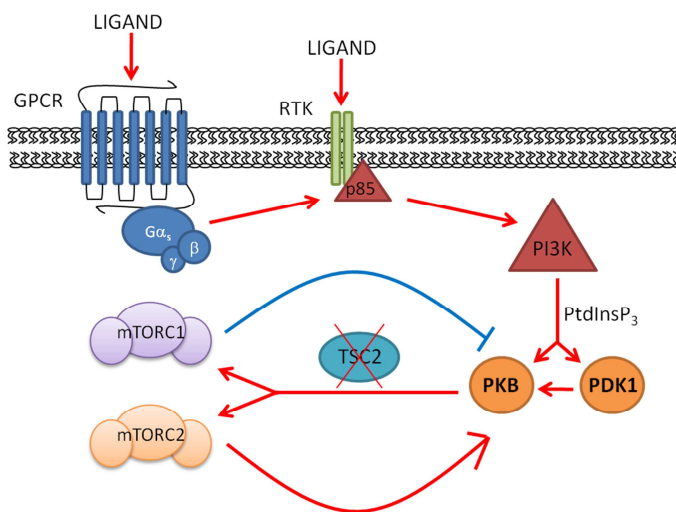


Figure 5. General scheme of PKB activation and feedback loops. RTK, receptor tyrosine kinase; p85, the regulatory subunit of PI3K.

PKB is also a principal upstream regulator of crucial intracellular processes responsible for cell survival, growth, proliferation, angiogenesis, metabolism, and probably cell migration and invasion [Manning B. D. and Cantley, 2007]. Interestingly, the PKB-catalyzed phosphorylation often serves for ‘switching off’ the functioning of its downstream targets; for example, the PKB-catalyzed phosphorylation of tuberous sclerosis 2 protein (TSC2), a component of the TSC1-TSC2 complex, inhibits the GTPase-activating protein function of TSC1-TSC2 and thus stimulates the GTP-loading of RheB, which in turn potently activates mTOR [Toker, 2008]. In this way, PKB attenuates the inhibitory effects of the TSC1-TSC2 complex on the mTOR complexes mTORC1 and mTORC2, and thus creates two important feedback loops, as mTORC2 acts as PKB activator (positive feedback), while mTORC1 has been demonstrated to inhibit PKB (negative feedback) [Huang J. and Manning, 2009].

1.3. PKs in disease

While the normal functioning of PKs is essential for the sustenance of life of an organism, the errors at DNA-level (*i.e.*, mutations of PK-encoding genes) or faults of PK expression, activation or feedback loops are connected to a variety of diseases [Chico *et al.*, 2009; Knight *et al.*, 2010; Manning B. D. and Cantley, 2007]. Probably the most explored group of diseases that are caused by deregulation of PKs is cancer. Within last decades, PKs and their direct activators

have evolved as the most frequently mutated oncogenes and tumor suppressors, thus representing the major path of signaling by which cancer cells evade normal physiological constraints on growth and survival [Zhang J. *et al.*, 2009]. Moreover, some PKs expressed in tumor or in the surrounding tissues contribute to disease progression as a result of their normal functioning by enabling tumor to acquire possibilities for angiogenesis and metastases [Knight *et al.*, 2010]. Whereas the identification of PKs contributing to tumor development and/or survival is a continuous process aided by the development of RNA-interference techniques and performance of large-scale forward and reverse genetic screens, the currently well-known examples of oncogenic PKs involve the following kinases [García-Echeverría *et al.*, 2000; Keri *et al.*, 2006; Knight *et al.*, 2010; Zhang J. *et al.*, 2009]:

- receptor tyrosine kinases – *i.e.*, BCR-Abl in chronic myeloid leukaemia, EGFR in lung, head, neck, pancreatic and colorectal cancers, HER2 in breast cancer, VEGFR-2 in ovarian and kidney cancers, and PDGFR in a variety of tumors;
- STE kinases, MAPK pathway PKs – *i.e.*, BRAF, MEK1 and MEK2 in ovarian and colorectal cancers;
- PI3K pathway PKs (including AGC-group) – *i.e.*, PKB in a variety of tumors.

The consequences of PK malfunctioning are also tightly connected with another large group of diseases – central nervous system (CNS) disorders [Chico *et al.*, 2009], although unveiling the role of PK in the CNS has been largely obstructed by the specific properties of the tissue itself (*i.e.*, existence of blood-brain-barrier). Interestingly, in case of CNS disorders the major 'culprits' are not represented by Tyr-kinases (as in case of cancers) but by Ser/Thr kinases from different groups [Chico *et al.*, 2009; Keri *et al.*, 2006; Virdee *et al.*, 2007]:

- CMGC-group – *i.e.*, GSK3 involved in a vast spectrum of disorders involving Alzheimer's and Parkinson's diseases, depression, HIV-associated dementia, traumatic brain injury, *etc.*;
- STE-group – *i.e.*, MAPK in Alzheimer's and Parkinson's diseases, cerebral ischaemia, spinal cord and traumatic brain injuries, *etc.*;
- AGC-group – *i.e.*, PKC and ROCK, both in Alzheimer's disease, cerebral ischaemia and vasospasm, and additionally, ROCK in multiple sclerosis and epilepsy;
- CAMK-group – *i.e.*, DAPK in acute brain injury and Alzheimer's disease.

The increased activity of a PK in the diseased tissue is in several cases accompanied by the increase of the concentration of the same PK in peripheral tissues, *i.e.*, body fluids. For instance, elevated levels of extracellular PKAc (ECPKA) and ECPKA autoantibodies have been detected in blood serum samples of patients with different malignant tumors (especially prostate, bladder, breast, and colon cancers) [Nesterova *et al.*, 2006]. Moreover, the valueability of ECPKA as a biomarker is not limited with diagnosis of cancer, but also allows monitoring and prognosis, as the good correlation between concentration of ECPKA and stage of disease or success of anti-cancer therapy has

been demonstrated in recent tests [Wang H. *et al.*, 2007]. Another PK suggested as a biomarker for cancers (*i.e.*, melanoma) according to the studies of xenograft mouse models is PKC α [Kang *et al.*, 2009]; moreover, the latter may also serve as a biomarker for Alzheimers disease, in parallel with other PKC isozymes [Barry *et al.*, 2010].

The examples mentioned above clearly illustrate that PKs belong to both, disease-associated and disease-modifying category of proteins, this fact rendering substantial interest in PKs as potential biological targets for pharmaceutical industry. Importantly, in order to be classified as a therapeutic target, a protein should also be termed ‘druggable’, *i.e.* it should possess a well-defined binding site capable of development of multiple strong and specific interactions with a small drug molecule [Hopkins and Groom, 2002]. PKs fulfill the druggability requirement by virtue of incorporation of at least one suitable site represented by the ATP-binding site, and therefore belong to ca 3000 therapeutic targets that comprise the ‘human druggable genome’ (which also includes GPCRs, nuclear hormone receptors, ion channels, metallopeptidases, proteases, PDEs, *etc*) [Hajduk *et al.*, 2005]. On the other hand, it should be kept in mind that therapeutic targets might also be represented by bacterial, viral, fungal or parasitic enzymes (as in case of malarial PKs) [Doerig *et al.*, 2010].

According to the currently reported state-of-the-art, there are only ca 330 targets that bind approved drugs, 270 encoded by the human genome and 60 belonging to pathogenic organisms; therefore, a vast majority of putative therapeutic targets remains to be explored [Landry and Gies, 2008]. In case of PKs, the difficulties for drug development rise not only due to the intrinsic complexity of PK signaling, but also due to the susceptibility of several therapeutically important PKs to mutations that trigger resistance towards drug candidates designed to interfere with the non-mutated target [Krishnamurty and Maly, 2010]. It is therefore evident that the discovery of novel compounds able to interact with and suppress the activity of the disease-modifying PKs remains of utmost importance. Consequently, there is also a strong requirement for methods enabling assessment of PK inhibitors, exploration of PK structure, functions and regulation mechanisms, and determination of protein kinase activity (*i.e.*, for PKs serving as biomarkers).

2. Protein kinase inhibitors

2.1. General features

Within the last 10 years, the development of PK inhibitors as potential drug candidates has become the major goal of pharmaceutical industry, with 1871 currently undergoing or completed clinical studies considering inhibition of PKs [Cohen P., 2010; Fedorov *et al.*, 2010; NIH Clinical Trials Homepage]. Furthermore, the field of application of PK inhibitors is not limited with pharmacy only. PK inhibitors may serve as valuable „devices“ for studying signaling of PKs and other up- and downstream cellular systems connected to PK activation and catalysis (*i.e.*, GPCRs, transcription factors) *in vivo* and in living cells/tissues, but also for *in vitro* biochemical assays aiming at surveillance of PK functioning and its modulation in simplified systems.

Dependent on the presumptive field of application, the development of PK inhibitors may focus attention on the achievement and improvement of different properties of the compounds. In 1997, Lipinski formulated a set of physico-chemical parameter ranges (often referred to as “Rule-of-Five”, ROF; Tabel 2) that were associated with 90% of orally active drugs that achieved phase II status [Lipinski *et al.*, 1997]. Basically, ROF and its further extensions state characteristics that should be fulfilled for the compounds that are under development as oral drugs, in order to reduce the number of compounds entering the clinical trials by exclusion of the “unsuitable” candidates already at the stage of design and preliminary selection.

Table 2. Rule-of-Five and its extensions

„Rule-of-Five“ ^a	Extensions
<ul style="list-style-type: none"> • Molecular weight ≤ 500 • $\log P \leq 5$ • Number of H-bond donors ≤ 5 • Number of H-bond acceptors ≤ 10 	<ul style="list-style-type: none"> • Polar surface area $\leq 140 \text{ \AA}^2$ <ul style="list-style-type: none"> ○ or sum of H-bond donors and acceptors ≤ 12 • Number of rotatable bonds ≤ 10

^a No more than one violation is allowed; $\log P$, octanol-water partition coefficient.

Despite the wide popularity of ROF criteria, it should be kept in mind that ROF applies only for orally administered compounds absorbed by passive mechanisms, and is hence not valid for immunotherapeutic vaccines, antisense technologies, and other novel biologic therapies [Grant, 2009; Keller *et al.*, 2006]. Moreover, several exceptions to ROF have been reported, *i.e.*, those represented by natural compounds [Clardy and Walsh, 2004]. Last but not least, a compound fulfilling the ROF criteria is not automatically an efficient drug, as ROF criteria do not take most of the issues of pharmacokinetics (*i.e.*, bioavailability, generation and excretion of metabolites, *etc*) and pharmacodynamics (*i.e.*, drug affinity and selectivity, therapeutic window, drug cytotoxicity and toxicity of metabolites, *etc*) into consideration [Chico *et al.*, 2009].

2.2. Characteristics and general principles of design of PK inhibitors

2.2.1. Affinity and inhibitory potency

Several of the previously mentioned properties of inhibitors cannot be reliably predicted at the initial stages of development, and sometimes are also not of major concern for PK inhibitors developed for biochemical assays *in vitro*; still, the high affinity (and high inhibitory potency) of an inhibitor towards its biological target is a primary goal for nearly all applications.

The affinity of a reversible ligand (*i.e.*, inhibitor, substrate, co-factor, *etc.*) towards an enzyme may mathematically be expressed as the equilibrium dissociation constant (K_D) of the complex consisting of the enzyme and the ligand (Equation 1A, 1B). Low dissociation constant value² means low susceptibility of the complex for dissociation and hence good affinity of the ligand towards the given enzyme.

$$K_D = \frac{[E][L]}{[EL]}$$

A

$$K_D = \frac{(E_t - [EL])(L_t - [EL])}{[EL]}$$

B

Equation 1. (A) K_D , dissociation constant of the enzyme-ligand complex; $[E]$, equilibrium concentration of free enzyme; $[L]$, equilibrium concentration of free ligand; $[EL]$, equilibrium concentration of the enzyme-ligand complex. (B) E_t , total concentration of enzyme; L_t , total concentration of ligand.

According to the basic principles of thermodynamics, an equilibrium constant of a reaction is related to the change of standard free energy of the reaction according to (Equation 2A). As association reaction (*i.e.*, binding of ligand) is the reverse process of the dissociation reaction, the relationship between the change of standard free energy of ligand binding (ΔG_B^0) and the equilibrium constant of the dissociation reaction (K_D) is expressed according to Equation 2B.

The change of standard free energy of binding (ΔG_B^0) is a sum of enthalpic and entropic terms (Equation 2C). Like any other spontaneous process, the binding of ligand to the enzyme takes place only in case of negative free energy of binding; therefore, the lower ΔH_B^0 and the higher ΔS_B^0 , the more negative is

² In biochemistry, all constants are by convention expressed as dissociation constants, and differently from physical chemistry not divided by standard concentration C_0 (1 mol/L); therefore, according Equation 1, biochemical constants usually possess a dimension [mol/L]. However, for mathematical equations containing logarithms of constants (*i.e.*, Equation 2), the division of corresponding constant by standard concentration is by default performed, and the dimensionless constant is then subjected to logarithm transformation.

ΔG_B^0 for the given reaction and the higher is the affinity of the inhibitor towards the given enzyme.

$$\Delta G^0 = -RT \ln K$$

$$\Delta G_B^0 = RT \ln K_D$$

$$\Delta G_B^0 = \Delta H_B^0 - T\Delta S_B^0$$

A

B

C

Equation 2. (A) ΔG^0 , change of standard free energy of a reaction; R, universal gas constant; T, absolute temperature; K, equilibrium constant of the reaction. (B) ΔG_B^0 , change of standard free energy of binding. (C) ΔH_B^0 , change of standard enthalpy of binding; ΔS_B^0 , change of standard entropy of binding.

While ΔH_B^0 decreases with an increasing number of favorable interactions in the system consisting of an inhibitor, an enzyme, and solvent, the increasing value of ΔS_B^0 reflects the rising amount of degrees of freedom. It is therefore evident that in several cases, enthalpic and entropic terms of inhibitor binding can compensate each other (*i.e.*, strong interactions between inhibitor and enzyme associated with low ΔH_B^0 cause ordering of both enzyme and inhibitor molecules and thus low ΔS_B^0), resulting in zero ΔG_B^0 and extremely low affinity of the inhibitor [Bissantz *et al.*, 2010]. Still, in other cases one of the ΔG_B^0 components may strongly outweigh another, triggering fully enthalpy- or fully entropy-driven binding.

While the affinity of a PK-targeted compound reflects the ability of the latter to bind to its target, the inhibitory potency characterizes its ability to block the phosphorylation reaction catalyzed by the PK of interest and thus cause reduction of the speed of formation of the phosphorylated product. According to the Michaelis-Menten kinetics [Segel, 1993], the initial velocity v_0 of one-substrate reaction (Scheme 3) reflects the change in concentration of reaction product in time (Equation 3A). The initial velocity might be expressed as Equation 3B, whereas the concentration of free enzyme $[E]$ is expressed as Equation 3C and an additional criterion $[S] \gg E_t$ is fulfilled, hence the reaction occurs at quasi-steady-state conditions ($[ES] = const$).



Scheme 3. Mono-substrate enzymatic reaction with formation of one product.

$$v_0 = \frac{d[P]}{dt} \quad v_0 = \frac{k_2 \cdot E_t \cdot [S]}{[S] + \frac{k_{-1} + k_2}{k_1}} \quad [E] = E_t - [ES]$$

A

B

C

Equation 3. (A) v_0 , initial velocity; $[P]$, concentration of product; t , time. (B) $[S]$, concentration of substrate. (C) $[E]$, concentration of free enzyme; $[ES]$, concentration of the enzyme-substrate complex.

The member $k_2 \cdot E_t$ is usually designated as the maximal velocity of an enzyme-catalyzed reaction (v_{max}); in order to compare different enzymatic reactions, the term turnover number is introduced, reflecting maximal catalytic activity of an enzyme. Turnover number is equal to the number of substrate molecules converted into product by enzyme per unit of time when the enzyme is fully saturated with substrate (Equation 4A); for different enzymes, k_{cat} may generally range from 1 s^{-1} to 10000 s^{-1} [Nelson *et al.*, 2000]. The member $(k_{-1} + k_2)/k_1$ in Equation 3B is termed Michaelis constant (K_m); mathematically, the K_m value is equal to the concentration of substrate enabling achievement of half of the maximal velocity of the reaction. Given the fact that several enzymatic reactions may occur at physiological conditions where $[S] \ll K_m$, the Equation 3B might be rewritten as Equation 4B; hence, the reaction resembles the bi-molecular reaction with pseudo-second order rate constant k_2/K_m . In case of most efficient enzymes, the value of the latter ratio is close to the diffusion limit (in the range of $10^9 \text{ M}^{-1} \text{ s}^{-1}$) [Nelson *et al.*, 2000].

$$k_{cat} = \frac{v_{max}}{E_t} \quad v_0 = \frac{k_2}{K_m} \cdot E_t \cdot [S]$$

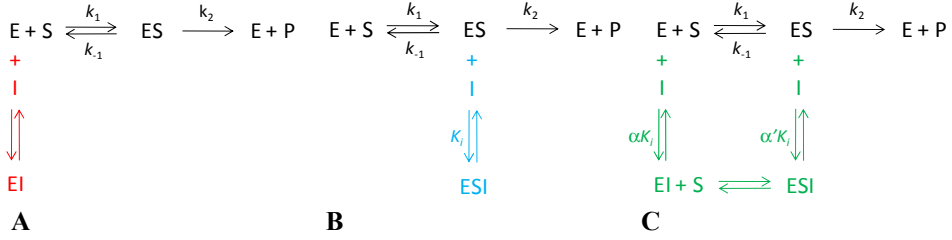
A

B

Equation 4. (A) k_{cat} , turnover number; v_{max} , maximum velocity. (B) K_m , Michaelis-Menten constant.

The inhibition of one-substrate reaction may be realized *via* several ways, including competitive, uncompetitive, and mixed mechanism of inhibition *versus* the substrate (Scheme 4), whereas the equation for inhibition constant K_i is dependent on the inhibition mechanism; only in case of competitive inhibition, the K_i may be expressed analogically to K_D [Segel, 1993]. The initial velocity of an inhibited reaction (v_0^{inh}) is correspondingly be expressed as Equation 5A, Equation 5B, or Equation 5C (in case if both $[S]$ and $[I]$ are remarkably larger than E_t). The comparison of the latter Equations with Equation 3B shows that in case of competitive inhibition, v_{max} is kept constant but the K_m value of the substrate is changed (the concentration of the substrate enabling

achievement of half of v_{max} at a fixed concentration of inhibitor is termed K_m^{app} , Equation 6A). In case of uncompetitive inhibition, both K_m and v_{max} are different from the non-inhibited reaction Equation 7A and 7B; the maximum velocity of the inhibited reaction at a fixed concentration of inhibitor is termed v_{max}^{app} . Both parameters are changed also in case of mixed inhibition (Equation 8A and 8B); however, if α equals to α' , the inhibition mechanism is termed non-competitive and only v_{max} is changed as compared to the non-inhibited reaction [Segel, 1993].



Scheme 4. Mechanisms of inhibition of a one-substrate reaction. (A) Competitive inhibition. (B) Uncompetitive inhibition. (C) Non-competitive inhibition.

$$v_0^{Inh} = \frac{v_{max} \cdot [S]}{[S] + K_m^{app}}$$

A

$$v_0^{Inh} = \frac{v_{max}^{app} \cdot [S]}{[S] + K_m^{app}}$$

B

$$v_0^{Inh} = \frac{v_{max}^{app} \cdot [S]}{[S] + K_m^{app}}$$

C

Equation 5. The initial velocities of the inhibited reactions. (A) Competitive inhibition; K_m^{app} , apparent Michaelis-Menten constant. (B) Uncompetitive inhibition; v_{max}^{app} , apparent maximum velocity. (C) Mixed inhibition.

$$K_m^{app} = K_m \cdot \left(1 + \frac{[I]}{K_i}\right)$$

A

$$\log\left(\frac{K_m^{app}}{K_m} - 1\right) = \log[I] - \log K_i$$

B

Equation 6. Parameters of the competitive inhibition. $[I]$, concentration of an inhibitor; K_i , inhibition constant.

$$K_m^{app} = \frac{K_m}{\left(1 + \frac{[I]}{K_i}\right)}$$

A

$$v_{max}^{app} = \frac{v_{max}}{\left(1 + \frac{[I]}{K_i}\right)}$$

B

Equation 7. Parameters of the uncompetitive inhibition.

$$K_m^{app} = \frac{K_m \cdot (1 + \frac{[I]}{\alpha K_i})}{(1 + \frac{[I]}{\alpha' K_i})} \quad v_{max}^{app} = \frac{v_{max}}{(1 + \frac{[I]}{\alpha' K_i})}$$

A

B

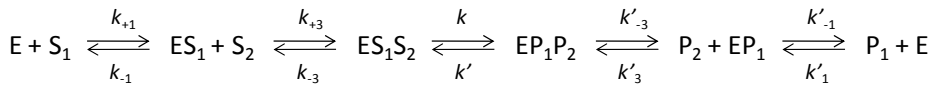
Equation 8. Parameters of the mixed inhibition.

In experiments where the detailed mechanism of inhibition is not of primary interest, it is convenient to introduce a quantity that reflects the potency of an inhibitor at the given assay conditions. The most popular of such quantities is IC_{50} , which is mathematically equal to the concentration of an inhibitor that causes 50% reduction of the reaction velocity as compared to that of non-inhibited reaction (*i.e.*, if $[I] = IC_{50}$, then $v_0^{inh} = 0.5 v_0$) [Segel, 1993]. In case of competitive inhibition, the IC_{50} value may be re-calculated to obtain K_i value according to the Cheng-Prusoff equation (Equation 9); however, it should be kept in mind that the latter is valid only in the assay conditions presupposed by Michaelis-Menten kinetics (*i.e.*, if $[S] \gg E_t$ and $[I] \gg E_t$) [Cheng Y. and Prusoff, 1973].

$$K_i = \frac{IC_{50}}{1 + \frac{[S]}{K_m}}$$

Equation 9. Cheng-Prusoff equation.

In case of bisubstrate reactions (as in case of PKs, where ATP is a co-substrate and the phosphorylatable protein/peptide serves as a substrate), the reaction scheme is substantially more complicated. Studies with PKAc have shown that the preferred order of substrate binding is ATP-first [Kong and Cook, 1988; Lew *et al.*, 1997b], and that the rate-limiting step of the reaction is generally not the phosphoryl transfer, but the dissociation of the co-product ADP (or the conformational change of PK associated with this dissociation) [Lew *et al.*, 1997b; Zhou J. and Adams, 1997]. The latter fact was also confirmed in studies with ROCK [Futer *et al.*, 2006]. Hence, the simplified reaction pathway may be depicted as Scheme 5, and the general expression for the reciprocal initial velocity of the reaction is then given as Equation 10, whereas the members φ_0 , φ_1 , φ_2 , and φ_{12} are calculated according to Equation 11A, 11B, 11C, and 11D, respectively [Dalziel and Dickinson, 1966].



Scheme 5. Bisubstrate enzymatic reaction with formation of two products and ordered mechanism of substrate binding and product dissociation.

$$\frac{1}{v_0} = \frac{1}{E_t} \left(\varphi_0 + \frac{\varphi_1}{[S_1]} + \frac{\varphi_2}{[S_2]} + \frac{\varphi_{12}}{[S_1][S_2]} \right)$$

Equation 10. The reciprocal initial velocity of the bisubstrate reaction corresponding to Scheme 5; $[S_1]$ and $[S_2]$ are the concentrations of substrates.

<p>A</p> $\varphi_0 = \frac{1}{k'_{-1}} + \frac{1}{k'_{-3}} + \frac{1}{k} \left(1 + \frac{k'}{k'_{-3}} \right)$	<p>B</p> $\varphi_1 = \frac{1}{k_{+1}}$
<p>C</p> $\varphi_2 = \frac{\left(1 + \frac{k'}{k'_{-3}} \right) k_{-3} + k}{kk_{+3}}$	<p>D</p> $\varphi_{12} = \frac{k_{-1} \left[\left(1 + \frac{k'}{k'_{-3}} \right) k_{-3} + k \right]}{k_{+1}kk_{+3}}$

Equation 11. Parameters of the constants from Equation 10.

Consequently, inhibition of the bisubstrate reaction can also occur *via* several routes, and it is substantially more convenient to use the IC_{50} value instead of calculating the true inhibition constant values by resolving complicated models of inhibition. Still, in case if the inhibition mechanism *versus* ATP or *versus* protein/peptide substrate is of primary interest, it is frequently established by fixation of concentration of a (co-)substrate, and measurement of the rate of the PK-catalyzed reaction at varied concentration of the other (co-)substrate [Segel, 1993]. The latter curve is then repeated at several fixed concentrations of an inhibitor, and the relative shift of the inhibited curves as compared to the non-inhibited curve (*i.e.*, the increase of K_m^{app} of the varied (co-)substrate at the growing concentration of the inhibitor) can be used to determine the inhibition mechanism. The true inhibition constant K_i of the inhibitor is then calculated from a double logarithmic Schild plot (for competitive inhibitors, see Equation 6B), or from the IC_{50} of the inhibitor according to the Cheng-Prusoff equation in case if competitive inhibition mechanism is established *versus* the (co-)substrate [Segel, 1993].

2.2.2. Rational design of PK inhibitors

The structure-aided development of PK inhibitors aims at pinpointing the crucial interactions between an inhibitor and a PK that need to be satisfied to achieve high efficiency of inhibitor binding, while being aware of flexibility of both inhibitor and PK molecules and the role of desolvation effects during inhibitor binding [Pratt *et al.*, 2004]. This goal is achieved by implementation of wealth of structural data considering PKs and their complexes resolved by crystallographic studies, NMR, *in silico* analysis and homology modeling, *etc.*

Probably the most important specific interactions for biomolecular recognition processes are hydrogen bonds, including strong “classical” H-bonds (*i.e.*, NH or OH as a donor and C=O as an acceptor) and weak H-bonds (*i.e.*, CH as a donor and C=O as an acceptor, or NH as a donor and π -system as an acceptor) [Bissantz *et al.*, 2010]. The bond distances and angular preferences of H-bonds follow strict rules, and apart from the nature of atoms forming the bond and from geometric parameters, the strength of a hydrogen bond is dependent on the neighboring atoms (*i.e.*, in some systems H-bonds with suboptimal geometries might be stabilized by flanking partners) [Bissantz *et al.*, 2010]. However, as formation of strong H-bond also implies high desolvation costs for both the donor and the acceptor, the net free energy gain may be minimal; hence, the molecular design of inhibitors should primarily aim at identification of H-bond donors and acceptors in the enzyme that are positioned in the clefts with decreased solvent accessibility.

The charge-assisted H-bonds (salt-bridges) between an inhibitor and a kinase should yield stronger interactions than those provided by neutral hydrogen bonds by virtue of the coulombic force component. However, in case of solvent-exposed salt-bridges, little gain in net free energy may be expected, as the free energy of salt-bridge formation has to exceed the solvation free energies of both, donor and the acceptor, which are initially strongly hydrated [Luo R. *et al.*, 1999]. Still, (partially) buried charged protein residues represent the extremely important spots for the structure-aided inhibitor design.

Several studies have demonstrated that the structural parameter of an inhibitor correlating best with its affinity towards an enzyme is the area of hydrophobic surface of the inhibitor buried upon binding to the enzyme [Engh and Bossemeyer, 2002; Vallone *et al.*, 1998]. The magnitude of this hydrophobic effect may be up to $125 \text{ J}/(\text{mol} \cdot \text{\AA}^2)$, with particularly large gains in binding energy obtained in cases where a non-polar ligand optimally occupies a hydrophobic narrow and poorly solvated pocket of protein [Southall *et al.*, 2002]. A separate group of hydrophobic interactions is represented by aryl-aryl interactions, where side-chains of aromatic amino acids of an enzyme form edge-to-face (T-shaped) or face-to-face (parallel) π - π interactions with aromatic fragments of an inhibitor; aryl-aryl interactions may additionally profit from charge transfer, if formed between an electron-rich and an electron-poor substituted aromatic system [Bissantz *et al.*, 2010]. Importantly, the majority of hydrophobic interactions between an enzyme and an inhibitor should also be entropically favorable. The presence of a hydrophobic solute causes ordering of surrounding water molecules, whereas the association of two hydrophobic solutes results in formation of water “cage” with smaller ordered surface area than the sum of ordered surface areas of “cages” for initial solutes [Bissantz *et al.*, 2010].

The structure-aided design of inhibitors represents one of two branches of a general strategy termed rational design. The other branch of this strategy is ligand-based design (or analogue-design [Zhang J. *et al.*, 2009]), taking advantage of published lead compounds (the “templates”, or “privileged structures”

[Keri *et al.*, 2006]) and selected features of catalytic cores of enzymes. Historically, several inhibitors with moderate to high affinity towards PKs have also been discovered as a result of screening of large collections of random compound (libraries) with intention to test a vast variety of different structures independently on their binding mode or mechanism [Lam *et al.*, 2003]. However, this approach has now mostly been claimed ineffective due to large overhead costs and relatively low outcome; instead, the design of focused libraries has become popular, consisting of compounds derived from scaffolds of well-known potent inhibitors and targeted to certain sites of enzyme known to ensure development of strong interactions (*i.e.*, ATP-binding site of PKs). Recently, several publications have emerged reporting successful combination of the ligand-based and the structure-aided design of PK inhibitors, especially in cases where computational approaches were used during the initial steps of inhibitor development [Fischer J. R. *et al.*, 2010; Fujiwara *et al.*, 2010; Tal-Gan *et al.*, 2010; Xu, *et al.*, 2009].

2.2.3. Selectivity issues

Apart from affinity, another characteristic that may be “tuned” with the aid of rational design of PK inhibitors is selectivity. Generally, selectivity of an inhibitor towards its target might be enhanced by two approaches:

- introduction of fragments that develop interactions with non-conserved or mutated residues in the catalytic core of a kinase (including cases where inhibitor sterically interferes with or disrupts interactions between such residues in non-target PKs; Figure 6A–B),
- or development of compounds that recognize the inactive state of a kinase (Figure 6B–D) [Grant, 2009; Morphy, 2010].

Additionally, targeting allosteric pockets characteristic of a target kinase only or also very closely related PKs yields compounds with a very narrow recognition profile (high selectivity), although such allosteric modulators are mostly discovered by chance and not designed rationally [Bogoyevitch and Fairlie, 2007].

The required degree of selectivity for a PK inhibitor is certainly dependent on its application. For instance, if the inhibitor under development will be used as a generic probe in assays for the screening of other inhibitors, or as an affinity support for the pull-down assays analyzing content of PK in various tissues, selectivity within the family of PKs would even be considered as disadvantage. Applications such as determination of certain kinomic biomarkers in tissues or use of inhibitor as a physiological modulator, on the other hand, traditionally require compounds with very high degree of selectivity not only within members of PK family but sometimes even within different isoforms of one PK [Hahmann and Schroeter, 2010].

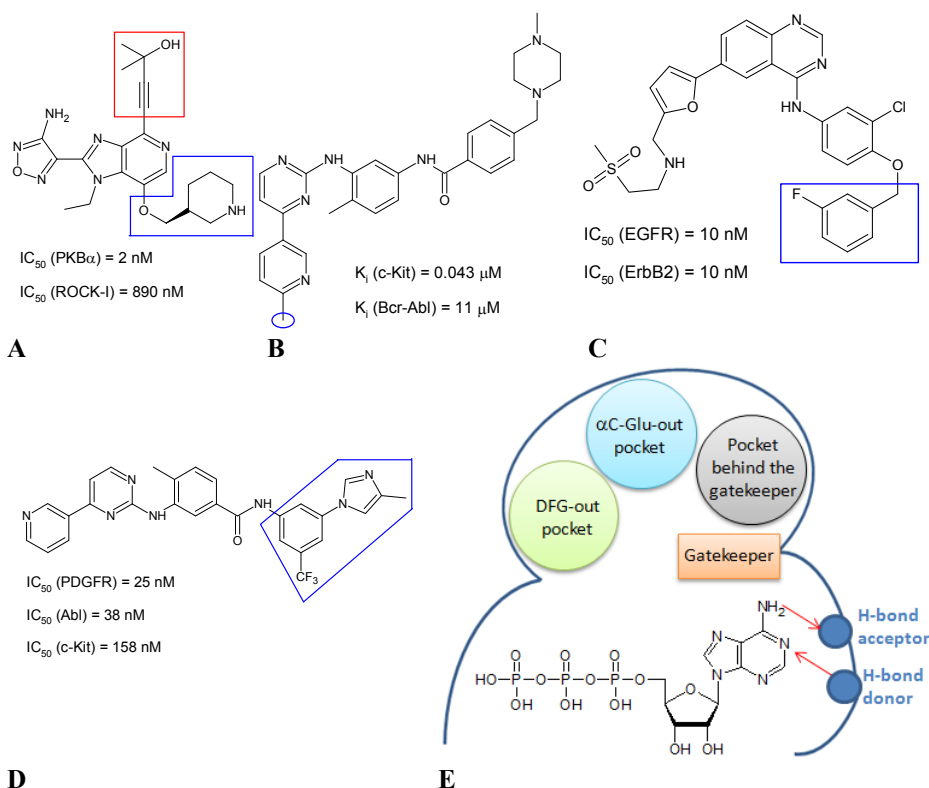


Figure 6. Inhibitors with enhanced selectivity. (A) GSK690693, targeting non-conserved residues of PKB isoforms: while red substituent at position 7 forms hydrogen bond with the side-chain of the conserved Glu236 and just enhances affinity, the blue substituent at position 4 targets the narrow back-pocket lined by Leu204 of PKB [Heerding *et al.*, 2008]. (B) Methylated imatinib (Gleevec), targeting c-Kit: the blue methyl group displaces water from the dehydron C673-G676 (a unique wrapping defect in soluble proteins where backbone hydrogen bonds in are partially exposed to water due to an insufficient number of neighboring nonpolar side-chain groups) [Zhang X. *et al.*, 2008]. (C) Lapatinib (Tykerb) targeting HER2 and EGFR: the blue fluoro-benzyloxy group improves the selectivity for HER2 and maintains affinity for EGFR; additionally, the inhibitor utilizes the “ α C-Glu-out” state of kinases, where rotation and outward shift of the C-helix opens up an additional pocket near the ATP-binding site [Wood E. R. *et al.*, 2004]. (D) Nilotinib (Tasigna), targeting Abl: the inhibitor utilizes the “DFG-out” state of a PK, where the “flip”-out of phenylalanine of the Asp-Phe-Gly motif blocks access of ATP and creates a new binding pocket [Weisberg *et al.*, 2005]. (E) Scheme of ATP-site and nearby pockets of PKs utilized by several selective inhibitors [according to Morphy, 2010].

However, even in case of pharmacologically active PK inhibitors, an idea for development of multi-targeted drugs has recently emerged [Grant, 2009; Knight *et al.*, 2010; Morphy, 2010; Zhang X. *et al.*, 2008]. After the break-through of Gleevec (Imatinib) achieving multi-year increase in survival of patients in the treatment of chronic myeloid leukemia (CML) [Druker and Lydon, 2000], the further progress of PK inhibitors in clinical trials and in clinical practice has been uneven, which might be (at least partially) attributed to several specific features of the kinase-connected diseases. PK inhibitors have been most successful in treatment of diseases driven by a single oncogenic PK (the so-called oncogene-addicted tumors); however, in case of diseases relying on several mechanisms (such as activation of surrogate kinases, inactivation of phosphatases, or activation of alternative redundant kinase pathways) treatment has been remarkably less efficient [Grant, 2009; Zhang J. *et al.*, 2009]. Moreover, some tumors may escape inhibition of single kinase by introducing resistance mutations causing lowered affinity of kinase towards drugs, or enhanced affinity towards natural drug competitors (*i.e.*, ATP) [Krishnamurthy and Maly, 2010]. Therefore, a multi-targeted compound (or a mixture of single-targeted compounds) able to inhibit both, initial PK and its mutated form, or able to block several tumor-maintaining PK pathways would be of considerable value.

Indeed, first steps have already been taken in this direction, including the examples listed below:

- sequential or combined therapy of CML patients with BCR-Abl inhibitors, of which some recognize the non-mutated form of the kinase and others may also inhibit different mutated forms (*i.e.*, first imatinib, then nilotinib or dasatinib, and finally so-called third-generation drugs) [Fuerst, 2010; Shah N. P. *et al.*, 2007];
- combined inhibition of VEGFR and PDGFR by the multi-targeted compounds sorafenib (Nexavar) and sunitinib (Sutent) [Gridelli *et al.*, 2007];
- clinical trials of dual PI3K and mTOR pathway inhibitors as well as mixtures of compounds targeting selectively one of these pathways [Fan and Weiss, 2006].

The first marketed multi-target drug is Lapatinib, with enhanced affinity towards both EGFR and HER2, the kinases overexpressed in a variety of human tumors [Lackey, 2006]. It should also be mentioned that several PK inhibitors initially designed as single-targeted drugs have subsequently demonstrated high affinity towards off-target PKs [Karaman *et al.*, 2008].

Off-target effects of PK inhibitors may generally be classified into two categories, non-PK selectivity issues (*i.e.*, inhibition of promiscuous proteins such as cytochrome P450 superfamily or hERG potassium ion channel) and kinase off-targeting; both may cause severe side-effects of drugs such as cardiotoxicity, dermatological toxicity, myelosuppression, neutropenia, *etc* [Chico *et al.*, 2009; Grant, 2009]. Additional factors that could trigger or diminish the risks for off-target inhibition include drug dosage (and dosing regimen, if several drugs are applied), cell membrane permeability and intracellular accu-

mulation, formation of active metabolites, *etc* [Grant, 2009]. Hence, accurate measurements of the selectivity profile of PK inhibitors preferably in the habitat of their potential application would unambiguously facilitate drug development, as well as disease diagnostics and monitoring, and other fields where PK inhibitors may be utilized [Grant, 2009; Morphy, 2010; Zhang J. *et al.*, 2009].

Up to date, there are several panels of PKs on the market that allow *in vitro* biochemical selectivity profiling of an inhibitor [Grant, 2009]. However, due to the high costs of these services, the compounds of interest are usually tested at a single concentration (100 nM to 10 μ M), and then dose-response curves of inhibitors are measured just with few members of the kinome [Grant, 2009; Zhang J. *et al.*, 2009]. Despite the indisputable value of biochemical kinase panels at the initial steps of inhibitor development, these trials may be compromised by the fact that the inhibitor is tested towards only a small fraction of kinome. Moreover, these assays are often performed at non-physiological conditions (*i.e.*, with low ATP concentrations, truncated and/or mutated forms of PKs, or artificial substrates), thus the results of such selectivity profiling should be cautiously interpreted [Grant, 2009; Morphy, 2010].

Another approach for the determination of selectivity of PK inhibitor is chemical proteomics (please refer to Section 2.3.1. Irreversible mono-ligand inhibitors), where the compound of interest is immobilized on solid beads and used as affinity support [Rix and Superti-Furga, 2009]. This method enables affinity-based profiling of the immobilized compound towards a natural system represented by the cell or tissue lysate; still, there might be complications arising from the inadequate PK activity caused by the loss of natural cellular environment, as well as from partial loss of inhibitor affinity resulting from immobilization.

Finally, intracellular selectivity of PK-targeted compounds may be assessed with the aid of cell lines engineered to respond to an increase or decrease of activity of a certain kinase. Mostly, these model cell lines have been developed from the murine Ba/F3 cell line, which under normal conditions requires the cytokine interleukin 3 to proliferate; however, transformation by an oncogenic kinase results in interleukin 3-independent proliferation [Warmuth *et al.*, 2007]. The rate of proliferation and survival thereby reflects the degree of activity of the given oncogenic kinase, and should be reduced after the application of a selective inhibitor targeted to the oncogene. Whereas these assays enable testing of an inhibitor in the intracellular milieu most close to that of the organisms, misleading information may be obtained in cases where the kinase expression profile in the model cell line differs from that in the diseased human tumor cells [Morphy, 2010]. To sum up, the achievement of optimal affinity, selectivity and other required properties of an inhibitor as well as the assessment of these properties in natural-like systems still remain a challenge, and the field of PK inhibitor research and development is far from depletion.

2.3. Main classes of PK inhibitors

PK inhibitors may be grouped into several types according to the following criteria:

- according to origin: natural, synthetic, or semi-synthetic inhibitors (*i.e.*, derivatives of natural inhibitors/substrates);
- according to the nature of bond formed in the PK-inhibitor complex: reversible or irreversible inhibitors;
- according to the kinetic mechanism of binding: competitive, uncompetitive or semicompetitive (including non-competitive) *versus* ATP and/or *versus* protein/peptide substrate, or allosteric inhibitors;
- according to the number of PK sites occupied by the compound: mono- or multi-ligand inhibitors.

Furthermore, the recent advances in the development of ATP-competitive tyrosine kinase inhibitors and their progression into drugs have necessitated introduction of one additional way of classification of compounds into Type-I and Type-II inhibitors [Johnson L. N., 2009; Noble *et al.*, 2004; Zhang J. *et al.*, 2009]. Type-I inhibitors bind to the active conformations of PKs (*i.e.*, those able to bind ATP and protein/peptide substrate); the pharmacologically important examples of Type-I inhibitors include gefitinib (Iressa) and erlotinib (Tarceva) targeting EGFR, and dasatinib (Sprycel) targeting members of Src family. All of these compounds bind to the ATP-cleft of the kinase, and may additionally occupy the adjacent pockets, *i.e.*, the hydrophobic pocket at the back of ATP-binding cleft. The latter is enlarged in some kinases (by virtue of incorporation of smaller amino acid residue positioned at the opening of the pocket, the so-called “gate-keeper” residue), and thus provides possibilities for introduction of selectivity determinants [Noble *et al.*, 2004].

Type-II inhibitors, by contrast, bind to and stabilize those inactive conformations of PKs (*i.e.*, “DFG-out” and “ α C-Glu-out”) where additional hydrophobic pockets are revealed in the region of the catalytic loop due to “opening” movement of adjacent helices or moieties of the kinase (Figure 6E) [Lee G. M. and Craik, 2009; Rabiller *et al.*, 2010]. The inactive conformations have been considered relatively non-conserved in different PKs and thus especially attractive for drug targeting; the examples Type-II inhibitors include well-known pharmacological drugs imatinib (Gleevec) and nilotinib (Tasigna) targeting BCR-Abl, lapatinib (Tykerb) targeting HER2, and sorafenib (Nexavar) targeting multiple receptor tyrosine kinases. However, it has recently been demonstrated that an inactive conformation may not always be unique for the certain PK, hence in some cases Type-II compounds might still possess lower selectivity towards their targets than Type-I compounds [Lewis, *et al.* 2008; Morphy, 2010]. Moreover, inactive conformations do not require preservation of kinase 3D structure needed for ATP binding, and are therefore more susceptible to resistant mutations.

2.3.1. Irreversible mono-ligand inhibitors

Irreversible inhibitors form a covalent bond (or several covalent bonds) upon binding to the kinase, and hence cannot be displaced by other inhibitors or substrates. According to the chemical properties, irreversible inhibitors can be divided into two groups: the compounds carrying reactive chemical groups (usually electrophiles) that instantly form a covalent bond with the PK upon binding, and compounds possessing so-called photo-affinity groups (usually aromatic azides or benzophenones) that serve as reversible inhibitors in the dark but become reactive upon UV-irradiation. The first irreversible inhibitors designed for kinases were ATP and cAMP analogues labeled with radioactive isotopes and incorporating either a photo-affinity azide-group or a chemically reactive p-fluorosulfonylbenzoyl moiety [Chuan *et al.*, 1989; Kerlavage and Taylor, 1980; Zoller *et al.*, 1981] (Figure 7A). These compounds were used for determination of residues in the kinase sites responsible for binding ATP or cAMP, respectively; after covalent modification, the kinases were subjected to proteolytic cleavage, and the radioactively labeled residues were isolated.

Later on, a similar approach named activity-based protein profiling (ABPP) was introduced, based on irreversible inhibitors termed activity-based probes (ABPs). An ABP consists of three fragments: a moiety endowed with affinity towards protein kinase(s) of interest, a chemical group responsible for generation of a covalent bond, and a reporter-tag for the detection of covalently modified PK (*i.e.*, a radioactive isotope, fluorescent dye, or biotin moiety) [Rix and Superti-Furga, 2009; Speers and Cravatt, 2004]. ABPs selective towards certain PKs have been used to “catch” the target protein(s) from the biological samples (*i.e.*, cell or tissue lysates), or to generate an affinity matrix where natural ligands interacting with enzyme (but not binding to the same site as ABP) may bind [Gayani *et al.*, 2008; Kalesh *et al.*, 2010]. Additional application possibilities are available for the generic ABPs, *i.e.*, those lacking selectivity within a certain group of PKs or most of the kinome). The latter may be used for identification of kinomic pattern of biological samples (so-called chemical proteomics), or for assessment of affinity and selectivity of non-covalent inhibitors added to the PK-containing sample prior to introduction of ABP [Ratcliffe *et al.*, 2007; Speers and Cravatt, 2004]. Apart from kinases, ABPs have been generated for over 20 enzyme classes, including major families of proteases, phosphatases, glycosidases and glutathione S-transferases, and a range of oxidoreductases [Saghatelian and Cravatt, 2005].

Another variant of irreversible inhibitors is represented by cross-linking compounds, which incorporate an affinity-fragment responsible for binding of compound to protein and two reactive groups responsible for covalent linking. One of the reactive groups generates a covalent bond with the PK (usually at the ATP-site), and the other reactive group forms a covalent bond with the protein or peptide binding to the substrate-binding site of the same PK [Liu K. *et al.*, 2008; Parang *et al.*, 2002b]. A cross-linking compound should therefore protrude into the substrate-site to modify covalently one of the protein/peptide

residues but not deep enough to interfere with its binding. Dialdehyde moieties have been frequently used as electrophilic moieties able to react irreversibly with nucleophilic groups of amino acid side-chains incorporated in the structure of kinase and substrate (Figure 7B). While in PKs, the reactive nucleophilic group is incorporated in the side-chain of the highly conserved Lys residue (corresponding to Lys72 in PKAc), the range of substrates suitable for trapping into cross-linked PK-substrate complexes is limited with Cys-containing pseudosubstrate-peptides [Kalesh *et al.*, 2010; Liu K. *et al.*, 2008; Maly *et al.*, 2004; Statsuk *et al.*, 2008]. Thus, dialdehyde-containing cross-linking compounds cannot be used for identification of novel kinase substrates in biological samples, but rather for selective detection of kinase itself, whereas selectivity may be achieved by use of a selective pseudosubstrate and/or a selective cross-linking compound. As an alternative, cross-linking compounds have been developed incorporating two azide groups that are both converted to reactive nitrene or diazaquinodimethane intermediates upon UV-irradiation (Figure 7C) [Parang *et al.*, 2002b; Polshakov, *et al.* 2005]. These intermediates are able to react with O-H and C-H bonds of proteins, and hence do not necessarily require presence of strong nucleophiles in the neighborhood of their binding site in order to form covalent bonds [Matheson *et al.*, 1977].

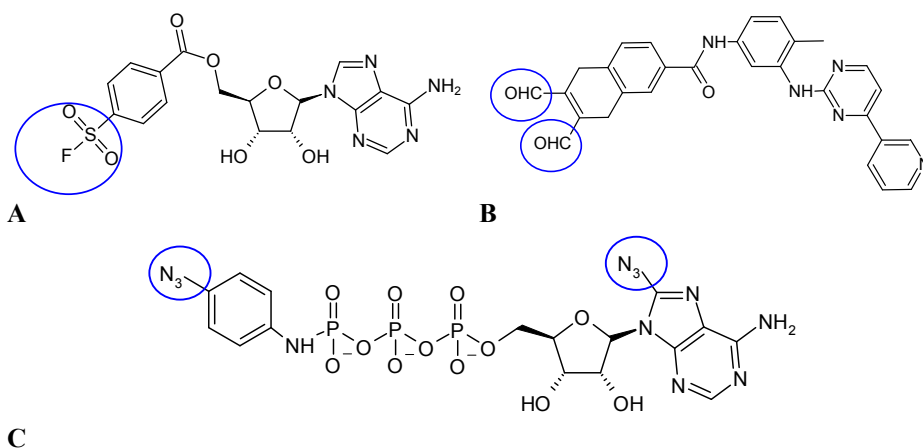


Figure 7. Examples of irreversible inhibitors. (A) FSBA [Ratcliffe *et al.*, 2007]. (B) Dialdehyde 7 [Kalesh *et al.*, 2010]. (C) Bifunctional azide-based crosslinker 5 [Parang *et al.*, 2002b].

The problematic issue of all aforementioned classes of irreversible inhibitors is loss of affinity and/or selectivity of the PK-binding fragment upon conjugation with reactive groups responsible for forming the covalent bonds. However, several irreversible inhibitors have been developed possessing sufficient affinity and selectivity for application as drugs (*i.e.*, for the treatment of non-small cell

lung cancer and other types of solid tumors). Most of the irreversible inhibitors undergoing clinical trials are targeted to ATP-sites of EGFR or HER2 and represent derivatives of quinazoline, anilinoquinoline, pyridopyrimidine, or pyrimidine incorporating unsaturated Michael acceptor groups that form covalent bond with Cys residues of tyrosine kinases (*i.e.*, Cys773 in EGFR, Cys805 in HER2) [Fry, 1999; Heymach *et al.*, 2006; Smaill *et al.*, 1999; Zhang J. *et al.*, 2009; Zhou W. *et al.*, 2009]. Recently, similar compounds targeting Bruton's tyrosine kinase and VEGFR-2 have been reported (Figure 8A). In the latter case, derivatives of quinazoline were used containing two reactive groups positioned in such way that one (Michael acceptor) generates a covalent bond with EGFR or HER2 and the other (benzoquinone moiety) with VEGFR-2 [García-Echeverría *et al.*, 2000; Wissner *et al.*, 2007; Zhang J. *et al.*, 2009]. Another selectivity-gaining binding mode was utilized by the natural compound lactoquinomycin, which formed covalent bonds with the residues Cys296 and Cys310 of the activation loop of PKB α [García-Echeverría and Sellers, 2008; Toral-Barza *et al.*, 2007]. Lactoquinomycin showed significant selectivity towards PKB α in a panel of 45 PKs and inhibited PKB-catalyzed phosphorylation in cells; however, the nonspecific redox-related cytotoxicity of this compound strongly limited its pharmacological applications. Last but not least, pyrrolopyrimidine derivatives containing either a chloromethylketone (CMK) or a fluoromethylketone (FMK) electrophile could also be successfully applied for irreversible inhibition of RSK isoforms 1, 2 and 4, and showed remarkable target selectivity not only in biochemical *in vitro* systems, but also in mammalian cells [Figure 8B; Cohen M. S. *et al.*, 2005]. The latter observation might be attributed to the incorporation of a second selectivity determinant into the structure of compounds, represented by a para-tolyl substituent targeted to the hydrophobic pocket at the back of the ATP-site that is lined by a compact gate-keeper residue (Thr) in case of RSK isoforms 1, 2 and 4.

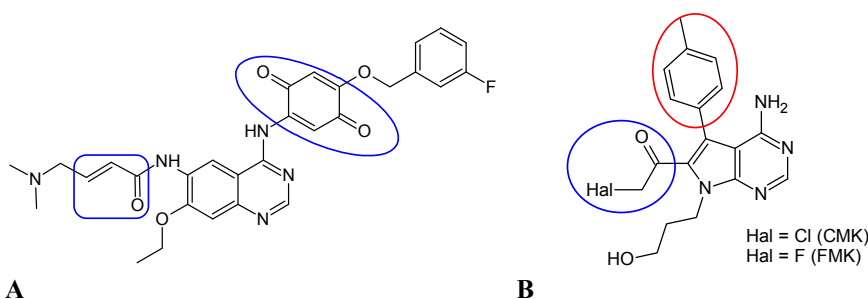


Figure 8. Examples of selective irreversible inhibitors. (A) Compound 17 [Wissner *et al.*, 2007]. (B) CMK and FMK; selectivity determinant marked with red oval [Cohen M. S. *et al.*, 2005].

To sum up, it should be mentioned that all irreversible inhibitors exhibit both time- and concentration-dependent manner of PK inactivation [Fry, 1999]. Moreover, in most cases the results of measurements of affinity and inhibition potency of irreversible inhibitors are dependent on the rate of formation of covalent bond with a kinase, and in case of chemically reactive compounds may even reflect affinity of both reversibly and irreversibly binding forms. The most problematic issue for the development of irreversible inhibitors remains exact identification of the positions in the inhibitor structure where reactive groups should be positioned to generate covalent binding to the protein residues. For irreversible inhibitors applied in crude biological systems, a problem of excessive activity may also evolve, *i.e.*, irreversible binding to the compounds containing nucleophilic centers and present in cell in high concentration (*i.e.*, glutathione) [Wissner *et al.*, 2007; Zhang X. *et al.*, 2008]. In case of pharmacological applications, the issue of selectivity might become especially important, as a covalent attachment to unanticipated targets should by all means be avoided to reduce the toxicity of irreversible inhibitors. The advantages of irreversible compounds, however, sometimes outweigh the potential risks, as covalent inhibitors ensure prolonged inhibition of enzyme and do not need to achieve high plasma concentrations in order to gain inhibitory potency [Fry, 1999; Morphy, 2010]. Moreover, ATP-site directed irreversible inhibitors do not suffer as much from the high intracellular concentrations of ATP as their reversible counterparts: once the covalent bond is formed between an inhibitor and a PK, the former cannot be displaced from the complex. Hence, covalently binding compounds are also of especial value for inhibition of proteins that acquire high affinity towards ATP as a result of mutation [Fry, 1999; Krishnamurthy and Maly, 2010].

2.3.2. Reversible mono-ligand inhibitors. Special case: ATP-competitive inhibitors

The majority of PK inhibitors being currently in clinical trials and probably also the majority of small-molecule PK inhibitors under development are represented by ATP-site targeted reversible compounds that compete with ATP for binding. This fact may seem surprising, considering the selectivity issues of targeting ATP-site possessed by all 518 PKs and over 1500 other proteins, and the need to compete with high intracellular concentrations of ATP (over 1 mM) [Fischer P. M., 2004]. However, wide popularity of ATP-competitive inhibitors (ACI) originates from the druggability approach previously discussed (please refer to Section 1.3. PKs in disease), as the ATP-site being deeply buried inside the PK molecule and allowing generation of multiple strong interactions between a ligand and a protein fits perfectly under definition of the druggable pocket.

Most of the ACIs are structurally similar to ATP itself, at least to a certain degree; typically, potent ACIs contain an aromatic system (or several aromatic

systems) incorporating nitrogen atom(s) that serves as H-bond donors or acceptors, and do not contain hydrolysable phosphates. The multiplicity of nitrogen-containing aromatic scaffolds used for the design of ACIs is illustrated below (Figure 9).

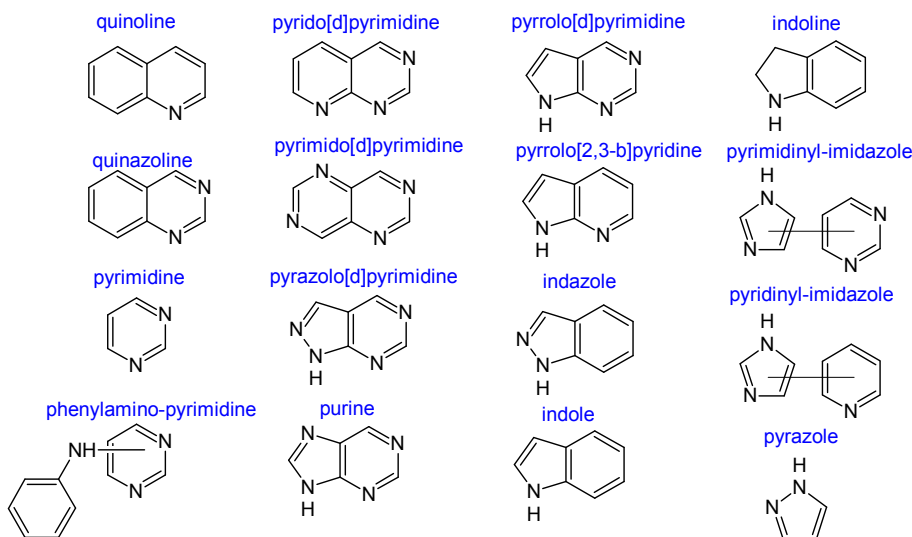


Figure 9. Aromatic scaffolds widely applied in ACIs.

Probably the best-known representatives of isoquinoline scaffold are so-called Hidaka-series compounds (H-inhibitors) first reported in 1984 and initially derived from calmoduline antagonist W-7 after replacement of naphthalene moiety with isoquinoline [Hidaka *et al.*, 1984]. The first generation of H-inhibitors consisted of relatively non-selective compounds, although later modifications resulted in an increase of selectivity towards certain targets, *i.e.* H-89 (Figure 10A) has been widely used as a PKAc-selective compound with a K_i value of 50 nM (although recent reports have demonstrated that H-89 is also a potent inhibitor of ROCK-II, MSK1, and S6K1) [Murray A. J., 2008; Ono-Saito *et al.*, 1999]. The efforts to generate a PKB-selective inhibitor based on isoquinoline scaffold have yielded compounds (Figure 10B–C) with a high affinity towards PKB β and the ability to inhibit PKB-catalyzed phosphorylation of GSK3 in cells; however, these compounds still exposed more potent inhibition of PKAc [Collins *et al.*, 2006; Li Q. *et al.*, 2006]. The most promising results were obtained with 1,4-diazepine conjugates of 5-isoquinoline-sulfonic acid, which revealed high affinity towards ROCK; one of these compounds is fasudil (HA-1077, Figure 10D), the first inhibitor approved for clinical use in Japan in 1995 for the treatment of cerebral vasospasm [Tamura *et al.*, 2005]. Fasudil inhibited ROCK-II with a K_i value of 330 nM, expressing a ca 10-fold

selectivity over PKG and a 30-fold selectivity over PKAc. A di-methylated form of fasudil, H-1152 (Figure 10E) revealed even better affinity towards ROCK-II ($K_i = 1.6$ nM) and improved selectivity *versus* PKAc and PKC, and has been recently used as a template for further derivatization aimed at improvement of inhibitory properties towards ROCK. Recently, a novel isoquinoline-derived ROCK-II inhibitor has been reported (Figure 10F), possessing a K_i value of 25 nM towards ROCK-II and exhibiting inhibition of ROCK-catalyzed MYPT1 phosphorylation in cells [Iwakubo *et al.*, 2007a].

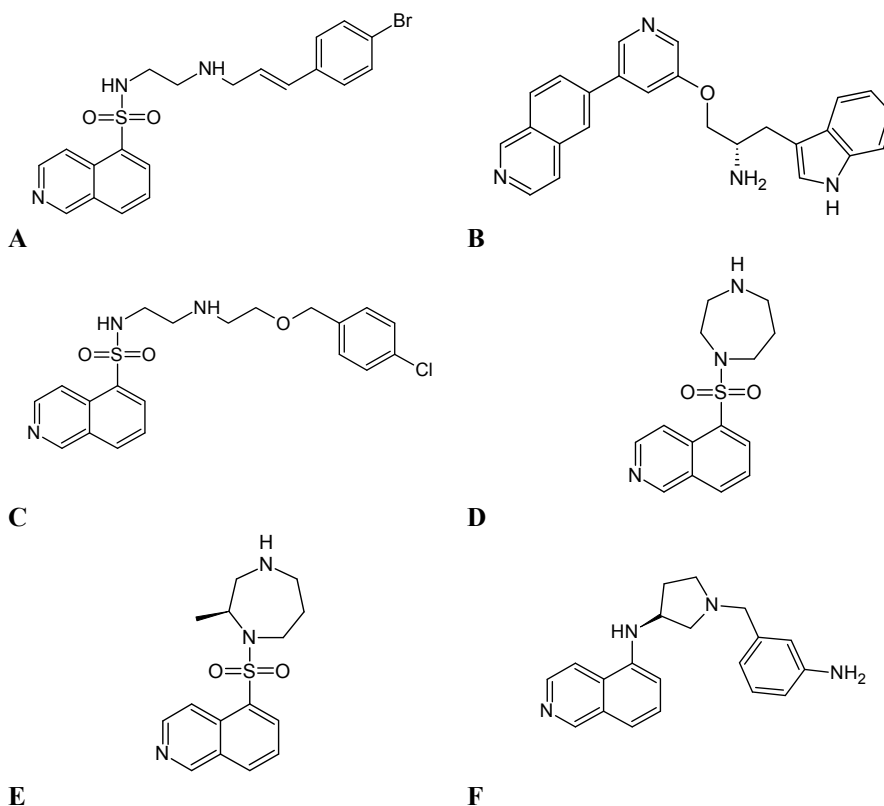


Figure 10. Examples of isoquinoline-containing ACIs. (A) H-89 [Ono-Saito *et al.*, 1999]. (B) Compound 13a [Li Q. *et al.*, 2006]. (C) Compound 9 [Collins *et al.*, 2006]. (D) HA-1077 [Tamura *et al.*, 2005]. (E) H-1152 [Tamura *et al.*, 2005]. (F) Compound 30-R [Iwakubo *et al.*, 2007a].

Another widely accepted class of ROCK inhibitors is based on pyridine and pyrrolo-pyridine scaffolds. One of the most prominent representatives is Y-27632 (Figure 11A), which has been widely applied as a ROCK-II inhibitor in smooth muscle assays; Y-27632 has a K_i value of 140 nM towards ROCK-I and a nearly 200-fold selectivity *versus* PKAc [Uehata *et al.*, 1997]. The replace-

ment of pyridine fragment of Y-27632 with pyrrolo-pyridine and elimination of chirality by introduction of phenyl moiety instead of cyclohexane resulted in an additional increase in affinity towards ROCK-II ($K_i = 3.6$ nM), and the compound Y-39983 (Figure 11B) is undergoing clinical trials as an anti-glaucoma agent [Tokushige *et al.*, 2007]. Pyrrolo-pyridine moiety has also been used in conjugation with difluoro-phenyl and diamino-pyrimidine fragments (Figure 11C), the resulting compound exhibiting high affinity towards ROCK and a good pharmacokinetical profile, and causing an effective reduction of blood pressure in anesthetized rats [Schirok *et al.*, 2008].

Interestingly, compounds based on pyrrolo-pyrimidine and structurally comparatively similar to Y-27632 and Y-39983 have been successfully applied as PKB α and PKB β inhibitors (Figure 11D–E), possessing a high affinity *in vitro* and anti-tumor effect *in vivo* [Caldwell *et al.*, 2008; Freeman-Cook *et al.*, 2010]. The pyrimidine core in conjugation with 5-amidothiophene also yielded a potent inhibitor of PKB isoforms α and γ (Figure 11F; IC_{50} values of 6 nM and 3 nM, respectively), although this compound was an even more potent inhibitor of PKAc (IC_{50} values of 0.1 nM) [Lin X. *et al.*, 2006]. Other scaffolds frequently adopted for the design of ACIs towards pharmacologically important PKs such as PKB and ROCK are represented by indazoles and pyrazoles [Chen *et al.*, 2008; Feng *et al.*, 2007; Goodman *et al.*, 2007; Iwakubo *et al.*, 2007b; Lin H. *et al.*, 2010; Saxty *et al.*, 2007; Sehon *et al.*, 2008, Zhu *et al.*, 2007].

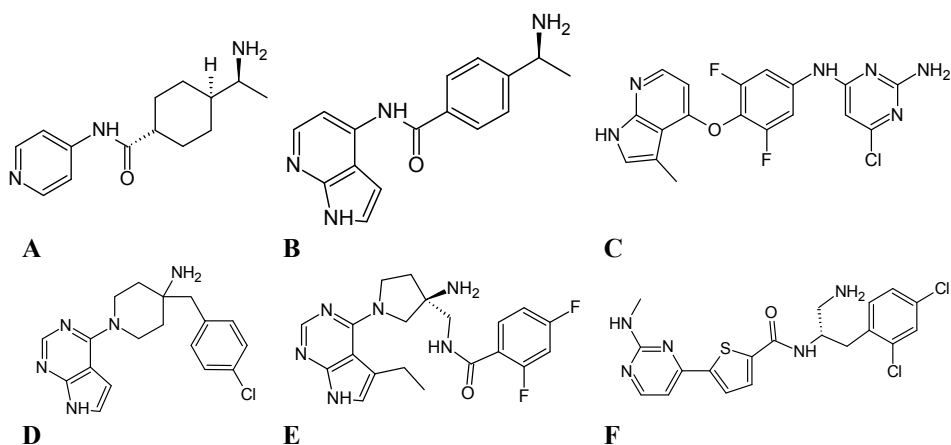


Figure 11. Examples of ACIs based on pyridine and pyrrolo-pyridine. (A) Y-27632 [Uehata *et al.*, 1997]. (B) Y-39983 [Tokushige *et al.*, 2007]. (C) Compound 32 [Schirok *et al.*, 2008]. (D) Compound 25 [Caldwell *et al.*, 2008]. (E) Compound 42 [Freeman-Cook *et al.*, 2010]. (F) Compound 2aa [Lin X. *et al.*, 2006].

One of the most promising pan-PKB inhibitors³ being currently in clinical trials is the azabenzimidazole-aminofurazan conjugate GSK690693 (Figure 12A), which despite a wide affinity-profile within the AGC-group of PKs has been successfully tested in mice bearing human ovarian, prostate, and breast carcinoma xenografts [Rhodes *et al.*, 2008]. Structurally similar conjugates (Figure 12B–C) have shown high affinity towards ROCK-I, and effectively reduced blood pressure in rats [Doe *et al.*, 2007; Stavenger *et al.*, 2007]. However, even a higher affinity was possessed by a conjugate of benzimidazole and chroman (Figure 12D), which strikingly demonstrated an over 400-fold selectivity *versus* PKAc and even higher selectivity indices *versus* other representatives of the AGC-group [Sessions *et al.*, 2008].

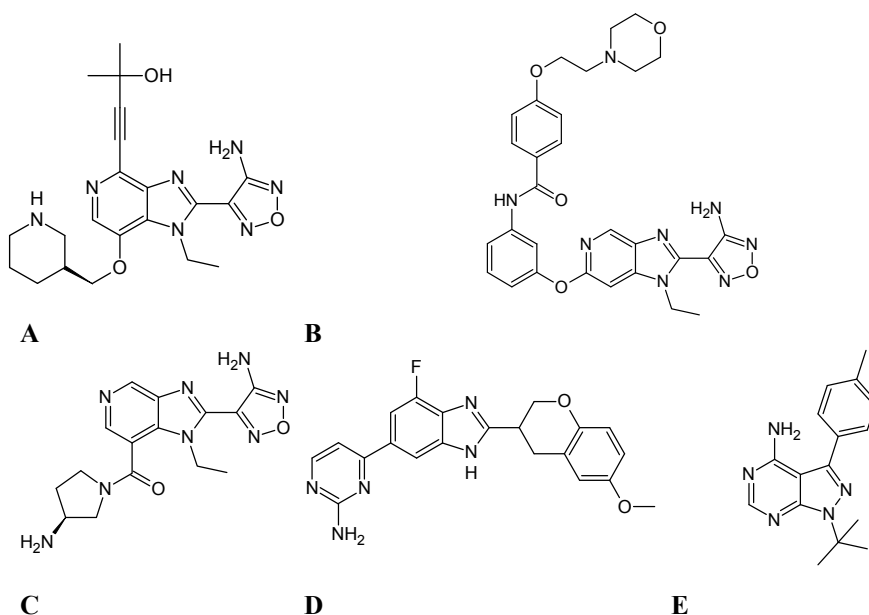


Figure 12. Examples of ACIs based on azabenzimidazole and indazole. (A) GSK690693 [Rhodes *et al.*, 2008]. (B) GSK269962A [Doe *et al.*, 2007]. (C) SB-772077-B [Doe *et al.*, 2007]. (D) SR4030 [Sessions *et al.*, 2008]. (E) PP1 [Liu Y. *et al.*, 1999].

³ Pan-inhibitor indicates a compound with high affinity towards all isoforms of the target PK.

Importantly, several natural compounds may serve as generic (promiscuous) ACIs of PKs, the best-known examples include the following compounds [Gani and Engh, 2010; Pande *et al.*, 2008; Shu, 1998]:

- balanol (isolated from the fungus *Verticillium balanoides*; structurally identical to azepinostatin isolated from *Fusarium merismoides*), (Figure 13A);
- flavopiridol (derivative of rohitukine, an alkaloid isolated from *Dysoxylum binectariferum*), (Figure 13B);
- staurosporine with its derivatives (initially isolated from microbial alkaloids of *Streptomyces staurosporeus* and other actinomycetes) (Figure 13C).

Balanol is a highly potent inhibitor of Ser/Thr kinases with especially high affinity towards most PKC isoforms, but lacking affinity towards casein kinase II or Tyr kinases; however, over 500 derivatives of balanol have been synthesized, of which several demonstrated an improved selectivity towards PKC *versus* other kinases (*i.e.*, PKAc) (Pande *et al.*, 2008; Shu, 1998). Flavopiridol inhibits most cyclin-dependent kinases and down-regulates the cyclins D1 and D3, thus inducing cell cycle arrest; by virtue of its anti-tumor effects in patients with renal, prostate and colon cancer, flavopiridol is currently undergoing Phase II trials [Senderowicz, 1999]. Staurosporine possesses probably the most wide affinity profile of all PK inhibitors, inhibiting 87% of PKs with a K_D value below 3 μ M [Karaman *et al.*, 2008]. It has also been one of the compounds being extensively used as a template in the ligand-based design, and the efforts in the field have yielded several staurosporine derivatives with improved selectivity, *e.g.*, bisindolyl maleimides targeted to PKC isoforms [Grodsky *et al.*, 2006; Komander *et al.*, 2004; Shu, 1998]. Several of the latter compounds are currently at different stages of clinical trials, *i.e.*, midostaurin PKC412 (inhibitor of PKC α , VEGFR-2, c-KIT, and PDGFR) or UCN-01 (inhibitor of PKC α , CDK2 and PDK1) [Fuse *et al.*, 2005; Komander *et al.*, 2003; Millward *et al.*, 2006]. Another well-known group of inhibitors sharing structure similarity with staurosporine are the so-called K-252-series compounds named after the natural non-selective inhibitor K252a, which inhibits Ser/Thr kinases as well as receptor Tyr kinases [Ruggeri *et al.*, 1999]. Its derivatives KT-5720 and KT-5823 (Figure 13D–E) have been widely used as PKAc and PKG-selective compounds, respectively [Kase *et al.*, 1987; Smolenski *et al.*, 1998]; however, several recent studies failed to report the *in vivo* effects of these compounds [Bain *et al.*, 2003; Burkhardt *et al.*, 2000; Murray A. J., 2008].

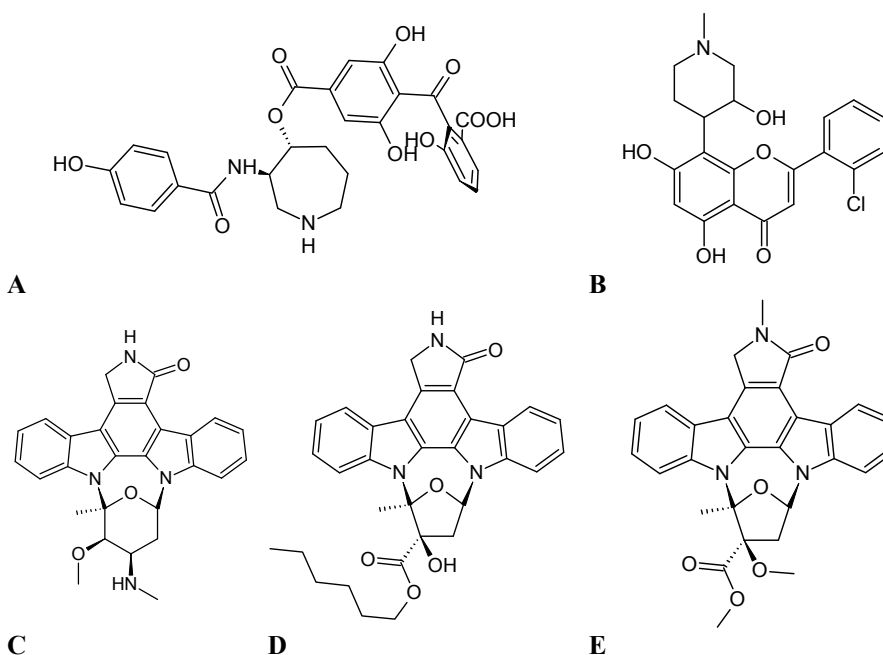


Figure 13. Examples of natural ACIs and their derivatives. (A) Balanol [Pande *et al.*, 2008]. (B) Flavopiridol [Senderowicz, 1999]. (C) Staurosporine [Gani and Engh, 2010]. (D) KT-5720 [Gani and Engh, 2010]. (E) KT-5823 [Kase *et al.*, 1987].

ACIs have been also used in chemical genetics approaches, where non-natural ligand/enzyme pairs are generated by point-mutation of the enzyme (*i.e.*, resulting in enlargement of certain pockets in the enzyme) and synthesis of sterically bulky ligand not able to bind the non-modified enzyme [Elphick *et al.*, 2007]. The idea behind the chemical genetics is to monitor the pathways of the point-mutated enzyme substituting the natural wild-type enzyme in its natural habitat; in case of PKs, the most frequently applied non-natural ligand is represented by the N6-substituted radioactively labeled ATP derivatives which function as ^{32}P -phosphoryl donors [Bishop *et al.*, 2001]. However, the latter compounds often yield extremely low signals, as their affinity towards the modified enzyme is not considerably better than that of ATP (but ATP is present in the cell in much higher concentration); additionally, they suffer from hydrolysis of phospho-diester bonds, and from poor cell membrane-penetrative properties. Therefore, ACIs have emerged as powerful alternative “devices”; for instance, derivatives of pyrazolo-pyrimidine inhibitor PP1 (Figure 12E) have been widely applied for the investigation of cellular responses to selective blocking of the PK of interest (*i.e.*, GRK2, v-Erb, CAMK-II, *etc.*) achieved by chemical genetics [Liu Y. *et al.*, 1999; Wang H. *et al.*, 2003].

2.3.3. Reversible mono-ligand inhibitors.

Special case: Protein/peptide substrate-competitive inhibitors

Inhibitors competing with protein substrates of PKs for binding represent another large group of PK inhibitors, which is under the scope of intense research. Protein substrate-competitive inhibitors (PCIs) have been considered very promising from the aspect of selectivity towards their PK targets, as PCIs bind to the site of PK responsible for recognition of specific substrates, and are thus potentially able to pinpoint the pattern of interactions characteristic of the target PK [Bogoyevitch *et al.*, 2005; Parang and Sun, 2004]. However, as the protein substrate-binding site of PKs is not well defined and opened to solvent, binding of compounds to this site is associated with large entropic costs that must be compensated by an extremely high enthalpy of binding, necessitating generation of multiple interactions between a PK and a PCI. The latter requirement, on the other hand, means that PCI itself can generally not be a small-molecular weight compound; large molecular weight and poor proteolytic stability of PCIs consisting of natural amino acids have substantially raised doubts about efficacy of PCIs as a class of inhibitors.

Still, PCIs are endowed with several remarkable properties that may outweigh disadvantages. First of all, compounds binding to the substrate site of PKs may express positive cooperativity with ligands binding to the ATP-site, as demonstrated by NMR studies with PKAc where affinity of substrate peptide Kemptide (Leu-Arg-Arg-Ala-Ser-Leu-Gly) was enhanced 3.4-fold in case of ATP-first mechanism of binding (as compared to Kemptide-first mechanism) [Masterson *et al.*, 2008]. Therefore, affinity of PCIs in the presence of high intracellular concentration of ATP is enhanced, not reduced as in case of ACIs. The exact mechanism of such positive cooperativity may vary between PKs, *i.e.*, PKAc relies on one residue (Tyr204) for the dispersion of perturbations from substrate-binding region to the distal sites of the PK molecule [Lew *et al.*, 1997a; Masterson *et al.*, 2008]. Secondly, it has been established that similar to protein-protein interfaces, the critical contribution to the binding energy of peptidic compounds results from interactions of only a small number of peptide residues with the protein molecule, creating so-called hot-spots of binding [London *et al.*, 2010]. Hence, identification of potential hot-spot regions in a PK and targeting those hot-spots with a PCI should enable reduction of molecular weight of the latter while preserving its affinity.

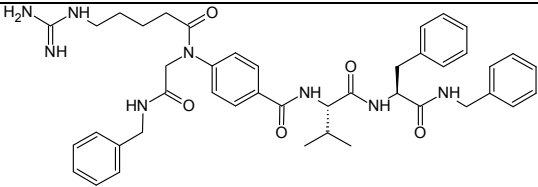
Generally, the strategies for PCI discovery either use information from the analysis of sequences of natural PCIs, substrates or pseudosubstrates (*i.e.*, autoinhibitory sequences) of PKs, or utilize libraries of peptides to determine the amino acid residues preferred by a PK in each position of the PCI sequence. The first strategy is probably best illustrated by PCIs of PKAc derived from the natural heat-stable protein kinase inhibitor (PKI). There are three isoforms of PKI expressed in human organism (PKI α , PKI β , and PKI γ), which have slightly different abundance in tissues (PKI α is the most abundant) and affinity towards

PKAc (K_i values⁴ of 0.2 nM, 7.1 nM, and 0.4 nM, respectively) [Dalton and Dewey, 2006]. All isoforms contain a highly ordered pseudosubstrate domain and a leucine-rich nuclear export signal, whereas the rest of the PKI molecules is disordered, which probably contributes to the thermostability of this protein. The biochemical analysis of PKI revealed that the shortest fragment with affinity comparable to that of full-length PKI is the 20-mer peptide PKI α (5–24) (K_i = 2.3 nM; Table 3A), whereas the minimal fragment of PKI α retaining relatively high affinity towards PKAc is 9-mer PKI α (14–22) with the amino acid sequence Gly-Arg-Thr-Gly-Arg-Arg-Ala⁵-Ile (K_i = 36 nM) [Bogoyevitch *et al.*, 2005]. Interestingly, the latter sequence is nearly identical to the “optimal sequence” of PKAc substrates as identified from subsequent screening of compound libraries, Arg/Xaa-Arg/Xaa-Xaa-Arg-Arg-Xaa-Ser-Hyd (where Xaa is any and Hyd is hydrophobic amino acid) [Pearce *et al.*, 2010]. Moreover, the same sequence is contained in PKArI and PKArII subunits with only difference in position P \pm 0, which is Ala in PKArI but Ser in PKArII; consequently, PKArI also serves as PCI of PKAc, with K_D value of 0.8 nM in the presence of ATP and in the absence of cAMP [Diskar *et al.*, 2007; Herberg and Taylor, 1993]. PKArII, on the other hand, may be either an inhibitor or a substrate of PKAc, with the dissociation constant values of 0.7 nM and 40 nM for non-phosphorylated and phosphorylated forms of PKArII, respectively (in the absence of cAMP) [Diskar *et al.*, 2007].

⁴ The K_i values provided in text for PKI and PKI fragments are valid in the presence of ATP; in the absence of ATP, the affinity of PKI is substantially lower (for instance, the K_D value for PKI α towards PKAc is 230 nM [Herberg and Taylor, 1993]).

⁵ The underlined Ala-residue corresponds to the phosphorylatable Ser/Thr residue in PKAc substrates.

Table 3. Structures of PCIs

<i>Code</i>	<i>Name</i>	<i>Structure</i>
A	PKI α (5–24) [Smith C. M. <i>et al.</i> , 1999]	Thr-Thr-Tyr-Ala-Asp-Phe-Ile-Ala-Ser-Gly-Arg- Thr-Gly-Arg-Arg-Asn- <u>Ala</u> ^a -Ile-His-Asp
B	Compound 36a [Kayser <i>et al.</i> , 2007]	
C	– [Ward and O'Brian, 1993]	Myr-Arg-Lys-Arg- <u>Thr</u> -Leu-Arg-Arg-Leu
D	– [House and Kemp, 1987]	Arg-Phe-Ala-Arg-Lys-Gly- <u>Ala</u> -Leu-Arg-Gln-Lys- Asn-Val-His-Glu-Val-Lys-Asn
E	myr- ψ PKC [Eichholtz <i>et al.</i> , 1993]	Myr-Phe-Ala-Arg-Lys-Gly- <u>Ala</u> -Leu-Arg-Gln
F	myr- ψ PKC ζ [Dominguez <i>et al.</i> , 1992]	Myr-Arg-Arg-Gly- <u>Ala</u> -Arg-Arg-Trp-Arg-Lys
G	WW21 [Dostmann <i>et al.</i> , 1999]	Thr-Gln-Ala-Lys-Arg-Lys-Lys- <u>Ala</u> -Leu-Ala-Met- Ala-NH ₂
H	W45 [Dostmann <i>et al.</i> , 2000]	Leu-Arg-Lys ₅ -His
I	DT-2 [Dostmann <i>et al.</i> , 2000]	Tyr-Gly-Arg-Lys-Lys-Arg-Arg-Gln-Arg-Arg-Arg- Pro-Pro-Leu-Arg-Lys ₅ -His
J	AKTide-2T [Luo Y. <i>et al.</i> , 2004]	Ala-Arg-Lys-Arg-Glu-Arg-Thr-Tyr-Ser-Phe-Gly- His-His-Ala
K	Peptide 2 [Luo Y. <i>et al.</i> , 2004]	Val-Glu-Leu-Asp-Pro-Glu-Phe-Glu-Pro-Arg-Ala- Arg-Glu-Arg-Thr-Tyr-Ala-Phe-Gly-His
L	IDA peptide [Fukami <i>et al.</i> , 1999]	Leu-Ala-Arg-Val-Ala-Asp-Pro-Asp-His-Asp-His- Thr-Gly-Phe-Leu- <i>Thr</i> ^b -Glu- <i>Tyr</i> -Val-Ala-thr-Arg- Trp-Tyr-Arg-Cys
M	KRX-123.302 [Goldenberg-Furmanov <i>et al.</i> , 2004]	Myr-Gly-Leu-Val-Thr-(3,5-diTyr)-(D-Lys)-Lys- Ile-(ϵ -abLys)-NH ₂
N	P15 [Perea <i>et al.</i> , 2004]	cyclic* Cys-Trp-Met-Ser-Pro-Arg-His-Leu-Gly- Thr-Cys

Code	Name	Structure
O	Compound 18 [Priestman and Lawrence, 2010]	

^a Underlined are the residues corresponding to P0 position of the substrate; ^b in italics is given the Tyr residue which serve as phosphorylation sites in a PK; * cyclic peptide generated *via* formation of S-S bond between the side-chains of Cys residues; Myr, myristoyl residue; 3,5-diITyr, 3,5-diiodo-tyrosine; ε-abLys, ε-aminobenzoyl-lysine. Red lines indicate positions where bonds are broken upon irradiation.

For PKB, several PCIs were designed based on the PKB substrate protein GSK3β, *i.e.*, the 6-mer mimicking the structure of the GSK3β sequence Gly-Arg-Pro-Arg-Thr-Thr-Ser-Phe (Table 3B); the N-terminal derivatization of this compound with cholesterol yielded the compound PTR6164, which effectively inhibited the growth of prostate cancer cells in xenograft models [Collins, 2009; Kayser *et al.*, 2007]. In case of PKC, one of the first examples was the N-myristoylated 8-mer derived from the major site of PKC-catalyzed phosphorylation on EGFR (Table 3C); interestingly, the latter served as an inhibitor of PKC despite containing a phosphorylatable Thr residue [Ward and O'Brian, 1993]. Other PKC-targeted PCIs based on the pseudosubstrate motif from the N-terminal regulatory domain of PKC were represented by the 18-mer peptide corresponding to residues 19–36 of PKCα and PKCβ (K_i value of 150 nM towards PKCα; Table 3D) [House and Kemp, 1987], and the myristoylated 9-mer myr-ψPKC (Table 3E) [Eichholtz *et al.*, 1993]. The same approach was also used to generate a highly selective PCI targeted to the PKCζ isoform (Table 3F), taking advantage of the fact that the pseudosubstrate motif of PKCζ differs from those of PKCα, PKCβ, and PKCγ isoforms [Dominguez *et al.*, 1992]. PCIs derived from the sequences of substrates and pseudosubstrates have also been designed for other Ser/Thr-kinases (*i.e.*, MLCK, MAP kinases) as well as Tyr-kinases (*i.e.*, Src) [Bogoyevitch *et al.*, 2005; Parang and Sun, 2004]. The best progress in the library-aided strategy of PCI discovery was demonstrated by the PKG-targeted compounds. Kinetic screening of exhaustive 8-mer, 12-mer and 14-mer substrate libraries (where an optimal amino acid residue out of 20 natural amino acids was found for every position in the peptide) identified sequences with high selectivity towards PKGIα *versus* closely related PKAc [Dostmann *et al.*, 1999; Tegge *et al.*, 1995]. The subsequent replacement of Ser with Ala in one of these substrates yielded a 12-

mer PCI with a K_i value of 7.5 μM and 100-fold selectivity *versus* PKAc (Table 3G). In analogical approach, kinetic screening of 8-mer PCI libraries identified the inhibitor W45 with a K_i value of 0.8 μM towards PKGI α and a 700-fold selectivity *versus* PKAc (Table 3H) [Dostmann *et al.*, 2000]. Conjugation of W45 with the membrane translocation signal of HIV-1 Tat-protein yielded inhibitor DT-2 (Table 3I), demonstrating an astonishing K_i value of 0.012 μM towards PKGI α and remarkable vasodilatory effects in isolated rat arteries [Dostmann *et al.*, 2000; Dostmann *et al.*, 2002; Taylor M. S. *et al.*, 2004]. DT-2 possessed a competitive mechanism of inhibition *versus* the substrate peptide; interestingly, the recent mass-spectroscopic studies of DT-2 complex with homodimeric PKGI α revealed that one DT-2 molecule binds simultaneously to both monomers of PKGI α [Pinkse *et al.*, 2009].

The library-aided strategy has also yielded high-affinity PCIs towards PKB, such as 14-mer AKTide-2T with a K_i value of 12 μM towards PKB α (Table 3J); interestingly, AKTide-2T acted as an inhibitor despite incorporation of Tyr and Ser residues [Cheng J. Q. *et al.*, 2005; Luo Y. *et al.*, 2004]. The subsequent modification of AKTide-2T and conjugation with the PKB substrate FOXO3 resulted in a 20-mer PCI with a K_i value of 110 nM towards PKB α and high selectivity towards PKB α *versus* closely related PKs (PKA, p70 S6K, PKC δ and γ , *etc*) [Table 3K; Luo Y. *et al.*, 2004]. This compound successfully inhibited PKB-catalyzed GSK3 phosphorylation in HeLa cell culture, but was not stable long enough to induce apoptosis. Finally yet importantly, peptide libraries have also been successfully used for generation of PCIs towards PKC [Lee J. H. *et al.*, 2004], and PKs from a substantially different group of kinome such as c-Src [Lam *et al.*, 1995].

An interesting approach for substrate-competitive inhibition of PKs has been proposed in 1999, with the rationale to protect PK substrates from phosphorylation by development of an inhibitor that binds these substrates (*i.e.*, a compound that actually competes with the PK for the substrates) [Fukami *et al.*, 1999]. Such a PCI should structurally correspond to a short segment of PK, or mimic a PK region situated near the catalytic site of a PK and composed of the amino acids unique for the PK of interest (or at least for the PK family of interest). For instance, the MAPK fragment situated between the highly conserved sequence Asp-Phe-Gly and triad Ala-Pro-Glu has been utilized for the design of inhibitors of the MAPK pathway (*i.e.*, Table 3L), demonstrating activity in both, *in vitro* and in oocytes [Fukami *et al.*, 1999]. Another example is represented by the substrate-binding loop of the Src family member Lyn, which was used as a template for the generation of 8-mer peptides with high sequence similarity; one of the resulting peptides, KRX-123.302 (Table 3M) inhibited the Lyn-catalyzed phosphorylation of physiological substrate Syk with an IC_{50} value of 300 nM [Bogoyevitch *et al.*, 2005; Goldenberg-Furmanov *et al.*, 2004]. The same principles were applied for the discovery of PCIs towards another Tyr-kinase c-Kit, and towards Ser/Thr-kinases PKB, PDK1 [Niv *et al.*, 2004]. An analogical compound P15 competing with CK2 for the substrates

was derived from the screening of the cyclic peptide phage display library towards a substrate of CK2 (Table 3N); upon conjugation with Tat-peptide, P15 revealed proapoptotic antitumor effects in mice bearing solid tumors [Perea *et al.*, 2004].

PCIs have been recently applied as so-called caged compounds, *i.e.*, compounds that acquire or lose inhibitory properties upon structural modification resulting from illumination of the sample [Lee H.-M. *et al.*, 2009]. Caged compounds are especially useful in cellular assays where a “switch” of PK activity is monitored, as those may induce such switch without altering the endogenous protein expression levels. Typically, a PCI is labeled with a photolabile group (*i.e.*, ortho-nitrobenzyl, hydroxyphenacyl, coumarin, or cinnamate moiety) that prevents binding of the PCI to its target; however, the inhibitor is present in the cellular environment, and when the photolabile group is cleaved by photolysis, the PCI is released that may inhibit its target PK [Priestman and Lawrence, 2010]. An elegant variant of caged PCI has been reported for PKAc (Table 3O), where a sequence derived from PKI was modified at the side-chain of Arg involved in forming of hot-spot interactions when binding to PKAc (corresponding to P-2 position of PKI); the caged compound had a K_i value of 20 nM towards PKAc. However, upon irradiation at 300...400 nm, the uncaged version of the same PCI was released, possessing a K_i value of 0.42 μ M and successfully blocking the morphological changes induced by a cell-permeable PKAc activator [Priestman and Lawrence, 2010].

In all of the aforementioned PCIs, the primary concern for usage inside the cell is the lack of ability of several peptides to cross the plasma membrane. Several techniques have been used for improvement of the membrane-penetrative properties of PCIs, including introduction of hydrophobic fragments (*i.e.*, myristoyl, palmitoyl, or cholesterol moieties, or conjugation with the peptide sequences endowed with cell membrane-penetrative properties [Collins, 2009; Dostmann *et al.*, 2000; Eichholtz *et al.*, 1993; Harris *et al.*, 1999; Perea *et al.*, 2004; Prudent and Cochet, 2004]. The latter sequences termed CPPs (cell-penetrating peptides) represent a variety of structures, differing in amino acid sequence and consequently, electrostatic charge; CPPs have been used to deliver a large variety of cargos into cells, such as peptides or proteins, and oligo-nucleotides [Fischer R. *et al.*, 2002; Watkins *et al.*, 2009]. The most widely applied CPPs (Table 4) are represented by fragments of transcription factors, *i.e.*, the antennapedia peptide derived from *Drosophila melanogaster* Antennapedia homeodomain protein (Antp), and the previously mentioned Tat-peptide derived from the HIV-1 Tat protein; other well-known CPPs are oligo-Arg peptides [Duchardt *et al.*, 2007; Fischer R. *et al.*, 2002; Watkins *et al.*, 2009].

Table 4. Structures of CPPs (according to [Duchardt *et al.*, 2007; Fischer R. *et al.*, 2002])

<i>Name</i>	<i>Sequence</i>
Antp	Arg-Gln-Ile-Lys-Ile-Trp-Phe-Gln-Asn-Arg-Arg-Met-Lys-Trp-Lys-Lys
MTS	Ala-Ala-Val-Ala-Leu-Leu-Pro-Ala-Val-Leu-Leu-Ala-leu-Leu-Ala-Pro
oligo-Arg	Arg ₆ ...Arg ₁₈
Tat-peptide	Tyr-Gly-Arg-Lys-Lys-Arg-Arg-Gln-Arg-Arg-Arg

MTS, Kaposi fibroblast growth factor (FGF)-derived membrane-translocating sequence.

Given the highly charged cationic nature of several CPPs (especially Tat and oligo-Arg), it is surprising that those are able to cross the lipophilic plasma membrane; despite the fact that the exact mechanism of membrane translocation of CPPs has been an object of thorough research, no consensus currently exists considering this issue. Endocytosis has been suggested as the major variant, further supported by several studies demonstrating the independence of cellular uptake of CPPs on temperature, receptors, or energy of ATP hydrolysis [Duchardt *et al.*, 2007; Watkins *et al.*, 2009]. However, other experiments have shown different mechanism of uptake at higher concentrations of CPPs, occurring at spatially restricted sites of the plasma membrane and leading to a rapid cytoplasmic distribution of CPPs without formation of endocytotic vesicles [Duchardt *et al.*, 2007; Watkins *et al.*, 2009]. All in all, it has been suggested that several mechanisms might be responsible for membrane translocation of CPPs, whereas the latter process may also be influenced by the cargo attached to the CPP. Considering the latter issue, the use of CPPs should be carefully guided, as cargo may influence the properties of CPP and *vice versa* [Fischer R. *et al.*, 2002]. For instance, the Tat-peptide has been shown to affect the affinity and selectivity of PCIs targeted to PKG, whereas recent studies indicated that the Tat-peptide itself acts as a potent PCI of PKC and PKA (IC₅₀ values of 22 nM and 1200 nM, respectively), and may also inhibit other representatives of AGC-group [Ekokoski *et al.*, 2010].

Another major concern from the aspect of intracellular applications of PCIs is the poor proteolytic stability of peptides composed of *L*-amino acids. The two major strategies to overcome this issue are represented by use of backbone-modified PCIs, or generation of peptidomimetics. The first strategy takes advantage of the fact that backbone-modified peptides may not be recognized by proteases, and therefore are more stable in complex biological systems; the main way of backbone modification is generation of enantio-, retro- or retro-inverso variants of the PCI (Figure 14) [Fischer P. M., 2003]. An enantio-peptide is composed of *D*-amino acids, whereas the sequence of AAs is exactly the same as in initial peptide; a retro-peptide, on the other hand, is composed of *L*-amino acids, but the sequence of amino acids in N → C direction of the retro-peptide corresponds to the same sequence of amino acids in C → N direction of the initial peptide. A retro-inverso peptide involves both changes of the initial peptide structure, being composed of *D*-amino acids with the reversed order of

amino acids in N \rightarrow C direction; such peptide may be regarded as a derivative of initial peptide where the relative topology of amino acid side-chains is maintained, but the backbone termini and the direction of peptide bonds is reversed [Fischer P. M., 2003]. All of these modifications may also be used just in some regions of the PCI, if the aim is to prevent the modification of the backbone of the whole molecule. Although an introduction of such profound changes into the structure of a PCI may raise doubts considering the affinity of the modified inhibitor, the backbone-modification strategy has proved its efficiency in several PCIs [Bonny *et al.*, 2001; Ricouart *et al.*, 1989; Phipps and Terreux, 2007; Wood J. S. *et al.*, 1996]. Probably the best illustration is represented by enantio- and retro-inverso variants of PKGI α -targeted DT-2 that had 15-fold and 2-fold lower K_i values, respectively, than DT-2 itself, and also possessed improved selectivity as well as enhanced cell membrane-penetrative properties [Nickl *et al.*, 2010].

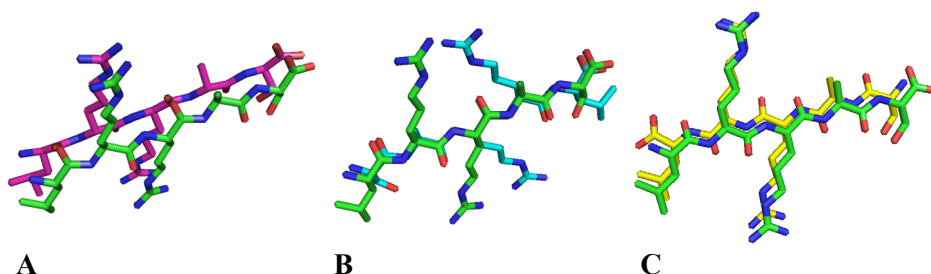


Figure 14. Backbone-modified variants of Leu-Arg-Arg-Ala-Ser peptide (the initial peptide is coloured green). (A) Enantio-variant (magenta). (B) Retro-variant (cyan). (C) Retro-inverso variant (yellow).

Peptidomimetics can be designed by the following ways (Figure 15A) [Grauer and König, 2009; Li S. and WenFang 2009]:

- modification of amino acid side-chains (*i.e.*, β -disubstitution for introduction of conformational restrictions);
- backbone modifications (*i.e.*, exchange/derivatization of N-H, C-H or C(=O) groups of backbone, extension of the peptide chains, or replacement of amide bonds);
- global restrictions (*i.e.*, head-to-tail or side chain-to-side chain cyclization).

Some of the backbone modifications could result in loss of chirality associated with replacement of $C\alpha$ atoms. For instance, in azapeptides (Figure 15C); synthesized from substituted hydrazines or hydrazides) the nitrogen atom is substituted for the $C\alpha$, and in peptoids Figure 15D; synthesized from bromoacetic acid and primary amines) the carbon atom corresponding to $C\alpha$ is not chiral (resembling Gly moiety) and the “side-chain” is attached to backbone nitrogen atom [Grauer and König, 2009]. Whereas elimination of chirality

provides several synthetic opportunities (*i.e.*, originating from the fact that deprotonation of C α would not cause enantiomerization), it may result in a considerable loss of affinity of PCI. However, peptidomimetics have been successfully applied as inhibitors of PKB; although being less potent than original peptidic inhibitors, these compounds demonstrate the potential of the whole peptidomimetic strategy [Collins, 2009; Tal-Gan *et al.*, 2010].

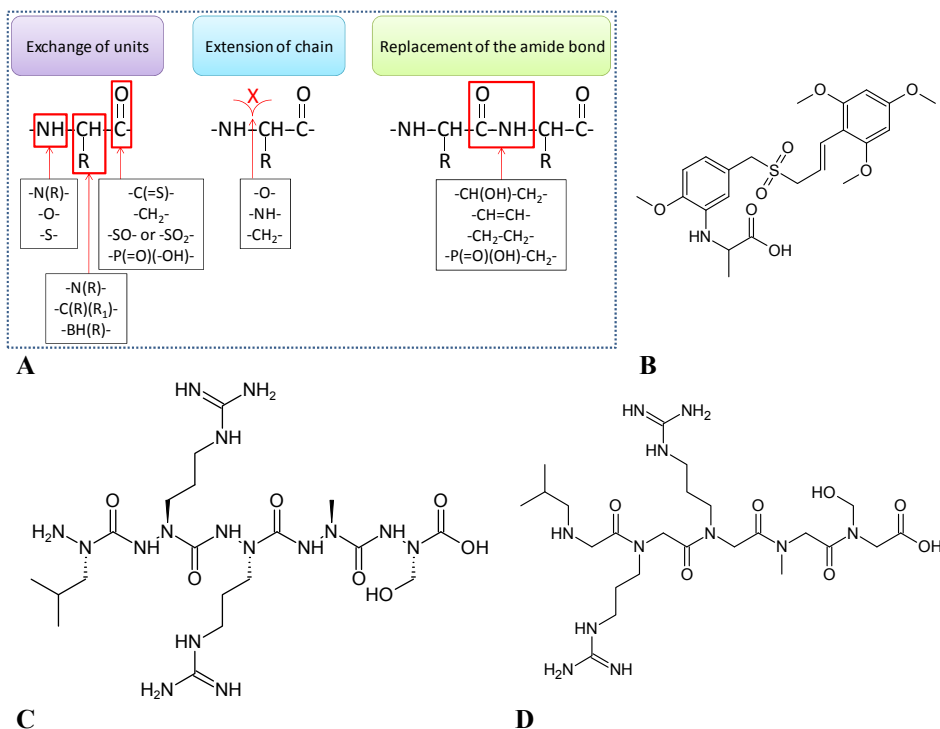


Figure 15. Examples of peptidomimetics and small molecular weight-PCIs. (A) Variants of peptidomimetics (adapted from [Grauer and König, 2009]). (B) ON012380 [Gumireddy *et al.*, 2005]. (C) Azapeptide variant of Leu-Arg-Arg-Ala-Ser peptide. (D) Peptoid variant of Leu-Arg-Arg-Ala-Ser peptide.

Finally, several small molecular weight-inhibitors have been recently discovered from screening of compound libraries, representing a variety of non-peptidic structures and expressing substrate-competitive inhibition patterns; the examples of PKs targeted by these compounds involve ERK, polo-like kinase-1, BCR-Abl, and IGFR1 [Bogoyevitch and Fairlie, 2007; Levitzki and Mishani, 2006]. One of the most potent small molecular weight-PCIs was the BCR-Abl inhibitor ON012380 (Figure 15B), possessing low nanomolar inhibition characteristics ($IC_{50} = 9$ nM), and inducing cell death at a 10 nM concentration of the inhibitor in cell lines expressing wild-type BCR-Abl or imatinib-resistant

Thr315Ile mutant BCR-Abl [Gumireddy *et al.*, 2005]. Moreover, ON012380 was effective in mice injected with cells expressing the T315I mutant, and showed no toxicity or other acute side-effects.

To sum up, the PCI strategies for inhibition of PKs have proved their efficiency both *in vitro* and *in vivo*, and are gradually evolving as physiologically active reagents in parallel to ACIs.

2.3.4. Reversible mono-ligand inhibitors. Special case: Allosteric inhibitors and inhibitors of activation

Apart from the design of ACIs and PCIs, another technique for the development of PK inhibitors is targeting remote sites and pockets not directly involved in catalytic functioning of kinases, *i.e.*, allosteric sites. Allosteric inhibitors (ALIs) do not directly compete with ATP⁶ or protein/peptide substrates but rather induce conformational changes in PK that indirectly lead to impedance of the phosphorylation reaction; thus, ALIs usually exhibit a non-competitive inhibition pattern *versus* both ATP and protein/peptide substrates [Bogoyevitch and Fairlie, 2007; Lewis *et al.*, 2008].

The binding sites of few ALIs have been determined after obtainment of the crystal structure of PK-ALI complexes. For instance, co-crystals of MEK1 and MEK2 with ATP and the allosteric inhibitor PD318088 (Figure 16A) revealed existence of a unique binding pocket adjacent to the ATP-site in kinases; this pocket probably also binds PD318088 analogue PD184352, which has demonstrated antiproliferative effects *in vivo* and is currently undergoing clinical trials [Ohren *et al.*, 2004]. Other methods for the identification of ALI binding sites involve the following approaches:

- deuterium-exchange mass-spectrometry (*i.e.*, applied for CMPD1 binding to p38 MAPK) (Figure 16B), [Davidson *et al.*, 2004]);
- proteolytic degradation and site-directed mutagenesis, *i.e.*, applied for polyoxometalates targeting CK2 [Prudent and Cochet, 2009], and for GNF-1 and GNF-2 targeting BCR-Abl (Figure 16C [Adrian *et al.*, 2006]);
- structure-activity relationships and molecular docking studies, *i.e.*, applied for thiadiazolidinone-derived ALIs binding to GSK3 β (Figure 16D, [Martinez *et al.*, 2002; Martinez *et al.*, 2005]) and for coumarine derivative G8935 inhibiting MEK1 (Figure 16E, [Han *et al.*, 2005]).

⁶ Type II-inhibitors are also frequently considered as allosteric, but in the context of given thesis the range of allosteric inhibitors is limited with compounds not binding to the catalytic cleft of PK.

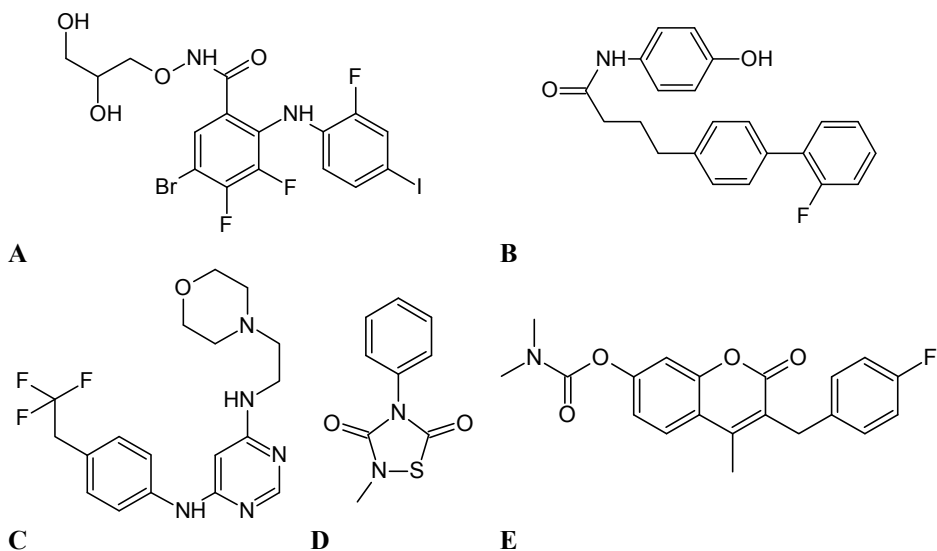


Figure 16. Examples of ALIs. (A) PD318088 [Ohren *et al.*, 2004]. (B) CMPD1 [Davidson *et al.*, 2004]. (C) GNF-1 [Adrian *et al.*, 2006]. (D) Compound 11 [Martinez *et al.*, 2002]. (E) G8935 [Han *et al.*, 2005].

By virtue of targeting unique pockets of PKs considerably less conserved than the catalytic cleft, ALIs are supposed to possess a higher selectivity than any other class of PK inhibitors. However, the development of ALIs is compromised by the fact that little is known about allosteric pockets of PKs as well as about structures of compounds that may fit these pockets. Historically, ALIs have been discovered as a result of screening of compound libraries, whereas the allosteric nature of inhibition of these compounds has been proven only during subsequent studies [Bogoyevitch and Fairlie, 2007; Lewis *et al.*, 2008].

Another class of compounds binding outside the catalytic cleft is represented by inhibitors of PK activation, which target pockets of catalytic or regulatory domains/subunits responsible for recognition of co-factors and secondary messengers. A well-known family of activation inhibitors is constituted by analogues of cyclic nucleotides, which interact with cyclic nucleotide-binding regions of PKAr and regulatory domains of PKG and thus stabilize interactions between the regulatory subunit/domains and the corresponding catalytic subunits. The examples of cyclic nucleotide analogues inhibiting activity of PKs (Figure 17A–B) involve Rp-cAMPS, Rp-8-Br-cAMPS, Rp-8-pCPT-cGMPS, Rp-8-Br-cGMPS and Rp-8-Br-PET-cGMPS; all of those share two structural features, presence of a sulfur atom bound to phosphorus and an R-configuration of the corresponding phosphorus atom [Anand *et al.*, 2010; Butt *et al.*, 1995; Poppe *et al.*, 2008; Smolenski *et al.*, 1998; Wei *et al.*, 1998]. Within these compounds, the best affinity as well as selectivity towards its target is possessed by Rp-8-Br-PET-cGMPS with a K_i value of 35 nM towards PKGI α and an over

500-fold selectivity *versus* PKA α I [Hofmann *et al.*, 2009]. In general, cGMP analogues demonstrate better selectivity towards PKG *versus* PKA α r than cAMP analogues towards PKA α r *versus* PKG, revealing the same trend as in case of cGMP and cAMP themselves. This fact has been attributed to the presence of single Thr177 residue in PKGI α (Ala211 in PKA α r), which specifically interacts with the 2-amino position of cGMP guanine base [Shabb and Corbin, 1992].

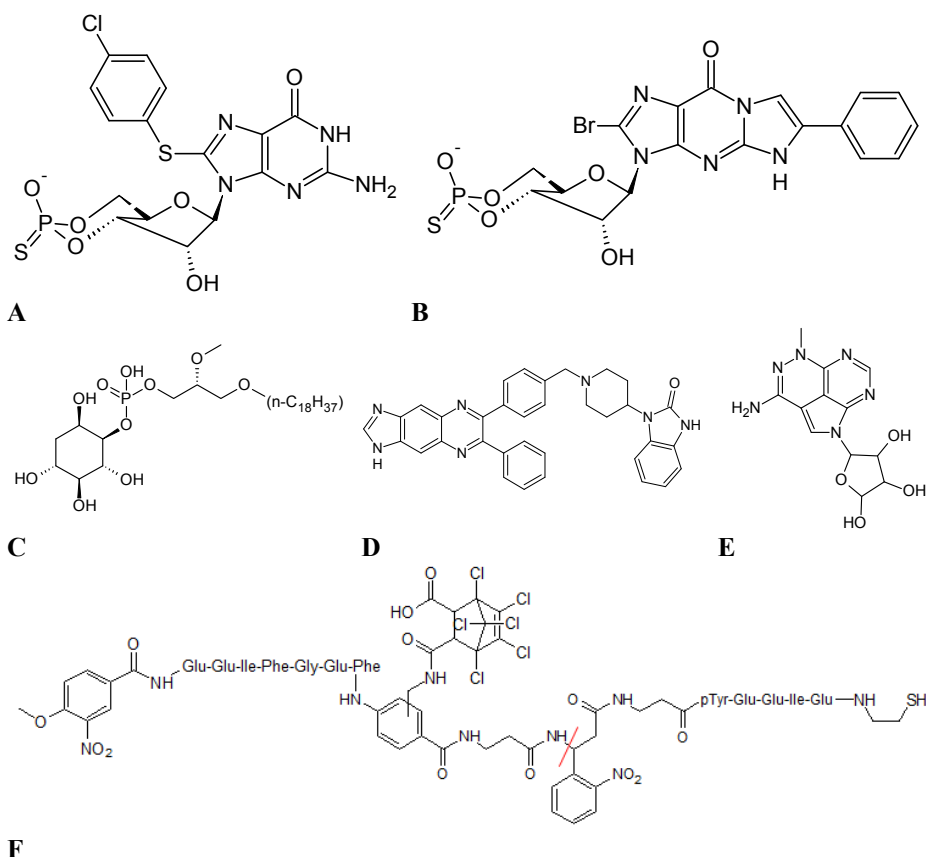


Figure 17. Examples of inhibitors of PK activation. (A) Rp-8-pCPT-cGMPS [Wei *et al.*, 1998]. (B) Rp-8-Br-PET-cGMPS [Butt *et al.*, 1995]. (C) DPIEL (PX-316) [Collins, 2009]. (D) AKT-I-1,2 [Lindsley *et al.*, 2005]. (E) API-2 (TCN) [Cheng J. Q. *et al.*, 2005]. (F) Compound 13 [Priestman and Lawrence, 2010]; red line indicates the position where bond is broken upon irradiation.

The PH-domain of PKB has also served as an attractive pocket for inhibitors preventing PKB activation by interfering with binding of PtdInsP₃, which recruits PKB to the plasma membrane. Currently, PH-targeting PKB inhibitors constitute a large group of compounds (Figure 17C–E) involving PtdInsP₃ analogues (*i.e.*, DPI, DPIEL, DCIEL, *etc.*), piperidiny benzimidazolone deriva-

tives (*i.e.*, AKT-I-1, AKT-I-2, and AKT-I-1,2), di- and tricyclic nucleosides (*i.e.*, API-1, API-2, TCN-P), benzene tetrakisphosphate, and alkylphospholipid perifosine (D-21266) [Bogoyevitch and Fairlie, 2007; Cheng J. Q. *et al.*, 2005; Collins, 2009; Kim D. *et al.*, 2010; Yang L. *et al.*, 2004]. Practically all of these compounds have demonstrated not only *in vitro* inhibition of PKB, but also showed antitumor effects in mice xenograft models; additionally, most compounds have been tested with PKB mutants lacking the PH-domain or myristoylated PKB (not requiring PtdInsP₃ for association with membrane) and exhibited either absent or considerably reduced affinity. Out of this set, the best properties from the aspect of inhibition potency and selectivity are possessed by AKT-I-1, AKT-I-2, and AKT-I-1,2, which are not only selective *versus* other kinases, but also distinguish between the isoforms of PKB. AKT-I-1 inhibits potently only PKB α (IC₅₀ = 760 nM), AKT-I-2 only PKB β (IC₅₀ = 325 nM), and AKT-I-1,2 both PKB α and PKB β (IC₅₀ values of 58 nM and 210 nM, respectively) but not PKB γ [Lindsley *et al.*, 2005; Zhao *et al.*, 2005].

Other examples of PK inhibitors preventing activation include cyclic peptides that disrupt the interactions between the CK2 catalytic and regulatory subunit, cyclic peptides and cyclin A-derived peptides that block binding of cyclin A to Cdk2, and compounds containing phosphorylated Tyr moieties or their analogues recognized by SH2 domains of various PKs [Bogoyevitch *et al.*, 2005; Parang and Sun, 2004; Prudent and Cochet, 2009]. The SH2-targeting compounds have also served as caged sensors of Lck (K_d values of 127 μ M and 2.6 μ M for caged and uncaged forms, respectively), and as photo-deactivatable probes of Src with photolabile moiety positioned between the inhibitor fragments targeting SH1 and SH2 sites of PK (Figure 17F) [Li H. *et al.*, 2008; Priestman and Lawrence, 2010]. The latter compounds (K_i value of 26 nM for the most potent representative) were cleaved into two fragments by photolysis, resulting in a 50-fold decrease of affinity; this rationale illustrated well the idea of affinity enhancement by linking two fragments targeting different sites of PKs, which had given stimulus for the development of biligand inhibitors.

2.3.5. Reversible biligand inhibitors.

Special case: Bisubstrate inhibitors

Biligand inhibitors are compounds that contain two interlinked fragments, whereas each fragment binds to one site of a target PK. The group of biligand inhibitors comprises compounds that target only sites distant from the catalytic core of PKs (*i.e.*, SH1 and SH2, or SH2 and SH3), the compounds which bind with one fragment targeting the distant site and another fragment targeting one of the sites in the catalytic core (*i.e.*, either ATP-site of protein/peptide substrate-site), and bisubstrate inhibitors [Parang and Cole, 2002a; Shen *et al.*, 2005].

Bisubstrate inhibitors (BSIs) constitute a sub-group of biligand inhibitors that incorporate two interlinked fragments targeting the binding site for ATP and the binding site for protein/peptide substrate, respectively. By virtue of

association with two sites of which one (ATP-site) enables development of multiple strong interactions and another (protein substrate-site) is responsible for selective recognition of ligands, BSIs should hypothetically be endowed with both, high affinity and high selectivity towards their PK-targets [Schneider *et al.*, 2005]. The realization of those hypothetic advantages presupposes exact pinpointing of crucial interactions without entropic penalty, which in turn necessitates the precise design of BSIs. Historically, the basic principles of BSI design have been connected to two methodologies widely used for drug development, the fragment-based drug design and the transition-state analogue inhibitor approach [Borsi *et al.*, 2010; Wolfenden, 1972].

The leading concept of the fragment-based approach implies that a high-affinity inhibitor can be constructed by tethering with a suitable linker two or more fragments (ligands) that bind to separate yet adjacent sites [Borsi *et al.*, 2010; Gill, 2004]. The fragment-based inhibitor discovery thus relies on the initial identification of moieties that bind to different sites of the target PK, and subsequent covalent linkage of these moieties. The choice of fragments in the initial step is generally performed by screening of large fragment libraries by NMR, by computational approaches, or by summarizing data from crystallographic studies; typically, the molecular weight of a fragment is below 150 Da [Akritopoulou-Zanze and Hajduk, 2009; Hajduk *et al.*, 2005; Vieth *et al.*, 2009]. The examples of two main approaches used for the conjugation of fragments are as follows [Akritopoulou-Zanze and Hajduk, 2009; Morphy, 2010]:

- “front-to-back”-mechanism when a hinge-binding fragment is first established and the rest of the compound is “grown” by the attachment of fragments targeting more distal sites;
- the opposing “back-to-front”-mechanism where expectedly selective fragment targeting a distal site is first identified and subsequently connected to less selective but more potent moieties.

Provided that the fragments and the linker(s) are properly arranged, the net binding free energy change of the formed conjugate (ΔG_B) should be equal to the sum of changes of the binding free energies of the fragments (ΔG_1 and ΔG_2) plus an additional linking gain (ΔG_L) according to Equation 12. The latter term is primarily explained by the relative entropic gain resulting from the interaction of a single molecule rather than multiple fragments with the protein molecule, which may contribute to the net increase in conjugate affinity (as compared to affinities of the initial fragments) up to three orders of magnitude [Borsi *et al.*, 2010]. Moreover, ΔG_L may reflect other effects, such as:

- unfavorable enthalpic contributions that arise from distortions of the fragment binding geometry;
- unfavorable entropic contributions originating from increased conformational flexibility in case of longer linkers (if the connected fragments bind to spatially distal sites);
- unfavorable or favorable interactions between the linker and the target;
- positive synergistic effects upon binding of one fragments of the conjugate.

$$\Delta G_B = \Delta G_1 + \Delta G_2 + \Delta G_L$$

Equation 12. The relationship between the change of the net binding free energy of the conjugate and the changes of the binding free energies of the fragments composing the conjugate.

The concept of the transition-state analogue inhibitor approach, on the other hand, lies in the notion that if enzymes *per se* are supposed to facilitate reaching the transition state for the reaction, they should possess especially high affinity towards the altered substrate in the transition state, exceeding that towards the initial form of the substrate [Wolfenden, 1972]. Consequently, PK inhibitors that are composed of two substrate-mimicking fragments should utilize the features of the PK-catalyzed reaction between the initial substrates. The first kinase inhibitors designed according to the transition-state analogue approach were reported in 1973, and since then this paradigm has been widely applied for the development of PK inhibitors [Lienhard and Secemski, 1973].

The first PK inhibitors utilizing ATP fragment were represented by the PKAc-targeted BSI composed of ATP linked to the PKAc substrate Kemptide *via* the oxygen atom of the Ser side-chain incorporated in Kemptide [Medzih-radszky *et al.*, 1994], and EGFR inhibitors composed of sulfobenzoyl-adenosine moieties linked covalently to small peptides *via* side-chain of the Tyr residue incorporated in peptide structures [Rosse *et al.*, 1997]. Unfortunately, all of these conjugates showed low affinity towards their target PKs, which in subsequent works was attributed to the utilization of a wrong model of the transition state for the phosphorylation reaction. On the basis of experimental studies with Tyr-kinases, it was proposed that PKs generally utilize the dissociative mechanism of phosphoryl transfer, hence the distance between the entering slightly nucleophilic oxygen and the attacked phosphorus should be over 4.9 Å [Kim K. and Cole, 1998]. The IRK-targeting inhibitor modified according to the latter model by introduction of the linker (Figure 18A) had considerably higher affinity (K_i value of 370 nM) than the composing fragments, ATP and substrate peptide (K_m values of 71 μM and 280 μM, respectively) [Parang *et al.*, 2001]. Later on, analogical constructs of ATP conjugated with substrate peptides or their analogues *via* short linker were designed as BSIs of PKAc (K_i value of 3.8 μM [Hines and Cole, 2004]), Csk (IC_{50} value of 600 nM [Shen and Cole, 2003]), CAMK-II (IC_{50} value of 22 nM [Ahn *et al.*, 2007]) or CDK2 (K_i value of 0.83 nM [Cheng K.-Y. *et al.*, 2006]). The latter compound (Figure 18B) represented a multiligand rather than a biligand class of inhibitors, as the fragment of the applied substrate peptide contained not only sequence binding to the protein/peptide substrate-site, but also the recognition motif Arg-Xaa-Leu which binds to the distal site located on CDK-2 activator cyclin A [Cheng K.-Y. *et al.*, 2006].

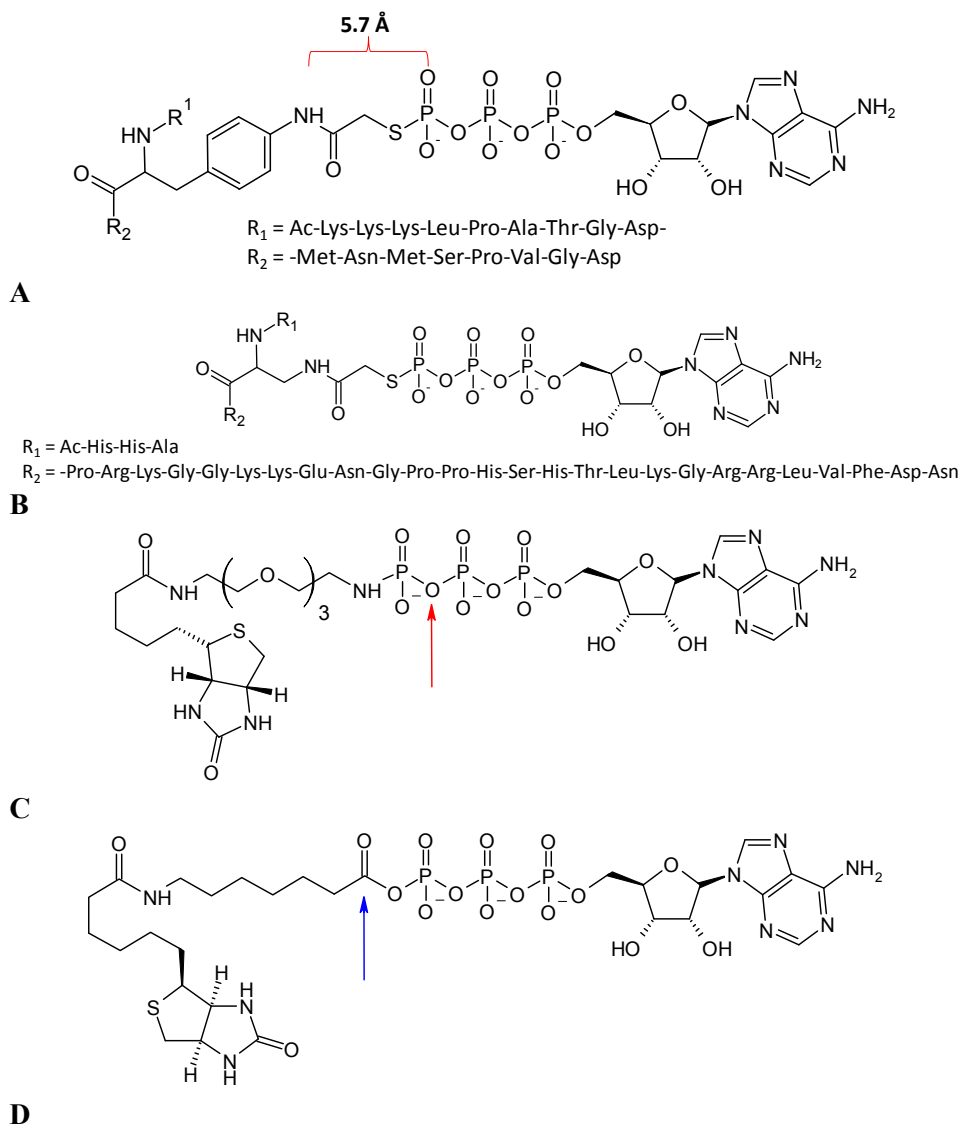


Figure 18. Examples of BSIs incorporating the ATP moiety. (A) Compound 2 [Parang *et al.*, 2001]. (B) CDC6 bispeptide [Cheng K.-Y. *et al.*, 2006]. (C) Compound 1b [Green and Pflum, 2007]; red arrow indicates the beginning of chain transferred to the hydroxyl group of phosphorylatable residue of a substrate. (D) BHAcATP [Patricelli *et al.*, 2007]; blue arrow indicates the beginning of chain transferred to the Lys residue of a PK.

Interestingly, recent studies have demonstrated that a conjugate where biotin was covalently attached to the γ -phosphorus of ATP *via* a hydrophobic flexible linker incorporating a nucleophilic NH group (Figure 18C) served as reagents for biotinylation of PK substrates, as PKs from different groups of kinome (*i.e.*, PKAc, CK2 and Abl) catalyzed transfer of biotin-modified phosphoryl groups from the conjugate to the substrate peptides [Green and Pflum, 2007]. By contrast, an analogical conjugate of biotin and ATP where the linker was shorter and incorporated an electrophilic carbonyl group (Figure 18D) could be applied for biotinylation of PKs themselves [Patricelli *et al.*, 2007]. The latter conjugate enabled biotinylation of an amazing amount of ATP-utilizing proteins, whereas 394 PKs from different proteomes were labeled [Patricelli *et al.*, 2007]. The mechanism of the biotinylation reaction involved attack of the highly conserved lysine residues in the catalytic cleft of kinases (corresponding to Lys 72 and Lys168 of PKAc) on the electrophilic center of the conjugate, causing covalent attachment of the linker-biotin moiety to the kinase *via* amide bond [Patricelli *et al.*, 2007].

The next step in the development of BSIs was the elimination of phosphoryl groups of ATP. The best-studied compounds of this type are probably exemplified by adenosine analogue-oligoarginine conjugates (ARCs); ARCs have evolved as a variety of structures, according to which these conjugates have been grouped into several “generations” [Lavogina *et al.*, 2010a]. Generations ARC-II and ARC-III constitute the object of investigation of the current thesis, and will be discussed in detail in the following sections; generation ARC-I is composed of conjugates consisting of adenosine-4'-dehydroxymethyl-4'-carboxylic acid moiety (Adc) and oligo-(L-arginine) joined by hydrophobic flexible linkers [Loog *et al.*, 1999]. The most potent representative of ARC-I generation possessed an IC₅₀ value of 700 nM towards PKAc (Figure 19A). It was also shown that ARC-I compounds could be derivatized with fluorescent dyes (Bodipy FL, TAMRA), PEG and biotin without remarkable loss of affinity of the conjugates, and applied as affinity supports for isolation and extraction of PKAc and other basophilic PKs from biological systems [Loog *et al.*, 2000; Uri *et al.*, 2002; Viht *et al.*, 2003]. Moreover, by virtue of incorporation of oligo-arginine, ARC-Is penetrated successfully plasma cell membrane and inhibited ROCK in living cells [Räägel *et al.*, 2009].

Logically, ATP moiety is not the only fragment to be incorporated into the composition of bisubstrate inhibitors of PKs. First of all, application of other nucleoside-triphosphate moieties and their analogues (*i.e.*, deoxy-variants) is possible, as it has been demonstrated that several PKs may utilize other phosphoryl donors than ATP, and large-scale utilization of ATP in the cellular signaling should primarily be attributed to the high concentration of the latter [Shugar, 1996]. Secondly, nucleoside-triphosphates and their close analogues do not possess high affinity towards PKs, whereas according to Equation 12, the higher affinity of the fragments is, the better is the binding of the conjugate. Thus, it would be more considerable to use potent ATP-competitive inhibitors than the ATP-site targeting fragments of BSIs.

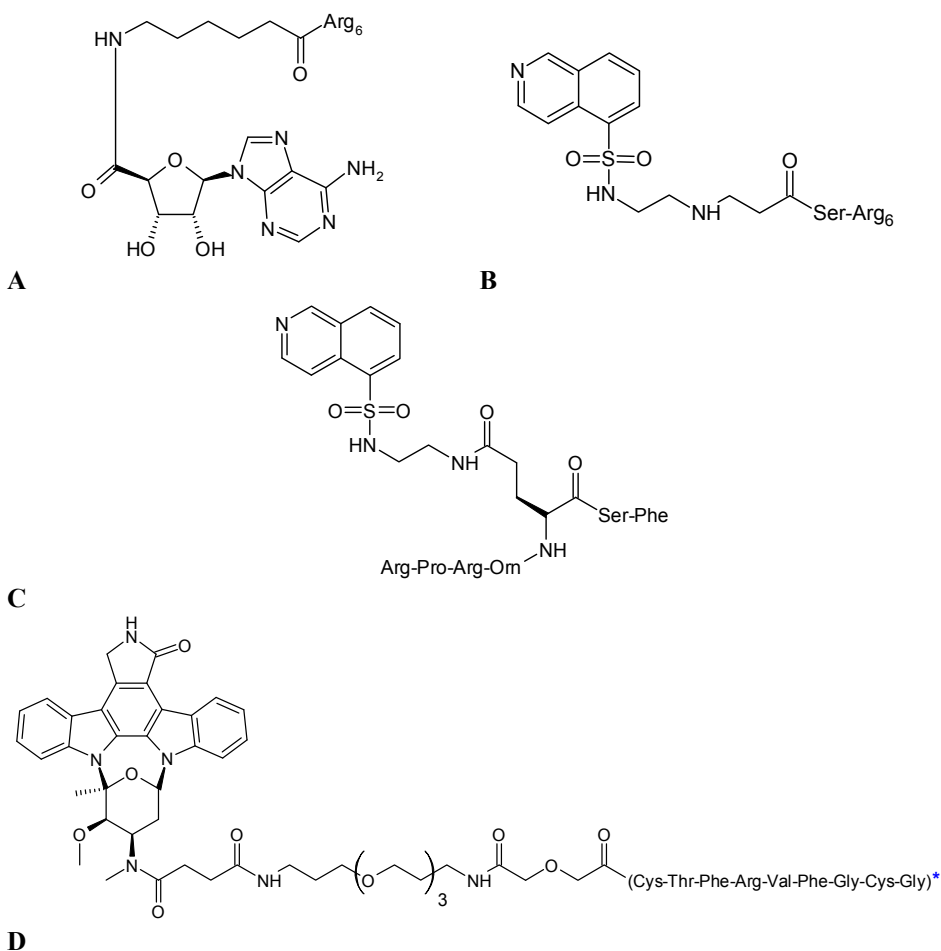


Figure 19. Examples of BSIs incorporating adenosine analogues. (A) Compound VII [Loog *et al.*, 1999]. (B) Compound 17 [Ricouart *et al.*, 1991]. (C) PTR-6132 [Livnah *et al.*, 2003]; Orn = ornithine. (D) Compound 1a [Shomin *et al.*, 2009]; * cyclic peptide generated *via* formation of S-S bond between the side-chains of Cys residues; the cyclic peptide fragment attached to the rest of the conjugate *via* the N-terminus of the Cys residue.

Indeed, the latter rationale has yielded several potent PK inhibitors, the first examples represented by conjugates of H-series inhibitors with oligo-arginine peptides; the most potent of these compounds (Figure 19B) possessed a K_i value of 100 nM towards PKC and 4 nM towards PKAc [Ricouart *et al.*, 1991]. Isoquinoline moieties have also been applied in conjugates with PKB-selective peptides to generate potent BSIs targeted to PKB; one of the most potent compounds (Figure 19C) exhibited a high affinity towards PKB (IC_{50} value of 20 nM) as well as PKAc, and efficiently inhibited cell growth of cancer cells [Livnah *et al.*, 2003; Livnah *et al.*, 2004]. The ATP-competitive inhibitor

staurosporine as well as its derivatives have also been used for the design of BSIs targeting CDK, PKC, or PKAc, whereas the most promising results from the aspect of both, affinity and selectivity, were achieved for PKAc-targeted BSIs [Schneider *et al.*, 2005; Shomin *et al.*, 2009]. The latter compounds involved a conjugate of the staurosporine derivative K252a with miniature protein derived from the recognition epitope of PKI, and a conjugate of another staurosporine derivative with cyclic peptide discovered from the phage-displayed library (Figure 19D); both conjugates possessed low nanomolar inhibition potencies towards PKAc (IC_{50} values of 3.6 nM and 2.6 nM, respectively) [Schneider *et al.*, 2005]. Moreover, both conjugates were profiled *versus* a panel of PKs and revealed enhanced selectivity towards PKAc; the latter phenomenon was especially pronounced in the case of K252a conjugate, which demonstrated an over 180-fold selectivity towards PKAc *versus* other tested PKs [Schneider *et al.*, 2005]. All in all, large increase in the selectivity of conjugates as compared to the corresponding non-selective staurosporine derivatives used as ATP-mimicking fragments confirms the hypothesis that BSIs may indeed join the advantages of highly potent ACIs and selective PCIs, and therefore represent one of the most attractive strategies for the development of PK inhibitors.

METHODS

This part will briefly introduce the principles, advantages and limitations of the main methods used for the accomplishment of the given thesis. Starting from the insight into compound synthesis *via* utilization of solid phase synthesis approach, the review will proceed to the biochemical *in vitro* assays for the measurement of inhibitory and affinity properties of PK inhibitors, focusing on the techniques with fluorescence detection. Finally, a highlight of protein crystallography will be provided, exemplified by a more detailed analysis of (co-)crystal structures of PKAc.

I. Solid phase peptide synthesis

The principle of solid phase peptide synthesis (SPPS) was introduced in 1963 by R. B. Merrifield [Merrifield, 1963], and the synthesis of compounds on solid phase has subsequently become an extremely popular technique not only for obtaining peptides, but also peptide analogues (*i.e.*, peptoids, azapeptides) oligonucleotides, *etc* [Desai *et al.*, 1994; Obrecht and Villalgorido, 1998]. The basic idea behind the SPPS protocol lies in the fact that a growing chain composed of monomers is covalently attached *via* one terminus to the porous insoluble solid support (so-called resin), so that each next monomer is incorporated only to the “free” terminus of the chain [Benoiton, 2005; Chan and White, 2000].

In order to understand the ultimate advantages of SPPS, one first needs to consider the structural crotchet of amino acids, namely incorporation of a nucleophilic amino group and an electrophilic carboxyl group within one amino acid molecule. Such combination of two mutually reactive fragments within one molecule necessitates the use of the so-called protective groups, *i.e.*, the entities that are conjugated with potentially reactive centers in the molecule in order to render the latter non-reactive until the protective group is removed [Green and Wuts, 1999]. In case of the “classical” solution synthesis methods, the obtainment of each peptide bond therefore presupposes protection of two groups:

- the protection of the amino acid at the N-terminus of forming the peptide bond (by groups withdrawing electron density),
- and the protection of the amino acid at the C-terminus of forming the peptide bond, to avoid the formation of by-products (by groups increasing electron density).

In SPPS, however, one of the termini (usually the C-terminus) of the growing chain is permanently protected by the insoluble resin bead until the whole chain is synthesized and then removed (cleaved) from the resin (Figure 20). Thus, the isolation of the intermediate product after every step of SPPS is usually performed barely by filtration, whereas the remaining reagents and by-products of the synthesis are flushed away. The latter fact in turn enables utilization of

high concentration of the reagents, which according to the mass law increases the rate of the reaction. On the other hand, the use of large amount of reagents and solvent increases the cost of SPPS; however, this downside is compensated by the high yield (usually, over 99% yield of each coupling step) and quickness [Benoiton, 2005; Chan and White, 2000].

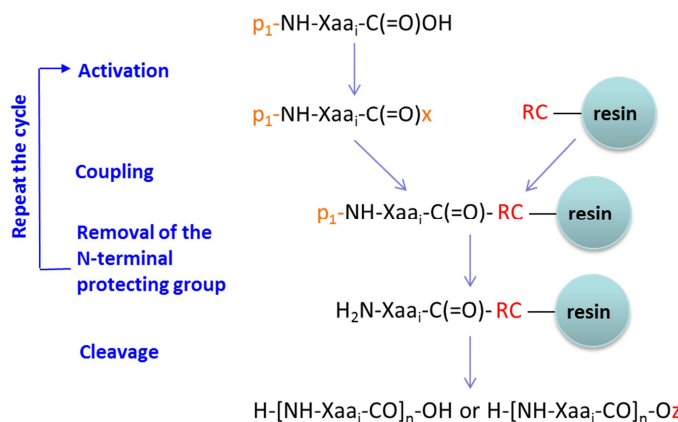


Figure 20. Scheme of SPPS. p_1 , N-terminal protecting group; x , activated C-terminus; RC, reaction center or growing chain; z , part of the initial reaction center of the resin (*i.e.*, amine group).

The question of the utmost importance for SPPS is the choice of the resin, formed by the polymeric beads usually composed of cross-linked polystyrene, polyacrylamide, or polyethylene glycol [Benoiton, 2005; Chan and White, 2000; Sigma-Aldrich® Resin Explorer]. Additionally, the beads bear the so-called reaction centers, where the growth of the peptide chain is initiated; dependent on the structure of the reaction center of the resin and on the cleavage conditions, part of the reaction center may remain attached to the resin, or become conjugated with the C-terminus of the growing chain after the cleavage. The amount of the reaction centers on and in the bead as related to the mass of the bead is expressed as loading, whereas the optimal loading number is dependent on the certain synthesis. If the loading number is high (2... 3 mmol/g), the density of the growing chains per bead will also be high, which may restrict the diffusion of reagents into and between the beads, and cause incomplete coupling of sterically hindered growing chains. On the other hand, the low loading number (below 0.1 mmol/g) will result in a low amount of the final product, as the loading also shows the maximal amount of the final product released after the cleavage per mass of the resin initially taken for the synthesis. The additional important criteria for the resin choice are as followed:

the resin must be physically stable, possess chemical inertness towards all reagents except those used for the attachment of the first monomer residue and for the final cleavage, and demonstrate good swelling in the solvent used for the synthesis. The most popular solvents are aprotic, and dependent on the synthesis may be either more or less polar (*i.e.*, *N,N*-dimethylformamide or dichloroethane, respectively), to secure good solubility of all applied reagents [Benoiton, 2005; Chan and White, 2000].

Each monomer added to the growing chain is generally initially protected at the terminus that should not participate in the coupling reaction. Thus, after the coupling, the growing chain is blocked on one terminus (usually, C-terminus) with the resin and on the other terminus (usually, N-terminus) with the protecting group, whereas the latter is removed prior to coupling of the new monomer. Additionally, as the side-chains of amino acids frequently bear other functional groups, side-chain protecting groups are also required. Importantly, the group protecting N-terminus should be removable in conditions different to those where side-chain protecting groups are removed or where the cleavage of the final product from the resin is performed; this orthogonality requirement is usually fulfilled by application of either the Boc- or the Fmoc-strategy (Figure 21) [Benoiton, 2005; Chan and White, 2000]. In the former, the Boc-group is used as the N-terminal protecting group that is be removed by treatment with trifluoroacetic acid, whereas the cleavage of the product is performed by HF; in the latter, Fmoc-group is used as the N-terminal protecting group removable by a weak base, usually piperidine, whereas the cleavage of the product is performed by treatment with trifluoroacetic acid [Greene and Wuts, 1999]. Thus, the Fmoc-strategy utilizes milder conditions, but is also more susceptible to side-reactions due to involvement of a base (*i.e.*, racemization of chiral amino acids caused by deprotonation of C α during the Fmoc-deprotection steps) [Benoiton, 2005].

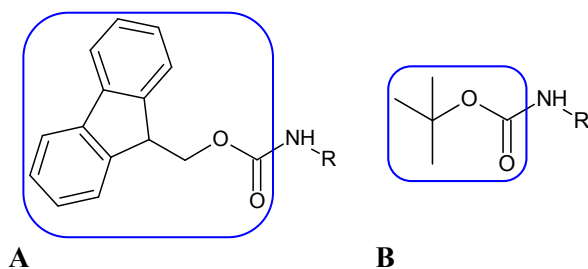


Figure 21. Structures of the most popular N-terminal protecting groups in SPPS. (A) Fmoc. (B) Boc.

The addition of a new monomer to the growing chain is comprised with the aid of the so-called activators. As the reaction between the carboxyl group and the amine group resulting in formation of the amide bond is associated with a very

high activation energy barrier, it is necessary to convert the carboxyl group to more reactive species (*i.e.*, *O*-acylisourea or triazol ester) prior to coupling [Benoiton, 2005; Chan and White, 2000]. This task is accomplished by addition of one or several activating reagents to the coupling mixture (Figure 22), which are afterwards removed during the washing step. In order to avoid the side-reactions originating from the excess reactivity of the activators, the amount of activators should be in general smaller than that of the monomer added to the growing chain.

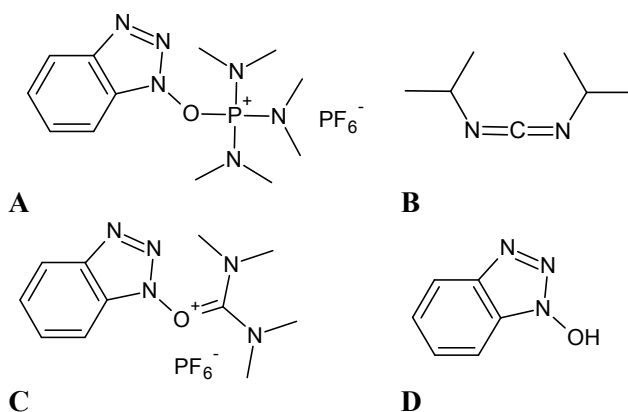


Figure 22. Structures of activators. (A) BOP. (B) DIC. (C) HBTU. (D) HOBt.

Probably the most pronounced downside of SPPS is the poor opportunity to monitor the course of reactions, as the resin bead interferes with the detection and quantification of the intermediate products attached to the resin. Despite the fact that several spectroscopic methods (*i.e.*, IR) have been suggested as possible variants for the establishment of the on-resin products, the most widespread techniques are still qualitative or semi-quantitative tests determining the presence or absence of certain chemical groups on the resin or in the solution collected from the resin (such as Kaiser-test or Fmoc-deprotection test) [Chan and White, 2000; Yan, 1998]. These tests utilize compounds that upon reaction with the isolated resin bead or the solution collected from the resin generate products with specific spectral properties (*i.e.*, a certain UV-VIS absorbance maximum), which are subsequently detected by a suitable technique. An alternative method is the isolation of a small portion of resin from the reaction vessel, cleavage of intermediate products, and subsequent qualitative or quantitative analysis (*i.e.*, by mass-spectroscopy); however, the latter variant is not suitable for the continuous usage, as it would remarkably decrease the net yield of the synthesis.

It should also be mentioned that the maximal size of the peptide “under construction” is limited in SPPS, in order to maintain the high yield of each

coupling step; the maximal number of monomers is dependent on the resin loading and on the structure of monomers, but is generally below 70 amino acids [Chan and White, 2000]. Still, longer chains may be obtained by separate synthesis of shorter fragments followed by the subsequent ligation. Moreover, several advancements in the field of SPPS (especially automation) have contributed to the development of other techniques enabling synthesis of large compound collections (libraries), either by parallel synthesis or by combinatorial approaches [Lam *et al.*, 1997; Maillard *et al.*, 2009; Obrecht and Villalgordo, 1998; Shin *et al.*, 2005]. Furthermore, combination of SPPS with solution synthesis (*i.e.*, where some fragments are synthesized in solution and subsequently conjugated with the growing chain on resin) provide additional possibilities for the synthesis of structurally variable compounds, such as conjugates of peptides or peptide analogues with (oligo)nucleotides, *etc* [Bonke *et al.*, 2008; Wu Y. and Xu, 2000].

2. Biochemical *in vitro* assays for the assessment of PK inhibitors

2.1. Inhibition assays versus binding assays

The biochemical *in vitro* assays for the assessment of PK inhibitors can be divided into two main groups according to the characteristics measured, inhibition assays and binding assays. The former group of assays takes advantage of the phosphorylation reaction catalyzed by the PK of interest, whereas the reference (non-inhibited) reaction is performed in the absence of an inhibitor and the trial reaction in the presence of the inhibitor. Generally, inhibition assays are performed in a form of kinetic studies, where the PK-catalyzed reaction (either in the absence or in the presence of the inhibitor) is artificially stopped at a certain point of time, *i.e.*, by dilution into concentrated acid; the phosphorylated product is subsequently isolated and quantified. Inhibition assays therefore measure the ability of the inhibitor to block the catalytic properties of PK and thus reduce the amount of the phosphorylated product formed (until the reaction was stopped). Additionally, from the non-inhibited reaction the activity of the PK in the given experiment may be established [Hastie *et al.*, 2006; Segel, 1993]. By variation of the concentration of the phosphoryl donor or phosphoryl acceptor in the presence of the same concentration of the kinase and inhibitor, it is also possible to determine the inhibition mechanism of the compound under investigation *versus* ATP or *versus* protein/peptide substrate, respectively [Segel, 1993].

As inhibition assays allow a direct determination of the ability of the inhibitor to protect the protein/peptide substrate from the phosphorylation (the ultimate goal of development of PK inhibitors), this group of biochemical *in vitro* assays have become a “classical” method for the characterization of PK inhibitors [Hastie *et al.*, 2006; Ma H. *et al.*, 2008]. However, their time-

consuming and multi-step nature, as well as the requirement for application of phosphoryl donor and phosphoryl acceptor, has triggered the search for and development of alternative assays more compatible with the HTS format, *i.e.*, binding assays [Degorce *et al.*, 2009].

In contrast to the inhibition assays, the binding assays do not utilize the PK-catalyzed reaction and thus do not require a phosphoryl donor or a phosphoryl acceptor; instead, the amount of a ligand (*i.e.*, an inhibitor) bound to the PK is detected *via* change of physical or physico-chemical characteristics of the system. Generally, the binding assays are performed at equilibrium conditions, and can be performed in direct binding format or displacement (competition) binding format [Segel, 1993]. While the former format allows determination of the degree to which the inhibitor is able to bind to the PK of interest (*i.e.*, the affinity of the inhibitor), the latter format measures the ability of the inhibitor to compete for binding to a PK with a ligand with previously determined affinity. Apart from assessment of the affinity characteristics, binding assays also enable determination of the PK site where the compound binds if the displacement of compound under investigation is performed by a ligand targeted to a certain binding site of a PK. While binding assays are generally less time-consuming and better amenable to automation than the inhibition assays, the major disadvantage of binding assays has been low affinity of ligands used in the displacement format experiments [Huang X., 2003], which in turn necessitates high consumption of the PK and limits the range of affinities of displacing compounds that can be reliably established. However, the recent advances in the field of PK-targeting compounds as well as detection techniques have remarkably dissipated the latter issues [Brown M. J., 2008; Degorce *et al.*, 2009; Lebakken *et al.*, 2007; Li Y. J. *et al.*, 2008].

The detection techniques are shared by both inhibition and binding assays, whereas the most common detection methods are radiometric and spectrophotometric [Li Y. J. *et al.*, 2008; Technikova-Dobrova *et al.*, 1991; Uri *et al.*, 2010]. The latter category includes fluorescence techniques, which have increasingly grown in number and popularity due to their low quantification limit and applicability for the *in vitro* assays in living cells and tissues.

2.2. Radiometric methods

Since the 1970s when first introduced for PKAc [Handa and Johri, 1977; Adelstein *et al.*, 1978], the majority of radiometric PK assays have been performed in a form of kinetic assays where the PK-catalyzed phosphorylation reaction is carried out in the presence of β -radioactive $\gamma^{32}\text{P}$ -ATP or $\gamma^{33}\text{P}$ -ATP mixed with non-radioactive ATP. As a result of the phosphorylation reaction, a fraction of the phosphoryl moieties introduced into substrate protein/peptide is also endowed with β -radioactivity; the phosphorylated substrate molecules are isolated from the reaction mixture and the amount of incorporated radioactive

phosphoryl is quantified by scintillation counting [Hastie *et al.*, 2006; Ma H. *et al.*, 2008].

The isolation step is most crucial for the whole strategy, as the method presupposes elimination of the non-reacted radioactive ATP from the mixture. Usually, the isolation of phosphorylated protein/peptide substrate is performed *via* dilution of the reaction mixture into concentrated phosphoric acid, and subsequent filtration through phosphocellulose paper. The latter is negatively charged and binds the protein/peptide substrates that are in turn positively charged due to protonation of basic amino acid side-chains after treatment with phosphoric acid (in order to bind to phosphocellulose paper, the substrates should possess a minimal charge of +2). The small peptide substrates that do not contain basic amino acid residues are modified prior to application in the given assay by addition of 2...3 Lys residues to the N-terminus or to the C-terminus of the substrate (*i.e.*, into positions where Lys would not interfere with binding of peptide substrate to the PK) [Hastie *et al.*, 2006]. The negatively charged ATP binds to the phosphocellulose filter only to the minor extent.

Recently, a new format of $\gamma^{32}\text{P}$ -ATP -based radiometric kinetic assay was introduced under the name scintillation proximity assay [PerkinElmer Scintillation Proximity Assay (SPA)]. This format utilizes microscopic beads that are added to the reaction mixture; these beads contain scintillant, which emits light upon stimulation with β -radiation if the β -emitter is bound to the surface of the bead. As the beads bind only protein or peptide substrate (the exact mechanism of recognition has not been reported by PerkinElmer) but not ATP, the need for isolation and washing steps is eliminated.

Apart from reliability and low quantification limit, the important advantage of the radiometric kinetic assays is their generic nature, *i.e.*, the possibility to utilize practically any PK and its protein/peptide substrate, whereas the size of the substrate is not limited [Hastie *et al.*, 2006]. However, the personal and environmental risks associated with the use of radioactive materials as well as the short half-life of $\gamma^{32}\text{P}$ -ATP (14 days) strongly limit the field of application of radiometric assays.

2.3. Fluorescence techniques

2.3.1. Fluorescence phenomenon

Fluorescence is one of the variants of luminescence, a phenomenon of light emission occurring from excited states of a molecule [Lakowicz, 2006]. An electron is excited by photon absorption from the ground singlet state (S_0) to higher singlet states (S_1 , or S_2); subsequently, in case of fluorescence a rapid relaxation to the lowest vibrational energy level of S_1 (so-called internal conversion) occurs within 10^{-12} s or less (Figure 23A). Finally, the return to the ground state takes place, which is associated with the emission of a photon; again, in case of fluorescence this return process occurs rapidly, with a typical

emission rate of more than 10^8 s^{-1} . In most cases, the electron returns to the higher vibrational energy level of S_0 , but then rapidly reaches the thermal equilibrium (within 10^{-12} s). As the energy of the photon used for excitation is generally higher than the energy of the emitted photon, the wavelength of the excitation photon is smaller than that of the emitted photon; this wavelength difference is called the Stokes shift, and it varies for different fluorescent compounds (fluorophores).

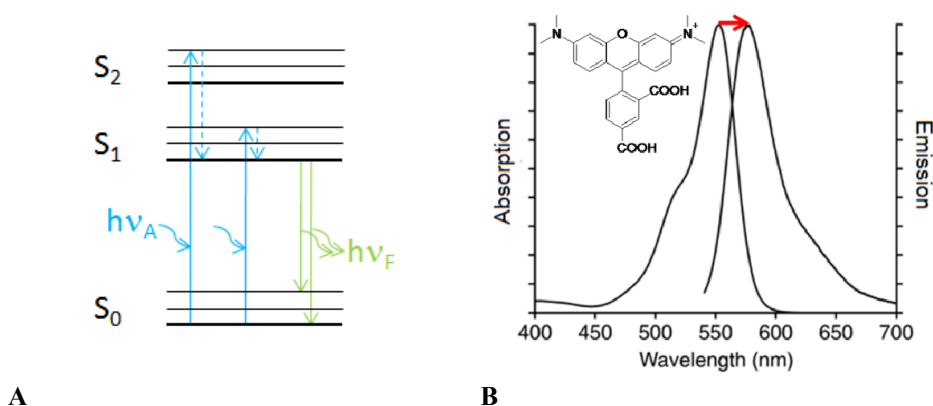


Figure 23. Principles of fluorescence. (A) Jablonski diagram of fluorescence. Absorption is shown as solid blue arrow, internal conversion as dotted blue arrow, and fluorescence emission as solid green arrow. S_0 , S_1 and S_2 are singlet states, $h\nu_A$ is exciting photon and $h\nu_F$ emitted photon. (B) Absorption (left) and emission (right) spectrum of 5-TAMRA at pH 7.0 (adapted from InvitrogenTM Product Spectra 5-TAMRA/pH 7.0). The Stokes shift is indicated with red arrow.

Structurally, fluorophores represent a variety of classes of organic as well as inorganic compounds. On the basis of size and chemical composition, three main groups of fluorophores can be distinguished:

- fluorescent proteins initially derived from living organisms (*i.e.*, jellyfish, corals) [Baird *et al.*, 1999; Cox *et al.*, 2007; Craggs, 2009; Tsien, 2009];
- small molecular-weight organic compounds (*i.e.*, fluorescein, rhodamine, *etc.*) usually containing conjugated aromatic cycles [Lakowicz, 2006];
- nanoparticles, which may either be fluorescent on their own (*i.e.*, semiconductor quantum dots), may acquire fluorescent properties upon ligation (*i.e.*, lanthanide ions), or can serve as compound enhancing or diminishing emission of other fluorophores (*i.e.*, gold and silver particles) [Moore *et al.*, 2009; Resch-Genger *et al.*, 2008; Seydack, 2005].

Each fluorophore has a characteristic spectrum of absorption, excitation and emission; in condensed phase, absorption and excitation spectra are nearly identical, and the discrete electronic transitions corresponding to the excitation and emission peaks are replaced by broader energy spectra (*i.e.*, Figure 23B)

[Lakowicz, 2006]. Consequently, the excitation of the fluorophore might be performed at a wavelength slightly different from the excitation maxima. Importantly, the profile of the fluorescence emission spectrum is independent of the excitation wavelength (logically, if excitation still occurs), due to the internal conversion occurring during the excited-state lifetime. However, the fluorescence emission intensity (or just fluorescence intensity) is proportional to the amplitude (intensity) of the fluorescence excitation spectrum at the given excitation wavelength, *i.e.*, the closer to the maximum the excitation is performed, the more intensive will be the emission within the whole range of emission wavelengths.

The latter fact also means that the more intensive is the maximal absorption of the fluorophore is, the more intensive will be the emission. According to the Beer-Lambert law, the absorbance at a certain wavelength is dependent on the extinction coefficient (ε) of the compound (Equation 13A); thus, a fluorophore with a higher ε value yields a stronger signal than the fluorophore with a lower ε value at the same concentration. However, the intensity of signal is also dependent on the quantum yield of the fluorophore, the ratio of the number of emitted photons to the number of absorbed photons; the value of quantum yield smaller than one results from the fact that depopulation of S1 may occur not only *via* photon emission but also *via* other non-radiative processes (Equation 13B). The product of values of the extinction coefficient at a certain wavelength and the quantum yield is defined as brightness, *i.e.*, the fluorescence output of the fluorophore; the higher is brightness value, the more preferable is the fluorophore for application in assays with low quantification limit.

<div style="text-align: center;"> $A_{\lambda} = \varepsilon_{\lambda} \cdot c \cdot l$ </div> <div style="text-align: center;"> A </div>	<div style="text-align: center;"> $Q = \frac{k_r}{k_r + \sum k_{nr}}$ </div> <div style="text-align: center;"> B </div>
<div style="text-align: center;"> $\tau = \frac{1}{k_r + \sum k_{nr}}$ </div> <div style="text-align: center;"> C </div>	<div style="text-align: center;"> $I_t = \sum_i \alpha_i \cdot e^{(-t/\tau_i)} + c$ </div> <div style="text-align: center;"> D </div>

Equation 13. Parameters of fluorescence. (A) A_{λ} , absorbance; ε_{λ} , molecular extinction coefficient; c , molar concentration of substance in solution; l , the length of the optical path; index λ indicates the wavelegth. (B) Q , fluorescence quantum yield; k_r , rate of the radiative decay; k_{nr} , rate of a non-radiative decay. (C) τ , fluorescence lifetime. (D) I_t , fluorescence intensity at time t ; α , scale factor; c , a time-independent component of the background noise.

Another important parameter of a fluorophore is the lifetime of its fluorescence (Equation 13C), which reflects the average time the fluorophore spends at the excited state before the return to the ground state. The return may occur *via* emission of photon, or *via* non-radiative processes, whereas the speed of the

latter strongly depends on the surrounding environment; in this case, measurement of fluorescence lifetime can be used as detection method for monitoring the binding of a fluorophore-containing ligand to the PK [Lakowicz, 2006; Lebakken *et al.*, 2007]. The typical fluorescence lifetime is $10^{-8} \dots 10^{-9}$ s, but in some fluorophores it may be exceptionally long (100 ns...few μ s) [Degorce *et al.*, 2009]. Such compounds are of especial value in applications where background fluorescence may be an issue, as the measurement of the emission after time delay should not influence the signal of a long lifetime-fluorophore, whereas the background noise is reduced (Equation 13D).

Finally, the criteria posed for the fluorophores also include high solubility, high stability, and low photobleaching; the latter parameter ensures that the fluorophore can be repeatedly excited and detected, which is a fundamental requirement for the low quantification limit of fluorescence detection [Lakowicz, 2006].

2.3.2. Measurement of fluorescence intensity (FI)

The measurement of FI requires the least complicated equipment, and may be performed with a simple fluorescence spectrometer. There are several types of assays that utilize FI detection, whereas the value of FI can increase or decrease as a result of certain molecular event, or remain the same:

- assays where a gain of FI takes place as a result of a change in the fluorophore structure (*i.e.*, gain of fluorescence associated with spatial convergence of fluorophore-composing fragments as a result of conformational change of PK substrate upon phosphorylation) [Souslova and Chudakov, 2007; Tsien and Baird, 2006];
- assays where a change of FI takes place as a result of a change in the fluorophore conformation (*i.e.*, change of FI associated with translation of conformational change to the fluorophore from the PK substrate upon phosphorylation or from the PK inhibitor upon binding) [Kawai *et al.*, 2004];
- assays where a change of FI takes place as a result of a change in the fluorophore environment (*i.e.*, change of pH or polarity associated with phosphorylation of the PK substrate [Sharma *et al.*, 2008; Wang Q. and Lawrence, 2005] or with binding of a PK inhibitor, or change of the spatial distance from the other chromophores or quenchers [Allen and Zhang, 2006; Rininsland *et al.*, 2004; Simard *et al.*, 2010], please refer to Section 2.3.3. Measurement of fluorescence intensity (FI). Special case: Förster-type resonance energy transfer (FRET));
- assays where a change of FI takes place as a result of induction of or interference with the cleavage of fluorophore (*i.e.*, upon phosphorylation of PK substrate) [Promega ProFluor® PKA Assay];
- separation-based assays where substrates and products of the PKAc-catalyzed reaction of the PK substrate, or PK-bound and non-bound forms of an inhibitor are isolated on the basis of other physical or chemical properties,

whereas the fluorophore retains its FI during isolation [Viht *et al.*, 2005] or is introduced after isolation [Charter *et al.*, 2006].

A representative of the latter category is the inhibition kinetic assay (so-called TLC-assay) that is based on a PK-catalyzed phosphorylation reaction utilizing ATP and a fluorescently labeled protein kinase substrate (*i.e.*, 5-TAMRA-Kemptide) [Viht *et al.*, 2005]. After the reaction, the non-phosphorylated substrate and phosphorylated product are separated with the aid of thin layer chromatography (TLC). The fluorescence intensity of both fluorescent compounds is measured on the TLC plate by fluorescence imaging, and the extent of phosphorylation is calculated. The ratiometric nature of the assay enables diminishing of artifacts such as well-to-well variation of the fluorescent compound concentration or pipetting errors.

TLC-assay is applicable for both, assessment of the PK activity (in this case, the reaction is performed in the absence of a PK inhibitor) as well as the determination of the inhibition properties of PK inhibitors (if the reaction is performed in the presence of a PK inhibitor). In the latter case, increase in concentration of ATP or labeled peptide substrate also allows determination of the inhibition mechanism of a PK inhibitor [Enkvist *et al.*, 2006]. Dependent on the labeled peptide substrate used for the phosphorylation reaction, the TLC-assay may be applied for different PKs; so far, it has been utilized for studies with PKAc and PKB γ inhibitors [Enkvist *et al.*, 2006; Enkvist *et al.*, 2009].

2.3.3. Measurement of fluorescence intensity (FI). Special case: Förster-type resonance energy transfer (FRET)

FRET is a form of non-radiative relaxation of the fluorophore, where the energy is transferred to a suitably oriented dipole moment of another spatially close non-excited fluorophore, if the emission spectrum of the first (donor) fluorophore overlaps with the excitation (absorption) spectrum of the second (acceptor) fluorophore [Gadella 2009; Lakowicz, 2006]. The efficiency of FRET is strongly dependent on the distance between the donor and acceptor (Equation 14A); the distance at which the probability of the FRET between fluorophores is equal to 50% is called the Förster distance (R_0 ; Equation 14B).

$$E = \frac{R_0^6}{R_0^6 + R^6} \qquad R_0^6 \approx \frac{9000(\ln 10)}{N_A \cdot 128\pi^5} \cdot \frac{\kappa^2 \cdot Q_D \cdot J}{n^4}$$

A

B

Equation 14. Parameters of FRET. (A) E , FRET efficiency; R_0 , Förster distance; R , distance between the FRET donor and acceptor. (B) κ^2 , dipole orientation factor; Q_D , fluorescence quantum yield of the FRET donor; J , spectral overlap between the donor emission spectrum and acceptor excitation spectrum; n , refractive index of the medium.

Typically, FRET occurs at distance of 20...90 Å between the donor and acceptor, which is hence comparable with the size of biological macromolecules [Lakowicz, 2006]. Detection of FRET enables the monitoring of several dynamic intra- and intermolecular processes; in case of PKs, the FRET phenomenon is most frequently utilized for monitoring the following events [Kalab and Soderholm, 2010; Wang H. *et al.*, 2009]:

- conformational changes of PKs (*i.e.*, upon binding of ligands), monitored by detection of FRET between the fluorophores attached to two different positions of the PK [Zaccolo *et al.*, 2002; Honda *et al.*, 2005];
- conformational changes of protein/peptide substrates of PKs (*i.e.*, upon phosphorylation), monitored by detection of FRET between the fluorophores attached to two different positions of the substrate [Allen and Zhang, 2006];
- binding of ligand(s) to the PK, monitored by detection of FRET between two fluorescently labeled ligands (*i.e.*, a protein substrate and an antibody [Kwan *et al.*, 2009]) or between a labeled ligand and a labeled PK [Vaasa *et al.*, 2010];
- phosphorylation of a PK protein/peptide substrate, monitored by detection of FRET between the fluorescently labeled substrate and a phosphoryl-specific fluorescently labeled antibody [Carlson *et al.*, 2009].

FRET might be detected in several ways, including the increase in acceptor fluorophore emission intensity (Equation 15A), decrease of donor fluorophore emission intensity (Equation 15B), or the change of the donor fluorophore lifetime (Equation 15C); the latter variant is possible by virtue of the fact that FRET increases the non-radiative relaxation rate of the donor and thus shortens the donor lifetime in the presence of the acceptor. A specific variant of FRET is represented by the fluorescence quenching, where the acceptor is not a fluorophore, *i.e.*, after excitation by energy transfer from the donor it does not emit a photon but undergoes non-radiative relaxation [Gadella 2009; Lakowicz, 2006; Sharma *et al.*, 2008]. Fluorescence quenching may accompany the “classical” FRET phenomenon (where the acceptor emits the photon), thus measurement of donor emission intensity or donor lifetime may provide more accurate data than measurement of acceptor emission intensity.

$$E = \frac{\varepsilon_A}{\varepsilon_D} \left(\frac{I_{AD}}{I_A} - 1 \right)$$

A

$$E = 1 - \frac{I_{DA}}{I_D}$$

B

$$E = 1 - \frac{\tau_{DA}}{\tau_D}$$

C

Equation 15. Measurement of FRET. (A) E , FRET efficiency; ε_A , molecular extinction coefficient of the acceptor; ε_D , molecular extinction coefficient of the donor; I_{AD} , intensity of the acceptor emission in the presence of the donor; I_A , intensity of the acceptor emission in the absence of the donor. The ratio of ε values should be taken into account as the acceptor may be directly excited at the same wavelength as the donor. (B) I_{DA} , intensity of the donor emission in the presence of the acceptor; I_D , intensity of the donor emission in the absence of the acceptor. (C) τ_{DA} , fluorescence lifetime of the donor in the presence of the acceptor; τ_D , fluorescence lifetime of the donor in the absence of the acceptor.

FRET offers several advantages as compared to the other fluorescence techniques, such as the possibility to perform measurements in a complex biological matrix (*i.e.*, cell lysate) and in several cases the ability to increase the selectivity of detection (*i.e.*, if one of the fluorescently labeled components is not selective towards the biological target on its own) [Gadella 2009; Lakowicz, 2006]. However, the quantitative measurement of FRET is frequently compromised by the excess donor (*i.e.*, due to the so-called bleed-through of the donor emission to the wavelength where the acceptor emission is measured), excess acceptor (*i.e.*, due to the off-peak excitation at the wavelength where the donor excitation is performed), and other factors [Włodarczyk *et al.*, 2008].

2.3.4. Measurement of fluorescence anisotropy (FA)

Fluorescence anisotropy measurements are based on the phenomenon of selective excitation of fluorophores by linearly polarized light [Jameson and Ross, 2010; Lakowicz, 2006]. In linearly polarized light, the electric field vector assumes only one unique oscillation axis, which is perpendicular to the light propagation direction. When the linearly polarized light impinges on a fluorophore, only those fluorophore molecules are excited which are appropriately oriented relative to the oscillation axis of the electric vector, *i.e.*, molecules that upon excitation are able to generate the induced dipole moment (so-called transition dipole) which is parallel to the oscillation axis of the electric vector. The radiation emitted by the fluorophore is also polarized, whereas dependent on the structure of fluorophore, the transition dipole corresponding to the emission of light may be either parallel or perpendicular to the excitation dipole. The actual oscillation axis of the electric vector of emitted light is determined by two polarizers oriented in parallel and in perpendicular directions relative to the initial oscillation axis. Fluorescence polarization (*FP*) is then defined as Equation 16A; an analogical term with identical information content as in the case of fluorescence polarization, is the fluorescence anisotropy (*FA*; Equation 16B); however, in case of the *FA* function the denominator represents the total intensity of emission.

$$\begin{array}{ll}
 \text{A} & \text{B} \\
 FP = \frac{I_{\parallel} - I_{\perp}}{I_{\parallel} + I_{\perp}} & FA = \frac{I_{\parallel} - I_{\perp}}{I_{\parallel} + 2 \cdot I_{\perp}} \\
 \\
 \text{C} & \text{D} \\
 \frac{1}{FA} = \frac{1}{FA_0} + \frac{R \cdot T \cdot \tau}{\eta \cdot V_{fl}} & V_{fl} = M \cdot (v + h)
 \end{array}$$

Equation 16. Measurement of FP and FA. (A), (B) I_{\parallel} and I_{\perp} are respectively the fluorescence intensities of the vertically and horizontally polarized components of emission, if the sample was excited with vertically polarized light. (C) FA_0 , limiting (intrinsic) anisotropy (in the absence of rotation of the fluorophore); R , universal gas constant; T , absolute temperature; τ , fluorescence lifetime; η , viscosity of the medium; V_{fl} , the effective molar volume of the fluorophore-containing unit. (D) M , molecular weight of the fluorophore-containing unit; v , partial specific volume; h , degree of hydration.

If the emitted light is completely polarized in the axis parallel to the polarization axis of the exciting light (*i.e.*, the polarization is totally maintained), the value of FA is +1; if the emitted light is totally polarized in the perpendicular axis, then the value of FA is -0.5. However, these theoretical limits are generally not realized: firstly, even in a highly viscous or frozen medium some of the dipoles excited will not be exactly parallel to the direction of the exciting light; secondly, in solutions the excited fluorophores may rotate during the lifetime of the excited state [Jameson and Ross, 2010; Lakowicz, 2006]. The latter phenomenon is dependent on the effective molar volume of the fluorophore-containing unit (V_{fl}); therefore, a relationship between the observed FA and V_{fl} can be derived (so-called Perrin equation, Equation 16C). As V_{fl} is in most cases linearly dependent on the molecular weight of the fluorophore-containing unit (Equation 16D), the complexation of the small-molecular weight fluorescent ligand with the large protein results in an increase of FA of the ligand, which is frequently used for development of assays based on FA detection.

One of such assays applicable for the assessment of the properties of PKs and PK inhibitors is the homogeneous FA-assay that utilizes ARC-derived fluorescent probes (ARC-Photo, molecular weight below 3 kDa) [Vaasa *et al.*, 2009]. The idea behind the FA-assay lies in the principle of the additivity of anisotropy (Equation 17A), meaning that in the mixture of free and bound ARC-Photo, both components contribute to the measured FA signal with different magnitudes (Equation 17B). The maximal and the minimal FA is correspondingly equal to the FA_{bound} and FA_{free} ; if the contribution of FA_{bound} is X_1 , the contribution of FA_{free} is $(1 - X_1)$, whereas X_1 hence reflects the ratio of bound ARC-Photo concentration to the total concentration of ARC-Photo [Vaasa *et al.*, 2009].

$$\langle FA \rangle = \sum_i f_i \cdot FA_i \qquad \langle FA \rangle = X_1 \cdot FA_{bound} + (1 - X_1) \cdot FA_{free}$$

A

B

Equation 17. FA-assay based on ARC-Photo. (A) $\langle FA \rangle$, observed anisotropy; FA_i and f_i , the anisotropy and the fractional contribution of the i^{th} specie. (B) FA_{bound} , anisotropy value of the PK-bound ARC-Photo; X_1 , the fractional contribution of FA_{bound} ; FA_{free} , anisotropy of the free ARC-Photo.

The FA-assay can be performed either as a direct binding format, or as a displacement (competition) binding format [Vaasa *et al.*, 2009]. In the first case, the binding of ARC-Photo to a PK is monitored by titration of a constant concentration of ARC-Photo with PK. In these conditions, X_1 is dependent on the total concentrations of ARC-Photo and PK, and on the affinity of ARC-Photo towards PK; additionally, the possible change of the fluorophore quantum yield caused by binding of fluorophore to the PK should be considered. Importantly, apart from the determination of the affinity of ARC-Photo, the binding format of the FA-assay also enables the assessment of the concentration of the active enzyme in the sample [Vaasa *et al.*, 2009].

In the second case, displacement of ARC-Photo from its complex with PK is performed by compounds targeting the ATP-site and/or protein substrate-site of PK; here, X_1 is additionally dependent on the concentration of the competing compound and its affinity towards PK [Vaasa *et al.*, 2009]. The higher the affinity is possessed by ARC-Photo, the wider is the range of affinities of competing compounds that can be reliably determined by the assay [Huang X., 2003]. It should also be noted that generic ARC-Photo probes are strongly preferred for the displacement (competition) binding format of an FA-assay, as the promiscuous nature of the probe allows the application of the assay for wide variety of PKs [Uri *et al.*, 2010].

3. Protein crystallography

3.1. General features

The physical phenomenon behind X-ray crystallography is the diffraction of X-rays from the crystal lattice, whereas the transformation of the detected diffraction picture yields the three-dimensional structure of the electron density for the atoms composing the given crystal (so-called crystal structure). The range of wavelengths of the X-radiation used for the crystallography is 0.4 to 25 Å, which is on the same scale as the chemical bond lengths between the atoms composing the crystal [Giacovazzo *et al.*, 2005]. According to the nature of a chemical bond within the object, several branches of crystallography may be

defined, utilizing metallic, ionic, covalent, molecular or macromolecular crystals, the latter group also involving protein crystals. Protein crystals are composed of the discrete molecular entities held together by intermolecular long-distance interactions (*i.e.*, weak dispersion or polar forces), whereas the variable intramolecular short-distance interactions are responsible for the conservation of the primary and higher structures of the protein. A characteristic feature of protein crystals is their large content of solvent (up to 70% of crystal volume [Matthews, 1968]), which enables preservation of the solubilized conformation of protein in the crystal; on the other hand, high water content may decrease the crystal symmetry, which in turn lowers the quality of diffraction.

The main steps for the obtainment of a crystal structure are represented by crystallization of the object of interest, measurement of diffraction from the crystal, and interpretation of diffraction data. The necessary condition for protein crystallization is a large amount (tens of milligrams) of pure material, which is one of the downsides of crystallography [Davis *et al.*, 2008; Wlodawer *et al.*, 2008]. Moreover, while the crystallization of water-soluble proteins is generally a matter of choosing right conditions, the crystallization of membrane proteins and proteins with large unordered regions still represents a challenge. The latter issue is pursued by different techniques, such as use of truncated forms of proteins, reduction of surface entropy, and enhancement of hydrophobicity of the protein surface to facilitate formation of intermolecular contacts [Argiriadi *et al.*, 2009; Joachimiak, 2009].

The crystallization process starts from the supersaturated protein solution and can be divided into two steps, nucleation and crystal growth. The supersaturating conditions can be obtained by addition/diffusion of precipitating solutions (salts, organic solvents and polyethylene glycols), and variation of pH, temperature, or concentrations of substances in the mother solution [Breitenlechner *et al.*, 2005; Giacobuzzo *et al.*, 2005]. Additional possibilities involve the addition of cofactors or metal ions, which should form conformationally fixed complexes with the protein of interest and possibly induce crystallization. Another approach is microseeding, where pieces of other protein crystals are added to the crystallization solution to form nucleation centers; this technique has proved especially useful in case if crystals of the same protein have already been obtained [Oswald *et al.*, 2008]. An important factor is also the incubation time, as the equilibrium between dissolved and crystallized protein may not be reached quickly; moreover, the amorphous precipitate can sometimes form ordered crystal structures after prolonged incubation. Finally, if the goal is to crystallize a complex of protein (*i.e.*, to generate a co-crystal), the necessary secondary messengers, substrates, inhibitors, *etc.* are added to the crystallization mixture. The addition can be performed either prior to formation of crystal, or *via* back-soaking after the initial crystal lattice of apoprotein is formed; in the latter case, the high water content of the crystal enables quick diffusion of the reagents added to the crystallization solution [Breitenlechner *et al.*, 2005]. Importantly, in all of the techniques mentioned above it is of utmost importance

to grow crystals in conditions maximally resembling the physiological environment, in order to restrict chemical and conformational changes in the protein and prevent obtainment of a crystal structure not applicable for studying naturally occurring processes [Davis *et al.*, 2008].

Prior to the measurement of diffraction, a procedure of cryoprocessing is frequently carried out, especially if synchrotron radiation is used as source of X-rays due to the elevated risk of damaging the crystal *via* generation of labile radicals. Performance of measurements at low temperatures decreases the mobility of free radicals, and also increases the maximum resolution of the diffraction pattern due to reduction of general thermal disorder [Giacovazzo *et al.*, 2005; Rogers, 1994]. The main task of cryogenic techniques is to cool the crystal without enabling the formation of crystalline ice, which could develop cracks in the crystal and damage the diffraction picture. The most applicable technique is flash-cooling, where the sample temperature is rapidly lowered (usually, by transferring the crystal into liquid nitrogen) so that the ice nucleation does not occur before the viscosity of the solution is high enough to prevent ice lattice formation [Rogers, 1994]. In order to avoid damaging of crystal, several precautions are applied before cooling the crystal, *i.e.*, immersion into hydrocarbon oil to remove the most of external liquid or addition of cryoprotective reagents (*i.e.*, glycerol, PEG, or methyl-pentanediol).

The measurement of diffraction might be performed *via* various techniques, which differ in the method of obtainment of the maximal number of diffraction maxima with one crystal set [Giacovazzo *et al.*, 2005]. Most of the techniques use monochromatic radiation, oscillating crystal mount and either a stationary or a moving detector; however, there are exceptions such as the Laue method, which uses polychromatic radiation. The advances in charge-coupled device technology have also enabled quick and precise detection of X-ray diffraction data with stationary crystal mount.

The detected diffractogram records the intensity of diffraction maxima (reflections), whereas the position of each atom in the crystal lattice influences the intensities of all the reflections and vice versa; this wealth of diffraction data is analyzed *via* Fourier transformation of the structure factors, yielding the three-dimensional electron density map for the given crystal [Giacovazzo *et al.*, 2005]. However, the equation for the Fourier transformation includes both the amplitudes and phases of the waves, whereas the X-ray detectors measure just the intensities (which are proportional to the square of the structure factor amplitudes), but not the phases (Equation 18A). This limitation is known as the phase problem, and recovering of phases may be performed *via* several methods, *i.e.*, multiwavelength anomalous diffraction, multiple isomorphous replacement, molecular replacement, or direct *ab initio* methods [Giacovazzo *et al.*, 2005; Hauptman, 1991].

$$\rho(x, y, z) = \frac{1}{V} \sum_h \sum_k \sum_l |F(h, k, l)| e^{i\varphi(h, k, l)} e^{-2\pi i(hx + ly + lz)}$$

A

$$R = \frac{\sum ||F_{obs}| - |F_{calc}||}{\sum |F_{obs}|}$$

B

Equation 18. Fourier transformation of the diffractogram and calculation of a quality parameter (R-factor). (A) $\rho(x, y, z)$, electron density in real space; V , volume of the unit cell; $|F(h, k, l)|$, structure factor amplitude (whereas h , k , and l are the coordinates in the reciprocal space); $\varphi(h, k, l)$, phase of the reflection. (B) $|F_{obs}|$, the observed reflection amplitudes; $|F_{calc}|$, reflection amplitudes calculated from the model.

The primary electron density map calculated by Fourier transformation from the set of experimental structure factor amplitudes and the modeled phases is named (F_{obs} , φ_{calc}) map, and represents an approximation of the true structure, with its quality dependent on the accuracy of the phase modeling [Wlodawer *et al.*, 2008]. Another type of electron density map is calculated using the differences between observed amplitudes and amplitudes calculated with phases, ($F_{obs} - F_{calc}$, φ_{calc}); this difference electron density map can be used to determine parts of the structure that can be used again to simulate a new set of phases [Wlodawer *et al.*, 2008]. The latter process involves repetitive rounds of automated optimization (according to the least-squares or maximum-likelihood algorithms) as well as manual corrections, until the previously defined quality parameters of the new density map reach their satisfactory values. Subsequently, the obtained electron map is interpreted in terms of positioning the atoms constituting protein, solvent and possible other components of crystallization mixture into the obtained density, and then subjected to the so-called refinement. The refinement procedure is performed both automatically and manually by variation of model parameters to achieve the best agreement between the observed reflection amplitudes (F_{obs}) and those calculated from the model (F_{calc}) [Wlodawer *et al.*, 2008]. After the refinement procedure, the final three-dimensional crystal structure is obtained, whereas the most important parameters of quality of the crystal structure are the following [Wlodawer *et al.*, 2008]:

- resolution, which reflects the minimum spacing of crystal lattice planes that may still provide measurable diffraction; the medium resolution value is in the range 2.0...2.7 Å;
- R-factor (Equation 18B), which includes both, the experimental errors and the information considering the deviation of model from reality; the medium R value is below 20%;

- R_{free} -factor, which is calculated analogically to the R-factor, but only for ca 1000 of randomly selected reflections that might have influenced the model definition but were not applied for model refinement; the value of R_{free} -factor should not differ from the R-factor more than 7%;
- R_{merge} , which reflects the deviation of the individual measurements of equivalent reflections; the medium R_{merge} value is below 5%;
- B-factors, also referred to as ‘temperature factors’ or Debye-Waller factors, which shows the degree of “mobility” of each atom (*i.e.*, the attenuation of X-ray scattering caused by thermal motion of the given atom); the values may range from 2 Å² (for atoms with fixed positions) to 100 Å² (for poorly fixed atoms).

Other important parameters involve completeness of the data, signal-to-noise ratio, root-mean-square deviations from geometrical standards, *etc* [Wlodawer *et al.*, 2008].

The main downside of protein crystallography lies in the fact that a crystal structure may provide only a static picture about the crystallized protein, *i.e.*, only one conformation (although a certain amount of information considering flexibility of different fragments of the protein may also be provided by the B-factors). Moreover, the crystal structures of protein complexes cannot predict the thermodynamical parameters such as binding energies, thus the application of information obtained from crystallographic studies for the design of protein-targeting compounds should be taken with some degree of reservation [Davis *et al.*, 2008].

3.2. Models of diffraction

The theory behind the phenomenon of diffraction of X-rays from the crystal ultimately relies on the high symmetry of the crystal lattice, which may be considered as a system formed by repetitive translation of identical three-dimensional smallest building blocks (unit cells) in space. By virtue of high molecular weight and folding into high-order structures, protein crystals generally possess a lower degree of symmetry than ionic or metallic crystals (*i.e.*, no axis or plane of symmetry may pass through the protein molecule). Hence, the basic principles of diffraction are more easily explained using the Bravais lattice as an example, *i.e.*, as an infinite set of points generated by a set of discrete translation operations described by the position vector **R**⁷ (Equation 19A) [Kittel, 1986].

One of the first models of diffraction of X-rays by crystal was proposed by W. L. Bragg and W. H. Bragg in 1913; this model considered the crystal as a set

⁷ In the text and legends for equations of the given section, vectors are denoted as bold underlined characters.

of discrete parallel atomic planes (Miller planes⁸) separated by a constant parameter d [Bragg, 1913] (Figure 24A). The incident X-ray emerging onto the lattice plane is elastically reflected, *i.e.*, the angle of incidence is equal to the angle of scattering (θ), whereas the wavelength of the photon is preserved. In this case, the waves scattered from the successive crystallographic planes are in constructive interference (*i.e.*, are in the same phase) if the difference of the path length of waves (Equation 19B) is equal to an integer multiple of the wavelength (Equation 19C).

$$\begin{array}{lll} \vec{R} = n_1 \vec{a}_1 + n_2 \vec{a}_2 + n_3 \vec{a}_3 & \Delta = 2d_{hkl} \sin \theta & 2d_{hkl} \sin \theta = m\lambda \end{array}$$

A B C

Equation 19. Real space and Bragg's law. (A) \vec{R} , position vector of the Bravais lattice; n , integer; \vec{a} , unit vector of the Bravais lattice (the length of the unit vector is called lattice parameter). (B) Δ , the difference of the path length of waves; d_{hkl} , distance between the planes; θ , angle of incidence. (C) m , integer; λ , wavelength of the incident X-radiation.

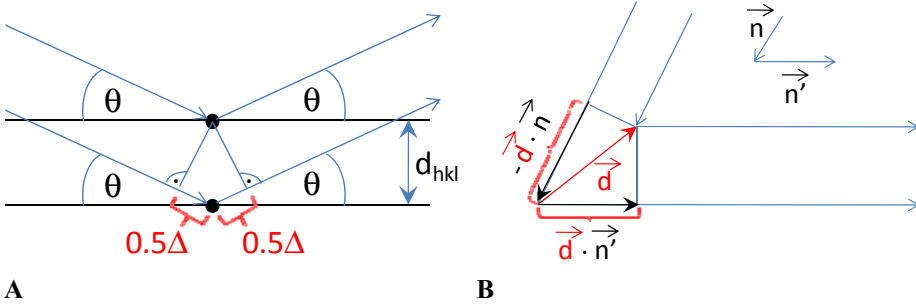


Figure 24. Models of laws of diffraction. (A) Bragg's law. (B) Laue's law.

An alternative model of diffraction from a crystal proposed by M. T. F. von Laue differs from the Bragg model in the aspect that no certain pattern is used to define the atomic planes within the crystal, and the scattering of X-rays is not considered as reflection [Figure 24B; Kittel, 1986]. Every particle positioned at the point R of the Bravais lattice may scatter the incident X-ray in different directions, but the diffraction maxima are observed only for those directions and wavelengths that yield constructive interference upon scattering from all points of lattice. If two parallel incident X-rays with the wave vector \underline{k} (Equation 20A)

⁸ Miller plane intercepts the three points $\vec{a}_1/h, \vec{a}_2/k, \text{ and } \vec{a}_3/l$, where $\vec{a}_1, \vec{a}_2, \vec{a}_3$ are the three lattice vectors and h, k, l are Miller indices proportional to the inverses of the intercepts of the plane in the basis of the lattice vectors.

propagating in direction \underline{n} are elastically scattered by lattice points positioned at distance d from each other, the rays scattered in direction \underline{n}' will yield constructive interference if the Equation 20B is fulfilled. If both sides of Equation 20B are multiplied by factor $2\pi/\lambda$ and scattering by all points of Bravais lattice is considered (given the fact that the points of Bravais lattice are positioned at distance R from each other), Equation 20C is obtained.

$$\begin{array}{lll} |\vec{k}| = \frac{2\pi}{\lambda} & \vec{d} \cdot (\vec{n}' - \vec{n}) = m\lambda & \vec{R} \cdot (\vec{k}' - \vec{k}) = 2\pi m \\ \text{A} & \text{B} & \text{C} \end{array}$$

Equation 20. Reciprocal space and Laue's law. (A) $|\underline{k}|$, length of wave vector; λ , wavelength. (B) \underline{d} , vector separating the two lattice points scattering X-radiation; \underline{n} , vector coinciding with the direction of the incident X-rays; \underline{n}' , vector coinciding with the direction of the scattered X-rays; m , integer. (C) \underline{R} , vector separating the lattice points scattering X-radiation; \underline{k} , wave vector of the incident wave; \underline{k}' , wave vector of the scattered wave; m , integer.

Basically, both, Bragg's law and Laue's law express the conservation of momentum transfer. Considering the reciprocal lattice⁹ where the set of Miller planes of the Bravais lattice is described by a vector \underline{K} normal to this set (Equation 21A), the Equation 20C means that the change of wave vector should be equal to a vector \underline{K} of reciprocal lattice. On the other hand, from the Figure 25 it can be seen that the length of vector \underline{K} may be defined as Equation 21B, thus the Equation 20C is equivalent to Equation 19C.

$$\begin{array}{ll} \vec{K} = h\vec{b}_1 + k\vec{b}_2 + l\vec{b}_3 & |\vec{K}| = 2|\vec{k}| \sin \theta \\ \text{A} & \text{B} \end{array}$$

Equation 21. Reciprocal space. (A) \underline{K} , position vector of the reciprocal lattice; h, k, l , Miller indices; \underline{b} , unit vector of the reciprocal lattice. (B) \underline{k} , wave vector of the incident wave; θ , angle of incidence.

⁹ The reciprocal lattice of a Bravais lattice is the set of all vectors \underline{K} such that for all lattice point position vectors \underline{R} , equation $\vec{R} \cdot \vec{K} = 2\pi m$ is valid.

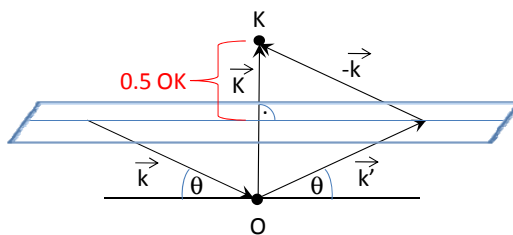


Figure 25. Model describing the diffraction conditions according to Bragg's and Laue's laws. The Bragg's plane is colored blue.

Overall, the wave vector of the scattered wave satisfies the conditions of Laue's and Bragg's laws only if the end of this vector lies in the Bragg's plane, *i.e.*, the plane which is perpendicular to the fragment of axis joining origin O with the point K of the reciprocal lattice, and divides fragment OK in two halves (Figure 25). As the length of fragment OK is defined by the crystal lattice, and the wavelengths of the incident and scattered waves are equal (due to elastic scattering), it is evident that either λ or θ may be varied to yield diffraction of X-rays from the given crystal, as described in the previous Section 3.1. General features.

3.3. Crystal structures of PKAc

3.3.1. General features

The first crystal structure of PKs was reported in 1991, and represented a ternary complex of PKAc with AMP-PNP and a fragment of PKI, PKI(5–24) [Knighton *et al.*, 1991]. This crystal structure (PDB code 1ATP) revealed several structural motifs that in subsequent studies proved to be common for the whole kinome, and important for the activation of PK, recognition of substrates, and catalysis of phosphoryl transfer. By virtue of good crystallizability, PKAc has been subsequently crystallized as apoenzyme, co-crystallized with a variety of physiological and synthetic regulators, and used as a model scaffold for other PKs (*i.e.*, after introduction of point-mutations into PKAc structure that were expected to simulate the modeled kinase) [Bonn *et al.*, 2006; Davies *et al.*, 2007; Taylor S. S. *et al.*, 2004].

PKAc is a globular enzyme with a bilobal structure of the catalytic core, a feature conserved within the whole family of PKs (Figure 26A); the small N-terminal lobe (residues 40...127) is mainly composed of β -strands, whereas the large C-terminal lobe (residues 128...300) mainly comprises α -helices. The N-terminal tail and the C-terminal tail span the surface of both lobes and serve as regulatory elements. The catalytic cleft is situated between the lobes, with the ATP-binding site buried deep inside the molecule, and the protein/peptide-substrate binding site positioned at the surface of the large lobe, being more opened to the solvent. The main motifs of secondary structure and connecting loops important from the point of PK functioning are presented in Table 5.

Table 5. Motifs and residues important for functioning of PKAc

<i>Motif</i>	<i>Number in PKAc</i>	<i>Important residues</i>
N-terminal tail, including Helix A	1...39 11...31	Trp30
β -strand 1, partially overlapped with Gly-rich loop	43...51 50...55	Lys47, Thr48 Gly50, Gly52, Ser53, Phe54, Gly55
β -strand 2	56...62	Arg56
β -strand 3	67...75	Lys72
Helix B	76...81	
Loop between Helix B and Helix C	82...84	Gln84
Helix C	85...97	His87, Glu91, Lys92, Arg93, Gln96
Loop between Helix C and β -strand 4	98...105	Phe100, Pro101, Phe102
β -strand 4	106...111	
β -strand 5	115...120	Met120
Loop between β -strand 5 and Helix D	121...127	Glu121, Val123, Glu127
Helix D	128...135	
Helix E	140...159	
β -strand 6	162...163	Arg165
Catalytic loop	166...171	Asp166, Lys168, Leu169, Glu170, Asn171
β -strand 7	172...174	
β -strand 8	180...182	
Mg ²⁺ -positioning loop	184...187	Asp184, Phe185, Gly186, Phe187
β -strand 9	189...190	Lys189, Arg190
Activation loop	191...197	Thr195, Trp196, Thr197
Peptide-positioning loop	198...208	Leu198, Gly200, Thr201, Pro202, Glu203, Tyr204, Leu205, Glu208
Helix F	218...233	Asp220, Trp221, Trp222, Glu230
Loop between Helix F and Helix G	234...242	Tyr235
Helix G	243...252	
Helix H	263...272	
Loop between Helix H and Helix I	273...288	Arg280
Helix I	289...292	
C-terminal tail, including Helix J	301...350 302...306	Tyr330

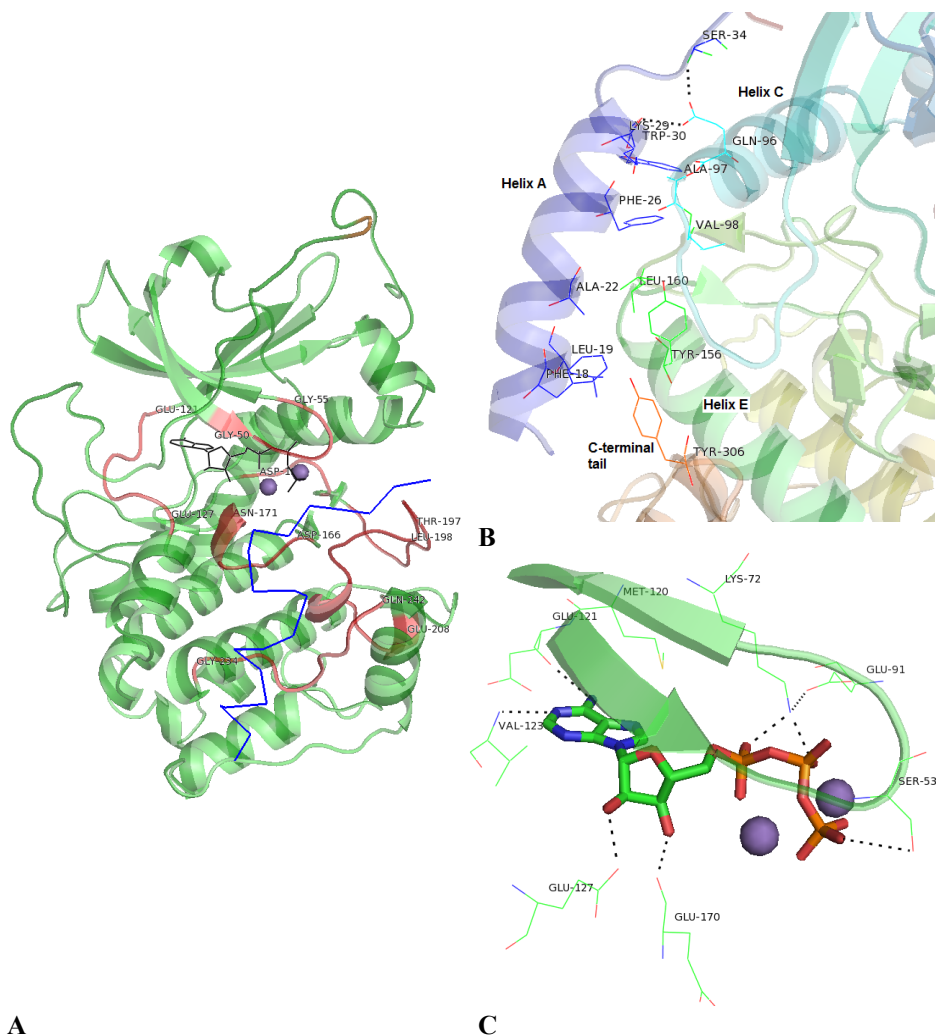


Figure 26. 1ATP. (A) PKAc shown as cartoon (with catalytically important loops colored red), ATP as black lines, Mg²⁺-ions as spheres, PKI(5–24) as blue ribbon. (B) Helix A. Phe26 and Trp30 fill the hydrophobic pocket lined by residues at the end of helix C (in the small lobe) and Arg190 from the β -strand 9 (in the large lobe, not shown). Backbone carbonyls of residues Lys29 and Ser34 at the end of Helix A make polar contacts to the Gln96 from the C-helix. (C) ATP-site (ATP shown as sticks, Gly-rich loop as cartoon). Met120 preceding the cleft serves as a gatekeeper residue¹⁰, closing the “entrance” to the pocket situated behind the cleft (near the N6 atom of

¹⁰ Importantly, the mutation of the gate-keeper residue is the common mechanism providing resistance of the disease-modifying PKs (*i.e.*, BCR-Abl, EGFR) towards therapeutic PK inhibitors [Krishnamurty and Maly, 2010; Zhang J. *et al.*, 2009]. Also, the mutation of the gate-keeper residue is frequently used in the chemical genetics approaches (please refer to Section 2.3.2. Reversible mono-ligand inhibitors. Special case: ATP-competitive inhibitors).

adenine moiety of ATP) and formed by residues 104...106 and 118..119. Glu121 and Val123 of the cleft form the hydrogen bonds considered as the interactions providing strong gain in binding energy of ligands binding to the ATP-site: in case of ATP, Glu121 accepts the hydrogen bond donated by N6 of adenine moiety, and Val123 donates hydrogen bond to N1 of purine ring. Additionally, Glu127 makes hydrogen bond with hydroxyl in 2' position of ribose moiety of ATP and is responsible for the recognition of Arg residue in the P-3 position of the substrate.

3.3.2. Ternary complex of PKAc with AMP-PNP and PKI(5...24)

The N-terminal tail of PKAc is comprised of thirty-nine residues and a myristoyl moiety attached to the N-terminal Gly. In the non-myristoylated protein (*i.e.*, recombinant PKAc expressed in *E.coli*) the first ten residues of the tail are disordered, but in the myristoylated PKAc those residues form a loop that serves as a node joining several parts of the molecule [Johnson D. A. *et al.*, 2001]. This loop folds onto the hydrophobic pocket formed by residues 100...102 of the loop between Helix C and β -strand 4, the end of the conserved C-lobe, and the beginning of C-terminal tail. The following residues 11...31 of the N-terminal tail form an amphipatic Helix A, which docks *via* its hydrophobic surface (Leu19, Ala22, Phe26, Trp30) to the residues of the large lobe (Ile 94, Ala 97, Val 98, Tyr156, Leu160, Leu162), and constitutes a “backbone” that fixes the mobility of the lobes in respect to each other (Figure 26B).

The small lobe is composed of five β -strands (1...5) constituting an anti-parallel β -sheet, and a conserved Helix C positioned between β -strands 3 and 4. In general, the parts of the small lobe distant from Helix A are uncoupled from the large lobe, with the exception of a hydrogen bond between His87 from Helix C and Thr197 from the activation loop which is formed only if the kinase is in closed conformation (please refer to Section 3.3.3. Conformational versatility of PKs). However, the ATP molecule bound to the cleft formed by the loop between β -strand 5 and Helix D (residues 121...127) serves as a “bridge” possessing multiple contacts to both lobes of PKAc (Figure 26C). From the top, the phosphate moieties of ATP are capped by the Gly-rich loop of the small lobe; at the top of this loop, a crucial contact is formed between the backbone amide of Ser53 and one of the oxygen atoms of the γ -phosphate. The highly conserved Gly50, Gly52 and Gly55 residues of Gly-rich also act in orchestra to position the γ -phosphate suitably for phosphoryl transfer [Cheng Y. *et al.*, 2005]. Other conserved residues in the small lobe are Lys72 and Glu91 that are within hydrogen bond distance from each other; while Lys72 anchors α - and β -phosphates of ATP and thus stabilizes the transition state, Glu91 is mainly important for the correct positioning of Lys72 [Cheng Y. *et al.*, 2005].

The large lobe contributes to the catalytic cleft with β -strands 6...9 and the loops positioned between the strands, catalytic loop (Figure 27), Mg^{2+} -positioning loop (Figure 28A), and peptide-positioning loop (Figure 29A). Not surprisingly, these loops are highly conserved within the family of PKs, which points to their significance for functioning of PK [Johnson D. A. *et al.*, 2001].

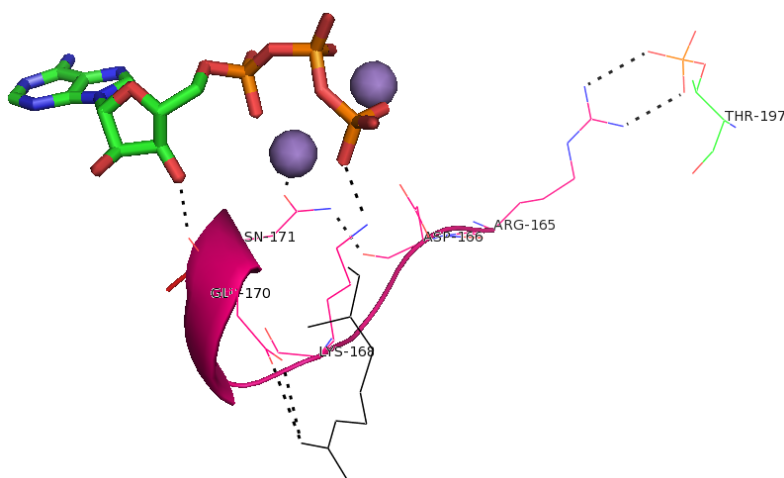
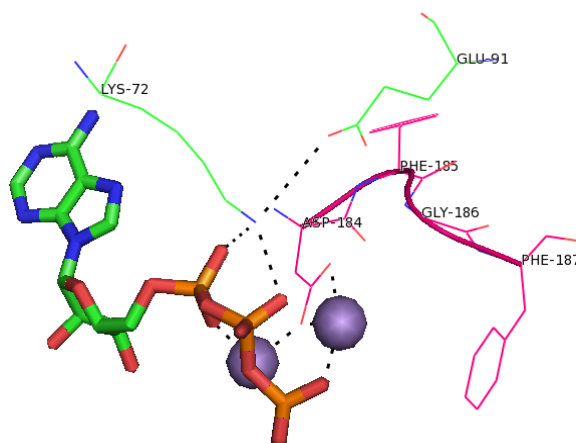
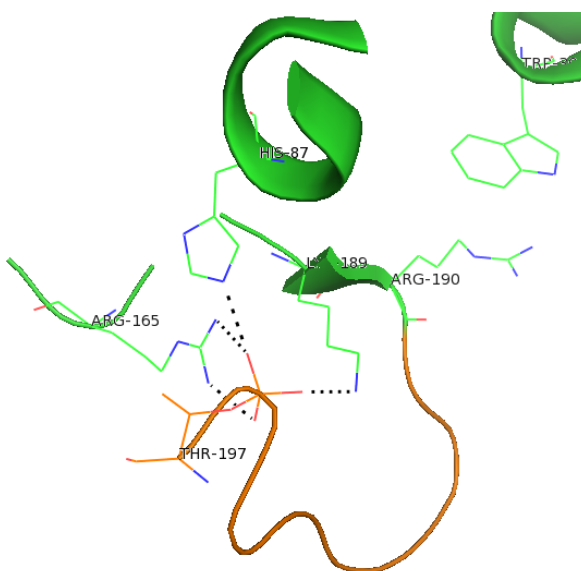


Figure 27. Catalytic loop (loop shown as magenta cartoon and lines, ATP as sticks, Mg^{2+} ions as spheres, Arg from P-2 position of PKI as black lines). Arg165 preceding the loop makes two hydrogen bonds with phosphorylated Thr197, providing a link between catalytic loop and activation loop. Asp166 from the catalytic loop serves as catalytic base to accept the proton delivered by the protein/peptide substrate. Lys168 interacts with the γ -phosphate of ATP and thus keeps ATP and the substrate in the reactive near-attack conformation. Glu170 is responsible for the recognition of Arg residue in the P-2 position of the substrate, and also forms a hydrogen bond with hydroxyl in 3' position of ribose moiety of ATP. Asn171 binds to the lower Mg^{2+} -ion, which is in turn bound to the α - and γ -phosphates of ATP (both Mg^{2+} -ions aid the catalysis, but the lower Mg^{2+} causes poor dissociation of the ADP from the PK after reaction [Cheng Y. *et al.*, 2005]). Asn171 also stabilizes the whole loop *via* formation of a hydrogen bond with the backbone carbonyl of Asp166.



A



B

Figure 28. Loops of PKAc. (A) Mg^{2+} -positioning loop (loop shown as pink cartoon and lines, ATP as sticks, Mg^{2+} ions as spheres, other interacting residues as green lines). Asp184 binds to the upper Mg^{2+} -ion bridging the β - and γ -phosphates of ATP, orients the γ -phosphate of ATP towards the substrate, and serves as a link between the small and the large lobe by forming catalytic triad with Lys72 and Glu91. Phe185 and Phe187 are responsible for exclusion of water from the site of phosphoryl transfer. (B) Activation loop (loop shown as orange cartoon with pThr-197 shown also as lines, other interacting residues as green lines and cartoons). Phosphorylated Thr197 forms multiple contacts with different parts of enzyme, ensuring adaptation of the catalytically active form of PKA; apart from formation of hydrogen bonds with His87 and Arg165, phosphorylated Thr197 also interacts with Lys189, which translates the conformational change to the Helix A (*via* interaction of Arg190 with Trp30).

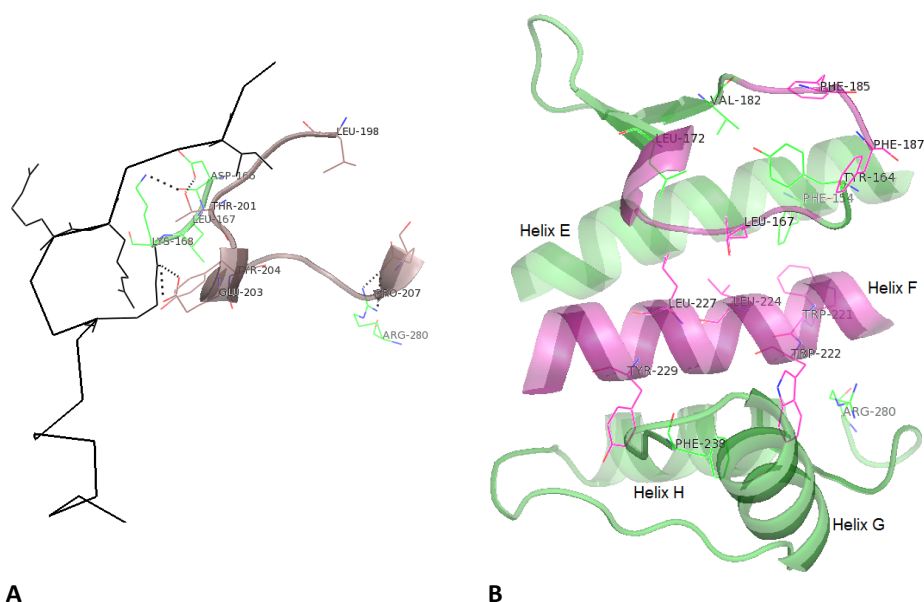


Figure 29. Peptide-positioning loop and interactions within the hydrophobic core. (A) Loop shown as brown cartoon and lines, PKI(5–24) as black ribbon (residues in positions P-6, P-3, P-2 and P+1 also as lines), interacting residues of PKAc as green lines. Pro202 and Leu205 form a hydrophobic pocket for accommodation of the hydrophobic residue in the P+1 position of the substrate. Thr201 makes hydrogen bonds with catalytic base Asp166 and with Lys168. Glu203 is responsible for the recognition of Arg residue in the P-6 position of the substrate. Tyr204 is critical for anchoring of the P+1 loop to the catalytic core, with the main contribution provided by hydrophobic interaction of Tyr204 with Leu167 of the catalytic loop and involvement of Tyr204 in the hydrophobic core formed by Helix E and Helix F [Yang J. *et al.*, 2004]. Glu208 forms the anchor for the P+1 loop by generating hydrogen bond with Arg280 from the loop between Helix H and Helix I. (B) Mg^{2+} -positioning loop, catalytic loop and Helix F are colored pink, the rest of PKAc is green. Below the Mg^{2+} -positioning loop and on the top of catalytic loop, a hydrophobic network is formed by Tyr164, Val182, Phe185, Phe187 and Trp221, whereas below the catalytic loop and on top of Helix F, another set of hydrophobic interactions is clustered around Leu167 and involves additionally Phe154, Leu172, Ala223 and Leu227. Trp222 below Helix F develops hydrophobic interactions with the Phe238 from the loop between the F and G helix, and links Helix F with peptide-positioning loop *via* with interaction with Arg280 that serves as a bridge.

The latter part of the large lobe is relatively hydrophobic, especially Helix F, which defines the hydrophobic core of PKAc. This core consists of two parts, one clustered around Tyr164 and another around Leu167 (Figure 29B); these two layers of interactions orchestrate the ordering of the large lobe of PKAc by signaling from the Mg^{2+} -positioning loop to the catalytic loop, and from the catalytic loop to the Helix F [Akamine *et al.*, 2003; Kornev *et al.*, 2006; Kornev and Taylor, 2010]. However, there are also two conserved charged residues in

Helix F, Asp220 and Glu230; while Asp220 forms hydrogen bonds with the amide hydrogen atoms of Tyr164 and Arg165 and thus contributes to the positioning of the catalytic loop, Glu230 is in parallel to Glu170 responsible for the recognition of Arg residue in the P-2 position of the substrate. Additionally, the interaction of Glu230 with Arg133 creates the upper part of the PKAc site for the recognition of the amphipathic helix of PKI in the position P-8...P-16 of the substrate, whereas the essential lower part of this site is formed by Phe239 of the loop between the Helix F and Helix G [Johnson D. A. *et al.*, 2001].

The C-terminal tail wraps around the surface of both lobes [Yang J. *et al.*, 2009], whereas the first fourteen residues are anchored to the large lobe and constitute a part of the hydrophobic pocket where the N-terminal myristoyl group binds. The intermediate part of the tail is relatively flexible; while residues 315...327 form a “gate” over the ATP-binding site, the residues 328...334 incorporating several acidic amino acids contribute to the recognition of protein/peptide substrate (*i.e.*, Tyr330 in parallel to Glu127 is responsible for the recognition of the Arg residue in the P-3 position of the substrate). The last four residues of the C-terminal tail are anchored to the small lobe, whereas Phe347 and Phe350 form the hydrophobic pocket which is also lined by residues of Helix C (Ile85, Leu89) and β -strand 5 (Leu116, Met118). Importantly, residues 347...350 of the C-terminal tail as well as the preceding residues 327...330 have also been shown to contribute to the recognition of PKAc by PDK1, the PK that performs phosphorylation of PKAc on Thr197 *in vivo*; additionally, the recognition of PKAc by PDK1 is facilitated by the phosphorylated state of Ser338 [Romano *et al.*, 2009].

3.3.3. Conformational versatility of PKs

Despite the fact that a protein crystal structure may provide only a static picture of the protein, the obtainment of several crystal structures from different complexes of one protein enables the construction of a model of conformational changes of the protein associated with its functioning. The crystal structure of the apoenzyme of PKAc (PDB 1J3H), in parallel with crystal structures of PKAc binary complexes with adenosine (PDB 1BKX) or PKI (PDB 2GFC), and quaternary complex with ADP, AlF₃ and the phosphorylatable analogue of PKI(5...24) (PDB 1L3R) reveal the dynamic changes in PKAc associated with the binding of ligands and performance of catalysis [Akamine *et al.*, 2003; Bonn *et al.*, 2006; Madhusudan *et al.*, 2002; Narayana *et al.*, 1997; Taylor S. S. *et al.*, 2004].

The crystal structure of the active PKAc apoenzyme (with phosphorylated Thr197) revealed that according to the B-factors, the small lobe is relatively dynamic in the absence of ligands, while the large lobe is remarkably stable and most of the catalytically residues from the large lobe are ready for the catalysis already in the apoenzyme [Akamine *et al.*, 2003]. PKAc adopts open conformation, *i.e.*, the part of the small lobe distant from the spanning Helix A is

moved away from the large lobe (*i.e.*, as compared to the previously discussed 1ATP structure). Numerically, the degree of openness of conformation is assessed according to the distances Tyr330...Glu127, Ser53... Asp166, and His87...phosphorylated Thr197 [Johnson D. A. *et al.*, 2001]; in apoenzyme, the corresponding distances are >20 Å, 12.8 Å and 10.4 Å (Figure 30A).

The residues of the small lobe responsible for the fixation of phosphate moieties of ATP are mostly disordered in the apoenzyme, *i.e.*, the side-chain of Lys72 is not visible, and the residues 52...55 of the Gly-rich loop possess very high B-factors [Akamine *et al.*, 2003]. On the contrary, the residues responsible for binding of adenine moiety of ATP are generally in the same positions as in the binary complex with adenosine, with exception of Val57, Met120, Leu173, and Phe327. Whereas the side-chains of Val57 and Leu173 are not visible in the apoenzyme crystal, Met120 (which otherwise serves as the gate-keeper residue) points away from the catalytic cleft, and the portion of the C-terminal tail including Phe327 is disordered. The latter fact demonstrates that the “gate” formed by the residues 315...327 and regulating access to the ATP-site is ordered only upon binding of the ligand to the ATP-site [Taylor S. S. *et al.*, 2004].

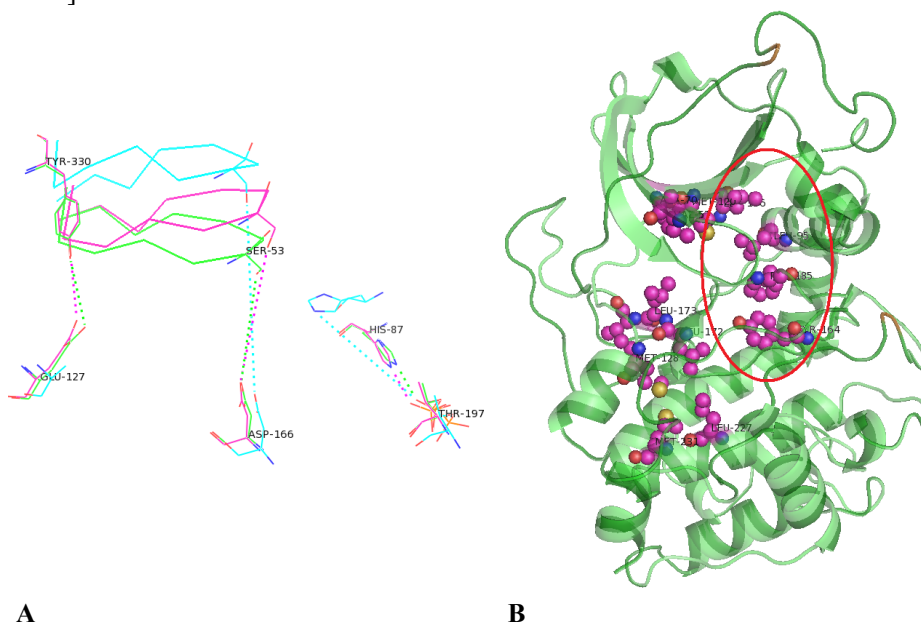


Figure 30. Conformational versatility of PKAc and interaction networks. (A) Superimposition of crystal structures 1ATP (ternary complex PKAc-AMPPNP-PKI(5–24); green), 1YDT (ternary complex PKAc-H89-PKI(5–24); magenta), and 1J3H (PKAc apoenzyme; cyan). (B) Hydrophobic network in PKAc. PKAc shown as green cartoon, hydrophobic residues constituting most important “spines” as magenta spheres; the main vertical spine surrounded with red oval is formed by Leu95 from Helix C, Leu106 from β -strand 4, Phe185 from Mg^{2+} -positioning loop, and Tyr164 from the region preceding catalytic loop [according to Kornev and Taylor, 2010].

The stable core of the apoenzyme is formed by Helix C, Helix D, Helix E, and β -strand 6; importantly, the catalytically crucial residues Asp166 and Lys168 belonging to this region are pre-positioned for catalysis [Akamine *et al.*, 2003]. Apart from those, several residues are pre-formed for binding of the protein/peptide substrate, *i.e.*, Glu170, Glu203, Glu230, and residues creating the P+1 pocket. However, residues Arg133 and Phe239 are not properly oriented, and the side-chain of Glu127 is not visible in the apoenzyme. The latter fact indicates that ordering of this residue occurs upon binding of ATP (*i.e.*, interaction with hydroxyl in 2' position of ribose moiety of ATP positions the side-chain of Glu127 suitably for the recognition of Arg residue in the P-3 position of the substrate) [Taylor S. S. *et al.*, 2004].

The observation considering the stability of the large lobe is also true for other crystal structures of active PKAc, as no major conformational changes are induced in the large lobe upon binding of ligands [Bonn *et al.*, 2006; Narayana *et al.*, 1997; Taylor S. S. *et al.*, 2004]. Instead, there are two major networks responsible for the communication of conformational changes in the active site to the remote regions of PKAc: the network started by ordering of Glu127, as discussed above, and the hydrophobic network (please also refer to Section 3.3.2. Ternary complex of PKAc with AMP-PNP and PKI(5...24)) [Akamine *et al.*, 2003; Kornev *et al.*, 2006; Kornev and Taylor, 2010]. The latter consists of two hydrophobic spines, one spine formed by the hydrophobic amino acid moieties from the ATP-binding hinge, Helix D and C-terminus of Helix F, and another spine incorporating residues from β -strand 4, Helix C, the region preceding catalytic loop and Mg^{2+} -positioning loop (Figure 30B).

The small lobe, still, can rotate and slide away in respect to the large lobe in different crystal structures, which allows the Gly-rich loop of PKAc to adopt a variety of intermediate conformations between the fully opened (corresponding to the apoenzyme) and fully closed (corresponding to the complex resembling the transition state). In case of fully closed conformation (*i.e.*, transition state model), the distances Tyr330...Glu127, Ser53...Asp166, and His87...phosphorylated Thr197 are 4.4 Å, 7.6 Å and 2.7 Å, respectively. In general, the crystal structure modeling of the phosphoryl transition state (where AlF_3 is used instead of the transferable phosphoryl group) is remarkably similar to the previously discussed ternary complex of PKAc with AMP-PNP and PKI(5...24) [Madhusudan *et al.*, 2002]. Importantly, the AlF_3 molecule is positioned between ADP and the phosphorylatable analogue of PKI(5...24) according to the dissociative mechanism of the direct in-line transfer, confirming the dissociative character of the phosphoryl transfer by PKs [Parang *et al.*, 2001].

Unfortunately, no crystal structure of the inactive state of PKAc (with non-phosphorylated Thr197) has so far been resolved. However, the comparison of crystal structures of various PKs in their activated *versus* inactivated states (Figure 31) allowed formulation of a model reflecting profound conformational changes in PKs associated with phosphorylation of the Thr residue from the

activation loop (corresponding to Thr¹⁹⁷ of PKAc¹¹) [Johnson, 2009; Kornev *et al.*, 2006]. Generally, there are several features of crystal structures of PKs characteristic of an inactive state (whereas for different PKs, different features are valid) [Huse and Kuriyan, 2002; Nolen *et al.*, 2004]:

- opening of the small lobe in respect to the large lobe;
- inordered activation loop, or the activation loop bound to the catalytic loop and thus serving as autoinhibitory domain;
- “swung-out” conformation of Helix C, where Glu⁹¹ is exposed to the solvent and its interaction with catalytically important Lys⁷² is disrupted;
- “DFG-out” state of the Asp-Phe-Gly motif of the Mg²⁺-positioning loop, where Asp¹⁸⁴ points out of the catalytic cleft (and no longer binds to the upper Mg²⁺-ion) and Phe¹⁸⁵ points into the catalytic cleft.

The “swing-in” movement of Helix C upon phosphorylation of Thr¹⁹⁷ from the activation loop results from the gain of interaction between phosphoryl of Thr¹⁹⁷ and Lys¹⁸⁹ or Thr¹⁹⁷ and Arg¹⁹⁰ (Figure 31A–D). In the “swung-out” Helix C, Glu⁹¹ pointing to the solvent usually forms a charge-assisted hydrogen bond to Arg¹⁹⁰; however, the phosphoryl of Thr¹⁹⁷ successfully outcompetes this interaction by forming the charge-assisted hydrogen bond with Arg¹⁹⁰ itself or the preceding residue (Lys¹⁸⁹) [Levinson *et al.*, 2006]. The reorganization of the “DFG-out” state of the Asp-Phe-Gly motif, on the other hand, involves several steps, but is also initiated by the interaction between Thr¹⁹⁷ and Lys¹⁸⁹, and another interaction between Thr¹⁹⁷ and Arg¹⁶⁵ (Figure 31E). Dephosphorylation of Thr¹⁹⁷ causes repulsion of Arg¹⁶⁵ and Lys¹⁸⁹, and thus destroys the ensemble of residues holding Asp¹⁸⁴ in the “DFG-in” state [Kornev *et al.*, 2006].

¹¹ Further on in this section, the residues of PKs corresponding to the residues of PKAc are denoted with three-letter code of the amino acid with superscript number of the residue in PKAc; *i.e.*, the Thr residue corresponding to Thr¹⁹⁷ in PKAc is denoted as Thr¹⁹⁷.

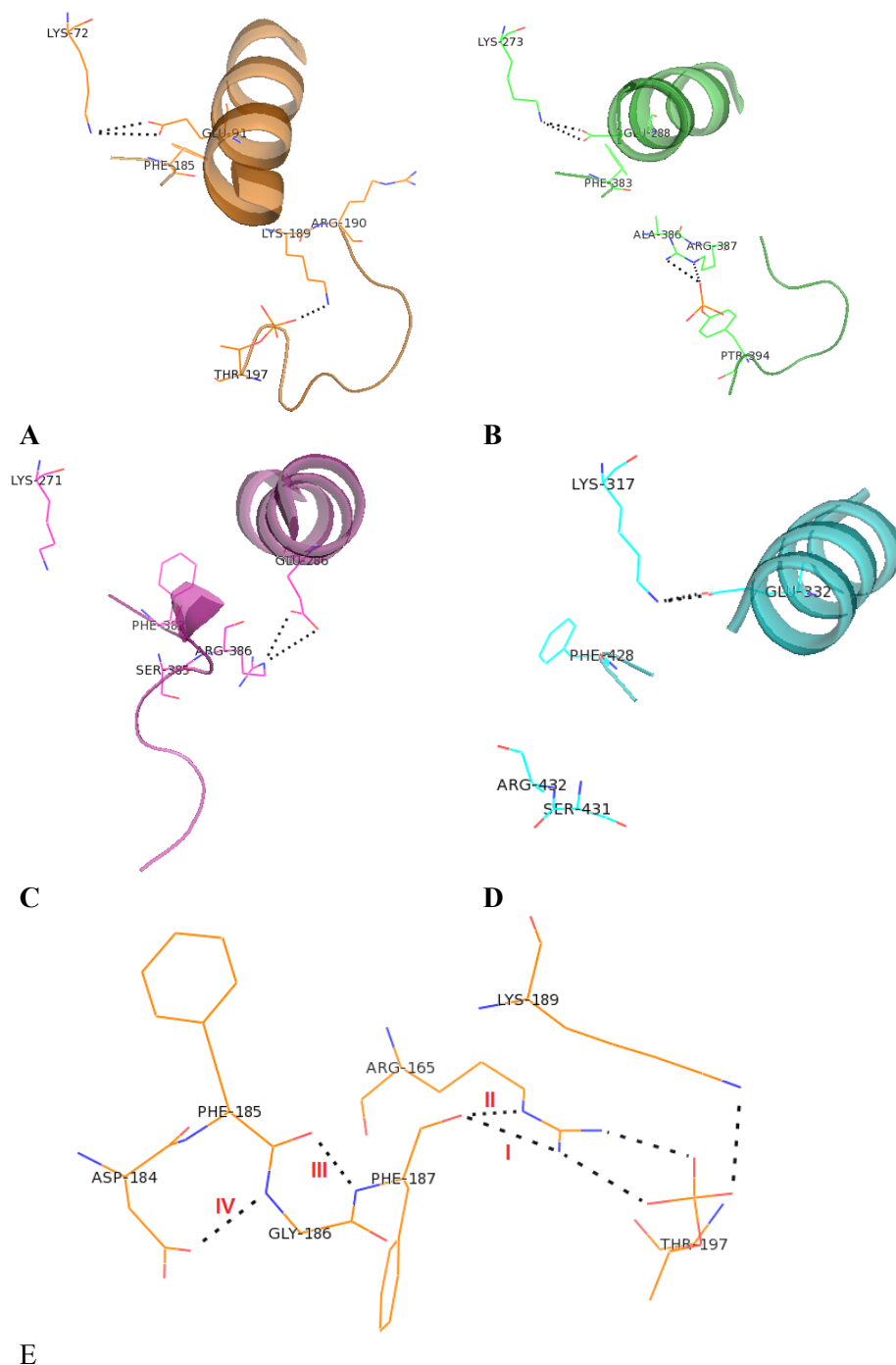


Figure 31. Comparison of active and inactive conformations of PKs. (A) 1ATP, representing the active conformation of a kinase (PKAc). Helix C, activation loop and Mg^{2+} -positioning loop shown as cartoon, residues responsible for active conformation

of Helix C and Asp-Phe-Gly triad shown as lines. (B) 3LCK, representing the active conformation of a kinase (LCK). (C) 2G1T, representing an inactive α C-Glu-out conformation of a kinase (Bcr-Abl). (D) 3GVU, representing an inactive DFG-out conformation of a kinase (Bcr-Abl); activation loop disordered. (E) 1ATP, organization of Asp-Phe-Gly motif by phosphorylated Thr¹⁹⁷. The positioning of Arg¹⁶⁵ resulting from interaction with Thr¹⁹⁷ triggers turning of the amide bond between DFG+1 and DFG+2 residues towards Arg¹⁶⁵, and formation of two additional hydrogen bonds (I and II). Subsequently, the amide bond between Phe¹⁸⁵ and Gly¹⁸⁶ turns and generates a hydrogen bond (III) with the amide hydrogen of DFG+2 residue. Additionally, this positioning of the amide bond between Phe¹⁸⁵ and Gly¹⁸⁶ favors formation of hydrogen bond (IV) between the amide hydrogen of Gly¹⁸⁶ and the side-chain of Asp¹⁸⁴, which finally fixes the catalytically correct position of the latter.

3.3.4. PKAr subunits and holoenzyme

PKAr subunits serve as physiological regulators of PKAc activity, and are also responsible for the intracellular localization of the enzyme *via* interaction with AKAPs. PKAr consists of the N-terminal docking/dimerization domain (D/D) and the C-terminal cAMP-binding domains A and B; these domains are joined by a linker that contains the so-called inhibitor sequence, *i.e.*, the fragment that can bind to the protein/peptide substrate-site of PKAc [Kinderman, *et al.* 2006; Sarma *et al.*, 2010]. According to its name, the main function of the D/D domain of PKAr is the formation of a dimer of PKAr subunits, whereas the joined D/D regions of two PKAr subunits constitute a motif for binding to AKAP, and the latter part of the PKAr dimer interacts with PKAc or with cAMP. Unfortunately, no crystal structure is available about the full-length PKAr; however, there are crystal structures of PKArI α and PKArII α D/D domains with or without AKAPs, and of N-terminally truncated PKArI α , PKArII α or PKArII β with PKAc α or with cAMP [Brown S. H. J. *et al.*, 2009; Kim C. *et al.*, 2007; Kinderman, *et al.* 2006; Sarma *et al.*, 2010; Wu J. *et al.*, 2007].

The dimerized PKArI α D/D domains as well as the dimerized PKArII α D/D domains have been co-crystallized with the dual-specificity AKAP, D-AKAP2 (PDB 3IM4 and PDB 2HWN, respectively) [Kinderman, *et al.* 2006; Sarma *et al.*, 2010]. Both crystal structures showed that the D/D dimer is in both cases formed by the XX-shaped antiparallel bundle of four helices, α_1 (residues 25...38 of PKArI α , 8...24 of PKArII α) and α_2 (residues 44...60 of PKArI α , 27...42 of PKArII α) from each monomer. Additionally, in 3IM4 two helices α_0 (residues 13...21) contribute to this surface, as the Cys16 from helix α_0 of each monomer forms disulfide bridge with Cys37 from helix α_1 of another monomer (Figure 32). The amphipathic helix of D-AKAP2 (residues 628–654 in 3IM4, residues 631...649 in 2HWN) binds diagonally across one face on the formed surface, and generates multiple contacts with helices α_1 of each monomer. Interestingly, in 2HWN the binding of the asymmetric sequence of D-AKAP2

induces an asymmetry of the PKArII α dimer: only in one monomer, the N-terminus (residues 1...8) preceding the helix α_1 is ordered, and the residues Ile3 and Ile5 interact with the D-AKAP2 helix [Kinderman, *et al.* 2006]. Such flexibility of structure probably contributes to the wider AKAP-selectivity profile of PKArII α as compared to PKArI α .

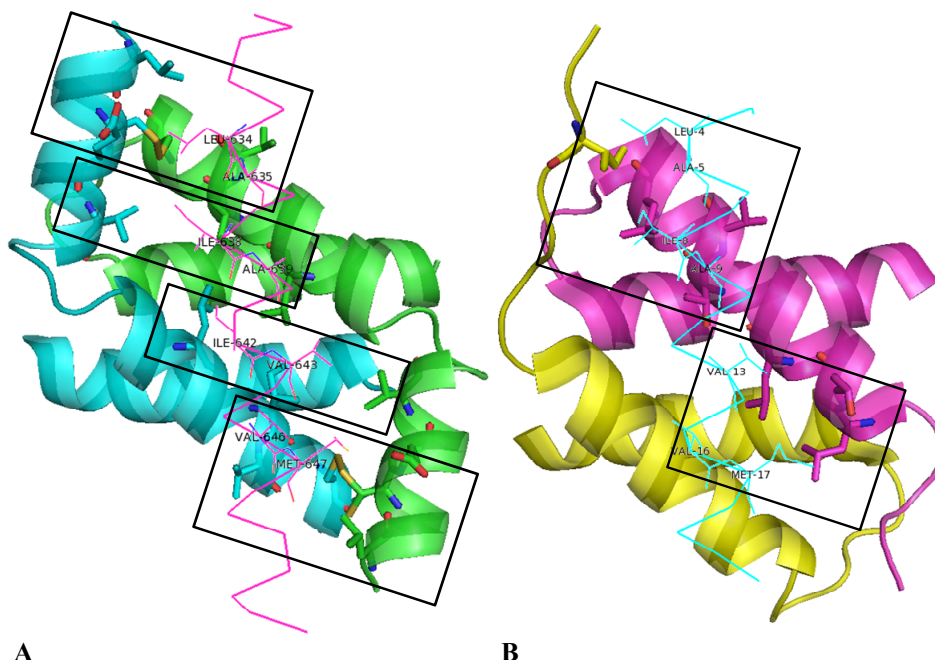


Figure 32. Interactions between PKArI α and D-AKAP2. (A) 3IM4. D/D fragments of PKArI α subunits are shown as cartoon (cyan for one subunit and green for another; residues participating in interactions with D-AKAP2 also shown as sticks), D-AKAP2 as magenta ribbon (the residues participating in strong interactions with PKArI α are also shown as lines and numbered). Black boxes indicate four main regions of binding at the interface. (B) 2HWN. D/D fragments of PKArII α subunits are shown as cartoon (yellow for the more ordered subunit and magenta for the less ordered one; residues participating in interactions with D-AKAP2 also shown as sticks), D-AKAP2 as cyan ribbon (the residues participating in strong interactions with PKArII α are also shown as lines and numbered). Black boxes indicate two main regions of binding at the interface.

Despite higher K_D value towards PKArI α (48 nM towards PKArI α , 2 nM towards PKArII α [Kinderman, *et al.* 2006]), the interface between PKAr and D-AKAP2 is larger in 3IM4 than in 2HWN: while in the former, there are four main regions of binding at the interface, in 2HWN there are only two regions (Figure 32). The formed interactions are mainly hydrophobic, although several polar contacts are also present. Interestingly, in co-crystal with PKArII α , a shift

of D-AKAP2 helix by one helix turn towards the N-terminus occurs in comparison to the co-crystal with PKArI α . Importantly, the pockets on the surface of dimerized PKAr subunits where residues of D-AKAP2 bind show preference for different hydrophobic residues (*i.e.*, as binding partners) dependent on the isoform of the PKAr, revealing the basis for selectivity of several AKAPs towards PKArI α [Kinderman, *et al.* 2006; Sarma *et al.*, 2010]. Analogically, different isoforms of PKAr display similar patterns of binding to the PKAc subunit and similar conformational changes upon binding of cAMP, although the details and the extent of these processes are dependent on the PKAr isoform [Brown S. H. J. *et al.*, 2009; Kim C. *et al.*, 2007; Wu J. *et al.*, 2007]. As the effects are most pronounced in case of PKArI α , the co-crystal of the truncated mutant form of PKArI α (91...379:Arg333Lys) with PKAc α and ATP (PDB 2QCS) and the co-crystal of another truncated form of PKArI α (113...376) with cAMP (PDB 1RGS) will be used as the illustrative examples [Kim C. *et al.*, 2007].

The PDB 2QCS co-crystal revealed that PKAc is in closed conformation, whereas PKArI α binds to PKAc in an extended conformation where cyclic nucleotide binding domains A and B are separated by the elongated helix B/C from domain A of PKArI α . There are four major sites on the surface of PKAc subunit involved in interactions with PKArI α [Kim C. *et al.*, 2007]:

- Site 1, spanning the C-terminal tail, protein/peptide substrate-site of PKAc, and P+1 loop (Figure 33A);
- Site 2, created by the hydrophobic surface of Helix G and P+1 loop (Figure 33B);
- Site 3, formed by the activation loop (Figure 33C);
- Site 4, involving the loop between Helix H and Helix I (Figure 33D).

The linker of PKArI α (residues 91...123, in full-length protein 45...123) binds to sites 1 and 2, domain A (123...258) binds to sites 2 and 3, and domain B (259...379) binds to sites 3 and 4 (Figure 34). Interestingly, the helix B/C from domain B of PKArI α is not elongated as its counterpart from domain A, but represents a construction containing three short segments, helices B, C, and C'.

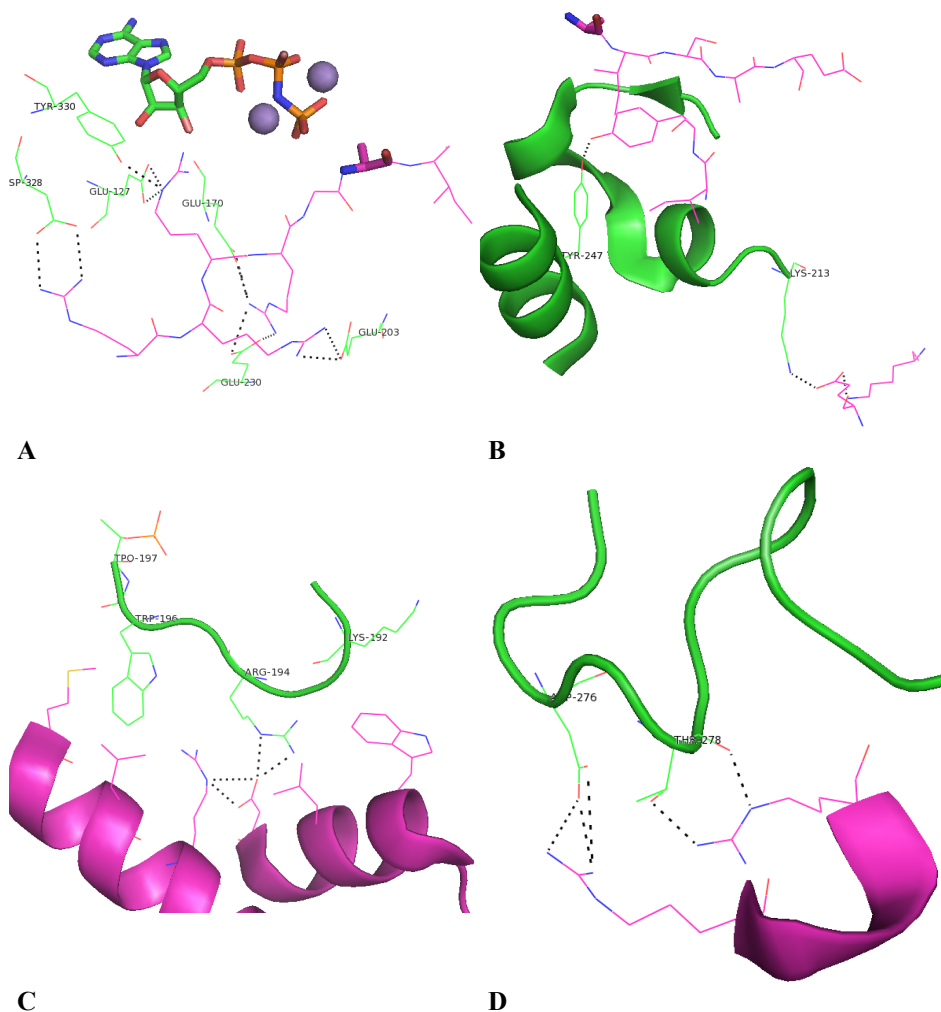


Figure 33. 2QCS, PKAc colored as green and PKArIα as magenta; numbers are given only for PKAc residues. (A) Site 1 is filled by the inhibitor sequence (residues 92...98) from the linker region of PKArIα; while Arg95 of PKArIα¹² (in position P-2) binds to Glu170^c and Glu230^c, Arg94^r (P-3) interacts with the side-chains of Glu127^c and Tyr330^c, Arg93^r (P-4) forms charge-assisted hydrogen bond to Glu203^c, and Arg92^r (P-5) makes two contacts with Asp328^c. Such hydrogen bond network is characteristic of PKArI isoforms, as only PKArI subunits (but not PKArII) contain Arg residues in positions P-4 and P-5. (B) Site 2 forms a hydrophobic interface with residues 97...101 and 204...205 of PKArIα; additionally, a hydrogen bond is generated between Tyr247^c and Tyr205^r, and polar interactions are developed between Lys213^c, Glu143^r, and Lys240^r. (C) The three “hot-spots” of binding between Site 3 and PKArIα are represented by the hydrophobic pocket formed by Trp196^c, Met234^r and Leu238^r, the

¹² Further on in this section, the residues of PKAc are denoted with superscript ^c, and the residues of PKAr with superscript ^r.

polar network of interactions between Arg194^c, Arg241^f and Asp267^f, and the hydrophobic contact area lined by Lys192^c, Trp260^f and Leu263^f. (D) In Site 4, the side-chains of Asp276^c and Thr278^c make a hydrogen bond to Arg352^f; additionally, Thr278^c *via* its side-chain and its backbone carbonyl group forms two hydrogen bonds to Arg355^f.

Binding of two cAMP molecules to PKA α induces a profound reorganization of the latter subunit, with the most drastic conformational change represented by bending of helix B/C from domain A, and rotation around the points in this helix corresponding to residues Arg226^f, Gly235^f, and Tyr244^f [Kim C. *et al.*, 2007]. As a result of such a bending and twisting movement, the cAMP-bound PKA α is folded into a globular structure (Figure 34B). In both domains A and B, the phosphate moiety of cAMP molecule makes multiple hydrogen bonds with the backbone nitrogen atoms of the short helix positioned inside the cAMP-binding site and termed phosphate-binding cassette (PBC, residues 200...205 in domain A, 324...329 in domain B). Additionally, in the cAMP-binding site of each domain a hydrogen bond is formed between the phosphate moiety of cAMP and the conserved arginine residue (Arg209^f in domain A, Arg333^f in domain B). Moreover, after cAMP-induced folding of PKA α , the residues Trp260^f and Tyr371^f are positioned under the five-stranded β -sandwiches of domain A and domain B, respectively, and become the “capping residues” for the cAMP-binding sites [Kim C. *et al.*, 2007]. By contrast, in PKAc-bound state, residue Trp260^f is involved in interactions with Site 3, and Tyr371^f is kept away from the rest of domain B by the intramolecular salt bridge formed by the preceding Arg366^f with Glu261^f.

As Tyr371^f is better accessible for cAMP than Trp260^f, the proposed mechanism for the cAMP-mediated activation of PKA starts from occupation of cAMP-binding site in domain B and “capping” of the bound cAMP molecule by Tyr371^f [Kim C. *et al.*, 2007]. The development of this hydrophobic interaction causes breakage of the salt bridge between Arg366^f with Glu261^f, and thus triggers bending of helix B/C from domain A; bending of the latter helix enables formation of the interface between the domains of PKA α . Finally, binding of another cAMP molecule to domain A necessitates “capping” of the bound cAMP molecule by Trp260^f, which causes dissociation of PKA α from PKAc.

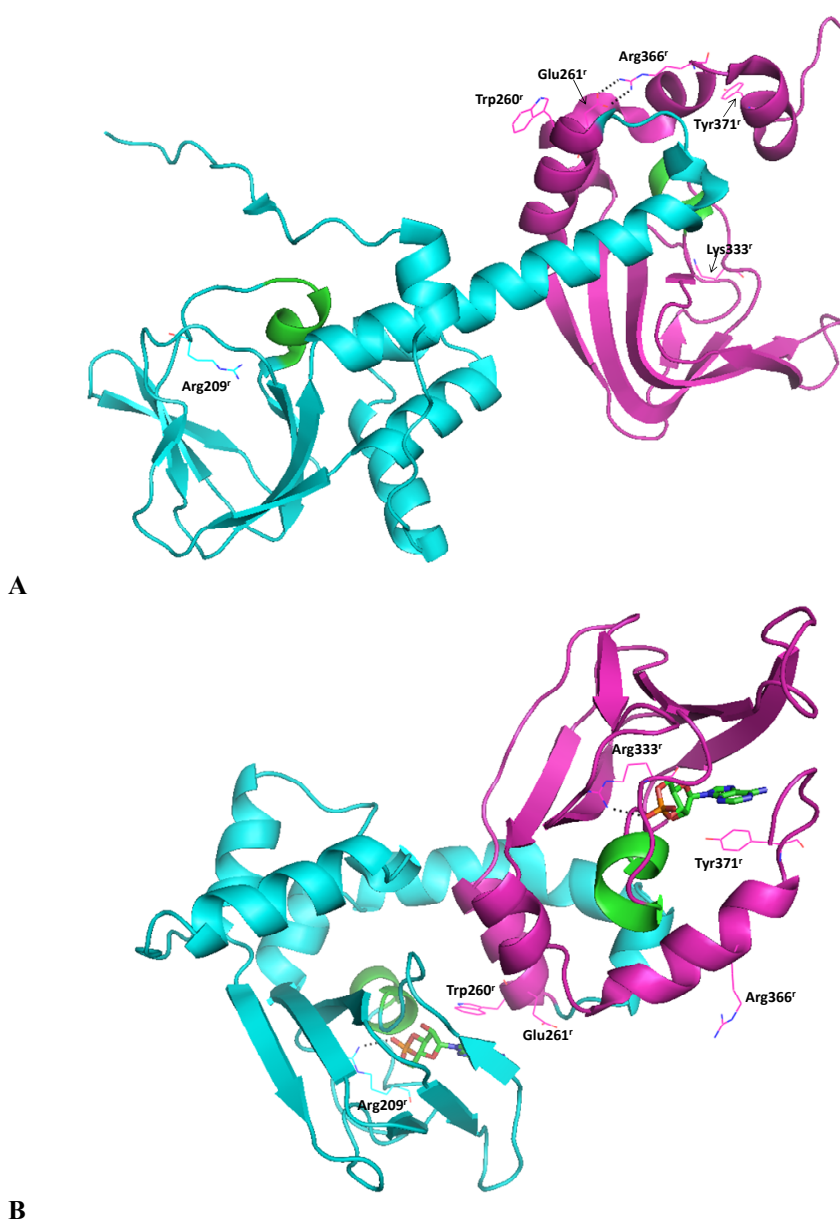


Figure 34. Conformational versatility of PKArl α . (A) 2QCS, PKAc-bound conformation of PKArl α . Domain A of PKArl α is shown as cyan cartoon, domain B as magenta cartoon, PBCs of either domain are colored green; residues important for cAMP binding are also shown as lines and numbered. (B) 1RGS, cAMP-bound conformation of PKArl α . The interface between the two lobes of the globular structure of cAMP-bound PKArl α is formed by the cAMP molecule binding to domain A, the kinked helix B/C from domain A, and helices A and B from domain B. The helices A and B from domain B are aligned parallel to each other and perpendicular in respect to the helix B/C from domain A.

This model is most likely valid for all isoforms of PKAr subunits, at least for PKArII α and PKArII β , as indicated by co-crystals of truncated forms of the latter with PKAc (PDB 2QVS and PDB 3IDC, respectively) [Brown S. H. J. *et al.*, 2009; Wu J. *et al.*, 2007]. However, there are other aspects in which PDB 2QVS and PDB 3IDC differ from 2QCS, such as conformation of PKAc subunit. In 2QVS, PKAc is in an open conformation due to the lack of ATP in the co-crystal, and the C-terminal tail of PKAc is disordered [Wu J. *et al.*, 2007]. By contrast, in 3IDC (similarly to 2QCS), the C-terminal tail of PKAc is ordered and the conformation of PKAc is more closed, but the hydrogen bond between Ser53^c and γ -phosphate moiety of ATP is absent [Brown S. H. J. *et al.*, 2009]. Still, in all three crystal structures the N-terminus of PKAr subunits becomes ordered as a result of binding to PKAc, in contrast to the unordered N-terminal linker of cAMP-bound PKAr subunits. Importantly, in case of 3IDC the linker residues 103...105 corresponding to the positions P-9...P-7 are not disordered as in 2QCS or 2QVS, but instead form an extended strand generating hydrophobic interactions with the loop between Helix F and Helix G of PKAc [Brown S. H. J. *et al.*, 2009]. The latter loop is also utilized as a binding partner by the amphipathic helix of PKI, but not by other isoforms of PKAr (as those possess an acidic linker that probably cannot bind to the hydrophobic surface) [Johnson D. A. *et al.*, 2001]; the latter fact emphasizes the multiplicity of mechanism for recognition of ligands binding to the protein/peptide substrate-site of PKAc.

AIMS OF THE STUDY

The main aims of this study were as follows:

- focussed design and synthesis of ARCs with improved proteolytic stability and enhanced affinity towards basophilic PKs;
- co-crystallization of ARCs with PKAc aimed at facilitation of the structure-aided design of new inhibitors;
- establishment of PK selectivity profiles for the most efficient ARCs, and determination of the fragments in the structure of ARCs responsible affecting their selectivity towards certain PKs;
- application of the most efficient ARCs for the *in vitro* experiments in living tissue by utilizing ability of ARCs to block certain PK pathways.

RESULTS AND DISCUSSION

I. Development of ARC-II conjugates [Paper 1: Enkvist *et al.*, 2006, Paper 3: Lavogina *et al.*, 2010a]

Despite several attractive properties such as combination of enhanced potency and selectivity, the bisubstrate inhibitors of protein kinases have been substantially less intensively explored than ATP-competitive compounds. One of the subgroups of BSIs is represented by ARCs, conjugates of an adenosine analogue (nucleosidic **Fragment 1**) and an arginine-rich peptide (peptidic **Fragment 2**), with **Fragment 1** targeted to the ATP-site and **Fragment 2** to the protein/peptide substrate-site of a PK (Figure 35).

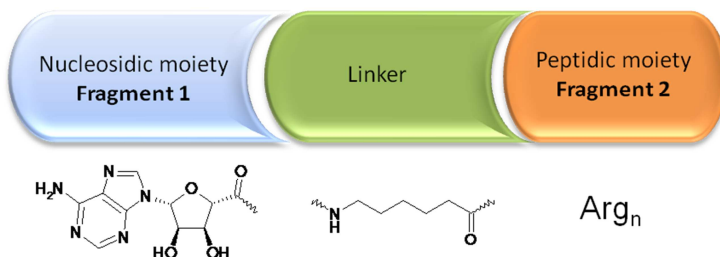


Figure 35. General scheme of ARC-I and ARC-II inhibitors. Below are shown examples of structures of **Fragment 1**, **Fragment 2**, and linker.

According to the initial design (prior to the given thesis) Adc moiety had been applied as **Fragment 1** and oligo-(L-arginine) as **Fragment 2**, linked *via* a hydrophobic flexible linker [Loog *et al.*, 1999]. By virtue of incorporation of highly charged cationic oligo-arginine peptide, ARCs had initially been developed as group-selective inhibitors targeting basophilic protein kinases (*i.e.*, PKAc, PKC, CAMK, *etc.*). The moderate inhibitory potency of the initial ARCs (IC₅₀ values in the submicromolar range) motivated the further optimization of the structure of these compounds aimed at increase of affinity towards PKAc. The latter was chosen as a model PK, as its mechanisms of activation and functioning are thoroughly described in the literature, and PKAc is available from several commercial resources in high purity and as the non-truncated active form.

The changes in the structure of initial ARCs included the following variations:

- amidation of the C-terminus of the conjugates;
- conversion of the peptidic **Fragment 2** to its enantio-modification, *i.e.*, use of D-arginines instead of L-arginines;

- modification of the linker part by reversion of direction of the amide bond between **Fragment 1** and **Fragment 2**, by N-methylation of the amide bond between **Fragment 1** and **Fragment 2**, and by introduction of rigid aromatic amino acids or additional hydrogen bond donors (*i.e.*, NH groups);
- conversion of the peptidic **Fragment 2** to its retro-analogue, *i.e.*, attachment of **Fragment 1** to the C-terminus of **Fragment 2**, not *vice versa*;
- modification of **Fragment 1** by elimination of ribose moiety of Adc, or by replacement of Adc with H-series inhibitor H-9 moiety (analogically to the work by Ricouart *et al.*, 1991).

In all novel conjugates, two structural units were preserved as in the initial ARCs: the length of the linker between **Fragment 1** and **Fragment 2**, and the use of oligo-arginine as **Fragment 2**. The structure of the first unit was optimized for inhibitory potency in studies with initial ARC-s by variation of the length of hydrophobic flexible linkers, and it had been shown that at the distance corresponding to the length of 6-aminohexanoic acid moiety, the highest affinity towards PKAc was achieved [Loog *et al.*, 1999]. The second unit, on the other hand, was kept intact because oligo-arginine had been demonstrated to provide conjugates with high affinity towards basophilic PKs as well as cell-penetrative properties [Uri *et al.*, 2002; Viht *et al.*, 2003]. It was acknowledged that application of oligo-arginine would possibly result in promiscuous nature of ARCs; however, at that point of ARC-development it was primarily important to achieve high affinity, not selectivity. The range of ARC-based applications was envisioned to be connected with generic affinity supports and fluorescent probes of PKs [Loog *et al.*, 2000], where selective pinpointing of certain PKs might be performed *via* other mechanisms (*i.e.*, elution/displacement with selective ACIs, PCIs, or BSIs). Moreover, it was presumed that in case if selectivity of ARCs would be set into the focus of attention, it could be possible to “tune” it by exchange of **Fragment 1** or linker. Twenty-five new ARCs were synthesized by combination of solid phase-peptide synthesis and solution synthesis approaches. The general synthetic scheme involved preparation of **Fragment 1** in solution and **Fragment 2** on solid phase, whereas the linker could be initially attached to either of the fragments and the procedure of conjugation could be performed either on solid phase or in solution, dependent on the course of preceding synthesis. The assessment of inhibitory potency of compounds towards PKAc was performed with the aid of non-radioactive TLC-based assay [Viht *et al.*, 2005], where the retarding effect of an inhibitor on PKAc-catalyzed phosphorylation reaction was monitored *via* the chromatographic separation of phosphorylated and non-phosphorylated forms of fluorescently labelled peptide substrate (5-TAMRA-Kemptide).

From the results of inhibition studies, the following modifications that significantly enhanced the inhibitory potency of ARCs were established (please refer to Table 1 from Paper 1):

- Amidation of the C-terminus of the conjugates resulted in 4–6-fold increase in potency, *i.e.*, IC₅₀ value of 170 nM for **ARC-341** (compound **3** from

Paper 1; (Figure 36A) *versus* IC₅₀ value of 700 nM for the corresponding non-amidated conjugate [Loog *et al.*, 1999].

- Use of D-arginines instead of L-arginines in **Fragment 2** resulted in a 20-fold increase in potency, *i.e.*, IC₅₀ value of 8.3 nM for **ARC-902** (compound **5** from **Paper 1**; Figure 36B) *versus* IC₅₀ value of 170 nM for the corresponding conjugate **ARC-341** containing oligo-(L-arginine) moiety (compound **3** from **Paper 1**). Moreover, application of D-arginines substantially improved the stability of novel ARCs towards proteolysis, as was detected in degradation experiments with fetal bovine serum and trypsin.
- Introduction of H-9 moiety as **Fragment 1** and Hex as linker resulted in slight increase in potency in case of conjugates containing oligo-(D-arginine), *i.e.*, IC₅₀ value of 5.3 nM for **ARC-903** (compound **26** from **Paper 1**; Figure 36D) *versus* IC₅₀ value of 8.3 nM for the corresponding conjugate **ARC-902** containing Adc moiety (compound **5** from **Paper 1**). However, the comparison of conjugates containing oligo-(L-arginine) revealed a 65-fold increase in potency, *i.e.*, IC₅₀ value of 30 nM for **ARC-349** (compound **25** from **Paper 1**; Figure 36E) *versus* IC₅₀ value of 2000 nM for the corresponding conjugate containing Adc moiety (compound **2** from **Paper 1**). All in all, as compared to the *Compound 17* reported in Ricouart *et al.*, 1991, the inhibitory properties of H-9-containing ARCs were not more efficient. However, in case of ARCs the all-D-arginine fragment was substituted for the all-L-arginine fragment of *Compound 17* unstable in biological systems, and the overall structure of the conjugate was also simplified by elimination of chiral and phosphorylatable Ser residue.

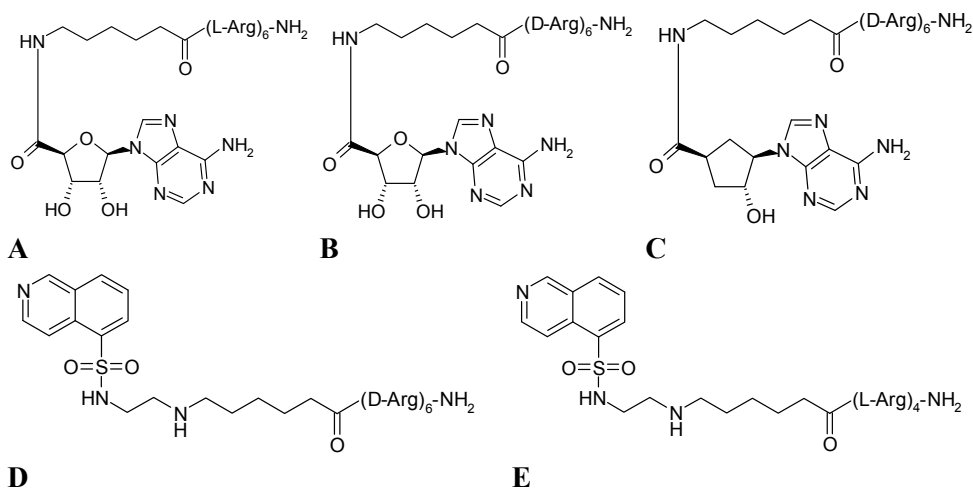


Figure 36. Examples of ARC-II. (A) **ARC-341**. (B) **ARC-902**. (C) **ARC-659-1b**. (D) **ARC-349**. (E) **ARC-903**.

Additionally, it was demonstrated that the most suitable arrangement of structural elements of ARCs was **Fragment 1** – linker – **Fragment 2** (*i.e.*, not the retro-modification of the conjugate **Fragment 2** – linker – **Fragment 1**), and that the linker moiety yielding highest potency of novel ARCs was 6-aminohexanoic acid moiety (Ahx), just as in case of the initial compounds. At this point, the latter result was slightly unexpected, as the flexible nature of Ahx raised doubts considering the entropic gain characteristic of ideally optimized BSIs (resulting from the interaction of a single BSI-molecule rather than its multiple fragments with the PK).

Overall, the most potent novel compounds towards PKAc were **ARC-902** and **ARC-903**; importantly, the IC₅₀ value of 8.3 nM for **ARC-902** was 130-fold lower than the product of IC₅₀ values of compounds used as **Fragment 1** (IC₅₀ value of 350 μM) and **Fragment 2** (IC₅₀ value ca 3000 μM). However, the IC₅₀ value of 5.3 nM for **ARC-903** was only 2-fold lower than the product of IC₅₀ values of **Fragment 1** (IC₅₀ value of 3.7 μM) and **Fragment 2** (IC₅₀ value ca 3000 μM), revealing that the optimal linkage of fragments had not been achieved. The latter fact in turn most probably pointed to a different mode of binding for H-9-containing compounds than for Adc-containing conjugates.

The profiling of **ARC-902** and **ARC-903** (each at concentration of 1 μM) *versus* a panel of 52 kinases revealed the promiscuous nature of these compounds, whereas **ARC-903** was more generic and slightly more effective than **ARC-902**. In addition to PKAc, both ARCs inhibited strongly ROCK-II, PKBβ, MSK1, and PRK2 (all representing AGC-group of kinome); as expected, neither compound inhibited acidophilic kinases (*i.e.*, CK1, CK2). In general, the profiling confirmed the tendency of ARCs to inhibit basophilic PKs, as all 14 kinases that were inhibited by both, **ARC-902** and **ARC-903** to an extent over 85%, represented basophilic PKs from AGC-group and from CAMK group.

It should also be mentioned that compound **ARC-659-1b** (Figure 36C) subsequently developed on the basis of **ARC-902** [Enkvist *et al.*, 2007], successfully confirmed the hypothesis that despite incorporation of non-selective oligo-(D-arginine) moiety, the selectivity of ARCs towards certain targets may be achieved by application of a selective ATP-mimicking entity as **Fragment 1**. In case of **ARC-659-1b**, the latter fragment was represented by the carbocyclic analogue of 3'-deoxyadenosine; the resulting conjugate demonstrated 3.5-fold increased affinity as compared to **ARC-902** (IC₅₀ values of 2.4 and 8.3 nM, respectively), and astonishingly increased the selectivity towards PKAc [Enkvist *et al.*, 2007]. When **ARC-659-1b** was profiled at 10 nM concentration towards a panel of 34 PKs, the determined residual activity of PKAc was 7%, whereas the only other kinases retaining less than 50% of the residual activity were ROCK-II (41%) and MSK1 (37%).

To sum up, the substantial improvement of inhibitory characteristics of oligo-(D-arginine)-containing amidated ARCs towards PKAc gave reason for introduction of two new terms, ARC-II and ARC-I, denoting respectively the set of compounds (“generation”) with structural features characteristic of the novel ARCs, and of the initial ARC-compounds [Lavogina *et al.*, 2010a].

2. Confirmation of the bisubstrate character of ARC-IIs

**[Paper 1: Enkvist *et al.*, 2006,
Paper 3: Lavogina *et al.*, 2010a]**

Notwithstanding the fact that BSIs have been developed as inhibitors of kinases since 1973 [Lienhard and Secemski, 1973], surprisingly little emphasis has been put on the confirmation of the bisubstrate nature of conjugates. While enhancement of affinity of a conjugate as compared to the composing fragments may indicate biligand (but not necessarily bisubstrate) binding, three main methods exist that may prove the bisubstrate inhibition character:

- kinetic analysis of the competitiveness of a BSI *versus* either substrate;
- binding studies where a BSI is displaced from its complex with a PK by either ATP- or protein substrate-competitive inhibitors;
- analysis of the BSI–PK co-crystal structures.

Additionally, improvement of selectivity of non-selective ATP-mimicking moiety upon conjugation with selective protein/peptide substrate-mimicking moiety also provides indirect evidence that the resulting conjugate is indeed a BSI.

Historically, kinetic studies of inhibition mechanism have been considered the most “universal” way for characterization of BSIs; as a first approximation, one would consider that a BSI should be competitive both *versus* ATP and *versus* a protein/peptide substrate. However, the studies of the mechanism of PKAc inhibition by **ARC-902** revealed competitive inhibition *versus* ATP and non-competitive inhibition *versus* peptide substrate (5-TAMRA-Kemptide), which was identical to the data obtained for several other BSIs, especially those targeted to PKAc [Parang and Cole, 2002a]. This phenomenon has been an object of thorough discussions [Lawrence and Niu, 1998; Lawrence, 2005; Magalhaes *et al.*, 2008], and it has been argued that a non-competitive inhibition mechanism *versus* one of the (co-)substrates (usually, the protein/peptide) does not rule out the bisubstrate character of inhibition, but is rather indicative of ordered (*i.e.*, ATP-first) mechanism of ligand binding by PK (please refer to Section 2.2.1. Affinity and inhibitory potency). Indeed, studies of Kemptide phosphorylation by PKAc indicated that the preferred kinetic pathway is an initial binding of ATP, which induces conformational changes facilitating binding of peptide substrate [Lew *et al.*, 1997a]. Another idea proposed for the explanation of the non-competitive inhibition mechanism of BSIs *versus* peptide substrates is an ordered mechanism of BSI binding [Ricouart *et al.*, 1991], where the ATP-mimicking moiety binds first and by triggering positive cooperative effects and/or by increasing the local concentration of the peptide substrate-mimicking moiety enables further binding of the latter to the PK.

The recent progress in the development of high-affinity probes has caused substantial rise of application of binding/displacement assays. Derivatives of **ARC-902** have been used as affinity sensors for SPR [Viht *et al.*, 2007], and as probes (**ARC-Photo**) for the assay with detection of fluorescence anisotropy/

polarisation [Vaasa *et al.*, 2009]. In the first case, biotinylated ARC-II compound **ARC-704** (Figure 37A) was immobilized on the SPR chip *via* streptavidin-biotin complex, yielding a high-affinity surface that bound efficiently PKAc and ROCK-II [M. Lust, unpublished data]. The solution competition experiments with compounds targeted to the ATP-site (*i.e.*, H-1152, H-89) and to the protein/peptide substrate-site (*i.e.*, PKArII α , GST-tagged PKI α) of PKAc showed that the latter could be displaced from its complex with immobilized **ARC-704** by both ACIs and PCIs, and thus confirmed the BSI nature of immobilized **ARC-704** [Viht *et al.*, 2007]. In the second case, labelling of an ARC-II representative with fluorescence dye 5-TAMRA yielded **ARC-583** (Figure 37B), which exhibited K_D values of 0.48 nM and 3.6 nM towards PKAc and ROCK-II, respectively, according to the direct titration experiments. Subsequently, **ARC-583** could be successfully displaced from its complex with PKAc by increasing concentrations of compounds targeted to ATP-site (*i.e.*, H-89) and to protein/peptide substrate-site (*i.e.*, PKArI α , PKArII α , PKI α) of the kinase, confirming again the bisubstrate nature of kinase inhibition by ARC-II compounds [Vaasa *et al.*, 2009].

The crystal structures of complexes of a PK inhibitor bound to its target allow unambiguous visualization of PK sites where the inhibitor binds as well as the interactions between the PK and the inhibitor; this information is crucially important for the structure-aided optimization of compounds. Therefore, co-crystallization of PKAc with several representatives of ARC-II inhibitors was carried out, and two crystal structures were resolved yielding the results presented below.

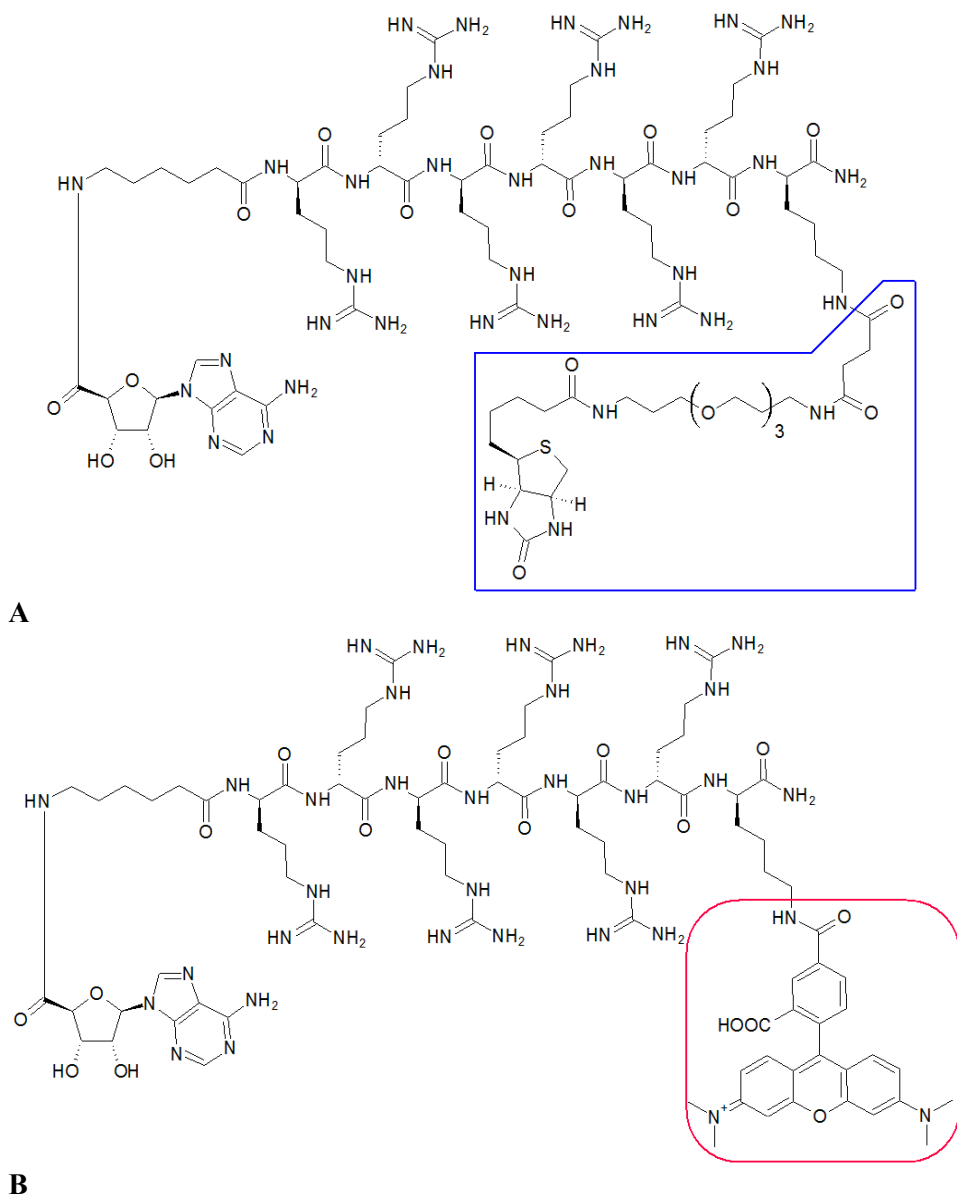


Figure 37. Examples of derivatized ARC-II. (A) **ARC-704**; blue polygon surrounds the attached biotin moiety. (B) **ARC-583**; red rounded rectangle surrounds the fluorescent dye TAMRA.

3. Crystallographic studies of ARC-II conjugates **[Paper 2: Lavogina et al., 2009, Paper 3: Lavogina et al., 2010a, Paper 5: Pflug et al., 2010]**

3.1. PKAc – ARC-1034 complex (PDB 3BWJ) **[Paper 2: Lavogina et al., 2009, Paper 3: Lavogina et al., 2010a]**

The first ARC-II representative yielding co-crystal structure with PKAc was **ARC-1034** (Figure 38A) incorporating amidated (D-Arg)₂-peptide and hence only partly representing the interactions between PKAc and longer ARC-II compounds (*i.e.*, conjugates containing amidated (D-Arg)₆-peptide). The electron density of the co-crystal indicated that two **ARC-1034** molecules (so-called “inner” and “outer”) were bound to one PKAc molecule, the “inner” **ARC-1034** expectedly positioned in the catalytic cleft and the “outer” molecule situated on the surface of PK in the contact region with the symmetry-related PKAc – **ARC-1034** complex. The presence of the “outer” **ARC-1034** was classified as a crystallographic artefact, as the evidence from SPR experiments [Viht *et al.*, 2007] as well as kinetic studies [Viht *et al.*, 2005] supported only an 1:1 stoichiometry of ARC-II binding to PKAc.

The electron density of the “inner” **ARC-1034** was well defined for the Adc-moiety occupying the ATP-site, and for the linker bound under the Gly-rich loop of PKAc. Apart from the “classical” pattern of hydrogen bond interactions developed by Adc-moiety with PKAc residues constituting ATP-binding hinge (*i.e.*, Glu121, Val123, Thr183 binding to purine of Adc and Glu127, Glu170 binding to hydroxyl groups of ribose moiety), a new interaction was spotted between the oxygen of carbonyl group of Adc and a water molecule situated inside the cleft (Figure 38B). This water molecule was itself connected *via* hydrogen bonds with side-chains of Thr183 and of the conserved residue Lys72; such network of interactions explained the previously reported higher affinity of Adc-containing ARC-IIs as compared to the analogical compounds containing adenine or adenosine fragments [Enkvist *et al.*, 2006].

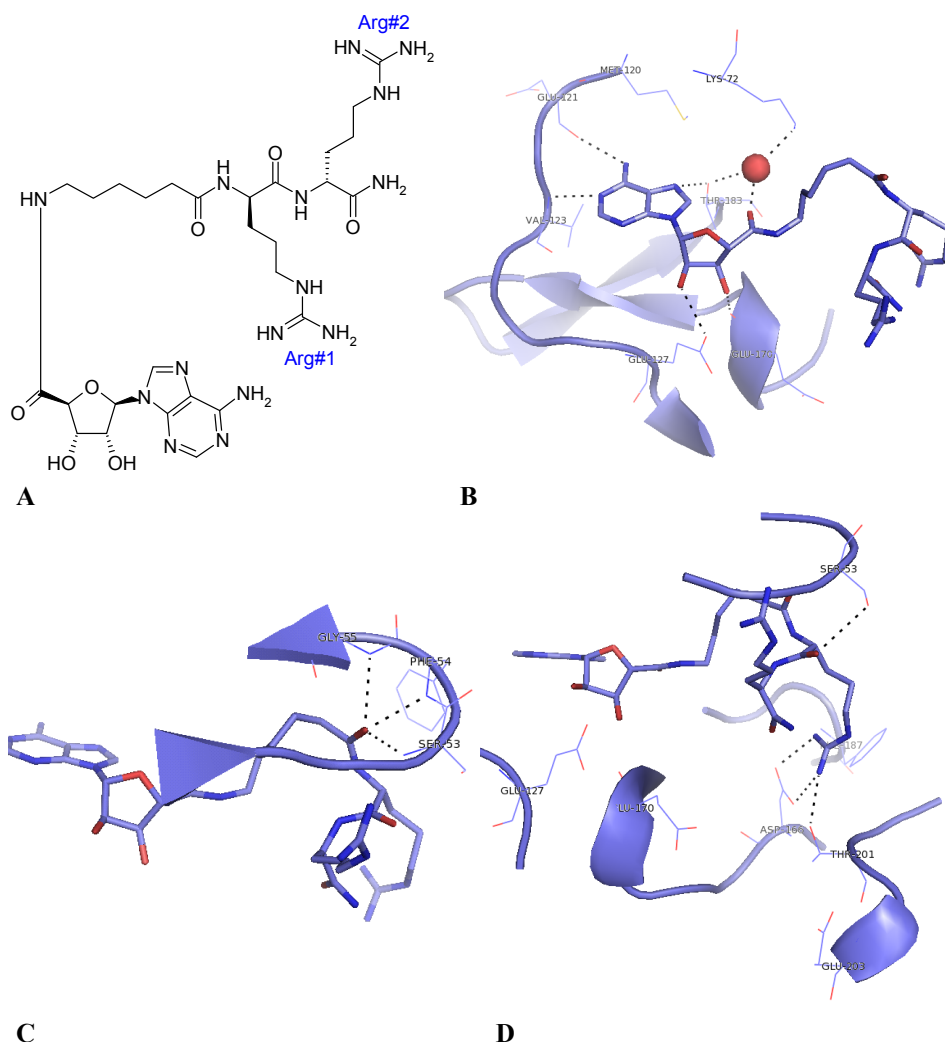


Figure 38. ARC-1034 and its co-crystal with PKAc. (A) Structure of **ARC-1034** with arginine residues numbered. (B) ATP-site of 3BWJ. **ARC-1034** is shown as sticks, water molecule as red sphere, PKAc as cartoon; the residues of the ATP-site of PKAc interacting with **ARC-1034** are shown as lines and numbered. (C) Interactions developed between the linker of **ARC-1034** and PKAc. (D) Interactions developed between the **Fragment 2** of **ARC-1034** and PKAc.

The binding mode of the linker, on the other hand, provided a good explanation for the previous observations that Ahx moiety was an optimal linking chain for both ARC-I and ARC-II compounds [Loog *et al.*, 1999; Enkvist *et al.*, 2006]. The length and flexibility of Ahx allowed positioning of the terminal carbonyl of the linker exactly below the flexible top of the Gly-rich loop, enabling generation of extensive hydrogen bond interactions between the terminal

carbonyl of the linker and the residues Ser53, Phe54, and Gly55 of PKAc, as well as above-plane hydrophobic interaction with the aromatic ring of Phe54 (Figure 38C). The conformation of PKAc was intermediate (half-closed), according to the distances Tyr330...Glu127 (4.7 Å), Ser53...Asp166 (10.5 Å), and His87...phosphorylated Thr197 (2.9 Å). In case of fully closed conformation (*i.e.*, transition state analogue), the corresponding distances are 4.4 Å, 7.6 Å and 2.7 Å (PDB 1L3R), and in case of fully open conformation (*i.e.*, apoenzyme) over 20 Å, 12.8 Å and 10.4 Å (PDB 1J3H). Overall, the conformation of the Gly-rich loop in PKAc – **ARC-1034** complex was similar to that reported for the binary complex PKAc – adenosine (PDB 1BKX) and for the ternary complex PKAc – H-89 – PKI(5-24) (PDB 1YDT) (Figure 39). However, in the former crystal the Gly-rich loop had not been fixed, and in the latter a hydrophobic above-plane interaction had been developed between the bromine group of H-89 and the aromatic ring of Phe54.

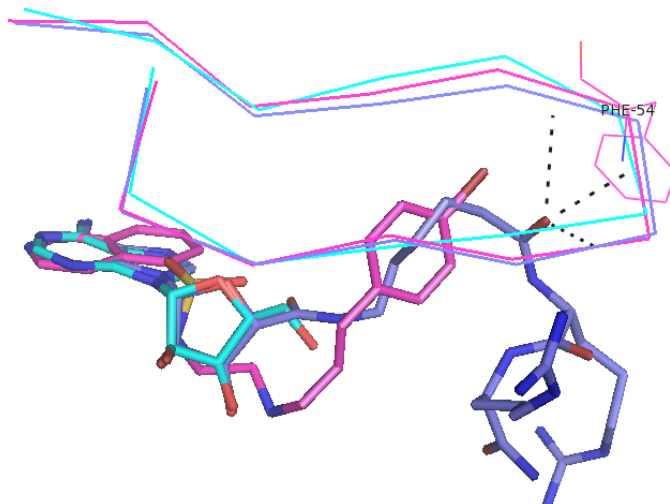


Figure 39. Overlay of Gly-rich loops of co-crystals PKAc – **ARC-1034** (3BWJ, blue), PKAc – adenosine (1BKX, cyan), and PKAc – H-89 – PKI(5-24) (1YDT, pink). Gly-rich loops of PKAc molecules are shown as ribbon and ligands as sticks; black dots indicate hydrogen bonds between **ARC-1034** and PKAc from 3BWJ, Phe54 of PKAc from 1YDT is shown as lines and numbered.

Prior to co-crystallization, it was expected that the D-Arg residues of **ARC-1034** develop interactions with Glu127 and Glu170 of PKAc, the residues responsible for recognition of PKAc protein/peptide substrates. It was also presumed that in case of longer ARC-II conjugates containing the amidated (D-Arg)₆-peptide, their D-Arg residues #3...#6 develop contacts with downstream amino acids of PKAc such as Glu203 and Glu230, both also involved in PKAc substrate recognition. Surprisingly, the electronic density of the amidated (D-Arg)₂-peptide incorporated in **ARC-1034** was not continuous and well-defined

only for the D-Arg residue closer to the linker moiety (Arg#1), whereas the D-Arg residue closer to the C-terminus of the conjugate (Arg#2) was exposed to the solvent. Moreover, Arg#1 did not protrude to Glu127 or Glu170 of PKAc but instead pointed “down” (Figure 38D), developing hydrogen bonds with side-chain groups of Asp166 and Thr201, and an in-plane interaction of the guanidinium-group with Phe187; additionally, the carbonyl of Arg#1 was an acceptor for the hydrogen bond donated by the side-chain of Ser53.

Overall, the absence of interactions between **Fragment 2** of **ARC-1034** and Glu residues of PKAc involved in binding of substrates demonstrated that **ARC-1034** did in fact not represent bisubstrate ARC-II compounds, but rather served as a simplified model for mapping interactions of **Fragment 1** and linker moiety with PKAc.

3.2. PKAc – ARC-670 complex (PDB 3AGM) [Paper 3: Lavogina et al., 2010a, Paper 5: Pflug et al., 2010]

Subsequently, a crystal structure of complex between PKAc and a representative of longer ARC-II compounds, **ARC-670** was solved; **ARC-670** contains a 6-derivatized purine analogue as **Fragment 1** linked *via* 1,8-octanedioic acid moiety to amidated (D-Arg)₆-peptide in **Fragment 2** (Figure 40A).

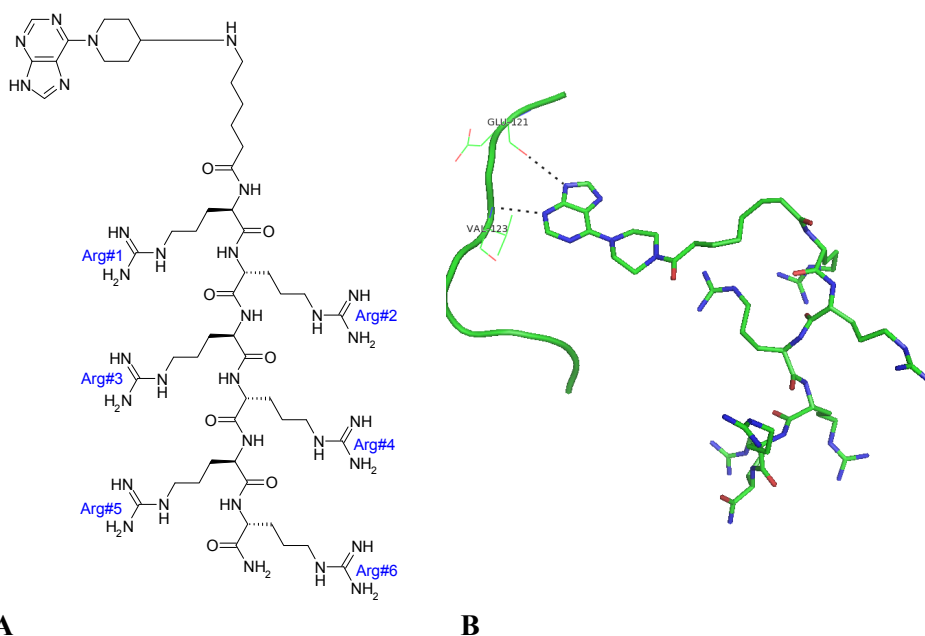


Figure 40. **ARC-670** and its co-crystal with PKAc. (A) Structure of **ARC-670** with arginine residues numbered. (B) ATP-site of 3AGM. **ARC-670** is shown as sticks, PKAc as cartoon; the residues of ATP-site of PKAc interacting with **ARC-670** are shown as lines and numbered.

The electronic density was well defined for the most of the **ARC-670** molecule; according to expectations, its **Fragment 1** occupied the ATP-site of the protein kinase, although the positioning of the purine moiety was different compared to the purine moiety of Adc contained in **ARC-1034**. In case of the latter crystal structure, three hydrogen bonds were developed with PKAc residues: the backbone amide carbonyl oxygen of Glu121 served as an acceptor for the N6 of Adc purine, the backbone amide nitrogen of Val123 was a donor for the N1, and the side-chain hydroxyl group of Thr183 was a donor for the N7. In case of **ARC-670** co-crystal, on the other hand, only two crucial hydrogen bonds were developed: Glu121 of PKAc served as an acceptor for the N9 of purine, and Val123 was a donor for the N3; the piperazine ring in the 6-position of purine developed no interactions with PKAc (Figure 40B). This binding mode of **Fragment 1** influenced the positioning of the linker moiety, directing the oxygen of carbonyl group closer to the **Fragment 1** out of the catalytic cleft; still, the carbonyl group closer to **Fragment 2** adopted the position highly similar to that of the corresponding carbonyl of the Ahx linker in the PKAc – **ARC-1034** complex. Due to the movement of the Gly-rich loop closer to β -stand 3 and helix B of PKAc (away from the C-tail) in the **ARC-670** co-crystal, the carbonyl of **ARC-670** was not positioned exactly below the Gly-rich loop and could develop interactions with only two residues of PKAc, Ser53 and Phe54 (Figure 41A). The part of the Gly-rich loop closer to the C-tail of PKAc was more opened than in the **ARC-1034** co-crystal resulting in distances Tyr330...Glu127 (6.9 Å) and Ser53...Asp166 (11.3 Å), whereas the part of the Gly-rich loop facing β -stand 3 and helix B was slightly more closed as reflected by the distance His87...phosphorylated Thr197 (2.6 Å) (Figure 41B).

Such movement of Gly-rich loop was needed to accommodate the **Fragment 2** of **ARC-670**, representing probably the most interesting feature of the given co-crystal (Figure 41C). Expectedly, the side-chain of Arg#1 of **ARC-670** developed the same interactions with Asp166 and Phe187 of PKAc as the Arg#1 of **ARC-1034**, although the hydrogen bond between **ARC-670** and Thr201 was much weaker. The carbonyl of Arg#1 of **ARC-670**, however, pointed towards the catalytic cleft (not towards the solvent as in **ARC-1034** co-crystal), and the side-chain of Arg#2 of **ARC-670** was therefore exposed to the solvent and not well covered with electron density. Arg#3, on the other hand, protruded deep into the catalytic cleft and was involved in interactions with Glu127 and Asp184 of PKAc; Arg#4, in its turn, pointed out of the catalytic cleft, but developed interactions with Glu203. Surprisingly, Arg#5 was solvent-exposed and poorly defined by the electron density, despite the fact that it protruded towards the Glu-rich C-tail of PKAc; by contrast, Arg#6 pointed deeply into the protein/peptide substrate-binding pocket of PKAc and developed hydrogen bonds with Glu230. Finally, an additional in-plane hydrophobic interaction was developed between the C-terminal amide of **ARC-670** and the aromatic side-chain of Phe129 of PKAc.

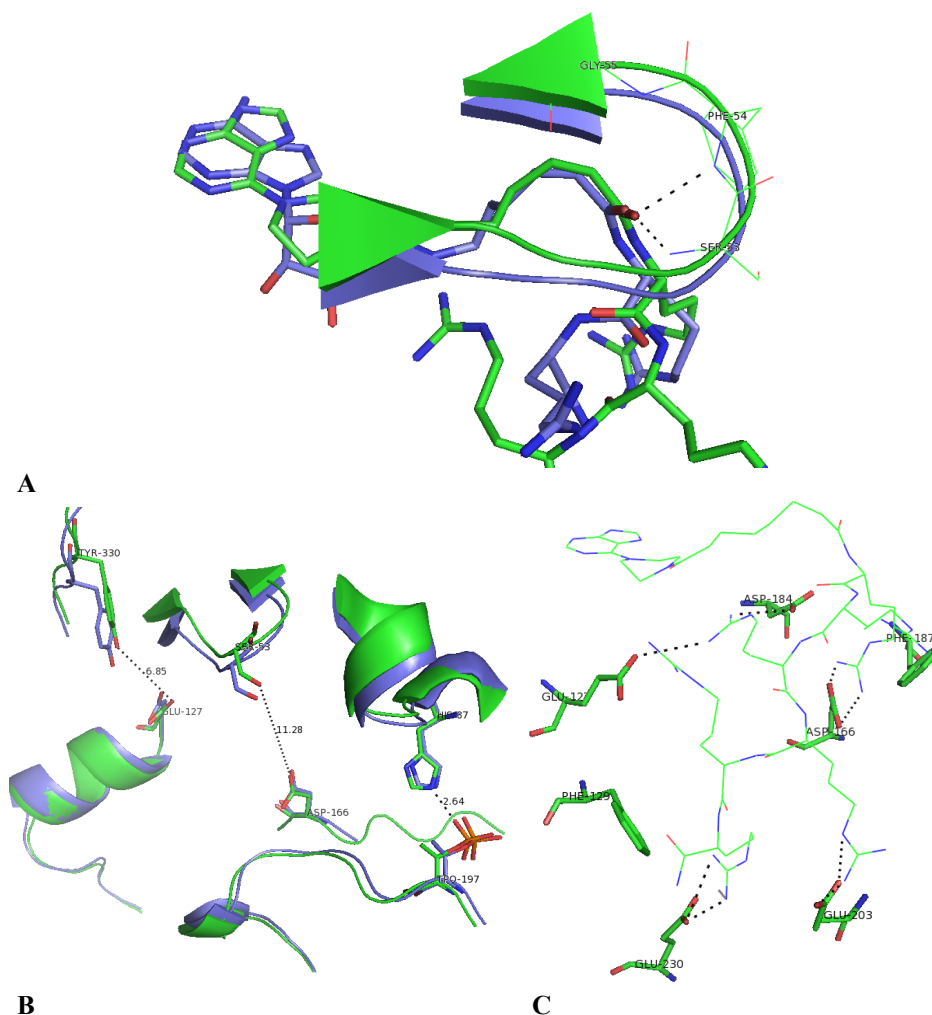


Figure 41. Comparison of 3AGM and 3BWJ. (A) Interactions developed between the linker of **ARC-670** and PKAc from 3AGM (green) overlaid with co-crystal PKAc – **ARC-1034** (3BWJ, blue). Ligands are shown as sticks, PKAc as cartoon; the residues of ATP-site of PKAc interacting with **ARC-670** are shown as lines and numbered. (B) Overlay of 3AGM (green) and 3BWJ (blue); distances between PKAc residues shown as sticks are measured for 3AGM only. (C) Interactions developed between the **Fragment 2** of **ARC-670** and PKAc; **ARC-670** is shown as lines, the residues of the protein substrate-site of PKAc interacting with **ARC-670** are shown as sticks and numbered.

Overall, the crystal structure of the PKAc – **ARC-670** complex clearly indicated the bisubstrate nature of binding of longer ARC-II conjugates, revealing interactions between the **Fragment 2** and the amino acid moieties of PKAc responsible for the protein/peptide substrate recognition (Glu127, Glu170, *etc.*).

Moreover, this co-crystal might provide an insight into the interactions underlying the binding of those PKAc substrates and PCIs that contain Arg residues in different positions than -2 and -3 prescribed by the consensus sequence of PKAc substrates Arg-Arg-Xaa-Ser-Hyd (Figure 42). The latter application of the **ARC-670** co-crystal is possible even despite the fact that ARC-IIs contain D-amino acid moieties, not L-amino acid moieties as in natural PKAc substrates; in fact, ARC-IIs may be considered as retro-inverso variants of PKAc substrate peptides comprised of L-amino acids. Namely, as the latter compounds bind with their N-terminus spatially close to the end of helix F and their C-terminus close to the phosphorylated Thr197 of PKAc, while the **Fragment 2** of **ARC-670** bound with its N-terminus near the pThr197 and its C-terminus near the end of helix F.

A more practical possibility for application of the data obtained from the **ARC-670** co-crystal would be the replacement of non-interacting D-Arg residues #2 and #5 with structural fragments bearing additional functionality (*i.e.*, fluorescent dyes, biotin, myristoyl, *etc.*) without risks to lose the affinity of the conjugate. Moreover, as the overlay of **ARC-670** and **ARC-1034** co-crystals showed that the positioning of the linker end closer to the **Fragment 2** practically coincided for both **ARC-670** and **ARC-1034**, the information about binding of **Fragment 2** obtained from **ARC-670** co-crystal may be extrapolated to ARC-II compounds that contain Adc as **Fragment 1** and Ahx as the linker (*i.e.*, **ARC-902**).

At the same time, it should be kept in mind that the conformational flexibility of ARC-II compounds might result in development of alternate strong interactions with the PK upon change of ARC-II structure, *i.e.*, preservation of high affinity after derivatization could still “mask” profound changes in mode of binding. For instance, when **ARC-902** [Adc-Ahx-(D-Arg)₆-NH₂] was subjected to Ala-scan where D-Arg residues of **Fragment 2** were one-by-one replaced with D-Ala, the obtained compounds inhibited PKAc with IC₅₀ values very similar to that of **ARC-902** itself [J. Rogozina, unpublished data]. This observation most likely indicates that the oligo-(D-arginine) serves to a certain limit as a “blanket” which might be shifted if necessary to “cover” all or most of the crucial binding partners (*i.e.*, Glu127, Glu170, Glu203, Glu230). Interestingly, the largest difference (3-fold higher IC₅₀ than that of **ARC-902**) was exhibited by a compound where D-Ala was substituted for Arg#1, indicating the importance of the latter residue as an “anchor” which stabilizes the PKAc conformation suitable for binding of **Fragment 1** and linker, and at the same time directs **Fragment 2** to the protein/peptide substrate-site of PK.

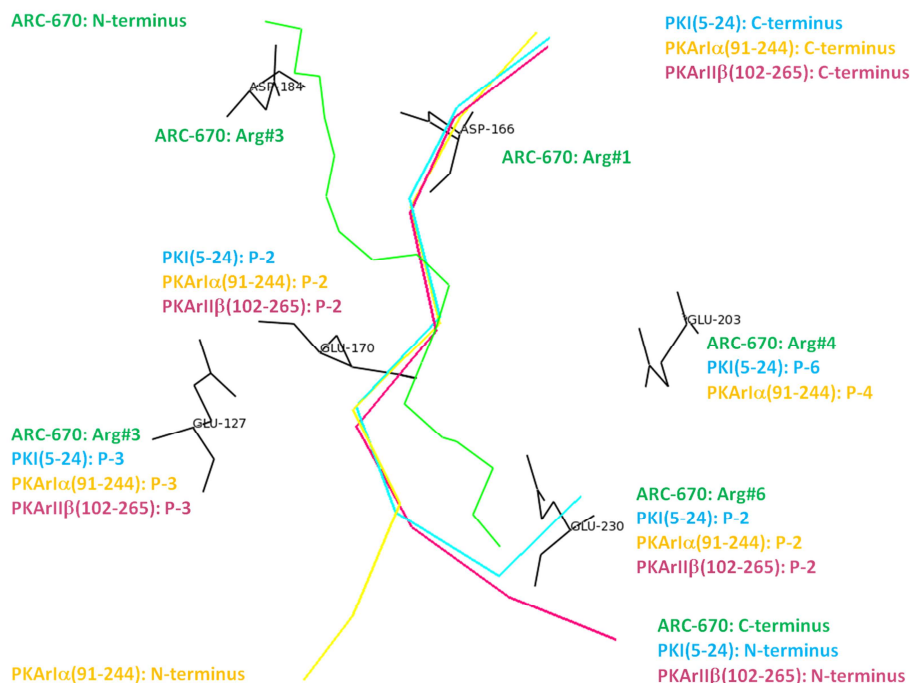


Figure 42. Overlay of co-crystals PKAc – **ARC-670** (3AGM, the backbone of **Fragment 2** of **ARC-670** shown as green lines), PKAc – AMPPNP – PKIα(5-24) (1ATP, residues 15-22 of PKI shown as cyan ribbon), PKAc – AMPPNP – PKArIα(91-244) (1U7E, residues 92-98 of PKArIα shown as yellow ribbon), and PKAc – AMPPNP – PKArIIβ(102-265) (3IDC, residues 106-113 of PKArIIβ shown as pink ribbon). PKAc residues involved in recognition of arginine moieties of the compounds targeting the protein substrate-site of PKAc shown as black lines and numbered; near each PKAc residue, the Arg residues of binding partners interacting with the given residue are indicated (the number of Arg residue corresponds to the position of the latter in the consensus sequence). In the corners, an approximate position of N- and C-termini of the compounds targeting the protein substrate-site of PKAc is shown.

4. Development of ARC-III conjugates [Paper 2: Lavogina et al., 2009, Paper 3: Lavogina et al., 2010a]

The crystal structure of the PKAc – **ARC-1034** complex pointed to several tendencies and structural features that could further be exploited for the design of two sets of compounds. The first set was designed to control the hypothesis that elimination of **Fragment 2** of **ARC-1034** should not influence the affinity of compound, as the most strong interactions contributing to the binding energy of **ARC-1034** originated from binding of **Fragment 1** and a linker. Consequently, the first set comprised “short” compounds that consisted just of **Fragment 1** and a linker, whereas in some cases one additional moiety (an amino acid or a diamine residue) at the C-terminus of the conjugate. The compounds were evaluated on the basis of their ability to displace an ARC-Photo fluorescent probe (**ARC-583**) from its complex with PKAc in an assay with fluorescence anisotropy detection, and the following structure-affinity relationship aspects were established (please refer to Table 2 from Paper 2):

- according to expectations, elimination of the Arg#2 residue from the structure of **ARC-1034** resulted in slight improvement of affinity, whereas the elimination of Arg#2 in combination with an additional replacement of Arg#1 with shorter an achiral diamine chain or a hydrophobic D-amino acid was not well tolerated by PKAc, which revealed the importance of the interaction between Arg#1 of **ARC-1034** and Asp166 of PKAc;
- the steepest drop of affinity (over 300-fold as compared to **ARC-1034**) was observed after elimination of Arg#2 and the replacement of Arg#1 by a hydrophobic L-amino acid, which also pointed to the importance of stereo-configuration of the chiral centre at the C-terminus of the linker;
- elimination of both, Arg#1 and Arg#2, resulted in a 7-fold decrease in affinity as compared to **ARC-1034**, whereas the introduction of a negative charge at the C-terminus of the resulting compound caused an additional 25-fold reduction in affinity.

Additionally, it was demonstrated that shifting of the carbonyl group of **Fragment 1** two bonds towards the C-terminus of the compound (further away from the ribose moiety as compared to Adc) resulted in an over 100-fold decrease in affinity as compared to **ARC-1034**. The latter observation thus indicated the importance of the hydrogen bond between this carbonyl in Adc and the water molecule in ATP-cleft of PKAc.

The idea behind the design of the second set of compounds originated from the fact that D-Arg moieties in **Fragment 2** of **ARC-1034** did not protrude to the region of PKAc responsible for binding of protein/peptide substrates; it was therefore decided to “elongate” **ARC-1034** by introduction of an additional linker moiety (so-called second linker). The structure-affinity relationship aspects were summarized in Table 3 from Paper 2; while the addition of another Ahx moiety to the Ahx linker of **ARC-1034** resulted in only 4-fold increase of affinity as compared to **ARC-1034**, whereas variation of the length of the

second linker did not improve the affinity. Next, it was decided to introduce not only the second linker, but also a “chiral spacer” between the two linkers in order to maintain the D-configuration of the Arg#1 of **ARC-1034**, which had previously shown its importance for directing the **Fragment 2** of ARC-II conjugates to the protein/peptide substrate site of PKAc. When D-Lys was used as a chiral spacer and Ahx as the second linker, the affinity of the resulting compound (**ARC-1012**, (Figure 43A) increased over 40-fold compared to **ARC-1034** (by contrast, the analogical compound with L-Lys as the chiral linker had lower affinity than **ARC-1034**). Interestingly, PKAc tolerated D-Ala as the chiral spacer equally well, as indicated by the affinity of the **ARC-1012** analogue incorporating D-Ala instead of D-Lys (**ARC-1039**, Figure 43B).

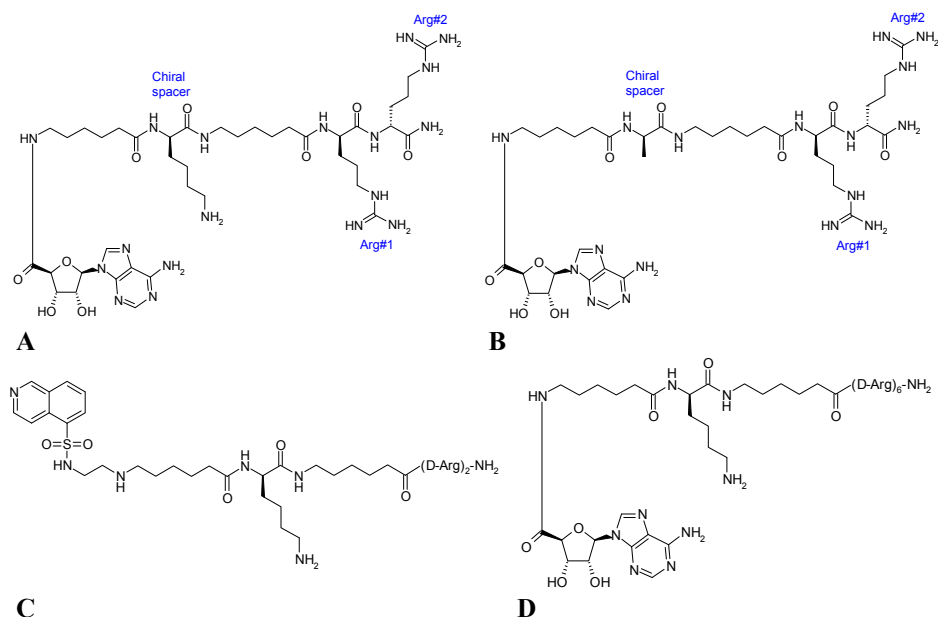


Figure 43. Examples of ARC-III. (A) **ARC-1012** with arginine residues numbered. (B) **ARC-1039** with arginine residues numbered. (C) **ARC-1074**. (D) **ARC-1028**.

Moreover, the **ARC-1012** analogue with H-9 moiety as **Fragment 1** and Hex as the first linker (**ARC-1074**, (Figure 43C) also had a higher affinity towards PKAc than the corresponding H-9-containing compound without the second linker or the chiral spacer [J. Rogozina, unpublished data]. The latter result was unexpected, as from the studies of ARC-II inhibitors it had been concluded that the mode of binding of H-9-containing compounds was different from that of Adc-containing compounds; hence, it was supposed that H-9 containing compounds would not profit from introduction of the second linker or the chiral spacer. However, it is possible that only the combination of H-9 moiety as **Fragment 1** and oligo(L-arginine), not oligo(D-arginine) as **Fragment 2**

yields conjugates with altered binding mode as compared to Adc-containing analogues. Furthermore, despite 10-fold difference in affinity of compounds with H9 and Adc used as **Fragment 1** in **ARC-1074** and **ARC-1012**, respectively, the IC_{50} values of **ARC-1074** and **ARC-1012** towards PKAc were nearly the same (10 nM and 7.6 nM, respectively). The latter fact indicated that the introduction of the second linker and the chiral spacer could still not hit the optimal geometry in case of H-9-containing compounds.

The substitution of an amidated (D-Arg)₆-peptide for the amidated (D-Arg)₂ of **ARC-1012** yielded compound **ARC-1028** (Figure 43D), which possessed a subnanomolar K_d value towards PKAc. The achievement of such a high affinity allowed the definition of the next generation of ARC-s, ARC-III (Figure 44) consisting of **Fragment 1** (ATP-mimics) and **Fragment 2** [oligo-arginine] joined by the sequence comprising two linker moieties and a chiral spacer (*i.e.*, amino acid moiety).

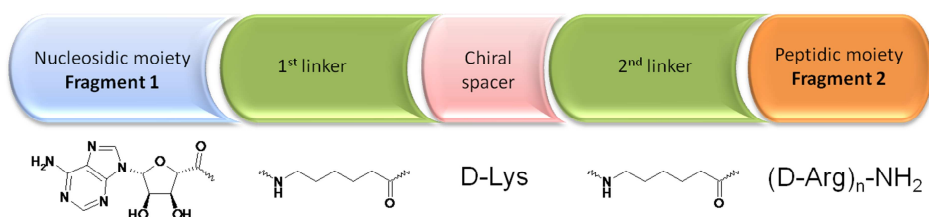


Figure 44. General scheme of ARC-III inhibitors. Below are shown examples of structures of **Fragment 1**, **Fragment 2**, linkers, and chiral moiety.

The profiling of **ARC-1028** towards a panel of 50 PKs (please refer to Table 5 from Paper 2) indicated that the general selectivity pattern of **ARC-1028** was similar to that of ARC-II representative **ARC-902**, whereas **ARC-1028** inhibited representatives of the AGC-group of kinome slightly better and the PKs of CAMK-group slightly worse than **ARC-902**. The PKs most efficiently inhibited by **ARC-1028** were PKAc, PKC isoforms (except atypical ι , ζ , and μ), ROCK isoforms, and ribosomal S6-kinases. A more detailed characterization of ARC-III representatives in the displacement assay towards ROCK-II and in the kinetic inhibition assay towards PKB γ (please refer to Table 4 from Paper 2) indicated that **ARC-1012** had an even better affinity towards ROCK-II than towards PKAc, but was a 7-fold less potent inhibitor of PKB γ compared to PKAc. **ARC-1028** had subnanomolar K_d values towards both PKAc and ROCK-II, and was also a potent inhibitor of PKB γ with IC_{50} value of 14.6 nM; all in all, the increase in the number of D-Arg moieties of **Fragment 2** evened out the differences in affinity and inhibitory potency towards different PKs.

Still, the most interesting result was the selectivity of **ARC-1039** towards PKAc, as the former displayed a 20-fold higher K_d towards ROCK-II and nearly 40-fold higher IC_{50} towards PKB γ compared to PKAc; in comparison to **ARC-1012**, **ARC-1039** bound to ROCK-II with an 85-fold lower affinity and

inhibited PKB γ with a 5-fold lower potency. This phenomenon could not be explained at that point of time, but it was utilized for the design of compound **ARC-1044** (Figure 45A) that was developed as an example of a highly selective ARC-III. **ARC-1044** incorporated the carbocyclic analogue of 3'-deoxyadenosine as **Fragment 1** (this moiety had previously demonstrated an increase of selectivity of ARC-II conjugates towards PKAc; [Enkvist *et al.*, 2007]) and the amidated (D-Arg)₂-peptide as **Fragment 2** joined by the sequence comprising two Ahx moieties as both the first and the second linker, and D-Ala as the chiral spacer. According to expectations, **ARC-1044** had an over 100-fold better affinity as well as nearly 100-fold better inhibitory potency towards PKAc *versus* ROCK-II and PKB γ , thus expressing the best selectivity towards its target PK of all ARCs developed so far. More importantly, the success of **ARC-1044** pinpointed two structural features (**Fragment 1** and the chiral spacer) that might strongly influence the selectivity of ARC-III compounds, suggesting that the right choice of these features might "tune" the affinity profile of conjugates according to the requirements of field of application (ideally from highly selective to generic). Indeed, the further variations of **Fragment 1** of ARC-III compounds have recently yielded **ARC-668** (Figure 45B), a generic inhibitor of the AGC-group of kinome as demonstrated by profiling towards a panel of 50 PKs [Enkvist *et al.*, 2009]. A few AGC-kinases inhibited to extent less than 90% by 100 nM concentration of **ARC-668** were PKB β (80%), PKGII (78%), PKC ζ (38%), and PKC ι (24%).

Based on **ARC-1028**, a fluorescent probe **ARC-1042** was developed [Adc-Ahx-(D-Arg)-Ahx-(D-Arg)₆(D-Lys{TAMRA})-NH₂] (Figure 45C) with a K_D value below 0.3 nM towards PKAc as determined in the direct binding FA-assay. **ARC-1042** could be successfully displaced from its complex with PKAc by compounds targeted to the ATP-site (*i.e.*, H-89) as well as to the protein/peptide substrate-site (*i.e.*, PKArl α , PKArII α , PKI α) of the kinase, and thus confirmed the bisubstrate character of ARC-III compounds incorporating amidated (D-Arg)₆-peptide as **Fragment 2**. Later on, the bisubstrate character of analogical ARC-III compounds possessing amidated (D-Arg)₂-peptide as **Fragment 2** was confirmed by co-crystal structures of **ARC-1012** and **ARC-1039** with PKAc [Pflug *et al.*, 2010].

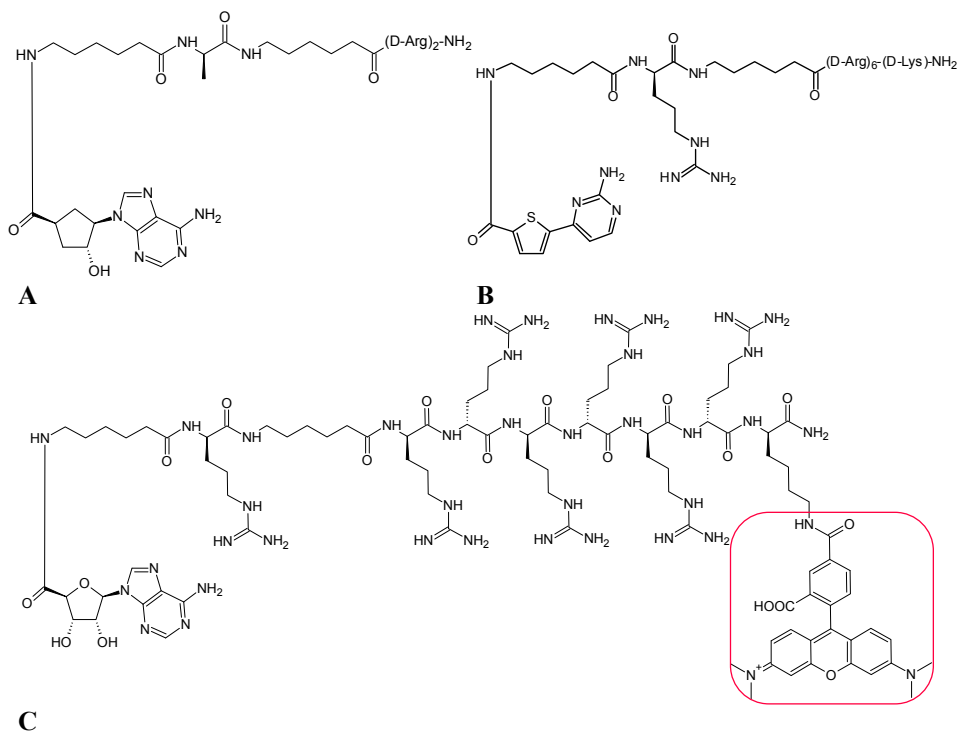


Figure 45. Illustration of tunable selectivity and derivatization potential of ARC-III. (A) **ARC-1044**. (B) **ARC-668**. (C) **ARC-1042**; red rounded rectangle surrounds the fluorescent dye TAMRA.

5. Crystallographic studies of ARC-III conjugates [Paper 5: Pflug *et al.*, 2010]

5.1. PKAc – ARC-1012 complex (PDB 3AG9)

The crystal structure of the PKAc – **ARC-1012** complex was resolved at a 2.0 Å resolution, but lacked electronic density for a part of the C-tail of PKAc (residues 317...332) and the second linker of **ARC-1012**. An asymmetric unit of crystal lattice included two PKAc molecules, of which only one was bound to **ARC-1012**; the latter observation could probably be attributed to the random effects of crystal packing, as no evidence from binding or inhibition studies had suggested a dimeric mechanism of inhibition of PKAc by **ARC-1012**.

As compared to the crystal structure of the PKAc – **ARC-1034** complex [Lavogina *et al.*, 2009], several changes in the interactions between PKAc and **Fragment 1** as well as first linker of **ARC-1012** were observed (Figure 46A). The Adc moiety in **Fragment 1** was buried deeper into the ATP-site and closer to the hinge, developing strong interactions with Glu121 and Val123, but only a weak hydrogen bond with Thr183. The most drastic difference was a change in conformation of ribose moiety of **Fragment 1**, which was tilted up and towards the C-tail of PKAc, losing the “classical” interaction between the 3' hydroxyl and Glu170 of PKAc (but probably gaining interaction with one of C-tail residues, which are not visible in the given crystal structure). Such movement of ribose also caused lifted position of the Gly-rich loop as compared to the **ARC-1034** co-crystal, as also indicated by distances Ser53...Asp166 (12.3 Å) and His87...phosphorylated Thr197 (4.55 Å) in the **ARC-1012** co-crystal. Still, the carbonyl group at the end of the first linker of **ARC-1012** made nearly the same interactions with the PKAc residues at the top of the Gly-rich loop as developed by the C-terminal carbonyl of the linker of **ARC-1034**; the only difference in the **ARC-1012** co-crystal was the weakened hydrogen bond with Gly55 of PKAc (Figure 46B).

The chiral moiety of **ARC-1012** adopted a position similar to that of Arg#1 in the **ARC-1034** co-crystal, developing hydrogen bonds with Asp166 (Figure 47A). However, in case of **ARC-1012** the hydrogen bond with Thr201 was absent due to the outward movement of the activation loop of PKAc, and the interaction with the aromatic ring of Phe187 of PKAc was also missing due to the absence of the guanidine group in the side-chain of chiral spacer. Similar to **ARC-670** and different from **ARC-1034** co-crystal, the carbonyl of the chiral spacer of **ARC-1012** pointed towards the catalytic cleft, but the electronic density for the following second linker as well as Arg#1 of **ARC-1012** was unfortunately ambiguous. However, the Arg#2 of **ARC-1012** developed multiple strong hydrogen bonds with Glu170 and Glu230, and an additional in-plane interaction of the guanidinium-group with Phe129, indicating that the major gain in affinity of **ARC-1012** compared to **ARC-1034** resulted from interactions of Arg#2 (Figure 47B). Importantly, the overlay of **ARC-1012** and **ARC-670** co-crystals showed that the side-chain of Arg#2 of **ARC-1012** aligned exactly with the side-chain of Arg#6 in **ARC-670**.

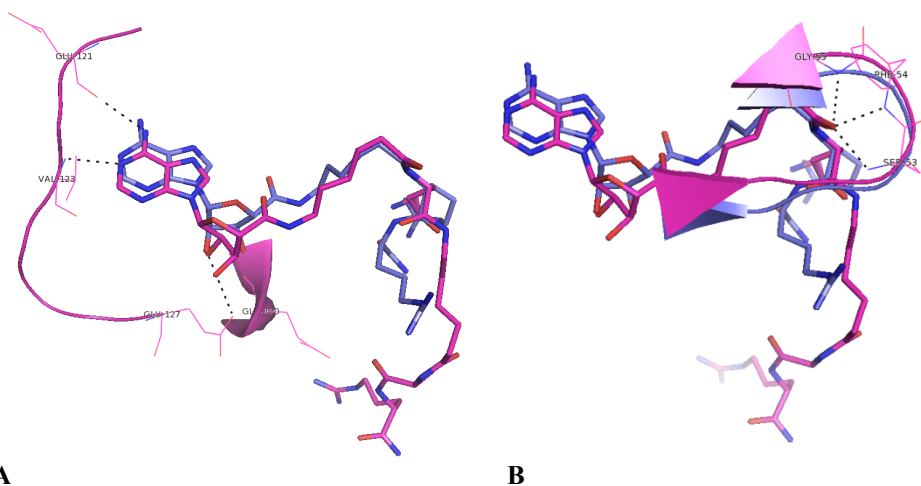


Figure 46. 3AG9. (A) Interactions developed between the **Fragment 1** of **ARC-1012** and the ATP-site of PKAc from 3AG9 (magenta) overlaid with the co-crystal PKAc – **ARC-1034** (3BWJ, blue). Ligands are shown as sticks, PKAc as cartoon; the residues of ATP-site of PKAc interacting with **ARC-1012** are shown as lines and numbered. (B) Interactions developed between the linker of **ARC-1012** and PKAc from 3AG9 (magenta) overlaid with co-crystal PKAc – **ARC-1034** (3BWJ, blue). Ligands are shown as sticks, PKAc as cartoon; the residues of Gly-rich loop of PKAc interacting with **ARC-1012** are shown as lines and numbered.

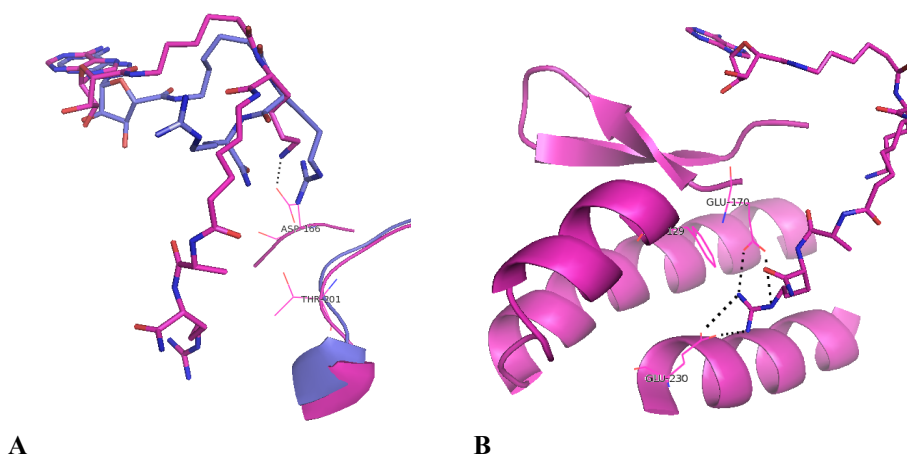


Figure 47. Comparison of 3AG9 and 3BWJ. (A) Interactions developed between the chiral moiety of **ARC-1012** and PKAc from 3AG9 (magenta) overlaid with the co-crystal PKAc – **ARC-1034** (3BWJ, blue). Ligands are shown as sticks, PKAc as cartoon; the residues of PKAc interacting with the chiral moiety of **ARC-1012** are shown as lines and numbered. (B) Interactions developed between the **Fragment 2** of **ARC-1012** and PKAc from 3AG9 (magenta) overlaid with co-crystal PKAc – **ARC-1034** (3BWJ, blue). Ligands are shown as sticks, PKAc as cartoon; the residues of protein substrate-site of PKAc interacting with **ARC-1012** are shown as lines and numbered.

Overall, the **ARC-1012** co-crystal allowed definition of the four major hot-spot fragments in **ARC-1012** developing strong interactions with PKAc:

- the purine moiety of **Fragment 1** binding to the ATP-site of PKAc,
- the carbonyl group of the first linker interacting with the residues of PKAc constituting the top of the Gly-rich loop,
- the side-chain of the chiral spacer (D-Lys) developing interactions with Asp166 of PKAc;
- Arg#2 binding Glu170 and Glu230 of PKAc responsible for recognition of protein/peptide substrate.

Most likely, the rest of the **ARC-1012** molecule was plainly arranged in a way that enabled exact pinpointing the aforementioned crucial contacts with the lowest entropic penalty; such hypothesis provides explanation for the tilted conformation of the ribose moiety, the poor fixation of Arg#1 and the second linker of **ARC-1012**, *etc.* Indeed, calorimetric studies [Rogozina and Pflug, unpublished] indicated rather entropy-driven mode of binding of **ARC-1012** as compared to **ARC-1034** (Table 6). Moreover, the recent thermodynamic analysis of multivalent interactions indicated that the use of flexible linkers in multi-ligand compounds is an effective strategy, and the loss of conformational entropy associated with the flexibility of linker may in several cases be only marginal [Kane, 2010].

Table 6. Data from calorimetric measurements of binding of ARCs to PKAc

<i>Compound</i>	<i>K_d, nM*</i>	<i>ΔH_B, kJ/mol</i>
ARC-1012	7.6	−60,7
ARC-1028	<0.1	−78,6
ARC-1034	250	−68,2

*proportional to ΔG_B

Possibly, in ARC-III conjugates incorporating the amidated (D-Arg)₆-peptide as **Fragment 2** (*i.e.*, **ARC-1028**), the hot-spot nature of Arg#2 is lowered, as there are other D-Arg residues in positions #3...#6 able to develop interactions with Glu203, Glu230, and other PKAc residues spatially closer to the end of helix F. In this context, the Pro-scan data of **ARC-1028** where D-Arg residues of **Fragment 2** were one-by-one replaced with D-Pro was of especial interest, indicating that the only modification resulting in an over 20-fold decrease in affinity (as compared to **ARC-1028**) was the replacement of Arg#1, whereas replacement of Arg#2 caused only a 3-fold loss of affinity [D. Lavogina, unpublished data]. These results indicate that the major importance of Arg#1 lies in its ability to direct the rest of **Fragment 2** of **ARC-1028** to the protein/peptide substrate-site of PKAc. Additionally, Pro-scan results may imply that lowering of hot-spot nature of Arg#2 allows rearrangement of conformation of **ARC-1028** as compared to **ARC-1012** so that Arg#1 is not exposed to solvent and may also develop interactions with PKAc. The indirect

confirmation for the latter statement is offered by the crystal structure of PKAc – **ARC-1039** complex, where elimination of another hot-spot fragment of ARC-III is possible due to substitution of D-Ala for D-Lys in the chiral spacer.

5.2. PKAc – ARC-1039 complex (PDB 3AGL)

The PKAc – **ARC-1039** complex crystallized with two PKAc molecules in the asymmetric unit, whereas both PKAc molecules were bound to **ARC-1039** (in contrast to **ARC-1012** co-crystal); the electron density was well defined for the whole **ARC-1039**.

The conformation of the **Fragment 1** of **ARC-1039** was nearly identical to that of **ARC-1034** (Figure 48A; [Lavogina *et al.*, 2009]), thus interactions with residues Glu121, Val123, Glu127, and Glu170 of PKAc were conserved, although the interaction between **ARC-1039** and Thr183 was weaker. The first linker of **ARC-1039** also adopted nearly the same shape as the linker of **ARC-1034** and hence also developed contacts with Ser53, Phe54, and Gly55 of PKAc, although the carbonyl group of the first linker of **ARC-1039** was positioned slightly closer to the end of the loop (Figure 48B). The conformation of the Gly-rich loop itself was again almost identical to that in the **ARC-1034** co-crystal, with similar distances Tyr330...Glu127 (5.0 Å), Ser53...Asp166 (10.2 Å), and His87...phosphorylated Thr197 (2.8 Å).

Analogically to Arg#1 of **ARC-1034** and differently from the chiral spacer of **ARC-1012**, the carbonyl group of the chiral spacer D-Ala in **ARC-1039** co-crystal pointed away from the catalytic cleft, and accepted hydrogen bond donated by the side-chain of Ser53 of PKAc (Figure 48C-D); the latter contact was the only direct interaction formed by D-Ala and PKAc. Importantly, due to an absent interaction of the chiral spacer with Asp166 of PKAc in the **ARC-1039** co-crystal, a strong hydrogen bond was formed between Asp166 and Thr201 (with length of 2.2 Å). The latter fact further confirms that **ARC-1039** served as bisubstrate inhibitor of PKAc, as the evidence from the literature has so far demonstrated that such hydrogen bond is present only in PKAc co-crystals with protein/peptide substrates or PCIs [Yang L. *et al.*, 2004].

Similar to **ARC-1012**, no interactions between the second linker of **ARC-1039** and PKAc were observed, although the electronic density was surprisingly well defined (in contrast with the second linker of **ARC-1012**); the latter fact might be attributed to good fixation of **Fragment 2** of **ARC-1039**. Differently from the **ARC-1012** co-crystal, Arg#1 of **ARC-1039** pointed towards the catalytic cleft and developed strong hydrogen bonds with Glu127 of PKAc, and an intramolecular hydrogen bond with the ribose residue from **Fragment 1**. The side-chain of Arg#2 of **ARC-1039** protruded to the same pocket as Arg#2 of **ARC-1012**, being involved in multiple polar contacts with Glu170 and Glu230 of PKAc, and an in-plane interaction of the guanidinium-group with Phe129.

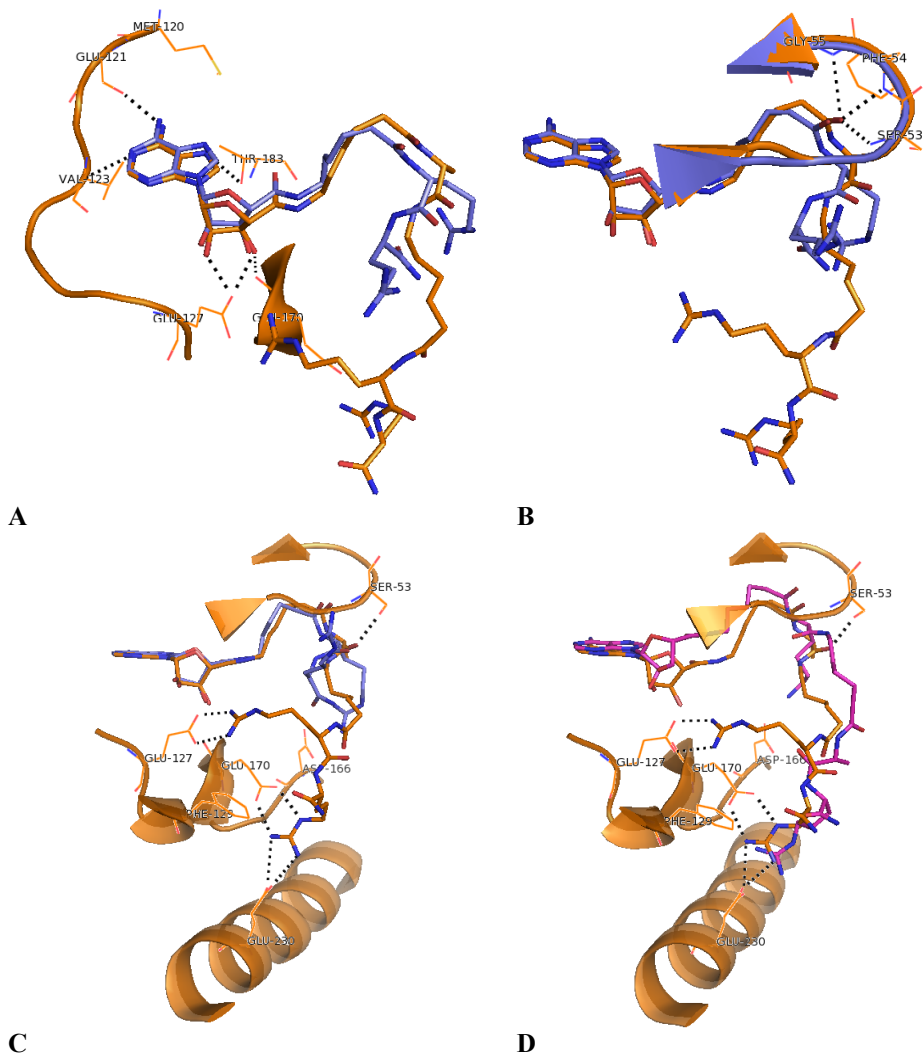


Figure 48. Comparison of 3AGL, 3BWJ and 3AG9. (A) Interactions developed between the **Fragment 1** of **ARC-1039** and ATP-site of PKAc from 3AGL (orange) overlaid with co-crystal PKAc – **ARC-1034** (3BWJ, blue). Ligands are shown as sticks, PKAc as cartoon; the residues of ATP-site of PKAc interacting with **ARC-1039** are shown as lines and numbered. (B) Interactions developed between the linker of **ARC-1039** and PKAc from 3AGL (orange) overlaid with the co-crystal PKAc – **ARC-1034** (3BWJ, blue). Ligands are shown as sticks, PKAc as cartoon; the residues of Gly-rich loop of PKAc interacting with **ARC-1039** are shown as lines and numbered. (C) Interactions developed between the **Fragment 2** of **ARC-1039** and PKAc from 3AGL (orange) overlaid with co-crystal PKAc – **ARC-1034** (3BWJ, blue). Ligands are shown as sticks, PKAc as cartoon; the residues of PKAc interacting with **ARC-1039** are shown as lines and numbered. (D) Interactions developed between the **Fragment 2** of **ARC-1039** and PKAc from 3AGL (orange) overlaid with co-crystal PKAc – **ARC-1012** (3AG9, magenta). Ligands are shown as sticks, PKAc as cartoon; the residues of PKAc interacting with **ARC-1039** are shown as lines and numbered.

Apart from revealing the multiplicity of binding modes of ARC-III compounds, the crystal structure of PKAc – **ARC-1039** complex provided an explanation for the enhanced affinity of **ARC-1039** towards PKAc *versus* ROCK-II. The hydrogen bond between Arg#1 of **ARC-1039** and Glu127 of PKAc is most likely lost in case of ROCK-II – **ARC-1039** complex, as the residue corresponding to Glu127 in ROCK-II is Asp176 with a shorter side-chain. In the PKAc – **ARC-1012** complex, Arg#1 pointed to solution and did not develop any interactions with Glu127, thus no interaction was lost in case of ROCK-II.

Overall, the change of one residue, the chiral spacer from D-Lys in **ARC-1012** to D-Ala in **ARC-1039** induced multiple differences in the **ARC-1039** co-crystal as compared to the **ARC-1012** co-crystal, which demonstrated once again the conformational flexibility of ARCs. In addition, the concept of mutual-induced fit [Williamson, 2000; Huang Z. and Wong, 2008] was clearly observable, where not only inhibitor adapted to the tertiary structure of enzyme, but the latter also showed local conformational flexibility (*i.e.*, illustrated by Gly-rich loop of PKAc). This evidence clearly points to limitations of structure-aided design performed by computational methods where the structure of an enzyme is considered as a fixed entity.

6. Application of ARC-II and ARC-III conjugates as inhibitors and fluorescent probes of PKGI α [Paper 4: Lavogina *et al.*, 2010b]

6.1. Development of assays

Having established the selectivity and affinity determinants of ARC-II and ARC-III conjugates towards PKAc [Enkvist *et al.*, 2006; Lavogina *et al.*, 2009], it was decided to test the affinity and inhibitory potency of ARCs towards a closely related kinase, PKGI α . Both PKA and PKG belong to family of cyclic nucleotide-dependent PKs, and possess high sequence homology of catalytic cores as well as cyclic nucleotide-binding domains (Figure 3) from the Section 1.2.2. PKG; [Hofmann *et al.*, 2009]); however, the structure-aided rational design of inhibitors for PKG is aggravated, as the latter has yielded no crystal structures so far. Therefore, PKA might be envisaged as a template for the design of PKG inhibitors, which may subsequently be optimized from the aspect of affinity and selectivity towards PKG in ligand-based design.

The first step for the screening of ARCs and reference compounds towards PKGI α was the establishment of a quick homogeneous assay enabling assessment of inhibitors within a wide range of inhibition/binding characteristics with sufficient accuracy. The most convenient way to accomplish this task was the adaptation of the previously reported ARC-Photo-based binding/displacement assay with fluorescence anisotropy/polarization detection (FA-assay), which had shown reliable results in experiments with PKAc and ROCK-II [Vaasa *et al.*, 2009]. The binding of four ARC-Photo probes representing generations ARC-II and ARC-III (**ARC-583**, **ARC-1042**, **ARC-669** [Figure 49A], and **ARC-1059** [Figure 49B]) was monitored in a direct binding FA-assay by titration with PKGI α (please refer to Table 1 from Paper 4); the lowest K_D value of 3.18 nM was obtained for the probe **ARC-1059** derived from the inhibitor **ARC-903**. In the presence of cGMP, the affinity of **ARC-1059** increased 8-fold, which was in good agreement with the fact that the catalytic activity of PKGI α increases 8...10-fold upon stimulation with cGMP; however, in the presence of both, cGMP and Mg^{2+} , the increase in affinity of **ARC-1059** was only 3-fold.

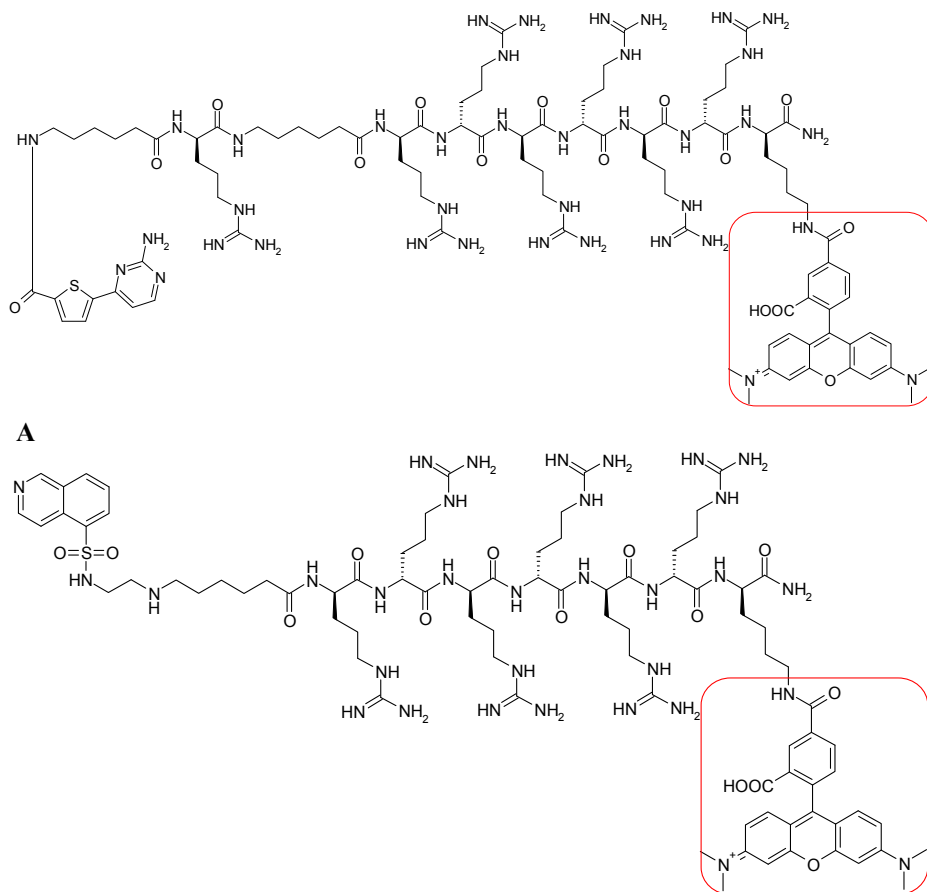


Figure 49. Examples of ARC-Photo. (A) ARC-669. (B) ARC-1059; red rounded rectangle surrounds the fluorescent dye TAMRA.

Interestingly, from the titration curves of **ARC-1059** it could be seen that the association of the latter into the complex with PKGI α not only caused an increase in fluorescence anisotropy of solution, but also led to a 3.5-fold enhancement of fluorescence intensity (FI). The change of FI of solution upon binding of ARC-Photo to the kinase had been previously reported for **ARC-583**, although in the latter case, the decrease in FI had been observed upon binding of **ARC-583** to PKAc [Vaasa *et al.*, 2009]. For this reason, the mathematical model of the FA-assay had been amended with a constant Q representing the ratio of FI for the bound and non-bound forms of ARC-Photo [Vaasa *et al.*, 2009]. The physical phenomenon behind the change of FI has not been unequivocally established. Most probably, Q values smaller than 1 may reflect the quenching of the ARC-bound fluorophore by an unfavourable environment in the complex with PK, and Q values larger than 1 may be caused

by partial intramolecular quenching of fluorophore in solution of free ARC-Photo (*i.e.*, by neighbouring aromatic systems) relieved upon binding of probe to a PK.

When the titration of **ARC-1059** by PKGI α in the presence of cGMP was monitored by the parallel measurement of FA and FI with microplate reader, the yielded curves were highly similar, and the K_D value of **ARC-1059** measured by FI detection was 0.44 nM. When the same titration was performed in a cuvette and FI was measured with a fluorescence spectrometer, the obtained K_D value of **ARC-1059** towards PKGI α in the presence of cGMP was 0.63 nM. The good correlation of results obtained from FA and FI read-outs (either with microplate reader or with spectrometer) demonstrated that in case of a sufficiently large Q value associated with binding of an ARC-Photo to a PK, the FA-assay might be converted to its analogue with FI-detection (FI-assay) that requires neither complicated equipment for FA measurement nor microplate format.

The concurrency of results measured by FA- and FI-assays was further confirmed by experiments where competitive displacement of **ARC-1059** from its complex with PKGI α in the presence of cGMP by ARCs or reference inhibitors was monitored (please refer to Table 2 from Paper 4). The reliability of FA- and FI-assays was verified by the “classical” radioactive kinetic assay, where the retarding effect of ARCs and reference compounds on the PKGI α -catalyzed phosphorylation of the peptide substrate TQAKRKSLAMA was measured in the presence of cGMP. The compounds with the best displacement as well as inhibition characteristics (*i.e.*, subnanomolar to low nanomolar displacement/inhibition IC_{50} values) were represented by ARC-II compounds containing H-9 as **Fragment 1** (*i.e.*, **ARC-349**, **ARC-903**), and ARC-III conjugates possessing an aminopyrimidine derivative as **Fragment 1** (*i.e.*, **ARC-663**, **ARC-664**, **ARC-668**). Similarly to the results of direct binding studies, ARCs containing Adc as **Fragment 1** exhibited a considerably poorer displacement and inhibition characteristics, indicating their poor affinity towards PKGI α .

Another binding/displacement assay format tested with the fluorescent probe **ARC-1059** was an assay with FRET detection; such assays are endowed with great potential from the point of view of intracellular application of ARCs. The FRET phenomenon has been widely applied for intracellular monitoring by virtue of ratiometric character of measurements and lower susceptibility to development of background signals. Previously, ARCs had been successfully applied in a biochemical assay where FRET had developed between a donor fluorophore FITC used for chemical labelling of PKAc, and the acceptor fluorophore TAMRA incorporated in the structure of **ARC-1042** [Vaasa *et al.*, 2010]. This time, fusion protein Cygnet 2.1 [Honda *et al.*, 2005] representing a construct of PKGI α fused *via* its C-terminus with fluorescent protein Citrine was used as a donor, and TAMRA of **ARC-1059** as an acceptor (please refer to Figure 4 from Paper 4). The FRET developed as a result of binding could be successfully disrupted by the non-fluorescent compound **ARC-903**, whereas both increase in the emission of donor (530 nm) and decrease in emission of

acceptor (580 nm) could be monitored either in the absence or in the presence of cGMP.

Overall, these experiments demonstrated the universal nature of ARC inhibitors from the aspect of applicability in assays with multiple fluorescence measurement techniques available for detection. Despite the fact that the structure-affinity relationship studies identified only generic ARCs as potent probes and inhibitors of PKGI α , this promiscuous nature of ARCs may prove advantageous for applications necessitating fluorescent detection or concomitant inhibition of several basophilic PKs; an example of such application is presented in Section 7. Measurement of physiological effects of ARC-903 in isolated rat arteries.

6.2. Studies of binding and inhibition mechanism

Before proceeding from *in vitro* bioanalytical methods with PKGI α to the experiments in living cells and tissues, the mechanism of PKGI α inhibition by most potent ARCs needed to be established. In FA- and FI-assays, **ARC-1059** could be successfully displaced from its complex with PKGI α by ATP and ACIs (*i.e.*, H9, H-89, staurosporine). However, the displacement of **ARC-1059** by the PKGI α peptide substrate TQAKRKKSLAMA and its non-phosphorylatable analogue TQAKRKKALAMA occurred only at high concentrations of displacing compounds, and could not be completed; moreover, **ARC-1059** could not be displaced by D-DT-2, a PKGI α -selective high-affinity PCI [Nickl *et al.*, 2010].

The kinetic studies of inhibition mechanism of PKGI α by ARCs revealed that **ARC-903** (used as an example of ARC) was competitive *versus* ATP, but clearly not competitive *versus* substrate peptide; moreover, in contrast to PKAc studies, the mechanism of inhibition *versus* substrate peptide of PKGI α resembled rather an uncompetitive than a non-competitive pattern (please refer to Figure 3 from Paper 4). The latter fact might indicate that ARCs are not bisubstrate inhibitors of PKGI α , but represent the group of biligand inhibitors with **Fragment 1** binding to the ATP-site of the PK, and **Fragment 2** binding to another distant site (*i.e.*, the Glu-rich C-tail of PKGI α ; Figure 3 from the Section 1.2.2. PKG). The biligand nature of ARCs is indirectly supported by the fact that these conjugates possess a higher affinity than the fragments composing those conjugates (*i.e.*, the K_i value of H9 towards PKGI α is 900 nM; [Ono-Saito *et al.*, 1999]).

7. Measurement of physiological effects of ARC-903 in isolated rat arteries [Paper 4: Lavogina *et al.*, 2010b]

The final step in progression from the rational design to assessment of properties of ARC-type inhibitors was confirmation of the ability of the latter to implement their high affinity and inhibition potential towards target PKs in biologically complex systems such as tissues and organs. As an example system, the smooth muscle tissue of rat cerebellum isolated intact arteries was chosen, due to the high content of PKAc and PKGI α , and a wealth of information in literature about effects resulting from inhibition of these PKs in this tissue.

First of all, the ability of ARC-Photos (**ARC-583**, **ARC-669**, and **ARC-1059**) to penetrate plasma membrane of smooth muscle cells in isolated arteries was tested. In accordance with the previously reported experiments in HEK-293 and CHO cell cultures [Uri *et al.*, 2002; Vaasa *et al.*, 2010], all compounds demonstrated cellular uptake after 1 h incubation of arteries in 10 μ M solution of ARCs at room temperature (Figure 50). The staining was characteristically pronounced in some regions of the arteries, and both, nuclear staining and diffused distribution in the cytoplasm could be indicated, whereas the proportion of distribution between the cytoplasm and the nucleus was dependent on the structure of the tested ARC (*i.e.*, **ARC-669** accumulated to nucleus, but **ARC-583** localization was more diffused, although still demonstrating nuclear inclusion). The studies of time- and concentration-dependent uptake of **ARC-1059** revealed that at a concentration of 10 μ M, the internalization of ARC was already observable after 20 min of incubation, although the nucleus was not yet stained (please refer to Figure 6 from Paper 4). By contrast, at 1 μ M or lower concentrations of **ARC-1059**, only minor extent of internalization was observed even after 60 min of incubation. The latter observation is also in good accordance with experiments in cell cultures [Vaasa *et al.*, 2010], which also indicated that a “critical” threshold of the ARC-Photo concentration had to be crossed in order to obtain effective internalization of conjugates into the cells.

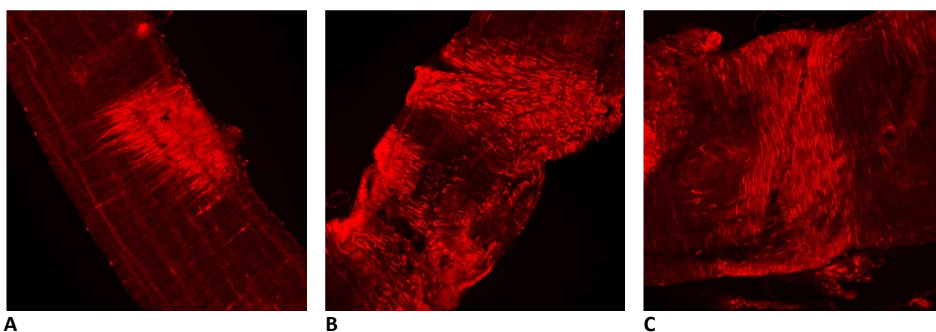


Figure 50. Staining of isolated rat cerebellum arteries by (A) 10 μ M **ARC-583**, (B) 10 μ M **ARC-669**, or (C) 10 μ M **ARC-1059** (in all cases, incubation time one hour at room temperature).

Next, measurement of the ability of **ARC-903** to inhibit PKGI α and PKAc at physiological conditions was performed by a pressure myography assay in the arteries isolated from rat cerebellum. Both PKGI α and PKAc trigger vasodilation *via* several mechanisms, with the net outcome in all cases represented by dephosphorylation of MLC₂₀; the inhibition of PKGI α or PKAc should therefore induce vasoconstriction (Scheme 1, Scheme 2 from the Section 1.2.2. PKG). Previously, vasoconstrictive effects had been demonstrated for the PKGI α -selective potent PCI D-DT-2 (concentration of 1...2 μ M in the superfusate; [Nickl *et al.*, 2010]), which relieved PKG- but not PKAc-induced vasodilation. The experimental set had comprised an isolated artery cannulised on glass pipettes and developing sustained myogenic tone upon pressurization to 80 mmHg. The change of the arterial diameter had been monitored in response to selective activators of PKG or PKAc (in order to discriminate the components of vasodilation triggered by either PK) and inhibitors applied *via* the superfusate. This time, the same technique was applied in tests with **ARC-903** (concentration of 4 μ M in the superfusate). **ARC-903** successfully abolished vasodilation induced by activators of both, PKGI α (*i.e.*, 8-Br-cGMP, MAHMA-NONOate) and PKAc (*i.e.*, Forskolin, 8-CPT-cAMP), confirming the ability of potent ARCs to inhibit PKs in physiological conditions (please refer to Figure 7 from Paper 4). Furthermore, the vasoconstriction of arteries induced by **ARC-903** occurred to an extent below the initial (basal) diameter, indicating that the basal activity of PKs was also inhibited; the latter result could also be repeated when **ARC-903** was applied to non-dilated artery.

Prior to the pressure myography experiments, **ARC-903** had revealed in bioanalytical *in vitro* assays highly potent inhibition of not only PKAc and PKG, but also ROCK [Enkvist *et al.*, 2006]. The promiscuous nature of **ARC-903** was therefore considered problematic, as in smooth muscle tissue, the pathways of cyclic-nucleotide dependent PKs oppose pathways of ROCK; it was therefore relieving to witness that **ARC-903** could still implement its high potency *via* inhibiting PKAc and PKGI α pathways in tissue. The reason why effects of inhibition of PKA and PKGI α on the one hand, and ROCK on the other hand did not mutually even out, probably lies in the fact that PKAc and PKG serve themselves as deactivators of ROCK, and therefore the latter was “switched off” during the whole course the experiment. In turn, the latter fact means that the constriction of artery upon application of **ARC-903** was achieved *via* ROCK-independent mechanisms, which might involve downregulation of telokin-induced MYPT activity and re-gain of function of Ca²⁺-pathways.

The application of a group-selective inhibitor with high affinity towards PKAc and PKGI α but not ROCK would probably yield more drastic and sustained effects in the given assay; still, this final set of pressure myography experiments convincingly demonstrated the wide field of application possibilities for the promiscuous nature of ARC-conjugates. Moreover, the ability of **ARC-903** to inhibit PKGI α - and PKAc-induced vasodilation in the arteries isolated from rat cerebellum represented the first clearly pronounced physiological effect of BSIs reported so far.

CONCLUSIONS

The present thesis focussed on design, synthesis and *in vitro* characterization of new conjugates of an adenosine analogue and an arginine-rich peptide as inhibitors of basophilic protein kinases. The progress within the given work comes to the fore by step-by-step evolution of ARCs from submicromolar to subnanomolar inhibitors of PKAc, PKG, ROCK and several other representatives of the AGC-group. Importantly, by virtue of enhanced proteolytic stability and relatively good cell membrane-penetrative properties, the most efficient ARCs are applicable both in biochemical assays and in living cells or tissues. Dependent on the character of application, different ARCs may be used as generic probes of basophilic PKs or as remarkably selective modulators of PK activity.

The main results of the thesis can be summarized as follows:

- Two new sets of ARCs (subsequently termed as ARC-II and ARC-III) have been designed and synthesized. The main modifications in the structure of new compounds as compared to the set of the initial ARCs (ARC-I) were as follows:
 - In case of ARC-II, the C-terminus of the compounds was amidated, D-Arg residues in the peptidic fragment were substituted for L-Arg residues, and H-9 moiety was incorporated as nucleosidic fragment. The most efficient representative of ARC-II was **ARC-903** with inhibition IC_{50} value of 5.3 nM towards PKAc.
 - In case of ARC-III, a second linker and the chiral moiety (amino acid) were introduced. The most efficient representative of ARC-III was **ARC-1028** with competitive displacement IC_{50} value of less than 0.5 nM towards PKAc.
- The bisubstrate character of ARCs was confirmed in displacement studies with PKAc (where the fluorescent ARC-probe could be successfully displaced from its complex with the kinase by compounds targeted to the ATP-site as well as the protein substrate site of PKAc), and by co-crystals of PKAc with representatives of ARC-III.
- The profiling of representatives of ARC-II and ARC-III towards a panel of PKs indicated that the novel ARCs were group-selective inhibitors possessing high affinity towards several PKs of the AGC-group; the more detailed studies with PKAc, PKGI α , PKB γ and ROCK-II revealed several structural elements (e.g., nucleosidic fragment or chiral moiety) which influence the inhibitory potency and enable tuning the selectivity of ARCs.
- The wide applicability of novel ARCs was confirmed by development of ARC-based biochemical *in vitro* assays for PKGI α with detection of change of fluorescence anisotropy (FA), fluorescence intensity (FI), or FRET. While the FA-assay was adapted from the previous PKAc studies, the FI- and FRET-assays were originally designed.

- The potential of novel ARCs as physiological modulators was demonstrated in the internalization studies with the isolated smooth muscle tissue, and in vasoconstriction experiments with isolated rat arteries (*via* targeting cAMP/PKA and cGMP/PKG pathways).

SUMMARY IN ESTONIAN

Adenosiini analoogi ja oligoarginiini konjugaatidel põhinevad proteiinkinaaside inhibiitorid

Valkude fosforüleerimisreaktsioon elusorganismides ning seda katalüüsivad valgud – proteiinkinaasid – on olnud loodusteaduste tähelepanu keskpunktis alates 1950-test aastatest, kui E. P. Kennedy, E. H. Fischer'i, E. G. Krebs'i, E. W. Sutherland'i ja W. D. Wosilait'i tööd avasid kinaaside ajastu [Cohen P., 2002]. Proteiinkinaasid osalevad enamikes raku elutegevuseks olulistes protsessides, seetõttu on häired nende ensüümide funktsioneerimises (eriti kõrgendatud aktiivsus) seotud mitmete haigustega (sealhulgas vähkkasvajad, diabeedid ja astma). Sellest tulenevalt keskenduvad nii akadeemiliste teadlaste kui ka farmaatsiafirmade ravimiarendajate huvid üha enam kinaaside toimemehhanismide uurimisele ja võimaluste selgitamisele rakusiseste valkude fosforüleerimistasaalude mõjutamiseks. Viimase ülesande lahendamisel on üheks perspektiivsemaks teeks proteiinkinaaside inhibiitorite arendus.

Käesolev töö kirjeldab adenosiini analoogi ja arginiinirikka peptiidi konjugaatide (ARC-de) arendamist proteiinkinaaside bisubstraatseteks kõrge inhibeerimispotentsiaaliga ligandideks, nende disaini ja sünteesi. Uudsete ARC-de arendamisel lähtuti tulemustest, mis saadi inhibiitorite struktuuri mõju uurimisel nende sidumis- või inhibeerimisomadustele cAMP-sõltuva proteiinkinaasiga (PKA) ning sama proteiinkinaasi ARC-dega kooskristalliseerimisel saadud struktuuride röntgenanalüüsil. Töö tulemusena õnnestus valmistada kaks uut ARC-tüüpi inhibiitorite põlvkonda (ARC-II ja ARC-III), mille esindajatel on võrreldes lähteühenditega (ARC-I) järgmised erinevused:

- ARC-II puhul amideeriti konjugaadi C-terminaalne karboksüülrühm ning peptiidides fragmendis asendati L-arginiinid D-arginiinidega; lisaks asendati mõnede ühendite nukleosiidses fragmendis adenosiini derivaat Hidaka inhibiitori H-9 jäägiga. ARC-II kõige efektiivsema esindaja (**ARC-903**) IC_{50} väärtus PKAc inhibeerimiskatsetes oli 5,3 nM.
- ARC-III puhul lisati konjugaatide struktuuri kiraalne element (aminohape) ja teine linker. ARC-III kõige efektiivsem esindaja oli **ARC-1028**, mille IC_{50} väärtus väljatõrjumiskatsetes PKAc-ga oli alla 0,5 nM.

Järgmise sammuna määrati ARC-II ja ARC-III kõige efektiivsemate ühendite selektiivsusprofiilid; ühendid osutusid rühm-selektiivseteks inhibiitoriteks mitmete basofiilsete proteiinkinaaside, eriti AGC-rühma esindajate suhtes. Detailsemates uuringutes proteiinkinaasidega PKGI α , PKB γ ja ROCK-II tehti kindlaks ka uute ARC-de struktuurifragmendid, mis mõjutavad inhibiitorite selektiivsust ühe või teise kinaasi suhtes.

Edasistes uuringutes tehti kindlaks, et tulenevalt uute ARC-de suhteliselt laia selektiivsusprofiilist oli võimalik rakendada ARC-del põhinevat sidumismeetodit (FA-meetod) kinaasiaktiivsuse hindamiseks ning proteiinkinaasi-inhibiitorite iseloomustamiseks mitte ainult eelnevalt mudelkinaasina kasutatud

PKA jaoks, vaid ka viimasega struktuurselt sarnase PKGI α jaoks. Lisaks eelnevale arendati uute ARC-de põhjal PKGI α jaoks veel kaks sidumismeetodit, milles inhibiitorite afiinsuse või kinaasi aktiivsuse määramiseks mõõdeti fluorestsentsi või FRET-i intensiivsuse muutust. Kõiki eespoolmainitud meetodeid on suure tõenäosusega võimalik kohandada ka mitme teise basofiilse proteiinkinaasi jaoks.

Töö viimases etapis demonstreeriti, et uute ARC-de rakendusala ei piirdu biokeemiliste *in vitro* mõõtmismeetoditega, vaid see on laiendatav *in vitro* katsetele elusrakkudes ja -kudedes. ARC-II ja ARC-III efektiivsemate esindajate proteolüütiline stabiilsus ja võime läbida raku plasmamembraani võimaldasid uurida uusi inhibiitoreid roti isoleeritud ajuarterite silelihaskoes. Nende katsetuste tulemusena selgus, et ARC-d suudavad inhibeerida cAMP/PKA ja cGMP/PKG radu füsioloogilistes tingimustes.

REFERENCES

- Adelstein R. S., Conti M. A., Hathaway D. R., Klee C. B., JBC (1978), 253, 8347–8350
- Adrian F. J., Ding Q., Sim T., Velentza A., Sloan C., Liu Y., Zhang G., Hur W., Ding S., Manley P., Mestan J., Fabbro D., Gray N. S., Nat. Chem. Biol. (2006), 2, 95–102
- Ahn D.-R., Han K.-C., Kwon H. S., Yang E. G., Bioorg. Med. Chem. Lett. (2007), 17, 147–151
- Airhart N., Yang Y.-F., Roberts C. T. Jr., Silberbach M., JBC (2003), 278, 38693–38698
- Akamine P., Madhusudan, Wu J., Xuong N.-H., Ten Eyck L. F., Taylor S. S., J. Mol. Biol. (2003), 327, 159–171
- Akropoulou-Zanze I., Hajduk P. J., Drug Disc. Today (2009), 14, 291–297
- Allen M. D., Zhang J., Biochem. Biophys. Res. Comm. (2006), 348, 716–721
- Alverdi V., Mazon H., Versluis C., Hemrika W., Esposito G., van den Heuvel R., Scholten A., Heck A. J. R., J. Mol. Biol. (2008), 375, 1380–1393
- Amano M., Chihara K., Nakamura N., Kaneko T., Matsuura Y., Kaibuchi K., JBC (1999), 274, 32418–32424
- Anand G. S., Krishnamurthy S., Bishnoi T., Kornev A., Taylor S. S., Johnson D. A., Mol. Cell. Proteomics (2010), doi: 10.1074/mcp.M900388-MCP200
- Argiriadi M. A., Sousa S., Banach D., Marcotte D., Xiang T., Tomlinson M. J., Demers M., Harris C., Kwak S., Hardman J., Pietras M., Quinn L., DiMauro J., Ni B., Mankovich J., Borhani D. W., Talanian R. V., Sadhukhan R., BMC Struct. Biol. (2009), 9, 16
- Bain J., McLauchlan H., Elliott M., Cohen P., Biochem. J. (2003), 371, 199–204
- Baird G. S., Zacharias D. A., Tsien R. Y., PNAS USA (1999), 96, 11241–11246
- Beene D. L., Scott J. D., Curr. Opin. Cell Biol. (2007), 19, 192–198
- Benoit N. L., Chemistry of peptide synthesis, CRC Press Taylor and Francis Group (2006)
- Bishop A. C., Buzko O., Shokat K. M., Trends Cell. Biol. (2001), 11, 167–172
- Bissantz C., Kuhn B., Stahl M., J. Med. Chem. (2010), 53, 5061–5084
- Bogoyevitch M. A., Barr R. K., Ketterman A. J., Biochim. Biophys. Acta (2005), 1754, 79–99
- Bogoyevitch M. A., Fairlie D. P., Drug Disc. Today (2007), 12, 622–633
- Bonke G., Vedel L., Witt M., Jaroszewski J. W., Olsen C. A., Franzyk H., Synthesis (2008), 15, 2381–2390
- Bonn S., Herrero S., Breitenlechner C. B., Erlbruch A., Lehmann W., Engh R. A., Gassel M., Bossemeyer D., JBC (2006), 281, 24818–24830
- Bonny C., Oberson A., Negri S., Sauser C., Schorderet D. F., Diabetes (2001), 50, 77–82
- Borsi V., Calderone V., Fragai M., Luchinat C., Sarti N., J. Med. Chem. (2010), 53, 4285–4289
- Bostrom S. L., Dore J., Griffith L. C., Biochem. Biophys. Res. Commun. (2009), 390, 1154–1159
- Bragg, W. L., Proc. Cambridge Philosoph. Soc. (1913), 17, 43–57
- Breitenlechner C. B., Bossemeyer D., Engh R. A., Bioch. et Bioph. Acta (2005), 1754, 38–49
- Brown M. J., Novel fluorescent kinase ligands and assays employing the same, WO2008071937 (2008)

- Brown S. H. J., Wu J., Kim C., Alberto K., Taylor S. S., *J. Mol. Biol.* (2009) 393, 1070–1082
- Burkhardt M., Glazova M., Gambaryan S., Vollkommer T., Butt E., Bader B., Heermeieri K., Lincoln T. M., Walter U., Palmetshofer A., *JBC* (2000), 275, 33536–33541
- Butt E., Pdhler D., Genieser H.-G., Huggins J. P., Bucher B., *Br. J. Pharmacol.* (1995), 116, 3110–3116
- Caldwell J. J., Davies T. G., Donald A., McHardy T., Rowlands M. G., Aherne G. W., Hunter L. K., Taylor K., Ruddie R., Raynaud F. I., Verdonk M., Workman P., Garrett M. D., Collins I., *J. Med. Chem.* (2008), 51, 2147–2157
- Calleja V., Alcor D., Laguerre M., Park J., Vojnovic B., Hemmings B. A., Downward J., Parker P. J., Larijani B., *PLoS Biol.* (2007), 5, 780–791
- Carlson C. B., Robers M. B., Vogel K. W., Machleidt T., *J. Biomol. Screen.* (2009), 14, 121–132
- Cary S. P. L., Winger J. A., Marletta M. A., *PNAS USA* (2005), 102, 13064–13069
- Casteel D. E., Zhang T., Zhuang S., Pilz R. B., *Cell. Signal.* (2008), 20, 1392–1399
- Chan W. C., White P. D., *Fmoc Solid Phase Peptide Synthesis*, Oxford University Press (2000)
- Chang L., Karin M., *Nature* (2001), 410, 37–40
- Charter N. W., Kauffman L., Singh R., Eglen R. M., *J. Biomol. Screen.* (2000), 11, 390–339
- Chen Y. T., Bannister T. D., Weiser A., Griffin E., Lin L., Ruiz C., Cameron M. D., Schürer S., Duckett D., Schröter T., LoGrasso P., Feng Y., *Bioorg. Med. Chem. Lett.* (2008), 18, 6406–6409
- Cheng J. Q., Lindsley C. W., Cheng G. Z., Yang H., Nicosia S. V., *Oncogene* (2005), 24, 7482–7492
- Cheng K.-Y., Noble M. E. M., Skamnaki V., Brown N. R., Lowe E. D., Kontogiannis L., Shen K., Cole P. A., Siligardi G., Johnson L. N., *JBC* (2006), 281, 23167–23179
- Cheng X., Ji Z., Tsalkova T., Mei F., *Acta Biochim. Biophys. Sin. (Shanghai)* (2008), 40, 651–662
- Cheng Y., Prusoff W. H., *Biochem. Pharmacol.* (1973), 22, 3099–3108
- Cheng Y., Zhang Y., McCammon J. A., *JACS* (2005), 127, 1553–1562
- Chico L. K., Van Eldik L. J., Watterson D. M., *Nat. Rev. Drug Discov.* (2009), 8, 892–909
- Chuan H., Lin J., Wang J. H., *JBC* (1989), 264, 7981–7988
- Clardy J., Walsh C., *Nature* (2004), 432, 829–837
- Cohen M. S., Zhang C., Shokat K. M., Taunton J., *Science* (2005), 308, 1318–1321
- Cohen P., *Nat. Cell. Biol.* (2002), 4, E127–E130
- Cohen P., *Biochem. J.* (2010), 425, 53–54
- Collins I., Caldwell J., Fonseca T., Donald A., Bavetsias V., Hunter L.-J. K., Garrett M. D., Rowlands M. G., Aherne G. W., Davies T. G., Berdini V., Woodhead S. J., Davis D., Seavers L. C. A., Wyatt P. G., Workman P., McDonald E., *Bioorg. Med. Chem.* (2006), 14, 1255–1273
- Collins I., *Anti-Cancer Agents Med. Chem.* (2009), 9, 32–50
- Cox G., Matz M., Salih A., *Microscopy Res. Tech.* (2007), 70, 243–251
- Craggs T. D., *Chem. Soc. Rev.* (2009), 38, 2865–2875
- Cross D. A. E., Alessi D. R., Cohen P., Andjelkovich M., Hemmings B. A., *Nature* (1995), 378, 785–789
- Currie R. A., Walker K. S., Gray A., Deak M., Casamayor A., Downes C. P., Cohen P., Alessi D. R., Lucocq J., *Biochem. J.* (1999), 337, 575–583

- Dalziel K., Dickinson F. M., *Biochem. J.* (1966), 100, 34–46
- Dalton G. D., Dewey W. L., *Neuropeptides* (2006), 40, 23–34
- Davidson W., Frego L., Peet G. W., Kroe R. R., Labadia M. E., Lukas S. M., Snow R. J., Jakes S., Grygon C. A., Pargellis C., Werneburg B. G., *Biochemistry* (2004), 43, 11658–11671
- Davies T. G., Verdonk M. L., Graham B., Saalau-Bethell S., Hamlett C.C. F., McHardy T., Collins I., Garrett M. D., Workman P., Woodhead S. J., Jhoti H., Barford D., *J. Mol. Biol.* (2007), 367, 882–894
- Davis A. M., St-Gallay S. A., Kleywegt G. J., *Drug Discovery Today* (2008), 13, 831–841
- De Barry J., Liégeois C. M., Janoshazi A., *Experim. Gerontology* (2010), 45, 64–69
- Degorce F., Card A., Soh S., Trinquet E., Knapik G. P., Xie B., *Curr. Chem. Genomics* (2009), 3, 22–32
- Desai M. C., Zuckermann R. N., Moos W. H., *Drug Dev. Res.* (1994), 33, 174–188
- Desch M., Sigl K., Hieke B., Salb K., Kees F., Bernhard D., Jochim A., Spiessberger B., Hocherl K., Feil R., Feil S., Lukowski R., Wegener J. W., Hofmann F., Schlossmann J., *Cardiovasc. Res. Adv. Acc.* (2010), 86, 496–505
- Di Benedetto G., Zoccarato A., Lissandron V., Terrin A., Li X., Houslay M. D., Baillie G. S., Zaccolo M., *Circ. Res.* (2008), 103, 836–844
- Dilly A. K., Rajala R. V. S., *IOVS* (2008), 49, 4765–4773
- Diskar M., Zenn H.-M., Kaupisch A., Prinz A., Herberg F. W., *Cell. Signal.* (2007), 19, 2024–2034
- Doe C., Bentley R., Behm D. J., Lafferty R., Stavenger R., Jung D., Bamford M., Panchal T., Grygielko E., Wright L. L., Smith G. K., Chen Z., Webb C., Khandekar S., Yi T., Kirkpatrick R., Dul E., Jolivet L., Marino J. P. Jr., Willette R., Lee D., Hu E., *J. Pharmacol. Exp. Ther.* (2007), 320, 89–98
- Doerig C., Abdi A., Bland N., Eschenlauer S., Dorin-Semblat D., Fennell C., Halbert J., Holland Z., Nivez M.-P., Semblat J.-P., Sicard A., Reininger L., *Biochim. Biophys. Acta* (2010), 1804, 604–612
- Dominguez I., Diaz-Meco M. T., Municio M. M., Berra E., de Herreros A. G., Cornet M. E., Sanz L., Moscat J., *Mol. Cell. Biol.* (1992), 12, 3776–3783
- Dostmann W. R. G., Nickl C., Thiel S., Tsigelny I., Frank R., Tegge W. J., *Pharmacol. Ther.* (1999), 82, 373–387
- Dostmann W. R. G., Taylor M. S., Nickl C. K., Brayden J. E., Frank R., Tegge W. J., *PNAS USA* (2000), 97, 14772–14777
- Dostmann W. R. G., Tegge W., Frank R., Nickl C. K., Taylor M. S., Brayden J. E., *Pharmacol. Ther.* (2002), 93, 203–215
- Druker B. J., Lydon N. B., *J. Clin. Invest.* (2000), 105, 3–7
- Du K., Montminy M., *JBC* (1998), 273, 32377–32379
- Duchardt F., Fotin-Mleczek M., Schwarz H., Fischer R., Brock R., *Traffic* (2007), 8, 848–866
- Dulin N. O., Niu J., Browning D. D., Ye R. D., Voyno-Yasenetskaya T., *JBC* (2001), 276, 20827–20830
- Eichholtz T., de Bont D. B., de Widt J., Liskamp R. M., Ploegh H. L., *JBC* (1993), 268, 1982–986
- Ekoski E., Aitio O., Törnquist K., Yli-Kauhaluoma J., Tuominen R. K., *Eur. J. Pharmaceutical Sci.* (2010), 40, 404–411
- Elphick L. M., Lee S. E., Gouverneur V., Mann D. J., *ACS Chem. Biol.* (2007), 2, 299–314
- Engh R. A., Bossemeyer D., *Pharmacol Ther.* (2002), 93, 99–111

- Enkvist E., Lavogina D., Raidaru G., Vaasa A., Viil I., Lust M., Viht K., Uri A., *J. Med. Chem.* (2006), 49, 7150–7159
- Enkvist E., Raidaru G., Vaasa A., Pehk T., Lavogina D., Uri A., *Bioorg. Med. Chem. Lett.* (2007), 17, 5336–5339
- Enkvist E., Kriisa M., Roben M., Kadak G., Raidaru G., Uri A., *Bioorg. Med. Chem. Lett.* (2009), 19, 6098–6101
- Facchinetti V., Ouyang W., Wei H., Soto N., Lazorchak A., Gould C., Lowry C., Newton A. C., Mao Y., Miao R. Q., Sessa W. C., Qin J., Zhang P., Su B., Jacinto E., *EMBO J.* (2008), 27, 1932–1943
- Fan Q. W., Weiss W. A., *Cell Cycle* (2006), 5, 2301–2305
- Fedorov O., Müller S., Knapp S., *Nat. Chem. Biol.* (2010), 6, 166–169
- Feng Y., Cameron M. D., Frackowiak B., Griffin E., Lin L., Ruiz C., Schröter T., LoGrasso P., *Bioorg. Med. Chem. Lett.* (2007), 17, 2355–2360
- Fischer J. R., Lessel U., Rarey M., *J. Chem. Inf. Model.* (2010), 50, 1–21
- Fischer P. M., *Curr. Prot. Pept. Sci.* (2003), 4, 339–356
- Fischer P. M., *Curr. Med. Chem.* (2004), 11, 1563–1583
- Fischer R., Waizenegger T., Köhler K., Brock R., *Biochim. Biophys. Acta* (2002), 1564, 365–374
- Frame S., Cohen P., *Biochem. J.* (2001), 359, 1–16
- Freeman-Cook K. D., Autry C., Borzillo G., Gordon D., Barbacci-Tobin E., Bernardo V., Briere D., Clark T., Corbett M., Jakubczak J., Kakar S., Knauth E., Lippa B., Luzzio M. J., Mansour M., Martinelli G., Marx M., Nelson K., Pandit J., Rajamohan F., Robinson S., Subramanyam C., Wei L., Wythes M., Morris J., *J. Med. Chem.* (2010), 53, 4615–4622
- Frei E., Huster M., Smital P., Schlossmann J., Hofmann F., Wegener J. W., *Am. J. Physiol. Gastrointest. Liver Physiol.* (2009), 297, G834–G839
- Fry D. W., *Pharmacol. Ther.* (1999), 82, 207–218
- Fuerst, M. L., *Onc. Times* (2010), 32, 5–7
- Fujiwara D., Ye Z., Gouda M., Yokota K., Tsumuraya T., Fujii I., *Bioorg. Med. Chem. Lett.* (2010), 20, 1776–1778
- Fukami Y., Tokmakov A. A., Konaka K., Sato K.-I., *Pharmacol. Ther.* (1999), 82, 399–407
- Fukata Y., Amano M., Kaibuchi K., *Trends Pharmacol. Sciences* (2001), 22, 32–39
- Fuse E., Kuwabara T., Sparreboom A., Sausville E. A., Figg W. D., *J. Clin. Pharmacol.* (2005), 45, 394–403
- Futer O., Saadat A. R., Doran J. D., Raybuck S. A., Pazhanisamy S., *Biochemistry* (2006), 45, 7913–7923
- Gadella T. W. J. (Editor), *FRET and FLIM techniques, Laboratory Techniques in Biochemistry and Molecular Biology* (2009), 33
- Gani O. A. B. S. M., Engh R. A., *Nat. Prod. Rep.* (2010), 27, 489–498
- Garcia-Echeverria C., Traxler P., Evans D. B., *Med. Res. Rev.* (2000), 20, 28–57
- Garcia-Echeverria C., Sellers W. R., *Oncogene* (2008), 27, 5511–5526
- Gayani B., Perera K., Maly D. J., *Mol. Bio. Syst.* (2008), 4, 542–550
- Giacovazzo C., Monaco H. L., Artioli G., Viterbo D., Ferraris G., Gilli G., Zanotti G., Catti M., *Fundamentals of crystallography.* Oxford University Press (2005)
- Gill A., *Mini Rev. Med. Chem.* (2004), 4, 301–311
- Goldenberg-Furmanov M., Stein I., Pikarsky E., Rubin H., Kasem S., Wygoda M., Weinstein I., Reuveni H., Ben-Sasson S. A., *Cancer Res.* (2004), 64, 1058–1066
- Goodman K. B., Cui H., Dowdell S. E., Gaitanopoulos D. E., Ivy R. L., Sehon C. A., Stavenger R. A., Wang G. Z., Viet A. Q., Xu W., Ye G., Semus S. F., Evans C.,

- Fries H. E., Jolivet L. J., Kirkpatrick R. B., Dul E., Khandekar S. S., Yi T., Jung D. K., Wright L. L., Smith G. K., Behm D. J., Bentley R., Doe C. P., Hu E., Lee D., J. Med. Chem. (2007), 50, 6–9
- Grant S. K., Cell. Mol. Life Sci. (2009), 66, 1163–1177
- Grauer A., König B., Eur. J. Org. Chem. (2009), 2009, 5099–5111
- Green K. D., Kay M., Pflum H., JACS (2007), 129, 10–11
- Greene T. W., Wuts P. G. M., Protective Groups in Organic Synthesis, John Wiley & Sons, Inc. (1999), 3rd edition
- Gridelli C., Maione P., Del Gaizo F., Colantuoni G., Guerriero C., Ferrara C., Nicoletta D., Comunale D., De Vita A., Rossi A., Oncologist (2007), 12, 191–200
- Grodsky N., Li Y., Bouzida D., Love R., Jensen J., Nodes B., Nonomiya J., Grant S., Biochemistry (2006), 45, 13970–13981
- Gumireddy K., Baker S. J., Cosenza S. C., John P., Kang A. D., Robell K. A., Reddy M. V. R., Reddy E. P., PNAS USA (2005), 102, 1992–1997
- Hahmann C., Schroeter T., Cell. Mol. Life Sci. (2010), 67, 171–177
- Hajduk P. J., Huth J. R., Tse C., Drug Disc. Targets (2005), 10, 1675–1682
- Han S., Zhou V., Pan S., Liu Y., Hornsby M., McMullan D., Klock H. E., Haugen J., Lesley S. A., Gray N., Caldwell J., Gu X. J., Bioorg. Med. Chem. Lett. (2005), 15, 5467–5473
- Handa A. K., Johri M. M., Plant Physiol. (1977), 59, 490–496
- Hanks S. K., Hunter T., FASEB J. (1995), 9, 576–596
- Hanks S. K., Genome Biol. (2003), 4, 111
- Hanoune J., Defer N., Annu. Rev. Pharmacol. Toxicol. (2001), 41, 145–174
- Harootunian A. T., Adams S. R., Wen W., Meinkoth J. L., Taylor S. S., Tsien R. Y., Mol. Biol. Cell. (1993), 4, 993–1002
- Harris T. E., Persaud S. J., Jones P. M., Mol. Cell. Endocrinology (1999), 155, 61–68
- Hastie C. J., McLauchlan H. J., Cohen P., Nat. Protoc. (2006), 1, 968–971
- Hauptman H. A., Rep. Prog. Phys. (1991), 54, 1427–1454
- Heerding D. A., Rhodes N., Leber J. D., Clark T. J., Keenan R. M., Lafrance L. V., Li M., Safonov I. G., Takata D. T., Venslavsky J. W., Yamashita D. S., Choudhry A. E., Copeland R. A., Lai Z., Schaber M. D., Tummino P. J., Strum S. L., Wood E. R., Duckett D. R., Eberwein D., Knick V. B., Lansing T. J., McConnell R. T., Zhang S., Minthorn E. A., Concha N. O., Warren G. L., Kumar R., J. Med. Chem. (2008), 51, 5663–5679
- Herberg F. W., Taylor S. S., Biochemistry (1993), 32, 14015–14022
- Herberg F. W., Doyle M. L., Cox S., Taylor S. S., Biochemistry (1999), 38, 6352–6360
- Heymach J. V., Nilsson M., Blumenschein G., Papadimitrakopoulou V., Herbst R., Clin. Cancer Res. (2006), 12, 4441s–4445s
- Hidaka H., Inagaki M., Kawamoto S., Sasaki Y., Biochemistry (1984), 23, 5036–5041
- Hines A. C., Cole P. A., Bioorg. Med. Chem. Lett., (2004), 14, 2951–2954
- Hofmann F., Bechtel P. J., Krebs E. G., JBC (1977), 252, 1441–1447
- Hofmann F., Ammendola A., Schlossmann J., J. Cell Science (2000), 113, 1671–1676
- Hofmann F., Bernhard D., Lukowski R., Weinmeister P., cGMP: Generators, Effectors and Therapeutic Implications (Handbook of Experimental Pharmacology), Springer (2009), 137–162
- Honda A., Sawyer C. L., Cawley S. M., Dostmann W. R., Methods Mol. Biol. (2005), 307, 27–43
- Hopkins A. L., Groom C. R., Nature Rev. Drug Discov. (2002), 1, 727–730
- House C., Kemp B. E., Science (1987), 238, 1726–1728
- Huang J., Manning B. D., Biochem. Soc. Trans. (2009), 37, 217–222

- Huang L. J., Durick K., Weiner J. A., Chun J., Taylor S. S., JBC (1997), 272, 8057–8064
- Huang Z., Wong C. F., J. Comput. Chem. (2008), 30, 631–644
- Huang X., J. Biomol. Screen. (2003), 8, 34–38
- Huse M., Kuriyan J., Cell Volume 109, Issue 3, 3 May 2002, Pages 275–282
- InvitrogenTM Human Kinome Map,
<http://www.invitrogen.com/site/us/en/home/LINNEA-Online-Guides/human-kinome-map/Search-The-Human-Kinome.html>, last viewed August 7, 2010
- InvitrogenTM Product Spectra 5-TAMRA/pH 7.0,
<http://www.invitrogen.com/site/us/en/home/support/Product-Technical-Resources/Product-Spectra.6121ph7.html>, last viewed August 16, 2010
- Iwakubo M., Takami A., Okada Y., Kawata T., Tagami Y., Sato M., Sugiyama T., Fukushima K., Taya S., Amano M., Kaibuchi K., Iijima H., Bioorg. Med. Chem. (2007a), 15, 1022–1033
- Iwakubo M., Takami A., Okada Y., Kawata T., Tagami Y., Ohashi H., Sato M., Sugiyama T., Fukushima K., Iijima H., Bioorg. Med. Chem. (2007b), 15, 350–364
- Jacobs M., Hayakawa K., Swenson L., Bellon S., Fleming M., Taslimi P., Doran J., JBC (2006), 281, 260–268
- Jameson D. M., Ross J. A., Chem Rev. (2010), 110, 2685–2708
- Joachimiak A., Curr. Opin. Struct. Biol. (2009), 19, 573–584
- Johannessen M., Moens U., Front. Bioscience (2007), 12, 1814–1832
- Johnson D. A., Akamine P., Radzio-Andzelm E., Madhusudan, Taylor S. S., Chem. Rev. (2001), 101, 2243–2270
- Johnson L. N., Quarterly Rev. Biophys. (2009), 42, 1–40
- Kaláb P., Soderholm J., (2010), 51, 220–232
- Kalesh K. A., Sim D. S. B., Wang J., Liu K., Lin Q., Yao S. Q., Chem. Commun. (2010), 46, 1118–1120
- Kane R. S., Langmuir (2010), 26, 8636–8640
- Kang J.-H., Asai D., Toita R., Kitazaki H., Katayama Y., Carcinogenesis (2009), 30, 1927–1931
- Karaman M. W., Herrgard S., Treiber D. K., Gallant P., Atteridge C. E., Campbell B. T., Chan K. W., Ciceri P., Davis M. I., Edeen P. T., Faraoni R., Floyd M., Hunt J. P., Lockhart D. J., Milanov Z. V., Morrison M. J., Pallares G., Patel H. K., Pritchard S., Wodicka L. M., Zarrinkar P. P., Nat. Biotechnol. (2008), 26, 127–132
- Kase H., Iwahashi K., Nakanishi S., Matsuda Y., Yamada K., Takahashi M., Murakata C., Sato A., Kaneko M., Biochem. Biophys. Res. Commun. (1987), 142, 436–440
- Kawai Y., Sato M., Umezawa Y., Anal. Chem. (2004), 76, 6144–6149
- Kayser K. J., Glenn M. P., Sebt S. M., Cheng J. Q., Hamilton A. D., Bioorg. Med. Chem. Lett. (2007), 17, 2068–2073
- Keller T. H., Pichota A., Yin Z., Curr. Opin. Chem. Biol. (2006), 10, 357–361
- Kéri G., Orfi L., Eros D., Hegymegi-Barakonyi B., Szintai-Kis C., Horvith Z., Wjczek F., Marosfalvi J., Szabadkai I., Pato J., Greff Z., Hafenbradl D., Daub H., Müller G., Klebl B., Ullrich A., Curr. Signal Transduction Therapy (2006), 1, 67–95
- Kerlavage A. R., Taylor S. S., JBC (1980), 255, 8483–8486
- Kim C., Cheng C. Y., Saldanha S. A., Taylor S. S., Cell (2007), 130, 1032–1043
- Kim D., Sun M., He L., Zhou Q.-H., Chen J., Sun X.-M., Bepler G., Sebt S. M., Cheng J. Q., JBC (2010), 285, 8383–8394
- Kim K., Cole P. A., JACS (1998), 120, 6851–6858
- Kinderman F. S., Kim C., von Daake S., Ma Y., Pham B. Q., Spraggon G., Xuong N.-H., Jennings P. A., Taylor S. S., Molecular Cell 24, 397–408, November 3, 2006

Kinnings S. L., Jackson R. M., *J Chem. Inf. Model.* (2009), 49, 318–329

Kittel, C. *Introduction to Solid State Physics*, John Wiley & Sons (1986), 2nd edition

Knight Z. A., Lin H., Shokat K. M., *Nature Rev. Cancer* (2010), 10, 130–137

Knighton D. R., Zheng J. H., Ten Eyck L. F., Ashford V. A., Xuong N. H., Taylor S. S., Sowadski J. M., *Science* (1991), 253, 407–414

Komander D., Kular G. S., Bain J., Elliott M., Alessi D. R., van Aalten D. M. F., *Biochem. J.* (2003), 375, 255–262

Komander D., Kular G. S., Schüttelkopf A. W., Deak M., Prakash K. R. C., Bain J., Elliott M., Garrido-Franco M., Kozikowski A. P., Alessi D. R., van Aalten D. M. F., *Structure* (2004), 12, 215–226

Kong C.-T., Cook P. F., *Biochemistry* (1988), 27, 4795–4799

Kornev A. P., Haste N. M., Taylor S. S., Ten Eyck L. F., *PNAS USA* (2006), 103, 17783–17788

Kornev A. P., Taylor S. S., *Biochim. Biophys. Acta* (2010), 1804, 440–444

Krishnamurty R., Maly D. J., *ACS Chem. Biol.* (2010), 5, 121–138

Kumar P., Walsh D. A., *Biochem. J.* (2002), 362, 533–537

Kuroki H., Imai A., Nashida T., Shimomura H., *Arch. Oral. Biol.* (2007), 52, 905–610

Kwan J., Ling A., Papp E., Shaw D., Bradshaw J. M., *Anal. Biochem.* (2009), 395, 256–262

Lackey, K. E., *Curr. Top. Med. Chem.* (2006), 6, 435–460

Lakowicz J. R., *Principles of fluorescence spectroscopy*, Springer (2006), 3rd edition

Lam K. S., Wu J., Lou Q., *Int. J. Pept. Protein Res.* (1995), 45, 587–592

Lam K. S., Lebl M., Krchnak V., *Chem. Rev.* (1997), 97, 411–448

Lam K. S., Liu R., Miyamoto S., Lehman A. L., Tuscano J. M., *Acc. Chem. Res.* (2003), 36, 370–377

Landgraf W., Hofmann F., *Eur. J. Biochem.* (1989), 181, 643–650

Landry Y., Gies J.-P., *Fundamental Clin. Pharmacol.* (2008), 22, 1–18

Lavogina D., Lust M., Viil I., König N., Raidaru G., Rogozina J., Enkvist E., Uri A., Bossemeyer D., *J. Med. Chem.* (2009), 52, 308–321

Lavogina D., Enkvist E., Uri A., *Chem. Med. Chem.* (2010a), 5, 23–34

Lavogina D., Nickl C. K., Enkvist E., Raidaru G., Lust M., Vaasa A., Uri A., Dostmann W. R., *Biochim. Biophys. Acta* (2010b), 1804, 1857–1868

Lawrence D. S., Niu J., *Pharmacol. Ther.* (1998), 77, 81–114

Lawrence D. S., *Inhibitors of Protein Kinases and Protein Phosphatases, Handbook of Experimental Pharmacology*, Springer (2005), 167

Lebakken C. S., Kang H. C., Vogel K. W., *J. Biomol. Screen.* (2007), 12, 828–841

Lee G. M., Craik C. S., *Science* (2009), 324, 213–215

Lee H.-M., Larson D. R., Lawrence D. S., *ACS Chem. Biol.* (2009), 4, 409–427

Lee J., Rudd J. J., *Trends Plant Sc.* (2002), 7, 97–98

Lee J. H., Nandy S. K., Lawrence D. S., *JACS* (2004), 126, 3394–3395

Leonard C. J., Aravind L., Koonin E. V., *Genome Res.* (1998), 8, 1038–1047

Levinson N. M., Kuchment O., Shen K., Young M. A., Koldobskiy M., Karplus M., Cole P. A., Kuriyan J., *PLoS Biol.* (2006), 4, e144

Lew J., Coruh N., Tsigelny I., Garrod S., Taylor S. S., *JBC* (1997a), 272, 1507–1513

Lew J., Taylor S. S., Adams J. A., *Biochemistry* (1997b), 36, 6717–6724

Lewis J. A., Lebois E. P., Lindsley C. W., *Curr. Opin. Chem. Biol.* (2008), 12, 269–280

Levitzki A., Mishani E., *Annu. Rev. Biochem.* (2006), 75, 93–109

Li H., Hah J.-M., Lawrence D. S., *JACS* (2008), 130, 10474–10475

Li Q., Woods K. W., Thomas S., Zhu G.-D., Packard G., Fisher J., Li T., Gong J., Dinges J., Song X., Abrams J., Luo Y., Johnson E. F., Shi Y., Liu X., Klinghofer V.,

- Jong R. D., Oltersdorf T., Stoll V. S., Jakob C. G., Rosenberg S. H., Giranda V. L., *Bioorg. Med. Chem. Lett.* (2006), 16, 2000–2007
- Li S., WenFang X., *Sci. China Series B: Chem.* (2009), 52, 535–548
- Li Y. J., Xie W. H., Fang G. J., *Anal. Bioanal. Chem.* (2008), 390, 2049–2057
- Lienhard G. E., Secemski I. I., *JBC* (1973), 248, 1121–1123
- Lin H., Yamashita D. S., Zeng J., Xie R., Wang W., Nidarmarthy S., Luengo J. I., Rhodes N., Knick V. B., Choudhry A. E., Lai Z., Minthorn E. A., Strum S. L., Wood E. R., Elkins P. A., Concha N. O., Heerding D. A., *Bioorg. Med. Chem. Lett.* (2010), 20, 673–678
- Lin X., Ayrapetov M. K., Sun G., *BMC Biochem.* (2005), 6, 25
- Lin X., Murray J. M., Rico A. C., Wang M. X., Chu D. T., Zhou Y., Del Rosario M., Kaufman S., Ma S., Fang E., Crawford K., Jefferson A. B., *Bioorg. Med. Chem. Lett.* (2006), 16, 4163–4168
- Lindsley C. W., Zhao Z., Leister W. H., Robinson R. G., Barnett S. F., Defeo-Jones D., Jones R. E., Hartman G. D., Huff J. R., Huberb H. E., Duggan M. E., *Bioorg. Med. Chem. Lett.* (2005), 15, 761–764
- Lipinski C. A., Lombardo F., Dominy B. W., Feeney P., *J. Adv. Drug Deliv. Rev.* (2001), 46, 3–26
- Liu K., Kalesh K. A., Ong L. B., Yao S. Q., *Chem. Bio. Chem* (2008), 9, 1883–1888
- Liu P., Cheng H., Roberts T. M., Zhao J. J., *Nat. Rev. Drug Disc.* (2009), 8, 627–644
- Liu Y., Bishop A., Witucki L., Kraybill B., Shimizu E., Tsien J., Ubersax J., Blethrow J., Morgan D. O., Shokat K. M. *Chem. Biol.* (1999), 6, 671–678
- Livnah N., Yechezkel T., Salitra Y., Perlmutter B., Ohne O., Cohen I., Litman P., Senderovitz H., Protein kinase inhibitors comprising ATP mimetics conjugated to peptides or peptidomimetics, WO2003010281, 2003
- Livnah N., Levitzki A., Senderovitz H., Yechezkel T., Salitra Y., Litman P., Ohne O., Cell permeable conjugates of peptides for inhibition of protein kinases, WO2004110337, 2004
- LoGrasso P. V., Feng Y., *Curr. Topics Med. Chem.* (2009), 9, 704–723
- London N., Movshovitz-Attias D., Schueler-Furman O., *Structure* (2010), 18, 188–199
- Loog M., Uri A., Raidaru G., Järvi J., Ek P., *Bioorg. Med. Chem. Lett.* (1999), 9, 1447–1452
- Loog M., Uri A., Raidaru G., Järvi J., Ek P., *FEBS Lett.* (2000), 480, 244–248
- Luo R., David L., Hung H., Devaney J., Gilson M. K., *J. Phys. Chem. B* (1999), 103, 727–736
- Luo Y., Smith R. A., Guan R., Liu X., Klinghofer V., Shen J., Hutchins C., Richardson P., Holzman T., Rosenberg S. H., Giranda V. L., *Biochemistry* (2004), 43, 1254–1263
- Ma H., Deacon S., Horiuchi K., *Expert Opin. Drug Discov.* (2008), 3, 607–621
- Ma Y., Pitson S., Hercus T., Murphy J., Lopez A., Woodcock J., *JBC* (2005), 280, 26011–26017
- Madhusudan, Akamine P., Xuong N. H., Taylor S. S., *Nat. Struct. Biol.* (2002), 9, 273–277
- Maekawa M., Ishizaki T., Boku S., Watanabe N., Fujita A., Iwamatsu A., Obinata T., Ohashi K., Mizuno K., Narumiya S., *Science* (1999), 285, 895–898
- Magalhaes M. L. B., Vetting M. W., Gao F., Freiburger L., Auclair K., Blanchard J. S., *Biochemistry* (2008), 47, 579–584
- Maillard N., Clouet A., Darbre T., Reymond J.-L., *Nat. Protoc.* (2009), 4, 132–142
- Maly D. J., Allen J. A., Shokat K. M., *JACS* (2004), 126, 9160–9161
- Manning B. D., Cantley L. C., *Cell* (2007), 129, 1261–1274

- Manning G., Whyte D. B., Martinez R., Hunter T., Sudarsanam S., *Science* (2002), 298, 1912–1934
- Martinez A., Alonso M., Castro A., Pérez C., Moreno F. J., *J. Med. Chem.* (2002), 45, 1292–1299
- Martinez A., Alonso M., Castro A., Dorronsoro I., Gelpí J. L., Luque F. J., Pérez C., Moreno F. J., *J. Med. Chem.* (2005), 48, 7103–7112
- Masterson L. R., Mascioni A., Traaseth N. J., Taylor S. S., Veglia G., *PNAS USA* (2008), 105, 506–511
- Matheson R. R., Jr., Van Wart H. E., Burgess A. W., Weinstein L. I., Scheraga H. A., *Biochemistry* (1977), 16, 396–403
- Matthews B. W., *J. Mol. Biol.* (1968), 33, 491–497
- Medzihradzky D., Chen S.L., Kenyon G.L., Gibson B.W., *JACS* (1994), 116, 9413–9419
- Merrifield R. B., *JACS* (1963), 85, 2149–2154
- Millward M. J., House C., Bowtell D., Webster L., Olver I. N., Gore M., Copeman M., Lynch K., Yap A., Wang Y., Cohen P. S., Zalcberg J., *Br. J. Cancer* (2006), 95, 829–834
- Miranda-Saavedra D., Stark M. J. R., Packer J. C., Vivares C. P., Doerig C., Barton G. J., *BMC Genomics* (2007), 8, 309
- Moore E. G., Samuel A. P. S., Raymond K. N., *Acc. Chem. Res.* (2009), 42, 542–552
- Morphy R., *J. Med. Chem.* (2010), 53, 1413–1437
- Mulder J., Ariaens A., van den Boomen D., Moolenaar W. H., *Mol. Biol. Cell* (2004), 15, 5516–5527
- Murray A. J., *Sci. Signal.* (2008), 1, re4
- Murray A. W., *Cell* (2004), 116, 221–234
- Murthy K. S., Zhou H., Grider J. R., Makhoul G. M., *Am. J. Physiol. Gastrointest. Liver. Physiol.* (2003), 284, G1006–G1016
- Murthy K. S., *Annu. Rev. Physiol.* (2006), 68, 345–374
- Muzaffar S., Jeremy J. Y., Sparatore A., Del Soldato P., Angelini G. D., Shukla N., *Br. J. Pharmacol.* (2008), 155, 984–994
- Nakayama M., Amano M., Katsumi A., Kaneko T., Kawabata S., Takefuji M., Kaibuchi K., *Genes to Cells* (2005), 10, 107–117
- Narayana N., Cox S., Xuong N.-H., Ten Eyck L. F., Taylor S. S., *Structure* (1997), 5, 921–935
- Nelson D. L., Lehninger A. L., Cox M. M., *Lehninger principles of biochemistry*, Worth Publishers (2000)
- Nesterova M. V., Johnson N., Cheadle C., Bates S. E., Mani S., Stratakis C. A., Kahn I., Gupta R. K., Cho-Chung Y. S., *Cancer Res.* (2006), 66, 8971–8974
- Nickl C. K., Raidas S. K., Zhao H., Sausbier M., Ruth P., Tegge W., Brayden J. E., Dostmann W. R., *Biochim. Biophys. Acta* (2010), 1804, 524–532
- Niv M. Y., Rubin H., Cohen J., Tsirulnikov L., Licht T., Peretzman-Shemer A., Cnaan E., Tartakovsky A., Stein I., Albeck S., Weinstein I., Goldenberg-Furmanov M., Tobi D., Cohen E., Laster M., Ben-Sasson S. A., Reuveni H., *JBC* (2004), 279, 1242–1255
- Noble M. E. M., Endicott J. A., Johnson L. N., *Science* (2004), 303, 1800–1805
- Nolen B., Taylor S., Ghosh G., *Mol Cell.*, Volume 15, Issue 5, 10 September 2004, Pages 661–675
- Obrecht D., Villalgorido J. M., *Solid-Supported Combinatorial and Parallel Synthesis of Small-Molecular-Weight Compound Libraries*, Elsevier Science (1998)

- Ohren J. F., Chen H., Pavlovsky A., Whitehead C., Zhang E., Kuffa P., Yan C., McConnell P., Spessard C., Banotai C., Mueller W. T., Delaney A., Omer C., Sebolt-Leopold J., Dudley D. T., Leung I. K., Flamme C., Warmus J., Kaufman M., Barrett S., Tecle H., Hasemann C. A., *Nat. Struct. Mol. Biol.* (2004), 11, 1192–1197
- Olson M. F., *Curr. Opin. Cell Biol.* (2008), 20, 242–248
- Ono-Saito N., Niki I., Hidaka H., *Pharmacol. Ther.* (1999), 82, 123–131
- Oswald C., Smits S. H. J., Bremer E., Schmitt L., *Int. J. Mol. Sci.* (2008), 9, 1131–1141
- Pande V., Ramos M. J., Gago F., *Anti-Cancer Agents Med. Chem.* (2008), 8, 638–645
- Parang K., Till J. H., Ablooglu A. J., Kohanski R. A., Hubbard S. R., Cole P. A., *Nat. Struct. Biol.* (2001), 8, 37–41
- Parang K., Cole P. A., *Pharmacol. Ther.* (2002a), 93, 145–157
- Parang K., Kohn J. A., Saldanha S. A., Cole P. A., *FEBS Lett.* (2002b), 520, 156–160
- Parang K., Sun G., *Curr. Opin. Drug Discovery Devel.* (2004), 7, 617–629
- Parsons M., Worthey E. A., Ward P. N., Mottram J. C. *BMC Genomics* (2005), 6, 127
- Patricelli M. P., Szardenings A. K., Liyanage M., Nomanbhoy T. K., Wu M., Weissig H., Aban A., Chun D., Tanner S., Kozarich J. W., *Biochemistry* (2007), 46, 350–358
- Paul B. Z. S., Daniel J. L., Kunapuli S. P., *JBC* (1999), 274, 28293–28300
- Pearce L. R., Komander D., Alessi D. R., *Nat. Rev. Mol. Cell. Biol.* (2010), 11, 9–22
- Perea S. E., Reyes O., Puchades Y., Mendoza O., Vispo N. S., Torrens I., Santos A., Silva R., Acevedo B., Lopez E., Falcon V., Alonso D. F., *Cancer Res.* (2004), 64, 7127–7129
- PerkinElmer Scintillation Proximity Assay (SPA),
<http://las.perkinelmer.com/Catalog/CategoryPage.htm?CategoryID=Scintillation+Proximity+Assay+%5bSPA%5d>, last viewed August 7, 2010
- Pflug A., Rogozina J., Lavogina D., Enkvist E., Uri A., Engh R. A., Bossemeyer D., *J. Med. Chem.* (2010), doi: 10.1016/j.jmb.2010.08.028
- Phipps J., Terreux R. Targeted protein kinase C inhibitors and uses thereof, WO2007016777 (2007)
- Pidoux G., Taskén K., *J. Mol. Endocrinol.* (2010), 44, 271–284
- Pinkse M. W. H., Rijkers D. T. S., Dostmann W. R., Heck A. J. R., *JBC* (2009), 284, 16354–16368
- Pinna L. A., Ruzzene M., *Biochim. Biophys. Acta* (1996), 1314, 191–225
- Polshakov D., Rai S., Wilson R. M., Mack E. T., Vogel M., Krause J. A., Burdzinski G., Platz M. S., *Biochemistry* (2005), 44, 11241–11253
- Poppe H., Rybalkin S. D., Rehmann H., Hinds T. R., Tang X.-B., Christensen A. E., Schwede F., Genieser H.-G., Bos J. L., Döskeland S. O., Beavo J. A., Butt E., *Nat. Methods* (2008), 5, 277–278
- Pratt D. J., Endicott J. A., Noble M. E., *Curr. Opin. Drug Discov. Devel.* (2004), 7, 428–436
- Priestman M. A., Lawrence D. S., *Biochim. Biophys. Acta* (2010), 1804, 547–558
- Profirovic J., Gorovoy M., Niu J., Pavlovic S., Voyno-Yasenetskaya T., *JBC* (2005), 32866–32876
- Promega ProFluor® PKA Assay,
http://www.promega.com/catalog/catalogproducts.aspx?categoryname=productleaf_1566, last viewed August 13, 2010
- Prudent R., Cochet C., *Chem. Biol.* (2009), 16, 112–120
- Puetz S., Lubomirov L. T., Pfister G., *Physiology* (2009), 24, 342–356
- Rabiller M., Getlik M., Klüter S., Richters A., Tückmantel S., Simard J. R., Rauh D., *Arch. Pharm. Chem. Life Sci.* (2010), 343, 193–206
- Ratcliffe S. J., Yi T., Khandekar S. S., *J. Biomol. Screen.* (2007), 12, 126–132

- Resch-Genger U., Grabolle M., Cavaliere-Jaricot S., Nitschke R., Nann T., *Nat. Meth.* (2008), 5, 763–775
- Rhodes N., Heerding D. A., Duckett D. R., Eberwein D. J., Knick V. B., Lansing T. J., McConnell R. T., Gilmer T. M., Zhang S.-Y., Robell K., Kahana J. A., Geske R. S., Kleymenova E. V., Choudhry A. E., Lai Z., Leber J. D., Minthorn E. A., Strum S. L., Wood E. R., Huang P. S., Copeland R. A., Kumar R., *Cancer Res.* (2008), 68, 2366–2374
- Ricouart A., Tartar A., Sergheraert C., Inhibition of protein kinase C by retro-inverso pseudosubstrate analogues, *Biochem. Biophys. Res. Commun.* (1989), 165, 1382–1390
- Ricouart A., Gesquiere J. C., Tartar A., Sergheraert C., *J. Med. Chem.* (1991), 34, 73–78
- Rininsland F., Xia W., Wittenburg S., Shi X., Stankewicz C., Achyuthan K., McBranch D., Whitten D., *PNAS USA* (2004), 101, 15295–15300
- Rix U., Superti-Furga G., *Nat. Chem. Biol.* (2009), 5, 616–624
- Rodgers D.W., *Structure* (1994), 2, 1135–1140
- Romano R. A., Kannan N., Kornev A. P., Allison C. J., Taylor S. S., *Prot. Science* (2009), 18, 1486–1497
- Rosenberg D., Groussin L., Jullian E., Perlemoine K., Bertagna X., Bertherat J., *Ann. N.Y. Acad. Sci.* (2002), 968, 65–74
- Rosse G., Sequin U., Mett H., Furet P., Traxler P., Fretz H., *Helvetica Chim. Acta* (1997), 80, 653–670
- Ruggeri B. A., Miknyoczki S. J., Singh J., Hudkins R. L., *Curr. Med. Chem.* (1999), 6, 845–857
- Rä ägel H., Sä älik P., Hansen M., Langel U., Pooga M., *J. Control Release* (2009), 139, 108–117
- Rybalkin S. D., Rybalkina I. G., Feil R., Hofmann F., Beavo J. A., *JBC* (2002), 277, 3310–3317
- Rybalkin S. D., Rybalkina I. G., Shimizu-Albergine M., Tang X.-B, Beavo J. A., *EMBO J.* (2003), 23, 469–478
- Saghatelian A., Cravatt B. F., *Nat. Chem. Biol.* (2005), 1, 130–142
- Sánchez A., Villalba N., Martínez A. C., García-Sacristán A., Hernández M., Prieto D., *Eur. J. Pharmacol.* (2008), 586, 283–287
- Sarbassov D. D., Guertin D. A., Ali S. M., Sabatini D. M., *Science* (2005), 307, 1098–1101
- Sarma G. N., Kinderman F. S., Kim C., von Daake S., Chen L., Wang B.-C., Taylor S. S., *Structure* 18, 155–166, February 10, 2010
- Saxty G., Woodhead S. J., Berdini V., Davies T. G., Verdonk M. L., Wyatt P. G., Boyle R. G., Barford D., Downham R., Garrett M. D., Carr R. A., *J. Med. Chem.* (2007), 50, 2293–2296
- Schirok H., Kast R., Figueroa-Pérez S., Bennabi S., Gnoth M. J., Feurer A., Heckroth H., Thutewohl M., Paulsen H., Knorr A., Hütter J., Lobell M., Münter K., Geiss V., Ehmke H., Lang D., Radtke M., Mittendorf J., Stasch J. P., *Chem. Med. Chem.* (2008), 3, 1893–1904
- Schlossmann J., Ammendola A., Ashman K., Zong X., Huber A., Neubauer G., Wang G.-X., Allescher H.-D., Korth M., Wilm M., Hofmann F., Ruth P., *Nature* (2000), 404, 197–201
- Schneider T. L., Mathew R. S., Rice K. P., Tamaki K., Wood J. L., Schepartz A., *Org. Lett.* (2005), 7, 1695–1698
- Scholten A., Aye T.-T., Heck A. J.R., *Mass Spectr. Rev.* (2008), 27, 331–353

- Schulz S., Chinkers M., Garbers D. L., FASEB J. (1989), 3, 2026–2035
- Segel I. H., Enzyme kinetics: behavior and analysis of rapid equilibrium and steady state enzyme systems, John Wiley & Sons, Inc. (1993)
- Sehon C. A., Wang G. Z., Viet A. Q., Goodman K. B., Dowdell S. E., Elkins P. A., Semus S. F., Evans C., Jolivet L. J., Kirkpatrick R. B., Dul E., Khandekar S. S., Yi T., Wright L. L., Smith G. K., Behm D. J., Bentley R., Doe C. P., Hu E., Lee D., J. Med. Chem. (2008), 51, 6631–6634
- Senderowicz A. M., Investig. New Drugs (1999), 17, 313–320
- Sessions E. H., Yin Y., Bannister T. D., Weiser A., Griffin E., Pocas J., Cameron M. D., Ruiz C., Lin L., Schürer S. C., Schröter T., LoGrasso P., Feng Y., Bioorg. Med. Chem. Lett. (2008), 18, 6390–6393
- Seydack M., Biosensors and Bioelectronics (2005), 20, 2454–2469
- Shabb J. B., Corbin J. D., JBC (1992), 267, 5723–5726
- Shabb J. B., Chem. Rev. (2001), 101, 2381–2411
- Shah B. H., Neithardt A., Chu D. B., Shah F. B., Catt K. J., J. Cell. Physiol. (2006), 206, 47–57
- Shah N. P., Skaggs B. J., Branford S., Hughes T. P., Nicoll J. M., Paquette R. L., Sawyers C. L., J. Clin. Invest. (2007), 117, 2562–2569
- Sharma V., Wang Q., Lawrence D. S., Biochim. Biophys. Acta (2008), 1784, 94–99
- Shen K., Cole P. A., JACS (2003), 125, 16172–16173
- Shen K., Hines A. C., Schwarzer D., Pickin K. A., Cole P. A., Biochim. Biophys. Acta (2005), 1754, 65–78
- Shin D.-S., Kim D.-H., Chung W.-J., Lee Y.-S., J. Biochem. Mol. Biol. (2005), 38, 517–525
- Shomin C. D., Meyer S. C., Ghosh I., Bioorg. Med. Chem. (2009), 17, 6196–6202
- Shu Y.-Z., J. Nat. Prod. (1998), 61, 1053–1071
- Shugar D., Acta Biochim. Pol. (1996), 43, 9–24
- Sigma-Aldrich® Resin Explorer, <http://www.sigmaaldrich.com/chemistry/drug-discovery/resin-explorer/solid-phase-resin.html>, last viewed August 7, 2010
- Simard J. R., Getlik M., Grütter C., Schneider R., Wulfert S., Rauh D., JACS (2010), 132, 4152–4160
- Skalhegg B. S., Johansen A. K., Levy F. O., Andersson K. B., Aandahl E. M., Blomhoff H. K., Hansson V., Tasken K., J. Cell. Physiol. (1998), 177, 85–93
- Skålhegg B. S., Funderud A., Henanger H. H., Hafte T. T., Larsen A. C., Kvissel A.-K., Eikvar S., Ørstavik S., Current Drug Targets (2005), 6, 655–664
- Smaill J. B., Palmer B. D., Rewcastle G. W., Denny W. A., McNamara D. J., Dobrusin E. M., Bridges A. J., Zhou H., Showalter H. D. H., Winters R. T., Leopold W. R., Fry D. W., Nelson J. M., Slintak V., Elliot W. L., Roberts B. J., Vincent P. W., Patmore S. J., J. Med. Chem. (1999), 42, 1803–1815
- Smith C. M., Radzio-Andzelm E., Madhusudan, Akamine P., Taylor S. S., Progress Biophys. Mol. Biol. (1999), 71, 313–341
- Smith J. A., Francis S. H., Walsh K. A., Kumar S., Corbin J. D., JBC (1996), 271, 20756–20762
- Smith J. A., Reed R. B., Francis S. H., Grimes K., Corbin J. D., JBC (2000), 275, 154–158
- Smolenski A., Burkhardt A. M., Eigenthaler M., Butt E., Gambaryan S., Lohmann S. M., Walter U., Naunyn-Schmiedeberg's Arch. Pharmacol. (1998), 358, 134–139
- Somlyo A. P., Somlyo A. V., J. Physiol. (2000), 522, 177–185
- Souslova E. A., Chudakov D. M., Biochemistry (Mosc). (2007), 72, 683–697

Southall, N. T., Dill, K. A., Haymet, A. D. J., *J. Phys. Chem. B* (2002), 106, 521–533

Speers A. E., Cravatt B. F., *Chem. Bio. Chem* (2004), 5, 41–47

Sriwai W., Zhou H., Murthy K. S., *Biochem. J.* (2008), 411, 543–551

Statsuk A. V., Maly D. J., Seeliger M. A., Fabian M. A., Biggs III. W. H., Lockhart D. J., Zarrinkar P. P., Kuriyan J., Shokat K. M., *JACS* (2008), 130, 17568–17574

Stavenger R. A., Cui H., Dowdell S. E., Franz R. G., Gaitanopoulos D. E., Goodman K. B., Hilfiker M. A., Ivy R. L., Leber J. D., Marino J. P. Jr., Oh H.-J., Viet A. Q., Xu W., Ye G., Zhang D., Zhao Y., Jolivet L. J., Head M. S., Semus S. F., Elkins P. A., Kirkpatrick R. B., Dul E., Khandekar S. S., Yi T., Jung D. K., Wright L. L., Smith G. K., Behm D. J., Doe C. P., Bentley R., Chen Z. X., Hu E., Lee D., *J. Med. Chem.* (2007), 50, 2–5

Steichen J. M., Iyer G. H., Li S., Saldanha S. A., Deal M. S., Woods V. L. Jr, Taylor S. S., *JBC* (2010), 285, 3825–3832

Tal-Gan Y., Freeman N. S., Klein S., Levitzki A., Gilon C., *Bioorg. Med. Chem.* (2010), 18, 2976–2985

Tamura M., Nakao H., Yoshizaki H., Shiratsuchi M., Shigyo H., Yamada H., Ozawa T., Totsuka J., Hidaka H., *Biochim. Biophys. Acta* (2005), 1754, 245–252

Tasken K., Aandahl E. M., *Physiol. Rev.* (2004), 84, 137–167

Taylor M. S., Okwuchukwuasanya C., Nickl C. K., Tegge W., Brayden J. E., Dostmann W. R. G., *Mol. Pharmacol.* (2004), 65, 1111–1119

Taylor S. S., Yang J., Wu J., Haste N. M., Radzio-Andzelm E., Anand G., *Biochim. Biophys. Acta* (2004), 1697, 259–269

Taylor S. S., Kim C., Cheng C. Y., Brown S. H. J., Wu J., Kannan N., *Biochim. Biophys. Acta* (2008), 1784, 16–26

Technikova-Dobrova Z., Sardanelli A. M., Papa S., *FEBS* (1991), 292, 69–72

Tegge W., Frank R., Hofmann F., Dostmann W. R. G., *Biochemistry* (1995), 34, 10569–10577

Toker A., *Mol. Cell* (2008), 31, 6–8

Tokushige H., Inatani M., Nemoto S., Sakaki H., Katayama K., Uehata M., Tanihara H., *Invest. Ophthalmol. Vis. Sci.* (2007), 48, 3216–3222

Toral-Barza L., Zhang W. G., Huang X., McDonald L. A., Salaski E. J., Barbieri L. R., Ding W. D., Krishnamurthy G., Hu Y. B., Lucas J., Bernan V. S., Cai P., Levin J. I., Mansour T. S., Gibbons J. J., Abraham R. T., Yu K., *Mol. Cancer Ther.* (2007), 6, 3028–3038

Tsien R. Y., Baird G., Circularly permuted fluorescent protein indicators, United States Patent 7060793 (2006)

Tsien R. Y., *Angew. Chem. Int. Ed.* (2009), 48, 5612–5626

Uehata M., Ishizaki T., Satoh H., Ono T., Kawahara T., Morishita T., Tamakawa H., Yamagami K., Inui J., Maekawa M., Narumiya S., *Nature* (1997), 389, 990–994

Uri A., Raidaru G., Subbi J., Padari K., Pooga M., *Bioorg. Med. Chem. Lett.* (2002), 12, 2117–2120

Uri A., Lust M., Vaasa A., Lavogina D., Viht K., Enkvist E., *Biochim. Biophys. Acta.* (2010), 1804, 541–546

Vaandrager A. B., Hogema B. M., de Jonge H. R., *Front. Biosci.* (2005), 10, 2150–2164

Vaasa A., Viil I., Enkvist E., Viht K., Raidaru G., Lavogina D., Uri A., *Anal. Biochem.* (2009), 385, 85–93

Vaasa A., Lust M., Terrin A., Uri A., Zaccolo M., *Biochem. Biophys. Res. Commun.* (2010), 397, 750–775

Vallone B., Miele A. E., Vecchini P., Chiancone E., Brunori M., *PNAS USA* (1998), 95, 6103–6107

- Walsh D. A., Perkins J. P., Krebs E. G., *J. Biol. Chem.* (1968), 243, 3763–3765
- Wang H., Shimizu E., Tang Y. P., Cho M., Kyin M., Zuo W., Robinson D. A., Alaimo P. J., Zhang C., Morimoto H., Zhuo M., Feng R., Shokat K. M., Tsien J. Z. *PNAS USA* (2003), 100, 4287–4292
- Wang H., Li M., Lin W., Wang W., Zhang Z., Rayburn E. R., Lu J., Chen D., Yue X., Shen F., Jiang F., He J., Wei W., Zeng X., Zhang R., *Cancer Epidemiol. Biomarkers Prev.* (2007), 16, 789–795
- Wang H., Nakata E., Hamachi I., *Chem. Bio. Chem.* (2009), 10, 2560–2577
- Wang Q., Lawrence D. S., *JACS* (2005), 127, 7684–7685
- Ward N. E., O'Brian C. A., *Biochemistry* (1993), 32, 11903–11909
- Warmuth, M., Kim, S., Gu, X. J., Xia, G. Adrian, F., *Curr. Opin. Oncol.* (2007), 19, 55–60
- Watkins C. L., Schmaljohann D., Futaki S., Jones A. T., *Biochem. J.* (2009), 420, 179–189
- Wei J.-Y., Cohen I. E. D., Genieser H.-G., Barnstable C. J., *J. Mol. Neurosci.* (1998), 10, 53–64
- Weisberg E., Manley P. W., Breitenstein W., Brügggen J., Cowan-Jacob S. W., Ray A., Huntly B., Fabbro D., Fendrich G., Hall-Meyers E., Kung A. L., Mestan J., Daley G. Q., Callahan L., Catley L., Cavazza C., Azam M., Neuberger D., Wright R. D., Gilliland D. G., Griffin J. D., *Cancer Cell.* (2005), 7, 129–141
- Wen W., Taylor S.S., Meinkoth J. L., *JBC* (1995), 270, 2041–2046
- Wen W., Liu W., Yan J., Zhang M., *JBC* (2008), 283, 26263–26273
- Vieth M., Erickson J., Wang J., Webster Y., Mader M., Higgs R., Watson I., *J. Med. Chem.* (2009), 52, 6456–6466
- Viht K., Padari K., Raidaru G., Subbi J., Tammiste I., Pooga M., Uri A., *Bioorg. Med. Chem. Lett.* (2003), 13, 3035–3039
- Viht K., Vaasa A., Raidaru G., Enkvist E., Uri A., *Anal. Biochem.* (2005), 340, 165–170
- Viht K., Schweinsberg S., Lust M., Vaasa A., Raidaru G., Lavogina D., Uri A., Herberg F. W., *Anal. Biochem.* (2007), 362, 268–277
- Virdee K., Yoshida H., Peak-Chew S., Goedert M., *FEBS Lett.* (2007), 581, 2657–2662
- Williamson J. R., *Nat. Struct. Biol.* (2000), 7, 834–837
- Wilson E. M., Chinkers M., *Biochemistry* (1995), 34, 4696–4701
- Wilson L. S., Elbatarny H. S., Crawley S. W., Bennett B. M., Maurice D. H., *PNAS USA* (2008), 105, 13650–13655
- Wissner A., Fraser H. L., Ingalls C. L., Dushin R. G., Floyd M. B., Cheung K., Nittoli T., Ravi M. R., Tan X., Loganzo F., *Bioorg. Med. Chem.* (2007), 15, 3635–3648
- Wlodarczyk J., Woehler A., Kobe F., Ponimaskin E., Zeug A., Neher E., *Biophys. J.* (2008), 94, 986–1000
- Wlodawer A., Minor W., Dauter Z., Jaskolski M., *FEBS J.* (2008), 275, 1–21
- Wolfenden R., *Accounts Chem. Res.* (1972), 5, 10–18
- Wood E. R., Triesdale A. T., McDonald O. B., Yuan D., Hassell A., Dickerson S. H., Ellis B., Pennisi C., Horne E., Lackey K., Alligood K. J., Rusnak D. W., Gilmer T. M., Shewchuk L., *Cancer Res.* (2004), 64, 6652–6659
- Wood J. S., Yan X., Mendelow M., Corbin J. D., Francis S. H., Lawrence D. S., *JBC* (1996), 271, 174–179
- Wooldridge A. A., MacDonald J. A., Erdodi F., Ma C., Borman M. A., Hartshorne D. J., Haystead T. A. J., *JBC* (2004), 279, 34496–34504
- Wu J., Brown S. H. J., von Daake S., Taylor S. S., 2007 VOL 318 *Science*, 274–279
- Wu Y., Xu J. C., *Chin. Chem. Lett.* (2000), 11, 771–774

- Xu Z., Nagashima K., Sun D., Rush T., Northrup A., Andersen J. N., Kariv I., Bobkova E. V., *J. Biomol. Screen.* (2009), 14, 1257–1262
- Yamaguchi H., Kasa M., Amano M., Kaibuchi K., Hakoshima T., *Structure* (2006a), 14, 589–600
- Yamaguchi H., Miwa Y., Kasa M., Kitano K., Amano M., Kaibuchi K., Hakoshima T., *J. Biochem.* (2006b), 140, 305–311
- Yan B., *Acc. Chem. Res.* (1998), 31, 621–630
- Yang J., Cron P., Good V. M., Thompson V., Hemmings B. A., Barford D., *Nat. Struct. Biol.* (2002), 9, 940–944
- Yang J., Ten Eyck L. F., Xuong N.-H., Taylor S. S., *J. Mol. Biol.* (2004), 336, 473–487
- Yang J., Kennedy E. J., Wu J., Deal M. S., Pennypacker J., Ghosh G., Taylor S. S., *JBC* (2009), 284, 6241–6248.
- Yang L., Dan H. C., Sun M., Liu Q., Sun X.-M., Feldman R. I., Hamilton A. D., Polokoff M., Nicosia S. V., Herlyn M., Sebt S. M., Cheng J. Q., *Cancer Res.* (2004), 64, 4394–4399
- Zaccolo M., Magalhães P., Pozzan T., *Curr. Opin. Cell Biol.* (2002), 14, 160–166
- Zhang H. H., Lipovsky A. I., Dibble C. C., Sahin M., Manning B. D., *Mol. Cell.* (2006), 24, 185–197
- Zhang J., Yang P. L., Gray N. S., *Nature Rev. Cancer* (2009), 9, 28–39
- Zhang X., Crespo A., Fernández A., *Trends Biotechnol.* (2008), 26, 295–301
- Zhao Z., Leister W. H., Robinson R. G., Barnett S. F., Defeo-Jones D., Jones R. E., Hartman G. D., Huff J. R., Huber H. E., Duggan M. E., Lindsley C. W., *Bioorg. Med. Chem. Lett.* (2005), 15, 905–909
- Zhong H., SuYang H., Erdjument-Bromage H., Tempst P., Ghosh S., *Cell* (1997), 89, 413–424
- Zhou J., Adams J. A., *Biochemistry* (1997), 36, 15733–15738
- Zhou W., Ercan D., Chen L., Yun C.-H., Li D., Capelletti M., Cortot A. B., Chirieac L., Jacob R. E., Padera R., Engen J. R., Wong K.-K., Eck M. J., Gray N. S., Jänne P. A., *Nature* (2009), 462, 1070–1074
- Zhu G.-D., Gong J., Gandhi V. B., Woods K., Luo Y., Liu X., Guan R., Klinghofer V., Johnson E. F., Stoll V. S., Mamo M., Li Q., Rosenberg S. H., Giranda V. L., *Bioorg. Med. Chem.* (2007), 15, 2441–2452
- Zoller M. J., Nelson N. C., Taylor S. S., *JBC* (1981), 256, 10837–10842

APPENDICES

Appendix I. Selectivity profiling of ARC-902, ARC-903, ARC-1028 and ARC-664

Protein kinase	Kinase group	Percent of inhibition			
		ARC-902, 1 microM	ARC-903, 1 microM	ARC-1028, 100 nM	ARC-664, 100 nM
AMPK A1/B1/G1	CAMK	52	61	51	41
Aurora A	other	nd	nd	10	46
CaMKI delta	CAMK	85	94	35	25
CaMKII alpha	CAMK	nd	nd	5	10
CaMKII beta	CAMK	nd	nd	16	22
CDK2/cyclin A	CMGC	12	27	0	6
CHK1	CAMK	84	69	88	82
CHK2	CAMK	86	78	62	33
CK1 alpha 1	CK1	-6	3	-30	-22
DAPK3 (ZIPK)	CAMK	nd	nd	22	44
GSK3 alpha	CMGC	nd	nd	16	8
GSK3 beta	CMGC	44	6	16	4
MELK	CAMK	nd	nd	84	83
MSK1	AGC	98	99	105	112
MSK2	AGC	nd	nd	109	112
p70 S6K	AGC	93	98	96	99
PAK3	STE	nd	nd	74	69
PAK4	STE	nd	nd	81	21
PAK6	STE	nd	nd	81	70
PDK1	AGC	38	44	45	65
PIM1	CAMK	nd	nd	96	97
PIM2	CAMK	62	91	79	95
PKAc alpha	AGC	89	94	104	104
PKB alpha (Akt 1)	AGC	98	98	89	97
PKB beta (Akt 2)	AGC	97	97	62	80
PKB gamma (Akt 3)	AGC	nd	nd	87	100
PKC alpha	AGC	69	85	94	92
PKC beta I	AGC	nd	nd	97	100
PKC beta II	AGC	nd	nd	94	104
PKC delta	AGC	nd	nd	97	97
PKC epsilon	AGC	nd	nd	106	103
PKC eta	AGC	nd	nd	106	106
PKC gamma	AGC	nd	nd	107	108
PKC iota	AGC	nd	nd	34	24
PKC mu	AGC	nd	nd	54	93
PKC zeta	AGC	nd	nd	53	38
PKC theta	AGC	nd	nd	97	91
PKD2	CAMK	nd	nd	37	79
PKD3	CAMK	nd	nd	55	90
PKGI	AGC	nd	nd	58	105
PKGII	AGC	nd	nd	16	78
PRKX	AGC	nd	nd	104	106
ROCK-I	AGC	nd	nd	105	106
ROCK-II	AGC	100	100	104	106
RSK1	AGC	72	100	98	97
RSK2	AGC	88	98	104	103
RSK3	AGC	nd	nd	99	97
SGK1	AGC	84	99	89	97
SGK2	AGC	nd	nd	76	91

Data integrated from Enkvist *et al.*, 2006; Enkvist *et al.*, 2009; Lavogina *et al.*, 2009

ACKNOWLEDGEMENTS

The support from the following institutions and organizations is gratefully acknowledged:

- Research group of Dr. Asko Uri, Chair of Bioorganic Chemistry, Institute of Chemistry, University of Tartu, Tartu, Estonia;
- Research group of Dr. Ago Rinken, Chair of Bioorganic Chemistry, Institute of Chemistry, University of Tartu, Tartu, Estonia;
- Research group of Dr. Dirk Bossemeyer, Research Group Structural Biochemistry, DKFZ, Heidelberg, Germany;
- Research group of Dr. Wolfgang R. Dostmann, Department of Pharmacology, College of Medicine, University of Vermont, Burlington VT, USA;
- Research group of Dr. Richard Engh, Department of Chemistry, Faculty of Science, University of Tromsø, Tromsø, Norway
- Graduate school “Functional materials and processes” receiving funding from the European Social Fund under project 1.2.0401.09-0079 in Estonia;
- Kristjan Jaagu stipendiumid, Sihtasutus Archimedes, Tallinn, Estonia;
- Programme “DoRa”, Sihtasutus Archimedes, Tallinn, Estonia.

PUBLICATIONS

CURRICULUM VITAE

General data

Name: Darja Lavõgina
Born: May 31, 1986, Tartu, Estonia
Citizenship: Estonian
Address: University of Tartu, Institute of Chemistry, 14A Ravila St.,
50411 Tartu, Estonia
E-mail: darja.lavogina@ut.ee

Education

2007–... University of Tartu, Institute of Chemistry, PhD student
2006–2007 University of Tartu, Faculty of Physics and Chemistry,
MSc student
2003–2006 University of Tartu, Faculty of Physics and Chemistry,
BSc student

Professional employment

2007–2009 University of Tartu, Faculty of Science and Technology, Institute
of Chemistry, Tartu University, Chair of Bioorganic Chemistry;
Extraordinary Researcher (0.20)
2008–2008 University of Tartu, Faculty of Science and Technology, Dean's
Office, Materjaliteaduse ja materjalide tehnoloogia doktorikool;
Extraordinary Researcher (0.08)

Professional self-improvement

2006–2007 Research Group Structural Biochemistry, DKFZ, Heidelberg,
Germany (4 months)
2009 Department of Pharmacology, College of Medicine,
University of Vermont, Burlington VT, USA (3 months)
2010 Sexual Medicine and Andrology Unit, Department of Clinical
Physiopathology, University of Florence, Florence, Italy
(2 weeks)
2010 Institute of Bioscience, Department of Physiology,
University of São Paulo, São Paulo, Brazil (2 months)

Scientific publications

- Pflug A., Rogozina J., **Lavogina D.**, Enkvist E., Uri A., Engh R. A., Bossemeyer D., Diversity of bisubstrate binding modes of adenosine analogue-oligoarginine conjugates in protein kinase A and implications for protein substrate interactions. *Journal of Molecular Biology* (2010), doi: 10.1016/j.jmb.2010.08.028
- Lavogina D.**, Nickl C. K., Enkvist E., Raidaru G., Lust M., Vaasa A., Uri A., Dostmann W. R., Adenosine analogue-oligo-arginine conjugates (ARCs) serve as high-affinity inhibitors and fluorescence probes of type I cGMP-dependent protein kinase (PKGI α). *Biochimica et Biophysica Acta-Proteins and Proteomics* (2010), 1804, 1857–1868
- Uri A., Lust M., Vaasa A., **Lavogina D.**, Viht K., Enkvist E., Bisubstrate fluorescent probes and biosensors in binding assays for HTS of protein kinase inhibitors. *Biochimica et Biophysica Acta* (2010), 1804, 541–546
- Lavogina D.**, Enkvist E., Uri A., Bisubstrate Inhibitors of Protein Kinases: from Principle to Practical Applications. *ChemMedChem* (2010), 5, 23–34
- Lavogina D.**, Lust M., Viil I., König N., Raidaru G., Rogozina J., Enkvist E., Uri A., Bossemeyer D., Structural Analysis of ARC-Type Inhibitor (ARC-1034) Binding to Protein Kinase A Catalytic Subunit and Rational Design of Bisubstrate Analogue Inhibitors of Basophilic Protein Kinases. *Journal of Medicinal Chemistry* (2009), 52, 308–321
- Vaasa A., Viil I., Enkvist E., Viht K., Raidaru G., **Lavogina D.**, Uri A., High-affinity bisubstrate probe for fluorescence anisotropy binding/displacement assays with protein kinases PKA and ROCK. *Analytical Biochemistry* (2009), 385, 85–93
- Enkvist E., Raidaru G., Vaasa A., Pehk T., **Lavogina D.**, Uri A., Carbocyclic 3'-deoxyadenosine-based highly potent bisubstrate-analog inhibitor of basophilic protein kinases. *Bioorganic & Medicinal Chemistry Letters* (2007), 17, 5336–5339
- Viht K., Schweinsberg S., Lust M., Vaasa A., Raidaru G., **Lavogina D.**, Uri A., Herberg F., Surface-plasmon-resonance-based biosensor with immobilized bisubstrate analog inhibitor for the determination of affinities of ATP- and protein-competitive ligands of cAMP-dependent protein kinase. *Analytical Biochemistry* (2007), 362, 268–277
- Enkvist E., **Lavogina D.**, Raidaru G., Vaasa A., Viil I., Lust M., Viht K., Uri A., Conjugation of adenosine and hexa-(D-arginine) leads to a nanomolar bisubstrate-analog inhibitor of basophilic protein kinases. *Journal of Medicinal Chemistry* (2006), 49, 7150–7159

ELULOOKIRJELDUS

Üldandmed

Nimi: Darja Lavõgina
Sünniaeg ja koht: 31. mai 1986, Tartu, Eesti
Kodakondsus: Eesti
Aadress: Tartu Ülikool, Keemia Instituut, Ravila 14A, Tartu 50411, Eesti
E-mail: darja.lavogina@ut.ee

Haridus

2007–... Tartu Ülikool, Keemia Instituut, Doktoriõpe
2006–2007 Tartu Ülikool, Füüsika-keemiateaduskond, keemia eriala, Magistriõpe
2003–2006 Tartu Ülikool, Füüsika-keemiateaduskond, keemia eriala, Bakalaureuseõpe

Teenistuskäik

2007–2009 Tartu Ülikool, Loodus- ja tehnoloogiateaduskond, Tartu Ülikooli Keemia Instituut, Bioorgaanilise keemia õppetool; Erakorraline teadur (0.20)
2008–2008 Tartu Ülikool, Loodus- ja tehnoloogiateaduskond, Loodus- ja tehnoloogiateaduskonna dekanat, Materjaliteaduse ja materjalide tehnoloogia doktorikool; Erakorraline teadur (0.08)

Erialane enesetäiendus

2006–2007 Research Group Structural Biochemistry, DKFZ, Heidelberg, Saksamaa (4 kuud)
2009 Department of Pharmacology, College of Medicine, University of Vermont, Burlington VT, USA (3 kuud)
2010 Sexual Medicine and Andrology Unit, Department of Clinical Physiopathology, University of Florence, Firenze, Itaalia (2 nädalat)
2010 Institute of Bioscience, Department of Physiology, University of São Paulo, São Paulo, Brasiilia (2 kuud)

Teaduspublikatsioonid

- Pflug A., Rogozina J., **Lavogina D.**, Enkvist E., Uri A., Engh R. A., Bossemeyer D., Diversity of bisubstrate binding modes of adenosine analogue-oligoarginine conjugates in protein kinase A and implications for protein substrate interactions. *Journal of Molecular Biology* (2010), doi: 10.1016/j.jmb.2010.08.028
- Lavogina D.**, Nickl C. K., Enkvist E., Raidaru G., Lust M., Vaasa A., Uri A., Dostmann W. R., Adenosine analogue-oligo-arginine conjugates (ARCs) serve as high-affinity inhibitors and fluorescence probes of type I cGMP-dependent protein kinase (PKGI α). *Biochimica et Biophysica Acta-Proteins and Proteomics* (2010), 1804, 1857–1868
- Uri A., Lust M., Vaasa A., **Lavogina D.**, Viht K., Enkvist E., Bisubstrate fluorescent probes and biosensors in binding assays for HTS of protein kinase inhibitors. *Biochimica et Biophysica Acta* (2010), 1804, 541–546
- Lavogina D.**, Enkvist E., Uri A., Bisubstrate Inhibitors of Protein Kinases: from Principle to Practical Applications. *ChemMedChem* (2010), 5, 23–34
- Lavogina D.**, Lust M., Viil I., König N., Raidaru G., Rogozina J., Enkvist E., Uri A., Bossemeyer D., Structural Analysis of ARC-Type Inhibitor (ARC-1034) Binding to Protein Kinase A Catalytic Subunit and Rational Design of Bisubstrate Analogue Inhibitors of Basophilic Protein Kinases. *Journal of Medicinal Chemistry* (2009), 52, 308–321
- Vaasa A., Viil I., Enkvist E., Viht K., Raidaru G., **Lavogina D.**, Uri A., High-affinity bisubstrate probe for fluorescence anisotropy binding/displacement assays with protein kinases PKA and ROCK. *Analytical Biochemistry* (2009), 385, 85–93
- Enkvist E., Raidaru G., Vaasa A., Pehk T., **Lavogina D.**, Uri A., Carbocyclic 3'-deoxyadenosine-based highly potent bisubstrate-analog inhibitor of basophilic protein kinases. *Bioorganic & Medicinal Chemistry Letters* (2007), 17, 5336–5339
- Viht K., Schweinsberg S., Lust M., Vaasa A., Raidaru G., **Lavogina D.**, Uri A., Herberg F., Surface-plasmon-resonance-based biosensor with immobilized bisubstrate analog inhibitor for the determination of affinities of ATP- and protein-competitive ligands of cAMP-dependent protein kinase. *Analytical Biochemistry* (2007), 362, 268–277
- Enkvist E., **Lavogina D.**, Raidaru G., Vaasa A., Viil I., Lust M., Viht K., Uri A., Conjugation of adenosine and hexa-(D-arginine) leads to a nanomolar bisubstrate-analog inhibitor of basophilic protein kinases. *Journal of Medicinal Chemistry* (2006), 49, 7150–7159

DISSERTATIONES CHIMICAE UNIVERSITATIS TARTUENSIS

1. **Toomas Tamm.** Quantum-chemical simulation of solvent effects. Tartu, 1993, 110 p.
2. **Peeter Burk.** Theoretical study of gas-phase acid-base equilibria. Tartu, 1994, 96 p.
3. **Victor Lobanov.** Quantitative structure-property relationships in large descriptor spaces. Tartu, 1995, 135 p.
4. **Vahur Mäemets.** The ^{17}O and ^1H nuclear magnetic resonance study of H_2O in individual solvents and its charged clusters in aqueous solutions of electrolytes. Tartu, 1997, 140 p.
5. **Andrus Metsala.** Microcanonical rate constant in nonequilibrium distribution of vibrational energy and in restricted intramolecular vibrational energy redistribution on the basis of Slater's theory of unimolecular reactions. Tartu, 1997, 150 p.
6. **Uko Maran.** Quantum-mechanical study of potential energy surfaces in different environments. Tartu, 1997, 137 p.
7. **Alar Jänes.** Adsorption of organic compounds on antimony, bismuth and cadmium electrodes. Tartu, 1998, 219 p.
8. **Kaido Tammeveski.** Oxygen electroreduction on thin platinum films and the electrochemical detection of superoxide anion. Tartu, 1998, 139 p.
9. **Ivo Leito.** Studies of Brønsted acid-base equilibria in water and non-aqueous media. Tartu, 1998, 101 p.
10. **Jaan Leis.** Conformational dynamics and equilibria in amides. Tartu, 1998, 131 p.
11. **Toonika Rinken.** The modelling of amperometric biosensors based on oxidoreductases. Tartu, 2000, 108 p.
12. **Dmitri Panov.** Partially solvated Grignard reagents. Tartu, 2000, 64 p.
13. **Kaja Orupõld.** Treatment and analysis of phenolic wastewater with micro-organisms. Tartu, 2000, 123 p.
14. **Jüri Ivask.** Ion Chromatographic determination of major anions and cations in polar ice core. Tartu, 2000, 85 p.
15. **Lauri Vares.** Stereoselective Synthesis of Tetrahydrofuran and Tetrahydropyran Derivatives by Use of Asymmetric Horner-Wadsworth-Emmons and Ring Closure Reactions. Tartu, 2000, 184 p.
16. **Martin Lepiku.** Kinetic aspects of dopamine D_2 receptor interactions with specific ligands. Tartu, 2000, 81 p.
17. **Katrin Sak.** Some aspects of ligand specificity of P2Y receptors. Tartu, 2000, 106 p.
18. **Vello Pällin.** The role of solvation in the formation of iotsitch complexes. Tartu, 2001, 95 p.

19. **Katrin Kollist.** Interactions between polycyclic aromatic compounds and humic substances. Tartu, 2001, 93 p.
20. **Ivar Koppel.** Quantum chemical study of acidity of strong and superstrong Brønsted acids. Tartu, 2001, 104 p.
21. **Viljar Pihl.** The study of the substituent and solvent effects on the acidity of OH and CH acids. Tartu, 2001, 132 p.
22. **Natalia Palm.** Specification of the minimum, sufficient and significant set of descriptors for general description of solvent effects. Tartu, 2001, 134 p.
23. **Sulev Sild.** QSPR/QSAR approaches for complex molecular systems. Tartu, 2001, 134 p.
24. **Ruslan Petrukhin.** Industrial applications of the quantitative structure-property relationships. Tartu, 2001, 162 p.
25. **Boris V. Rogovoy.** Synthesis of (benzotriazolyl)carboximidamides and their application in relations with *N*- and *S*-nucleophiles. Tartu, 2002, 84 p.
26. **Koit Herodes.** Solvent effects on UV-vis absorption spectra of some solvatochromic substances in binary solvent mixtures: the preferential solvation model. Tartu, 2002, 102 p.
27. **Anti Perkson.** Synthesis and characterisation of nanostructured carbon. Tartu, 2002, 152 p.
28. **Ivari Kaljurand.** Self-consistent acidity scales of neutral and cationic Brønsted acids in acetonitrile and tetrahydrofuran. Tartu, 2003, 108 p.
29. **Karmen Lust.** Adsorption of anions on bismuth single crystal electrodes. Tartu, 2003, 128 p.
30. **Mare Piirsalu.** Substituent, temperature and solvent effects on the alkaline hydrolysis of substituted phenyl and alkyl esters of benzoic acid. Tartu, 2003, 156 p.
31. **Meeri Sassian.** Reactions of partially solvated Grignard reagents. Tartu, 2003, 78 p.
32. **Tarmo Tamm.** Quantum chemical modelling of polypyrrole. Tartu, 2003. 100 p.
33. **Erik Teinemaa.** The environmental fate of the particulate matter and organic pollutants from an oil shale power plant. Tartu, 2003. 102 p.
34. **Jaana Tammiku-Taul.** Quantum chemical study of the properties of Grignard reagents. Tartu, 2003. 120 p.
35. **Andre Lomaka.** Biomedical applications of predictive computational chemistry. Tartu, 2003. 132 p.
36. **Kostyantyn Kirichenko.** Benzotriazole — Mediated Carbon–Carbon Bond Formation. Tartu, 2003. 132 p.
37. **Gunnar Nurk.** Adsorption kinetics of some organic compounds on bismuth single crystal electrodes. Tartu, 2003, 170 p.
38. **Mati Arulepp.** Electrochemical characteristics of porous carbon materials and electrical double layer capacitors. Tartu, 2003, 196 p.

39. **Dan Cornel Fara.** QSPR modeling of complexation and distribution of organic compounds. Tartu, 2004, 126 p.
40. **Riina Mahlapuu.** Signalling of galanin and amyloid precursor protein through adenylate cyclase. Tartu, 2004, 124 p.
41. **Mihkel Kerikmäe.** Some luminescent materials for dosimetric applications and physical research. Tartu, 2004, 143 p.
42. **Jaanus Kruusma.** Determination of some important trace metal ions in human blood. Tartu, 2004, 115 p.
43. **Urmas Johanson.** Investigations of the electrochemical properties of polypyrrole modified electrodes. Tartu, 2004, 91 p.
44. **Kaido Sillar.** Computational study of the acid sites in zeolite ZSM-5. Tartu, 2004, 80 p.
45. **Aldo Oras.** Kinetic aspects of dATP α S interaction with P2Y₁ receptor. Tartu, 2004, 75 p.
46. **Erik Mölder.** Measurement of the oxygen mass transfer through the air-water interface. Tartu, 2005, 73 p.
47. **Thomas Thomborg.** The kinetics of electroreduction of peroxodisulfate anion on cadmium (0001) single crystal electrode. Tartu, 2005, 95 p.
48. **Olavi Loog.** Aspects of condensations of carbonyl compounds and their imine analogues. Tartu, 2005, 83 p.
49. **Siim Salmar.** Effect of ultrasound on ester hydrolysis in aqueous ethanol. Tartu, 2006, 73 p.
50. **Ain Uustare.** Modulation of signal transduction of heptahelical receptors by other receptors and G proteins. Tartu, 2006, 121 p.
51. **Sergei Yurchenko.** Determination of some carcinogenic contaminants in food. Tartu, 2006, 143 p.
52. **Kaido Tamm.** QSPR modeling of some properties of organic compounds. Tartu, 2006, 67 p.
53. **Olga Tšubrik.** New methods in the synthesis of multisubstituted hydrazines. Tartu. 2006, 183 p.
54. **Lilli Sooväli.** Spectrophotometric measurements and their uncertainty in chemical analysis and dissociation constant measurements. Tartu, 2006, 125 p.
55. **Eve Koort.** Uncertainty estimation of potentiometrically measured pH and pK_a values. Tartu, 2006, 139 p.
56. **Sergei Kopanchuk.** Regulation of ligand binding to melanocortin receptor subtypes. Tartu, 2006, 119 p.
57. **Silvar Kallip.** Surface structure of some bismuth and antimony single crystal electrodes. Tartu, 2006, 107 p.
58. **Kristjan Saal.** Surface silanization and its application in biomolecule coupling. Tartu, 2006, 77 p.
59. **Tanel Tätte.** High viscosity Sn(OBu)₄ oligomeric concentrates and their applications in technology. Tartu, 2006, 91 p.

60. **Dimitar Atanasov Dobchev.** Robust QSAR methods for the prediction of properties from molecular structure. Tartu, 2006, 118 p.
61. **Hannes Hagu.** Impact of ultrasound on hydrophobic interactions in solutions. Tartu, 2007, 81 p.
62. **Rutha Jäger.** Electroreduction of peroxodisulfate anion on bismuth electrodes. Tartu, 2007, 142 p.
63. **Kaido Viht.** Immobilizable bisubstrate-analogue inhibitors of basophilic protein kinases: development and application in biosensors. Tartu, 2007, 88 p.
64. **Eva-Ingrid Rõõm.** Acid-base equilibria in nonpolar media. Tartu, 2007, 156 p.
65. **Sven Tamp.** DFT study of the cesium cation containing complexes relevant to the cesium cation binding by the humic acids. Tartu, 2007, 102 p.
66. **Jaak Nerut.** Electroreduction of hexacyanoferrate(III) anion on Cadmium (0001) single crystal electrode. Tartu, 2007, 180 p.
67. **Lauri Jalukse.** Measurement uncertainty estimation in amperometric dissolved oxygen concentration measurement. Tartu, 2007, 112 p.
68. **Aime Lust.** Charge state of dopants and ordered clusters formation in $\text{CaF}_2\text{:Mn}$ and $\text{CaF}_2\text{:Eu}$ luminophors. Tartu, 2007, 100 p.
69. **Iiris Kahn.** Quantitative Structure-Activity Relationships of environmentally relevant properties. Tartu, 2007, 98 p.
70. **Mari Reinik.** Nitrates, nitrites, N-nitrosamines and polycyclic aromatic hydrocarbons in food: analytical methods, occurrence and dietary intake. Tartu, 2007, 172 p.
71. **Heili Kasuk.** Thermodynamic parameters and adsorption kinetics of organic compounds forming the compact adsorption layer at Bi single crystal electrodes. Tartu, 2007, 212 p.
72. **Erki Enkvist.** Synthesis of adenosine-peptide conjugates for biological applications. Tartu, 2007, 114 p.
73. **Svetoslav Hristov Slavov.** Biomedical applications of the QSAR approach. Tartu, 2007, 146 p.
74. **Eneli Härk.** Electroreduction of complex cations on electrochemically polished Bi(*hkl*) single crystal electrodes. Tartu, 2008, 158 p.
75. **Priit Möller.** Electrochemical characteristics of some cathodes for medium temperature solid oxide fuel cells, synthesized by solid state reaction technique. Tartu, 2008, 90 p.
76. **Signe Viggor.** Impact of biochemical parameters of genetically different pseudomonads at the degradation of phenolic compounds. Tartu, 2008, 122 p.
77. **Ave Sarapuu.** Electrochemical reduction of oxygen on quinone-modified carbon electrodes and on thin films of platinum and gold. Tartu, 2008, 134 p.
78. **Agnes Kütt.** Studies of acid-base equilibria in non-aqueous media. Tartu, 2008, 198 p.

79. **Rouvim Kadis.** Evaluation of measurement uncertainty in analytical chemistry: related concepts and some points of misinterpretation. Tartu, 2008, 118 p.
80. **Valter Reedo.** Elaboration of IVB group metal oxide structures and their possible applications. Tartu, 2008, 98 p.
81. **Aleksei Kuznetsov.** Allosteric effects in reactions catalyzed by the cAMP-dependent protein kinase catalytic subunit. Tartu, 2009, 133 p.
82. **Aleksei Bredihhin.** Use of mono- and polyanions in the synthesis of multisubstituted hydrazine derivatives. Tartu, 2009, 105 p.
83. **Anu Ploom.** Quantitative structure-reactivity analysis in organosilicon chemistry. Tartu, 2009, 99 p.
84. **Argo Vonk.** Determination of adenosine A_{2A}- and dopamine D₁ receptor-specific modulation of adenylate cyclase activity in rat striatum. Tartu, 2009, 129 p.
85. **Indrek Kivi.** Synthesis and electrochemical characterization of porous cathode materials for intermediate temperature solid oxide fuel cells. Tartu, 2009, 177 p.
86. **Jaanus Eskusson.** Synthesis and characterisation of diamond-like carbon thin films prepared by pulsed laser deposition method. Tartu, 2009, 117 p.
87. **Margo Lätt.** Carbide derived microporous carbon and electrical double layer capacitors. Tartu, 2009, 107 p.
88. **Vladimir Stepanov.** Slow conformational changes in dopamine transporter interaction with its ligands. Tartu, 2009, 103 p.
89. **Aleksander Trummal.** Computational Study of Structural and Solvent Effects on Acidities of Some Brønsted Acids. Tartu, 2009, 103 p.
90. **Eerold Vellemäe.** Applications of mischmetal in organic synthesis. Tartu, 2009, 93 p.
91. **Sven Parkel.** Ligand binding to 5-HT_{1A} receptors and its regulation by Mg²⁺ and Mn²⁺. Tartu, 2010, 99 p.
92. **Signe Vahur.** Expanding the possibilities of ATR-FT-IR spectroscopy in determination of inorganic pigments. Tartu, 2010, 184 p.
93. **Tavo Romann.** Preparation and surface modification of bismuth thin film, porous, and microelectrodes. Tartu, 2010, 155 p.
94. **Nadežda Aleksejeva.** Electrocatalytic reduction of oxygen on carbon nanotube-based nanocomposite materials. Tartu, 2010, 147 p.
95. **Marko Kullapere.** Electrochemical properties of glassy carbon, nickel and gold electrodes modified with aryl groups. Tartu, 2010, 233 p.
96. **Liis Siinor.** Adsorption kinetics of ions at Bi single crystal planes from aqueous electrolyte solutions and room-temperature ionic liquids. Tartu, 2010, 101 p.
97. **Angela Vaasa.** Development of fluorescence-based kinetic and binding assays for characterization of protein kinases and their inhibitors. Tartu 2010, 101 p.

98. **Indrek Tulp.** Multivariate analysis of chemical and biological properties. Tartu 2010, 105 p.
99. **Aare Selberg.** Evaluation of environmental quality in Northern Estonia by the analysis of leachate. Tartu 2010, 117 p.